THE ASTROPHYSICAL JOURNAL

An International Review of Spectroscopy and Astronomical Physics

FOUNDED IN 1895 BY GEORGE E. HALE AND JAMES E. KEELER

VOLUME 104

JULY–NOVEMBER 1946

THE UNIVERSITY OF CHICAGO PRESS
CHICAGO, ILLINOIS

CAMBRIDGE UNIVERSITY PRESS, LONDON

PUBLISHED JULY, SEPTEMBER, NOVEMBER, 1946

COMPOSED AND PRINTED BY THE UNIVERSITY OF CHICAGO PRESS
CHICAGO, ILLINOIS, U.S.A.

CONTENTS

NUMBER 1

Concentrations of the Interstellar Medium. Fred L. Whipple 1

The Motions of the Stars within 20 Parsecs of the Sun. Gustaf Strömberg . . 12

A Comparative Study of the Spectra of α Boötis and 70 Ophiuchi A. Suzanne E. A. van Dijke 27

The Diameters of Globular Clusters. Albert G. Mowbray 47

The Distribution of Brightness at the Extreme Limb of the Sun. Zdeněk Kopal . 60

The Photographic Light-Curve of T Coronae Borealis. Cecilia Payne-Gaposchkin and Frances W. Wright 75

The Internal Temperature-Density Distribution of Main Sequence Stars Built on the Point-Convective Model. II. Sirius A. R. E. Marshak and G. Blanch 82

The Effect of the Absorption Lines on the Temperature Distribution of the Solar Atmosphere. Guido Münch 87

On the Radiative Equilibrium of a Stellar Atmosphere. XI. S. Chandrasekhar . 110

Curve of Growth of γ Cygni. Jorge Sahade and Carlos U. Cesco 133

An Interesting Phenomenon in Stellar Spectroscopy. Otto Struve 138

The Reflection Effect in Eclipsing Binary Stars. Paris Pişmiş 141

Reviews 146

NUMBER 2

Rectification of the Light-Curves of Eclipsing Variables. Henry Norris Russell 153

A Study of the Extended Envelope Surrounding the Wolf-Rayet Component of V 444 Cygni. Zdeněk Kopal and Martha B. Shapley 160

The Infrared Spectrum of υ Sagittarii. Jesse L. Greenstein and Paul W. Merrill . 177

On the Radiative Equilibrium of a Stellar Atmosphere. XII. S. Chandrasekhar . 191

On the Helium Content of the Sun. Martin Schwarzschild 203

Ultraviolet Absorption Spectrum of Air in the Region λλ 600–2000. J. J. Hopfield. 208

On the Direction of Rotation in Spiral Nebulae. Bertil Lindblad and Rolf Brahde 211

Structure and Mass of Cometary Nuclei. B. Vorontsov-Velyaminov 226

Dwarf M Stars Found Spectrophotometrically. Second List. A. N. Vyssotsky, E. M. Janssen, W. J. Miller, S.J., and M. E. Walther 234

Motions and Absolute Magnitudes of Dwarf M Stars. A. N. Vyssotsky . . . 239

On the Interstellar Reddening in the Region of the North Polar Sequence and the Normal Color Indices of A-Type Stars. W. W. Morgan and W. P. Bidelman 245

Spectrographic Observations of Fourteen Eclipsing Binaries. Otto Struve . . 253
Spectroscopic Observations of θ Aquilae. Carlos U. Cesco and Otto Struve . . 282
Spectroscopic Observations of ζ^1 Ursae Majoris. Carlos U. Cesco 287
The Radial Velocities of Fifty Globular Star Clusters. N. U. Mayall . . . 290
Notes
Some Remarks on the Nova Phenomenon. Svein Rosseland 324
Note on the Spectral and Luminosity Classification of Stars from Spectra of Low Dispersion. Bertil Lindblad 325
The Occurrence of Cycles in *He* I. Anne B. Underhill 327
Reviews 330
Erratum 332

NUMBER 3

On the Dynamical Stability of Stars. P. Ledoux 333
The Atmosphere of 10 Lacertae. Lawrence H. Aller 347
The Light-Curves of R Aquarii. Cecilia Payne-Gaposchkin and Constance Boyd . 357
The Light-Curves of Z Andromedae and AX Persei. Cecilia Payne-Gaposchkin . 362
The Eclipsing System UV Leonis. Sergei Gaposchkin 370
The Eclipsing System RX Geminorum. Sergei Gaposchkin 376
The Eclipsing System RY Geminorum. Sergei Caposchkin 383
Some Radial-Velocity and Line-Intensity Measures in the Spectrum of β Canis Majoris. Anne B. Underhill 388
Spectrographic Observations of RY Persei and RZ Ophiuchi. W. A. Hiltner . . 396
The Ratio of Interstellar Absorption to Reddening. Jesse L. Greenstein . . . 403
Continuous Emission in the Orion Nebula. Jesse L. Greenstein 414
On the Continuous Absorption Coefficient of the Negative Hydrogen Ion. III. S. Chandrasekhar and Frances Herman Breen 430
The Continuous Spectrum of the Sun and the Stars. S. Chandrasekhar and Guido Münch 446
Notes
Luminosity Characteristics on Low-Dispersion Spectra of Stars of Types M0–M4. P. C. Keenan and J. J. Nassau 458
The Radial Velocity of 27 Canis Majoris. O. Struve 459
On the Possibility of Tracing Polarization Effects in the Rotational Profiles of Early-Type Stars. Yngve Öhman 460
Reviews 463
Erratum 464
Index 465

VOLUME 104 NUMBER 1

THE ASTROPHYSICAL JOURNAL

AN INTERNATIONAL REVIEW OF SPECTROSCOPY AND ASTRONOMICAL PHYSICS

JULY 1946

CONCENTRATIONS [illegible] INTERSTELLAR MEDIUM . . . *[illegible]* [illegible]

THE MOTIONS OF [illegible] WITHIN 20 PARSECS OF THE SUN . . . *[illegible]* [illegible]

A COMPARATIVE STUDY OF THE SPECTRA OF α BOÖTIS AND 70 O[illegible] A
[illegible] [illegible]

THE DIAMETERS OF [illegible] CLUSTERS . . . *[illegible]* [illegible]

THE DISTRIBUTION OF [illegible] AT THE EXTREME LIMB OF [illegible]
[illegible] [illegible]

THE PHOTOGRAPHIC [illegible] OF T CORONAE BOREALIS
Cecilia Payne-Gaposchkin and [illegible] [illegible]

THE INTERNAL [illegible]-DENSITY DISTRIBUTION OF MAIN [illegible] STARS BUILT ON THE [illegible]-CONVECTIVE MODEL. II. SIRIUS A
[illegible] [illegible]

THE EFFECT OF THE [illegible] LINES ON THE TEMPERATURE [illegible]TION OF THE SOLAR [illegible] . . . *[illegible]* [illegible]

ON THE RADIATIVE [illegible] OF A STELLAR ATMOSPHERE. [illegible]
[illegible] [illegible]

CURVE OF GROWTH OF [illegible] CYGNI . . . *Jorge Sahade and [illegible]* [illegible]

AN INTERESTING [illegible] IN STELLAR SPECTROSCOPY . . . *[illegible]* [illegible]

THE REFLECTION [illegible] IN ECLIPSING BINARY STARS . . . *[illegible]* [illegible]

REVIEWS . . . [illegible]

THE UNIVERSITY OF CHICAGO PRESS
CHICAGO, ILLINOIS, U.S.A.

July 1946 Vol. 104, No. 1

THE ASTROPHYSICAL JOURNAL

AN INTERNATIONAL REVIEW OF SPECTROSCOPY AND ASTRONOMICAL PHYSICS

The Astrophysical Journal is published bimonthly by the University of Chicago at the University of Chicago Press, 5750 Ellis Avenue, Chicago, Illinois, during July, September, November, January, March, and May. ¶The subscription price is $10.00 a year; the price of single copies is $2.00. Orders for service of less than a full year will be charged at the single-copy rate. ¶Postage is prepaid by the publishers on all orders from the United States and its possessions, Argentina, Bolivia, Brazil, Chile, Colombia, Costa Rica, Cuba, Dominican Republic, Ecuador, Guatemala, Haiti, Republic of Honduras, Mexico, Morocco (Spanish Zone), Nicaragua, Panama, Paraguay, Peru, Rio de Oro, El Salvador, Spain (including Balearic Islands, Canary Islands, and the Spanish Offices in Northern Africa; Andorra), Spanish Guinea, Uruguay, and Venezuela. ¶Postage is charged extra as follows: for Canada and Newfoundland, 42 cents on annual subscriptions (total $10.42); on single copies, 7 cents (total $2.07); for all other countries in the Postal Union, 96 cents on annual subscriptions (total $10.96), on single copies 16 cents (total $2.16). ¶Patrons are requested to make all remittances payable to The University of Chicago Press, in United States currency or its equivalent by postal or express money orders or bank drafts.

The following are authorized agents:

For the British Empire, except North America, India, and Australasia: The Cambridge University Press, Bentley House, 200 Euston Road, London, N.W. 1, England. Prices of yearly subscriptions and of single copies may be had on application.

Claims for missing numbers should be made within the month following the regular month of publication. The publishers expect to supply missing numbers free only when losses have been sustained in transit, and when the reserve stock will permit.

Business correspondence should be addressed to The University of Chicago Press, Chicago 37, Illinois.

Communications for the editors and manuscripts should be addressed to: Otto Struve, Editor of THE ASTROPHYSICAL JOURNAL, Yerkes Observatory, Williams Bay, Wisconsin.

Line drawings and photographs should be made by the author, and all marginal notes such as co-ordinates, wave lengths, etc., should be included in the cuts. It will not be possible to set up such material in type.

One copy of the corrected galley proof should be returned as soon as possible to the editor, Yerkes Observatory, Williams Bay, Wisconsin. Authors should take notice that the manuscript will not be sent to them with the proof.

The cable address is "Observatory, Williamsbay, Wisconsin."

The articles in this journal are indexed in the *International Index to Periodicals*, New York, N.Y.

Applications for permission to quote from this journal should be addressed to The University of Chicago Press, and will be freely granted.

Entered as second-class matter, July 31, 1940, at the Post-Office at Chicago, Ill., under the act of March 3, 1879.
Acceptance for mailing at special rate of postage provided for in United States Postal Act of October 3, 1917, Section 1103, amended February 28, 1925.

[PRINTED IN U.S.A.]

THE ASTROPHYSICAL JOURNAL

AN INTERNATIONAL REVIEW OF SPECTROSCOPY AND ASTRONOMICAL PHYSICS

VOLUME 104 JULY 1946 NUMBER 1

CONCENTRATIONS OF THE INTERSTELLAR MEDIUM*

FRED L. WHIPPLE
Harvard College Observatory

Received April 23, 1946

ABSTRACT

A suggested process for the origin of stars by the concentration of interstellar dust particles is discussed. In the initial stages the process depends upon the mutual attraction of particles under the force of light-pressure in the galactic-radiation field, as proposed by Spitzer. A chance concentration of particles will become an attractive center of force and will grow exponentially with time, as particles percolate through the gaseous substratum. Only in the darkest obscuring clouds, away from hot bright stars, is the theoretical growth found to be sufficiently rapid for serious consideration. After the initial concentration has become moderately opaque, the growth is linear with time, until a sufficient mass has accumulated for gravity to become effective. Then a much slower exponential growth with time can complete the prestellar accumulation of mass, if the interstellar medium is sufficiently quiescent. The conditions of quiescence are found to be exceedingly severe. If these conditions can be satisfied in actual obscuring clouds, stars can evolve from interstellar matter in a space of time of the order of 10^9 years. Galactic clusters of stars would generally be expected rather than individual isolated stars. Various observational evidence points to the likelihood of some such evolutionary process.

During the past decade our knowledge of the nature of the matter between the stars has increased at an exceedingly rapid pace. The dust and gases that constitute the interstellar material have now become no less important than the stars themselves in cosmological studies. Information has been gathered by many investigators, who used many different techniques of observation and theory.

Star counts, particularly in and about the obscured regions of the Milky Way, have led to a knowledge of the distribution in position, extent, and obscuring power of the dust clouds, which are concentrated in and near the galactic plane. Measures of the apparent distribution of the external galaxies have contributed materially to a knowledge of the distribution of near-by dark matter, as has a study of the dependence on distance of the apparent diameters of galactic star clusters.

Photoelectric, photographic, and photovisual observations of obscured stars have given the wave-length dependence (approximately $1/\lambda$) of the scattering produced by the particles of the dust clouds. The mode of reflection has been observed in the reflection nebulae near intrinsically bright stars. Such observations, combined with theoretical studies, have given evidence as to the approximate frequency distribution in size of the particles. A rough upper limit for the number of the particles per unit volume in space has been obtained from observations of meteors.

* Presented in February, 1942, at the Inter-American Congress of Astrophysics, Tonanzintla, Mexico, under the title, "Theory of the Interstellar Medium." Because of various circumstances the publication has been delayed. It is now presented in its original form, without change except for title.

The gases of interstellar space have been studied by spectrographic methods, first, by their absorption lines superimposed upon the spectra of stars and, second, by their emission lines observed in the nonstellar luminous background of the Milky Way. Astrophysical theory applied to these observations has indicated the abundances of various atoms and molecules, as well as the electron densities and state of ionization in certain regions of space.

Finally, an upper limit to the density of the composite interstellar medium in the neighborhood of the sun has been obtained from the observations of stellar motions as analyzed by Oort.[1]

General studies of the interstellar medium have been made by Dunham,[2] Struve,[3] Spitzer,[4] and others. Their investigations summarize the extensive observational material and present a fairly consistent picture of physical conditions between the stars.

Because the integrated mass of the interstellar material is comparable to the total mass concentrated in the stars, any possible process of stellar origin from interstellar material deserves careful consideration. No known physical process of energy generation can maintain the radiation of the supergiant stars for three billion years, the short-time scale of the universe. Some process for the contemporary formation of stars appears to be needed, and the necessity becomes imperative if a time scale even longer than three billion years is assumed. The interstellar matter provides the only obvious source of stellar building material. Furthermore, Spitzer's studies of the dynamics of the interstellar medium in gravitational systems suggests that the lack of supergiant stars in the spheroidal galaxies may well be associated with the lack of large aggregations of interstellar material in these systems. He shows that, in the spiral types possessing great angular momentum, extensive obscuring clouds and layers can be maintained by rotation, and he notes that supergiant stars are numerous. The present paper presents a preliminary exploration of a process whereby interstellar matter may possibly be concentrated to form a star.

The process depends primarily upon the attractive force set up between dust particles by the galactic-radiation field, light-pressure, and shadow effect suggested by Spitzer. This analysis follows in some respects as a sequel to his investigations; his general assumptions and conclusions are adopted for the sake of uniformity and simplicity.

An average region of the galactic plane is assumed to consist of a substratum of hydrogen (about 1 atom per cubic centimeter) containing sufficient dust particles of a uniform size to produce an average visual absorption of 1 mag. per kiloparsec. In this medium are the stars that produce the general radiation field. The presence of other atoms or molecules is ignored explicitly, but not implicitly, because in regions distant from the hotter and brighter stars the photoelectric ionization of these atoms is required to maintain the high kinetic temperature of the hydrogen substratum, a temperature taken on the average to be 10,000° K. The frequency distribution of particle sizes is mostly ignored in order to simplify the analysis for order-of-magnitude conclusions.

In such a medium near the galactic plane the hydrogen substratum will act as a fluid, maintaining practically a constant density against the relatively small forces of gravity or light-pressure, so long as the kinetic temperature remains constant. The interspersed dust particles, however, will come practically to rest with respect to the hydrogen substratum and will diffuse exceedingly slowly under their own partial pressure. Hence a minor concentration of dust, such as might be produced by diffusion through the hydrogen under the pressure of nonisotropic light from passing stars, will remain as a minor irregularity for a long period of time.

[1] *B.A.N.*, No. 238, 1932.

[2] *Proc. Amer. Phil. Soc.*, **81**, 277, 1939.

[3] *Washington Acad. Sci.*, **31**, 217, 1941.

[4] *Ap. J.*, **93**, 369, 1941; **94**, 232, 1941; **95**, 329, 1942.

Let us now investigate the development of such a minor concentration of dust in an otherwise homogeneous medium that is quiescent. Suppose the concentration is spherical, of radius r, and that it contains a uniform excess-particle density of N_d cm^{-3}, in addition to the average particle density of n_d cm^{-3}. So long as the cloud possesses a low opacity, each excess particle of radius σ, mass m_d, and scattering area $\pi\sigma^2 Q$ will act independently to shadow the general radiation from particles outside the concentration. Here Q is the ratio of the effective scattering area of the particle to the blocking area. Since only the effective absorbing area of each particle will be efficient in reducing the radiation traversing the concentration, the scattering area of a particle must be reduced by the factor $(1 - \gamma)$, where γ is the albedo. Hence the concentration directionally reduces the radiation at a distance R from its center by the factor $\pi\sigma^2 N_d r^3 (1 - \gamma) Q/3R$.[2] If the radiation field, of energy density U, is otherwise isotropic, a similar particle at R experiences a centrally directed acceleration g, given by the expression

$$g = \frac{\pi^2 \sigma^4 N_d r^3 (1 - \gamma) Q^2 U}{3 m_d R^2} . \tag{1}$$

In this equation it is assumed that the light-pressure on a particle is proportional to the total scattering area of the particle, the increased pressure of light thrown backward compensating for the greater intensity of the light scattering in the direction of the beam. Also Q and γ are functions of the wave length of the radiation, as well as functions of the sizes and composition of the particles. The quantity $(1 - \gamma)Q^2U$ should be averaged with respect to the wave length. For the case in which a mixture of particle sizes is assumed, the precise equation for g as a function of particle size is easily set up mathematically, but it involves double integrals in λ and σ. The integrals are so difficult to evaluate numerically that a rough average of $(1 - \gamma)Q^2U$ is preferable for the present discussion.

With respect to the hydrogen substratum, the particle will diffuse toward the concentration with a velocity, V_d, given by

$$V_d = K g , \tag{2}$$

where

$$K = \frac{K_0 m_d}{\sigma^2 n_H m_H V_H} . \tag{3}$$

Here the subscript H refers to hydrogen atoms, V_H being the root-mean-square velocity. The quantity K_0 is a dimensionless factor.

As Strömgren[5] has demonstrated, hydrogen will be completely ionized in regions of space near the hotter stars but will be practically neutral in regions away from them. The dimensionless coefficient, K_0, is of the order of unity for neutral hydrogen atoms but depends somewhat upon the precise nature of the collisions of the atoms with the dust particles. The value of $K_0 = 2/\pi$, given by Spitzer, will be adopted. In regions of ionized hydrogen, $K_0 = (3\sqrt{6})/(4\sqrt{\pi}32.9\gamma_e^2)$, where γ_e is a number that measures the negative voltage of the dust particles. Spitzer shows that $\gamma_e = 2.51$ in average regions of ionized hydrogen. Hence $K_0 = 5 \times 10^{-3}$ for these regions. The electrons attached to the particles increase the effective collisional areas for protons so greatly that in regions of ionized hydrogen the velocities of diffusion for dust particles are reduced by a factor of 100 as compared to the velocities in regions of neutral hydrogen.

Equations (1) and (2) show that the velocity of a particle toward the concentration will vary inversely as the square of the distance from the center, or inversely as the surface area of the sphere concentric with the concentration. Since the space density of the particles outside the concentration is assumed to be constant at the beginning, the density will remain constant with time as the particles diffuse toward the concentration. In a

[5] *Ap. J.*, **89**, 526, 1939.

quiescent medium, therefore, the concentration containing a mass, M, in excess of the original uniform density of interstellar material, will grow at a rate

$$\frac{1}{M}\frac{dM}{dt} = \frac{\pi^2\sigma^4 K n_d (1-\gamma) Q^2 U}{m_d}. \tag{4}$$

Thus the mass of the concentration increases exponentially, with the time, independently of the radial distribution of the particles within the concentration and independently of the radius or change in radius of the concentration. Equation (4) holds as long as the opacity of central cross-section remains moderately small. The mass will increase by a factor of e in a time, τ_r, given by the expression

$$\tau_r = \frac{n_H m_H V_H}{\pi^2\sigma^2 K_0 n_d (1-\gamma) Q^2 U}, \tag{5}$$

where the right member of equation (3) has been substituted for K.

In the determination of τ_r for average regions of the galactic plane, we may adopt a kinetic temperature of 10,000° K for the hydrogen atoms, a density of 1 hydrogen atom per cubic centimeter, Dunham's value of 5.2×10^{-13} erg per cubic centimeter for the radiation density and a general opacity of 1 mag. per kiloparsec. To investigate order-of-magnitude effects we note that $\pi\sigma^2 n_d Q$ represents the general opacity per centimeter if mean values, approximating an average with wave length, are taken for the variables in $(1-\gamma)Q^2U$. Hence in equation (5) only the expression $(1-\gamma)Q$ is now dependent upon particle size.

The quantity Q represents the ratio of the effective scattering area of a particle to its actual area, while γ is the albedo. Schalén,[6] Greenstein,[7] and Henyey and Greenstein[8] have extended the calculations of radiation scattering by small particles, according to the theory presented by Mie. For metallic particles of iron and nickel in the critical range of radii from 0.2×10^{-5} cm to 2.0×10^{-5} cm, the values of Q vary from 0.3 to 4.0, generally remaining above unity. The value of Q tends to increase with the frequency of radiation from λ 10,000 to λ 1,000 and also to increase with particle size. The albedo increases from about 0.03 to 0.5 with increasing particle size, so that the variation of $(1-\gamma)$ acts in a direction to compensate the variation of Q. Although the compensation is not exact, $(1-\gamma)Q$ may be roughly approximated by the numerical value 1.0 over the range of particle sizes above, with allowance for the averaging effect of the variation of the radiation density with wave length.

In regions of ionized hydrogen the value of τ_r becomes 7×10^{10} years. This period of time is much too great to permit any development of a dust concentration into a star, even on a long-time scale. Effects of galactic rotation and disturbances by stars penetrating the concentration would prevent effective growth at such a slow theoretical rate.

In regions of neutral hydrogen $\tau_r = 6 \times 10^8$ years, covering three complete rotations of the galaxy at the sun's distance from the center. Such a slow process appears to be unlikely as a direct means of star formation. The effects of light-pressure and shadowing by dust clouds must certainly be an important factor in the formation and preservation of the great clouds observed near the plane of the galaxy, but the growth of a small isolated cloud in average regions of interstellar space is seen to be very slow and precarious.

Great clouds of obscuring matter, however, are observed to exist. Their opacity indicates that their mean density is sufficient to maintain them gravitationally against the shearing effects of galactic rotation. McCuskey[9] has shown that the central region of the Taurus cloud, with a diameter of the order of 5 pc, has a longitudinal opacity of 5 mag.

[6] *Upsala Medd.*, **64**, 1936; *Upsala Astr. Obs.*, Vol. **1**, No. 2, 1939.

[7] *Harvard Circ.*, No. 422, 1937.

[8] *Ap. J.*, **88**, 580, 1938

[9] *Ap. J.*, **94**, 468, 1941.

Since the central region must be approximately symmetrical in form, this observation suggests that the opacity is of the order of 1 mag. per parsec near the center, a thousand times the opacity of average interstellar regions.

The radiation density in such an obscuring cloud will not be lowered by a great factor. Allowing 2.5 mag. of scattering from edge to center, the radiation loss will be less than $(1 - \gamma) \times 10$, or a factor of 10, as an upper limit for particles of low albedo. Stars imbedded in the cloud will somewhat increase the average radiation density above this lower limit, so that we may adopt the factor 5 as a representative value for average regions near the center of the cloud. The spectroscopic observations by Struve and Elvey[10] fail to indicate bright hydrogen lines in luminous rims of dark nebulae in Taurus and suggest that a hydrogen substratum in this region of space would probably be neutral.

Except for a considerable deviation from isotropy in the radiation field and minor effects from cooling of the hydrogen substratum, we may now apply equation (5) for the rate of growth of a particle concentration in such a large cloud. The deviation from isotropy need not concern us at the moment, as it tends only to produce a net force toward the center of the large cloud, while the cooling of the substratum can increase n_H and decrease V_H only slightly. Adopting $U = 1.0 \times 10^{-13}$ ergs per cubic centimeter and an absorption of 1 mag. per parsec, we find $\tau_r = 1.4 \times 10^6$ years, if the substratum consists of neutral hydrogen. This value of τ_r, however, is so small that it must be corrected for the time required for a particle to be accelerated to the velocity given by equation (2). A simple analysis of the accelerations on the particle shows that, in a time t, V_d will attain the value given in equation (2), corrected by a factor of $1 - \exp(-t/K)$, under a constant acceleration. We allow quite sufficiently for the lag in equation (2) by adding $2K$ to the value of τ_r. Since $K = 2.2 \times 10^6$ years in the problem under consideration, the corrected value of τ_r becomes 6.0×10^6 years.

It is interesting to note that the above value of τ_r is practically a minimum for the given space densities of particles and radiation. If the space density of hydrogen is increased up to a factor of 4, τ_r of equation (5) is increased proportionately, while the time lag from K is reduced proportionately. For still greater densities of hydrogen, τ_r increases. If the density of hydrogen is decreased, the time lag increases, and the material can fall into the concentration only a little more rapidly. The form of equation (4) would be changed, however, for less hydrogen.

The process of growth is here sufficiently rapid that a concentration would grow by a factor of 10^{150} in 10^9 years if equation (4) were valid for high space densities of dust. The exponential growth, however, changes to a linear growth with time as the scattering of light across the concentration increases above approximately 1 mag. The absolute absorption of light will be somewhat less than the scattering opacity because of the $(1 - \gamma)$ factor. A conservative value of the particle density, N_d, at the transition period can then be derived from the equation

$$2\pi r \sigma^2 Q N_d (2.5 \text{ Mod.}) = 1 \text{ mag.}, \tag{6}$$

if the density is assumed to be uniform.

The mass, M_r, of the concentration, is, then,

$$M_r = \frac{2.5 \text{ Mod.} \; 8 m_d r^2}{3 \sigma^2 Q}. \tag{7}$$

For iron particles of radius 10^{-5} cm and $Q = 3$, equation (7) becomes

$$M_r = 5.2 \times 10^{22} (r \text{ a.u.})^2 \text{ gm}, \tag{7a}$$

where (r a.u.) represents r expressed in astronomical units.

[10] *Ap. J.*, **89**, 119, 1939.

An opaque concentration, under the conditions of the derivation of equation (1), will produce an acceleration on an exterior particle given by

$$g_r = \frac{\pi \sigma^2 Q U r^2}{4 m_d R^2} . \tag{8}$$

The particles will diffuse toward the concentration in the same fashion as in the derivation of equation (4); and the rate of increase of the mass of the concentration is given by

$$\frac{dM}{dt} = \pi K (\pi \sigma^2 n_d Q) U r^2 . \tag{9}$$

For the concentration within a large obscuring cloud, as above, equation (9) takes the numerical form

$$\frac{dM}{dt} = 4.5 \times 10^{22} (r \text{ a.u.})^2 \text{ gm } 10^{-6} \text{yr}^{-1} . \tag{9a}$$

This linear growth with time can proceed until the acceleration of gravity on an exterior particle is comparable to the acceleration of radiation pressure. The critical mass, M_{gr}, at which the two accelerations are equal is obtained by equating the gravitational acceleration, GM/R^2, to g_r of equation (8):

$$M_{gr} = \frac{\pi \sigma^2 Q U r^2}{4 m_d G} . \tag{10}$$

The critical mass for the concentration within a large cloud becomes

$$M_{gr} = 2.8 \times 10^{24} (r \text{ a.u.})^2 \text{ gm} . \tag{10a}$$

A comparison of equations (9*a*) and (10*a*) shows that, within about 10^8 years after the cloud has become opaque, the gravitational attraction equals the light-pressure on small particles. Henceforth the gravitational force predominates and draws in not only the small particles but also any larger ones that may be present in the large cloud. The gravitational growth is exponential with time, and, under the assumptions of the present analysis, the time τ_g for a mass increase by a factor e is given by

$$\tau_g = (4 \pi G K n_d m_d)^{-1} . \tag{11}$$

By the nature of the derivation of M_{gr}, τ_g is also identical with the time required for the opaque cloud to increase its mass by M_{gr}, under the action of radiation pressure alone. The time τ_g is clearly a maximum value because the large particles will diffuse more rapidly than the small ones under gravity. In a large cloud, however, the frequency distribution of particle sizes is quite possibly determined by the effects of light-pressure and diffusion, so that an assumption that a considerable fraction of the mass is contained in large particles is unwarranted. In the large cloud under consideration, $\tau_g = 6.0 \times 10^7$ years, neglecting the relatively small time lag in equation (2).

Let us now retrace the growth of a mass equal to that of the sun. If we allow 10^9 years for the growth under gravity alone, we find a growth factor of 10^7. Hence $M_{gr} = 2 \times 10^{26}$ gm, at a time when light-pressure ceased to play an important role. The radius of the concentration was then less than 10 a.u., according to equation (10*a*). An interval of 6×10^7 years carries the concentration back to a state of low opacity, if the radius remained unchanged and the material was uniformly distributed. At that time the mass was 5×10^{24} gm, by equation (7*a*).

A sphere of radius 10 a.u. in an average region of the large dust cloud contains a mass of 1.2×10^{20} gm. If we allow an original concentration of dust with an excess density equal to the average density over this volume, the factor of growth before the cloud be-

came opaque was 4×10^4. Hence, if $\tau_r = 6.0 \times 10^6$ years, an interval of 9.1×10^7 years was required for the first growth under radiation pressure. The total time for the growth of the solar mass is then 1.15×10^9 years.

Most striking in this outlined history of a star's growth is the relatively small mass of the concentration at the time that gravity is assumed to become dominant as a building force. Mars has a mass some three times this value. Would planetary bodies in the large cloud be able to grow by accretion sufficiently rapidly to become stars in a reasonable period of time? If absolutely at rest with respect to the interstellar medium, a planet would grow at the rate given by equation (11), but the introduction of a very small motion will reduce the rate enormously. An upper limit to the rate will be given by the growth of the planetary mass according to the equations of the ordinary two-body problem.[11] A body of radius r and mass M, moving at a velocity v through the cloud of dust particles, will have a collisional radius, σ_p, given by

$$\sigma_p^2 = \frac{2GMr}{v^2} + r^2 . \tag{12}$$

The r^2 term will generally be small compared to the term in r and can be neglected. Hence the growth in mass is exponential with time, the mass increasing by a factor e in a time τ_p, given by

$$\tau_p = v\,(2\pi G m_d n_d r)^{-1} . \tag{13}$$

In our large obscuring cloud the numerical value becomes

$$\tau_p = 5.5 \times 10^8 v\,(r \text{ a.u.})^{-1} \text{ yr} . \tag{13a}$$

If r is of planetary dimensions and the velocity is as great as a few centimeters per second, the rate of growth is negligible in 3×10^9 years. Planetary bodies, therefore, will not grow by accretion at an appreciable rate in the large dust cloud. Even for the postulated prestellar concentration of radius 10 a.u., equation (13*a*) requires that the velocity should not exceed 1 cm/sec^{-1} in order that $\tau_g = 6 \times 10^7$ years. More generally, by comparison of equations (11) and (13), $\tau_g = \tau_p$ if $r = 2\text{K}\,v$. With the assumed value of K for neutral hydrogen,

$$v\,(\text{cm/sec}^{-1}) = 0.11\,(r \text{ a.u.}) . \tag{14}$$

This stipulation of extreme quiescence for the concentration with respect to the interstellar medium and the concomitant quiescence of the medium itself presents the most serious handicap to the process of stellar evolution from interstellar material. Whether the stipulations can be met in an actual obscuring cloud, such as the one in Taurus, it is difficult to ascertain.

We may reasonably postulate a larger radius for the initial concentration, perhaps $r = 1000$ a.u. or more. Such a radius is less than 1 per cent of a parsec, and the concentration would not be likely to be disrupted by a passing star in an interval of 10^9 years. The mass attainable by light-pressure alone would then be of the order of 10^{29} gm by equation (7*a*), if the conditions of quiescence are satisfied. Such a mass would have a good chance of continuing to grow fairly rapidly under the combined forces of light-pressure and gravity, even though its relative velocity might eventually exceed 1 meter per second, as set by equation (14). Gravitational forces within the large cloud would act on the concentration and the interstellar medium in the same manner, but differentially in direction over large volumes. The interstellar medium could be moved with respect to the concentration by the pressure of nonisotropic radiation and also by the shear-

[11] See Eddington, *Internal Constitution of the Stars*, p. 391, 1926.

ing effects of galactic rotation, although the large clouds would have sufficient density ($\rho > 10^{-23}$ gm per cubic centimeter) to be stable against the action of galactic rotation.[12]

If, then, a volume of interstellar material, with radius 10,000 a.u. can become sufficiently quiescent to permit the growth of a concentration some 1000 a.u. in radius, the suggested process of stellar evolution may be considered to show considerable promise. The viscosity of neutral hydrogen, η, is 2.8×10^{-3}, according to Spitzer.[4] In the large cloud the space density of the dust particles amounts to about six times the density of hydrogen. Since equipartition of energy is assumed for the relatively massive particles, they do not contribute to the viscosity. Jeans has shown[13] that inequalities of angular momentum between two points separated by a distance d will be reduced to half in a time, $\rho d^2/\eta$. In the large cloud, for $d = 10{,}000$ a.u., the angular momentum will be halved in 3×10^6 years. Consequently, if the currents are not continuously maintained, the viscosity of the interstellar medium will provide the desired degree of quiescence in a period of time less than 10^9 years.

It is of considerable interest to note that the viscosity of ionized hydrogen is much less than that of neutral hydrogen. Hence regions of ionized hydrogen are not sufficiently viscous to acquire the quiescence necessary for star formation from a concentration of particles. It has already been noted that the diffusion of particles through ionized hydrogen is also too slow to recommend the process in these regions. Radiative viscosity is negligibly small because of the great dilution.

Although viscosity can satisfactorily reduce the motions over a volume of radius approximately 10,000 a.u., the material for a star of the sun's mass must be drawn from a volume of about a parsec in radius. Viscosity cannot damp out large-scale currents over such a volume in 10^9 years; indeed, it can hardly halve them in this time. Furthermore, the shearing of galactic rotation may tend to renew some such currents. In addition, we should expect some currents or rotation in the large dust cloud to maintain it against contraction under its own gravitational field. The densest portion of the Taurus cloud, with diameter 5 pc, must comprise a mass of at least 10 solar masses. The virial theorem[14] requires random motions of the order of 0.1 km/sec.

It is possible, of course, that the large cloud has little, if any, angular momentum. It is located in a region of the galaxy where the linear velocity of rotation decreases with the distance from the galactic center. If the large cloud itself is in the process of contraction and, at the same time, is growing in mass by accretion from the substratum of interstellar dust, a state of zero angular momentum in the cloud can conceivably be maintained. Possibly, too, the dense "F" region observed by McCuskey in the Taurus cloud is in the process of condensing to become a single massive star.

In such a small cross-section of the galactic plane the interstellar medium would possess angular momentum in a sense opposite to that of galactic rotation. During contraction the regions away from the galactic center would increase their linear velocity. Those regions toward the galactic center would decrease their linear velocity. The result would be a decrease in the angular momentum of the cross-section with contraction, until a zero or an opposite rotation was attained. To what extent this process would occur in actuality it is difficult to judge.

Over most of the observable area of the Andromeda nebula, where the linear velocity of rotation is increasing with distance from the center,[15] contraction of the interstellar medium would result in a continued increase of the angular momentum as measured in the region of contraction. Hence a contraction process from the interstellar medium

[12] See Bok, *Harvard Circ.*, No. 384, p. 12, 1934.

[13] *Astronomy and Cosmogony*, p. 269, 1929.

[14] See Smart, *Stellar Dynamics*, p. 310, 1939.

[15] Babcock, *Lick Obs. Bull.*, **19**, 41, 1939.

cannot generally lead to a local cloud with small angular momentum. On the other hand, Babcock's determination of the mass distribution in the Andromeda nebula indicates that the ratio of mass to luminosity increases toward the outer regions. This observation suggests that nonluminous interstellar matter may become relatively more abundant with increasing distance from the center of the nebula. The supergiant (young) stars also are observed to be relatively more abundant in these regions. The direct evidence, therefore, favors an evolutionary connection between the nonluminous matter and the young stars.

Upon the chance motions of a region in the large dust cloud depends largely the eventual history of a concentration growing by accretion under the action of light-pressure and gravity. In a large region of absolute quiescence the material would rapidly settle to the center and, when the mass was sufficiently great, would become a star. Growth would stop when the light-pressure on the dust particles counterbalanced the attraction of gravity. For a star of mass M, total radiation E ergs/sec^{-1}, and surface temperature a few thousand degrees, the light-pressure equals gravity when

$$\frac{E}{M} = \frac{4\,cGm_d}{\sigma^2(1-\gamma)Q}. \tag{15}$$

Setting $(1 - \gamma)Q$ equal to unity for iron particles of radius $\sigma = 10^{-5}$ cm, we find that the gravitational attraction is canceled by the radiation pressure when the star radiates about 2 ergs per gram per second. This rate of energy output corresponds closely to that of the sun. Were the mass-luminosity relation valid for the early stages of a star's evolution, we should expect stars of approximately the sun's mass to be formed in absolutely quiescent regions of space. The application of this relation, however, is purely speculative. Thermonuclear reactions of light-elements, such as lithium, beryllium, and boron, if present, might be expected to provide energy[16], [17] in the early part of a star's life. Energy from pure contraction would also be released. Prediction of the limiting masses produced by accretion is consequently difficult. Lyttleton and Hoyle[18] consider it likely that accretion is also an important factor in the maturer stages of a star's existence.

A certain amount of turbulence in the interstellar medium is essential to the production of a massive star by the proposed process, and probably also to the production of a small star. The prestellar concentration must remain large in the radiation-pressure stage of evolution in order to grow to an appreciable mass (see eq. [7]), and in the gravitational stage in order that a small velocity relative to the medium will not prevent growth. Very small motions in the medium would prevent the concentration from contracting as new material is added. Somewhat more rapid motions would cause it to grow. The balance would be very delicate, and it is difficult to estimate the currents to be expected. Relatively rapid currents could permanently prevent further growth at any stage and could easily disrupt the concentration in the radiation-pressure stage.

We should expect generally, therefore, that the majority of chance concentrations of particles would be destroyed at an early stage. Some would grow to asteroidal or planetary masses before the growth process was terminated, while a few would continue to grow, eventually forming stars. The stipulations of quiescence, however, are so severe that a very small minority of the concentrations could produce stars.

A star, if formed by a condensation of interstellar material, would generally be expected to possess a relatively large amount of angular momentum. The velocity of rotation would, of course, be small and inconspicuous in the early stages of development while the radius was large. If the star later contracts to a small radius with a high temperature, a

[16] Bethe, *Phys. Rev.*, **55,** 434, 1939.

[17] Gamow, *Phys. Rev.*, **55,** 718, 1939.

[18] *Proc. Cambridge Phil. Soc.*, **35,** 592, 1939.

high velocity of rotation might be expected. Rotational instability, in fact, would frequently occur, particularly in early spectral types. Struve's[19] observations of rapid stellar rotation and even instability among the hot stars are of the greatest interest in this connection.

Fission might also be expected to occur at almost any stage in the contraction of the prestellar mass. Double or multiple stars would, therefore, be expected to occur frequently—in harmony with observation. We might also expect, however, that double stars would be frequent among stars of high angular momentum, such as the hot stars of the Pleiades observed by Struve, while, in fact, the contrary situation appears to exist.

Stars formed by concentration of the interstellar material would be expected to occur in clusters rather than singly. The average space density of particles, as was shown above, is too low to permit a sufficiently rapid growth of initial concentration in average regions of the galactic plane. Only within large dust clouds can the process function satisfactorily. These large clouds are comparable to the galactic star clusters in several respects. Both types of object are very highly concentrated to the galactic plane. The denser obscuring clouds are only a few parsecs in diameter, not dissimilar in size to the galactic star clusters.[20] Much larger and more transparent clouds, however, are frequent, as are smaller ones. The masses of the clouds are difficult to estimate with accuracy. Certainly, the denser ones contain a minimum of several solar masses and are probably of the same order of mass as the galactic clusters.

The spatial motions of the clusters and obscuring clouds also appear to be of the same order of magnitude. Miss Hayford[21] finds that the galactic clusters show average random radial velocities of about 9 km per second. The radial velocities of obscuring clouds can only be inferred from indirect evidence. Multiple interstellar absorption lines show a total range in radial velocity of about 30 km per second, according to Mount Wilson observations.[22] We are possibly justified in assuming that dust clouds will show ranges in velocity comparable to those of clouds of interstellar atoms. Wilson and Merrill[23] and Wilson[24] have analyzed the curves of growth of the interstellar sodium and calcium lines. They interpret the observations in terms of kinetic motions of the atoms, about 7.5 km per second for sodium and 22 km per second for calcium. Very high temperatures (50,000° K for sodium and 860,000° for calcium) would be required to account for these motions thermally. Perhaps the velocities represent random motions of smaller volumes in the general interstellar medium. The order of magnitude of the velocities is the same as for the galactic clusters, but the observations await further interpretation.

The possible chemical composition or hydrogen content of stars originating in the proposed manner is a subject of considerable interest but is rather speculative. Kuiper,[25] basing his analysis on a study by Strömgren,[26] has shown that the hydrogen content of stars in a given cluster is probably about constant. Should we expect a uniform hydrogen content for stars originating from an interstellar medium of uniform composition? So long as the concentration remains large, of the order of 1000 a.u., the velocity of escape will never exceed the average velocity of the hydrogen atoms in the substratum. In the radiation-pressure stages of the evolution the concentration will consist almost wholly of particles. The pressure of the gas within the cloud must equal that outside. As the concentration becomes opaque, the kinetic temperature of the gas will drop markedly. At the same time the opacity and reduced ionization within the cloud will decrease the rate of radiation of energy acquired by contraction and by absorption of radiation. Hence the

[19] Abstracts, Inter-American Congress of Astrophysics, 1942, unpublished. *Pop. Astr.* **53,** Nos. 5 and 6, 1945.

[20] Trumpler, *Lick. Obs. Bull.*, **14,** 154, 1930.

[21] *Lick. Obs. Bull.*, **16,** 53, 1932.

[22] Adams, *Ap. J.*, **97,** 105, 1943.

[23] *Ap. J.*, **86,** 129, 1937.

[24] *Ap. J.*, **90,** 427, 1939.

[25] *Ap. J.*, **86,** 176, 1937.

[26] *Zs. f. Ap.*, **7,** 222, 1933.

absolute temperature, as measured by the total energy density, will rise from a few degrees absolute to an increasingly high value as the concentration grows. A real contraction of the hydrogen substratum will occur in the early stages of development. This contraction should be of substantial aid in drawing matter from great distances but should not greatly increase the mass of hydrogen.

The density of hydrogen within the concentration can increase above that of the neighboring space only by the ratio of the temperature outside to that inside. This ratio can hardly exceed a factor of a few hundred times. The total mass of the hydrogen acquired in this fashion will be negligible in terms of stellar masses. The indirect effect of molecule formation may be of greater importance. Solid hydrogen cannot be expected to form so readily within the concentration as in the neighboring regions of space, but we may assume that each nonhydrogen atom (except helium) will combine with at least 1 hydrogen atom. The hydrogen content acquired in this manner is perhaps a lower limit. In the later stages of development the acquisition of hydrogen by the prestellar mass will depend largely upon the radius, mass, and consequent surface gravity. The upper limit of the hydrogen content will equal the hydrogen content of the surrounding interstellar medium.

Since the mass of the star will also depend strongly upon the radius of the concentration in the later stages, we may expect that the hydrogen content within a cluster of stars formed by concentration of the interstellar medium will be fairly accurately a function of the mass of the individual star. A one-dimensional family of stars should result. The main sequence of the Russell-Hertzsprung diagram should therefore be narrow for stars in a cluster and might vary from cluster to cluster, in keeping with observation. Until the mass-luminosity relation for the giant branches of the diagram is better explained and until the detailed steps of stellar evolution are better understood, further prediction of details in the diagram would be purely speculative.

The suggested origin of stars requires that young stars be highly concentrated to the galactic plane and that they generally be associated with obscuring clouds. The extremely luminous O and B stars are highly concentrated in a plane near that of the Milky Way but tend somewhat to avoid the most highly obscured regions. Probably the obscuration itself is responsible for this avoidance.

THE MOTIONS OF THE STARS WITHIN 20 PARSECS OF THE SUN*

GUSTAF STRÖMBERG
Mount Wilson Observatory
Received April 9, 1946

ABSTRACT

The purpose of this investigation is to provide a representative sample of the motions of the stars in the neighborhood of the sun. The three components of the velocities of 444 stars within 20 parsecs from the sun have therefore been computed from their proper motions, radial velocities, and parallaxes.

The constants for the velocity ellipsoids were determined for all the spectral types involved and are referred to the system of galactic co-ordinates. The velocities of the stars were then projected on the "dynamical axes" of the galaxy, the x_1-axis being directed toward galactic longitude 339°, the y_1-axis toward galactic longitude 69°, and the z_1-axis toward the galactic pole. The x_1-axis points approximately toward the center of the galaxy; the y_1-axis is the axis of asymmetry in stellar motions. This asymmetry is very evident among the stars studied.

Attempts were made to establish correlations between the motions of the stars and their masses, the bolometric magnitude M_b being used as a measure of the masses of the stars. For all the velocity components studied a definite correlation was established, although the variation with mass is not very pronounced. The z_1-components, referred to the galactic plane and taken without regard to sign, show a higher speed for the less massive stars than for the more massive. Both the x_1-components and the y_1-components yield definite values for which the mass is a maximum. These values are $x_1 = +5$ and $y_1 = -9$ km/sec, both referred to the sun. Values of $v^2 = (x_1 + 17)^2 + (y_1 + 300)^2 + (z_1 + 7)^2$ were computed and were assumed to represent the velocity of a star relative to the center of the galaxy in a nonrotating system of co-ordinates. These values show a maximum mass for a root-mean-square value of v equal to 295 km/sec. All these effects can be understood on the hypothesis that the more massive a star, the greater is the probability that it moves in an exact circle around the center of the galaxy and that its orbit lies in the galactic plane.

The observed relationship between stellar motions and stellar masses has been interpreted as the effect of internal friction in a prestellar system of gas or dust, in accordance with theories previously advanced.

Many studies of the motions of the stars have been made on the basis both of radial velocities and of proper motions. The stars studied have ordinarily been selected on the basis of apparent brightness, large proper motion, spectral characteristics, or association with particular star systems. Because of the great dispersion in stellar motions and the many established or suspected correlations involved, it is important to find a representative sample of the motions of all the stars in a particular region of the galaxy. Several questions connected with the dynamics of the galaxy and with the causes of the present distribution of stellar velocities would be elucidated if such a sample were available and, in particular, if a definite effect of the masses of the stars involved could be established. The region of the galaxy for which we have the most complete data is, of course, the neighborhood of the sun. The present study aims, therefore, at providing such a sample; it relates to all the stars within a distance of 20 parsecs for which both proper motions and radial velocities are available.

OBSERVATIONAL DATA AND METHODS OF COMPUTATION

The data used in this study were collected by Dr. Ralph E. Wilson some time ago, and I am greatly indebted to him for letting me use his compilation. All those stars for which the weighted mean parallax is equal to or greater than 0".05 were included, except a few for which radial velocities or proper motions had not been determined. The total number of stars available was 444. The proper motions from the *General Catalogue*[1] and for some of the fainter stars from the catalogues of the Cincinnati Observatory[2] were converted into linear tangential velocities. Since the parallaxes are relatively large, the effect

* *Contributions from the Mount Wilson Observatory, Carnegie Institution of Washington*, No. 722.

[1] *Carnegie Inst. Washington, Pub.* 468, 1937. [2] *Pub. Cincinnati Obs.*, No. 18, 1918; No. 20, 1930.

of the errors in the parallaxes could be neglected. Weighted means were formed for the radial velocities taken from all available sources, mainly from Moore's Catalogue.[3] For double stars the velocity of the center of mass was used. The visual absolute magnitudes (M_v) were derived from the apparent magnitudes (m_v), which for the brighter stars were taken from the *H.D. Catalogue*. For double stars the magnitude and the spectral type of the brighter component were used. The visual absolute magnitude was converted into absolute bolometric magnitude (M_b) with the aid of data determined by Pettit and Nicholson.[4] The actual reduction (ΔM) used in this paper is given in Table 1. It is well known that the bolometric magnitude of a star is correlated with its mass. The latest determination of this mass-luminosity relation is that by G. P. Kuiper.[5] The values of the geometric mean mass (m) in Table 2 in terms of the sun's mass have been read off from his diagram.

TABLE 1

REDUCTIONS TO BOLOMETRIC MAGNITUDE

Sp.	ΔM	Sp.	ΔM	Sp.	ΔM	Sp.	ΔM
A0	−0.3	dG5–dG9	0.0	dM0	−1.3	gG3	−0.1
A2	−0.1	dK0	−0.1	dM3	−1.9	gK1	−0.4
A3–A4	0.0	dK3	−0.4	dM5	−2.5	gK5	−1.1
A5–dG4	+0.1	dK6	−0.7	dM6	−2.8	gM2	−1.8

TABLE 2

RELATIONSHIP BETWEEN BOLOMETRIC ABSOLUTE MAGNITUDE AND MASS

$\bar{M}_b$	$\underline{m}$	$\bar{M}_b$	$\underline{m}$	$\bar{M}_b$	$\underline{m}$	$\bar{M}_b$	$\underline{m}$
+10	0.10	+7	0.56	+4	1.20	+1	2.40
9	0.26	6	0.76	3	1.48	0	3.2
+ 8	0.40	+5	0.96	+2	1.86	−1	4.3

Since the relationship between bolometric magnitude and mass is statistical and since there still may be systematic errors in the mass-luminosity curve, the mean bolometric magnitude has been retained as the principal measure of the mean mass of the stars in the various groups.

The formulae for computing the velocity components, relative to the sun, of a star in right ascension α and declination δ are given below.

$$\left.\begin{aligned} \xi &= V\cos\alpha\cos\delta - \frac{k}{\pi}(\mu_1\sin\alpha + \mu_2\cos\alpha\sin\delta), \\ \eta &= V\sin\alpha\cos\delta + \frac{k}{\pi}(\mu_1\cos\alpha - \mu_2\sin\alpha\sin\delta), \\ \zeta &= V\sin\delta + \frac{k}{\pi}\mu_2\cos\delta . \end{aligned}\right\} \qquad (1)$$

Here V is the radial velocity of the star; $\mu_1 = \mu_\alpha\cos\delta$ and $\mu_2 = \mu_\delta$ are the components of its proper motion in the direction of increasing α and δ, respectively, expressed in

[3] *Pub. Lick Obs.*, Vol. **18**, 1932.

[4] *Mt. W. Contr.*, No. 369; *Ap. J.*, **68**, 279, 1928.

[5] *Ap. J.*, **88**, 489, 1938.

seconds of arc per year; π is the parallax; and k is the factor 4.74 km year/sec. The ξ-axis is directed toward the vernal equinox (1900.0), the η-axis is in the equator and in a right ascension equal to 90°, and the ζ-axis is directed toward the north celestial pole.

The equatorial velocity components were converted into galactic components with the aid of the following formulae:

$$\left.\begin{aligned} x &= -\xi \sin A + \eta \cos A \ , \\ y &= -\xi \cos A \sin D - \eta \sin A \sin D + \zeta \cos D \ , \\ z &= +\xi \cos A \cos D + \eta \sin A \cos D + \zeta \sin D \ . \end{aligned}\right\} \tag{2}$$

Here A and D are the right ascension and declination of the north galactic pole. The x- and y-axes are in the galactic plane in galactic longitude 0° and 90°, respectively. The z-axis is directed toward the north pole of the galaxy. Using the standard values $A = 190°$ and $D = +28°$ (1900.0), we find

$$\left.\begin{aligned} x &= +0.1736\xi - 0.9848\eta \ , \\ y &= +0.4624\xi + 0.0815\eta + 0.8829\zeta \ , \\ z &= -0.8695\xi - 0.1533\eta + 0.4695\zeta \ . \end{aligned}\right\} \tag{3}$$

Finally, the velocities were projected on what we may call the "dynamical axes of the galaxy." The x_1-axis in this system of co-ordinates is directed toward the mass center of the galaxy; the y_1-axis is also in the galactic plane and perpendicular to the x_1-axis; and the z_1-axis is directed toward the north pole of the galaxy. The y_1-axis coincides, at least approximately, with what I have called "the axis of asymmetry in stellar motions." The galactic longitude of the center of the galaxy is known to be in the neighborhood of 330°, and the axis of asymmetry has a longitude between 60° and 70°. The longitude of the x_1-axis has been made to coincide with that of the major axis of the velocity ellipsoid when all the stars are combined. The value found for this longitude, L, is 339°, as seen in Table 5. We have, then,

$$\left.\begin{aligned} x_1 &= x \cos L + y \sin L \ , \\ y_1 &= -x \sin L + y \cos L \ , \\ z_1 &= z \ . \end{aligned}\right\} \tag{4}$$

It lies in the nature of things that the orientation of the dynamical axes in the galactic plane cannot be determined with high accuracy. An uncertainty of several degrees is, however, of no great importance in the present study.

RESULTS OF COMPUTATIONS

After the stars were grouped according to spectral type, the velocity ellipsoids were computed from the galactic-velocity components. The stars actually used in this computation numbered 419. Only 16 giants and subgiants were found in the volume with a radius of 20 parsecs; these are listed in Table 3. Their apparent and absolute visual magnitudes are given, as well as their galactic-velocity components in kilometers per second.

In Table 4 are listed the stars which have unusual velocities in any one of the galactic co-ordinates. These stars, together with most of the stars in Table 3, were excluded, although the few giant stars in the list do not exhibit any marked peculiarities in their motion when compared with the dwarf stars in general. Only one isolated white dwarf (Cin. 58) was included in the list. It is of interest to note that this star and another faint F star (Cin. 706) have abnormally large velocities perpendicular to the galactic plane.

Table 5 shows the constants for the velocity ellipsoids. The galactic components of

the group motion are indicated by the symbols $\bar{x}$, $\bar{y}$, and $\bar{z}$. The opposite velocity vector is the sun's motion relative to the particular group and is given in equatorial co-ordinates. The velocity dispersions along the principal axes of the velocity ellipsoids are denoted by σ_1, σ_2, and σ_3. The first represents the maximum dispersion, and the last the dispersion along the principal axis which has the highest galactic latitude. The directions of the principal axes are given in galactic co-ordinates.

TABLE 3

GIANTS AND SUBGIANTS

Star	Sp.	m_v	M_v	x	y	z
GC 158	G7	3.9	2.6	−13	− 11	+11
865	G7	2.2	1.0	−19	+ 6	−12
2339	G4	3.7	2.7	−51	+ 16	+11
2538	K1	2.2	0.8	−14	− 21	+ 4
4517	G9	3.8	2.8	−36	− 38	−24
5194	K5	4.4	3.2	0	− 25	−19
5605	K8	1.1	0.1	−50	+ 14	−22
6427	G1	0.2	−0.4	−38	+ 7	− 8
10438	G9	1.2	1.2	−11	+ 12	−24
18666	M6	4.4	3.1	+ 5	− 39	+15
19033	G9	2.3	1.1	−48	− 28	−23
19242	K0	0.2	0.2	−39	−103	− 2
22502	G4	3.6	2.1	+12	− 3	+ 2
25046	G8	3.4	1.9	+ 1	− 82	+15
30289	K0	3.7	2.7	−10	− 35	−13
32875	K1	3.4	2.4	− 1	− 44	0

TABLE 4

STARS WITH UNUSUAL VELOCITIES

Star	Sp.	m_v	M_v	x	y	z
GC:						
1360	G4	5.3	5.9	−116	−107	− 32
6369	K2	8.5	10.6	−137	−248	− 54
15183	M2	7.6	10.5	+ 9	− 71	− 76
16253	G5	6.5	6.6	+157	−297	− 16
22728	G9	6.8	5.7	+ 9	−138	+ 5
Cin. 18:						
58	F3	12.3	14.3	− 32	+ 86	−228
153	M3	10.5	9.8	+103	− 83	−107
217	K5	11.0	9.7	+ 1	−203	− 19
462	M6	12.5	13.4	+ 23	−161	− 51
706	F2	8.8	7.3	− 14	−111	+123
1136	M4	11.2	11.3	− 48	+ 9	− 80

Figure 1 shows the position of the intersection of the velocity ellipsoids with the galactic plane. Figure 2 shows the intersections of the velocity ellipsoids with a plane perpendicular to the galactic plane and through the axis of asymmetry, that is, through the axis y_1 in galactic longitude 69°.

The distribution of the individual velocity vectors referred to the sun as origin and projected on the galactic plane is shown in Figure 3. The distributions of the dynamical

TABLE 5

VELOCITY ELLIPSOIDS

Quantity	Spectrum and Number of Stars					
	A(26)	F(83)	G(104)	K(108)	M(98)	All (419)
x (km/sec)	− 10.0	− 14.8	− 30.9	− 24.6	− 21.5	− 22.6
y (km/sec)	− 2.0	− 3.6	− 11.1	− 15.1	− 16.2	− 11.3
z (km/sec)	− 7.8	− 6.2	− 7.9	− 5.1	− 7.7	− 6.8
V_0 (km/sec)	12.9	16.5	33.8	29.3	28.0	26.2
α_0 (degrees)	249.1	265.7	276.7	286.1	282.0	278.2
δ_0 (degrees)	+ 24.9	+ 21.8	+ 23.7	+ 32.4	+ 39.7	+ 30.2
σ_1 (km/sec)	17.2	25.1	39.9	45.5	48.4	40.4
L_1 (degrees)	350.4	334.2	346.7	338.5	330.8	338.9
B_1 (degrees)	+ 8.0	− 6.3	− 5.1	− 4.3	+ 0.9	− 2.7
σ_2 (km/sec)	5.6	16.2	24.4	24.8	28.0	24.4
L_2 (degrees)	77.8	69.1	74.5	68.5	60.6	58.8
B_2 (degrees)	− 17.3	− 37.4	+ 21.4	− 2.2	− 10.0	+ 1.3
σ_3 (km/sec)	8.2	18.9	18.9	17.5	18.9	18.3
L_3 (degrees)	104.9	56.2	269.5	5.7	65.4	312.6
B_3 (degrees)	+ 71.4	+ 51.8	+ 67.9	+ 85.2	+ 80.0	+ 87.0

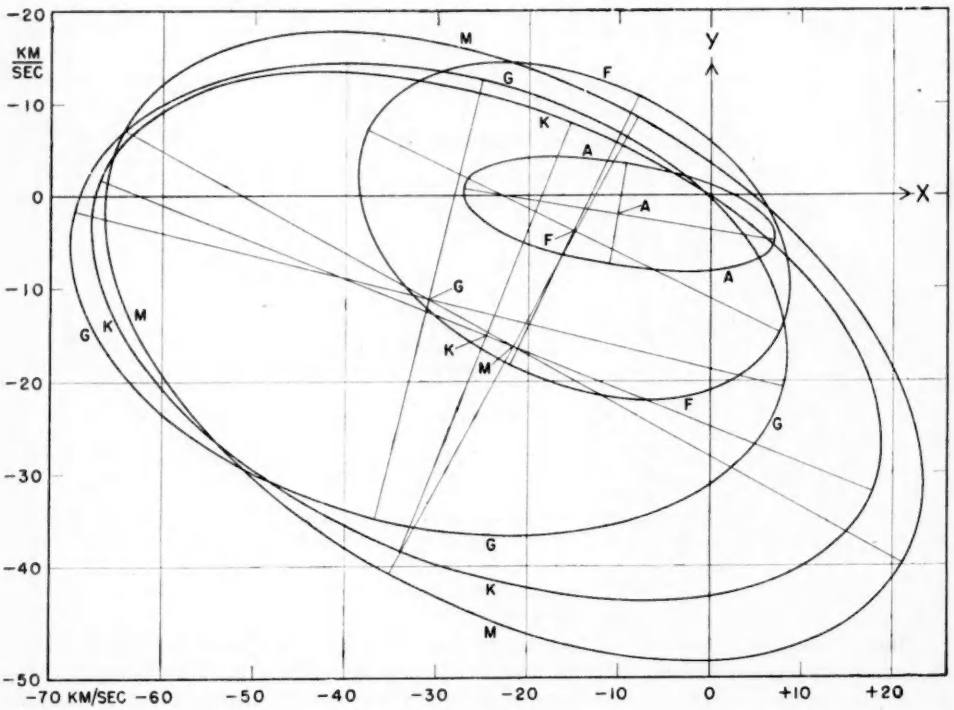

FIG. 1.—Projections of the velocity ellipsoids for different spectral types on the galactic plane. The sun is at the origin, and the x-axis is in galactic longitude 0°.

velocity components, when all the types are combined, are given in Table 6 and are shown graphically in Figure 4. The distribution in the normal error-curves based on the constants in Table 5 and projected on the dynamical axes is given in tabular and graphic forms.

The results of this analysis agree closely with those derived from the motions of the stars in general. There is a steady increase in velocity dispersion as we proceed along the main sequence to stars of later spectral types, and at the same time there is an increase in the numerical value of the group motion. The last phenomenon is a result of the now well-established asymmetry in stellar motions. This asymmetry is clearly shown in Figure 3

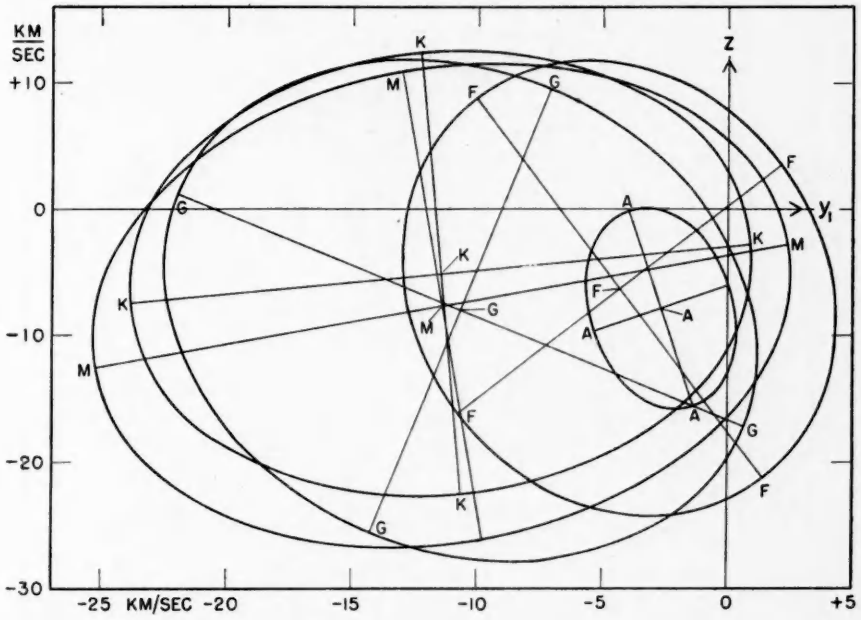

FIG. 2.—The velocity ellipsoids for different spectral types projected on a plane in galactic longitude 69° and perpendicular to the galactic plane. The sun is at the origin.

as a wide scattering of high-velocity stars in the third quadrant and the complete absence of stars with a velocity, relative to the sun, greater than 100 km/sec in the first quadrant. The asymmetry is brought to light in the most striking way in the distribution of velocities projected on the axis of asymmetry (the y_1-axis) when all the stars are combined. As shown in Table 6 and in Figure 4, the distribution of the y_1-components is exceedingly asymmetric and can by no means be represented by a normal error-curve.

STELLAR MOTIONS AND MASSES

The asymmetry in the motions of the stars in our region of the galaxy has previously been established for practically all types of stars. References to its significance in the dynamics of the galaxy and in the theory of the formation of the galaxy will be given later. In order to give a dynamical interpretation of stellar motions it is essential to ascertain whether and to what extent they can be correlated with the masses of the stars in-

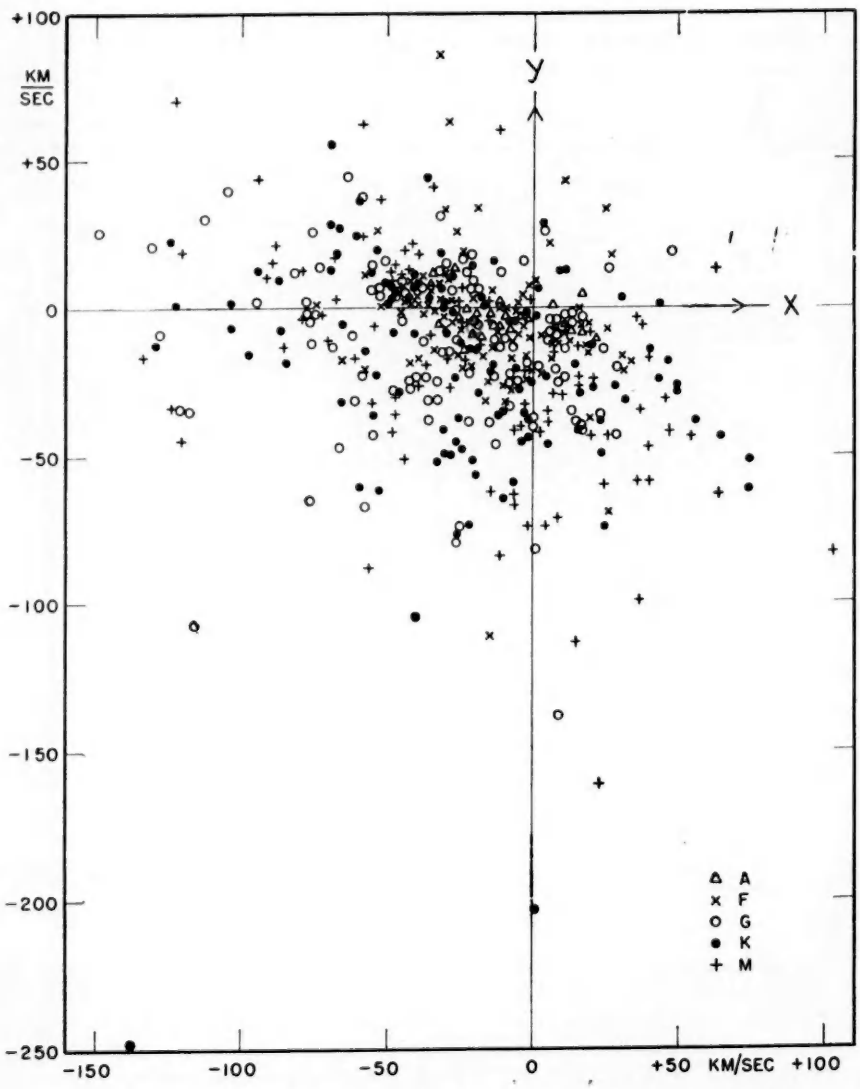

FIG. 3.—The velocities of the stars projected on the galactic plane. The sun is at the origin, and a line from the origin to a particular point indicates the velocity vector of a star projected on the galactic plane and referred to the sun.

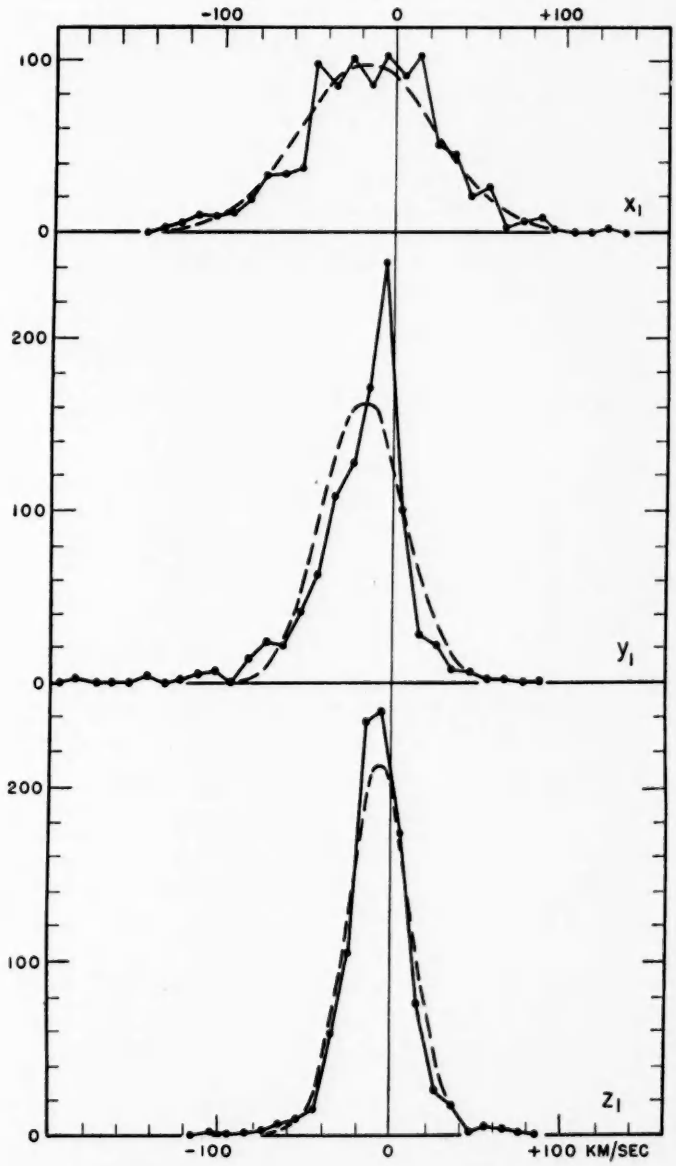

FIG. 4.—Distribution-curves for the velocities projected on the dynamical axes. The x_1-axis is in galactic longitude 339° and points approximately toward the center of the galaxy; the y_1-axis is in galactic longitude 69° and coincides with the axis of asymmetry in stellar motions. The z_1-axis points toward the north pole of the galaxy. The dashed curves are normal error-curves.

TABLE 6

Distribution of Velocities

Velocity (Km/Sec)	A						F						G						K						M						All					
	$F(x_1)$		$F(y_1)$		$F(z_1)$		$F(x_1)$		$F(y_1)$		$F(z_1)$		$F(x_1)$		$F(y_1)$		$F(z_1)$		$F(x_1)$		$F(y_1)$		$F(z_1)$		$F(x_1)$		$F(y_1)$		$F(z_1)$		$F(x_1)$		$F(y_1)$		$F(z_1)$	
	O	C	O	C	O	C	O	C	O	C	O	C	O	C	O	C	O	C	O	C	O	C	O	C	O	C	O	C	O	C	O	C	O	C	O	C
Between																																				
$-\infty$ and -100	....	....	....	....	....	....	....	....	12	....	11	....	45	29	36	1	....	....	27	35	26	1	....	....	49	38	29	3	10	....	29	20	25	....	4	....
-100 -90	....	....	....	....	....	....	....	1	0	....	0	....	9	21	0	1	....	....	26	20	0	2	....	....	10	20	0	6	0	....	11	15	0	2	0	....
-90 -80	....	....	....	....	....	....	....	2	0	....	0	....	22	32	27	5	....	....	26	30	9	8	....	....	29	28	19	13	5	....	19	25	14	4	1	....
-80 -70	....	....	....	....	....	....	6	8	0	....	0	....	49	45	40	15	....	1	39	40	35	18	....	....	38	38	19	26	14	1	33	35	24	11	3	....
-70 -60	....	1	....	....	....	....	12	18	0	1	12	1	36	61	9	32	18	3	35	51	9	38	....	1	58	48	72	47	0	2	34	49	21	27	7	2
-60 -50	....	6	....	....	....	....	46	38	12	7	0	6	63	76	22	63	0	13	35	62	110	70	9	5	14	58	19	73	29	11	37	64	41	54	9	7
-50 -40	....	24	....	....	....	....	116	69	6	27	12	23	58	88	89	102	27	37	114	73	79	107	9	19	134	68	77	104	14	33	98	78	62	91	15	26
-40 -30	107	71	....	....	36	4	128	107	52	73	35	63	71	98	139	140	71	80	61	82	114	142	66	56	82	76	144	126	63	77	85	89	108	130	59	68
-30 -20	143	148	36	12	18	66	93	140	145	147	70	129	156	100	134	162	138	138	66	87	140	159	74	120	77	80	111	140	159	138	101	97	126	156	106	133
-20 -10	196	219	196	228	239	325	81	159	227	213	279	195	80	98	161	160	210	186	88	87	140	152	259	191	58	83	159	135	187	191	85	99	170	161	239	195
-10 0	303	229	696	556	500	432	180	151	308	222	233	218	76	88	192	131	214	196	105	85	189	124	246	221	10	81	183	115	221	202	103	94	243	140	245	213
0 $+10$	36	169	54	195	71	157	128	124	157	169	221	181	98	76	89	91	152	161	114	77	70	86	210	189	43	77	106	87	154	166	91	85	99	103	176	176
$+10$ $+20$	179	89	18	9	36	16	105	87	12	92	75	111	116	61	31	54	125	104	61	68	53	51	44	119	115	68	14	58	72	103	104	72	28	64	77	108
$+20$ $+30$	36	33	....	....	....	....	47	52	23	36	6	51	49	45	22	26	9	52	48	57	26	25	48	55	62	60	19	35	43	51	51	57	21	34	26	49
$+30$ $+40$	....	9	....	....	....	....	46	26	6	11	23	17	36	32	9	12	18	21	35	44	....	11	17	18	77	49	19	18	19	18	45	43	8	15	18	18
$+40$ $+50$	....	2	....	....	....	....	6	12	29	2	0	4	9	21	....	3	9	6	44	34	....	4	0	5	29	38	0	9	0	6	21	30	6	6	2	4
$+50$ $+60$	....	....	....	....	....	....	6	4	0	....	0	1	9	13	....	2	9	2	31	25	....	2	9	1	67	29	10	3	0	1	27	20	2	1	5	1
$+60$ $+70$	....	....	....	....	....	....	....	2	11	....	0	....	0	8	....	....	....	....	0	16	....	....	9	....	14	22	....	1	10	....	3	13	2	1	4	....
$+70$ $+\infty$	....	....	....	....	....	....	....	....	....	....	23	....	18	8	....	....	....	....	45	27	....	....	....	....	34	39	....	1	....	....	23	15	....	....	4	....

volved. The absolute bolometric magnitudes (M_b) were therefore derived, as mentioned before, and the stars were grouped according to certain characteristics of their motion, the mean bolometric magnitude being derived for each group.

First, the distribution of the bolometric magnitudes for each spectral type was determined. The results are given in Table 7 as percentages. The first grouping was made to ascertain whether or not there was any tendency toward equipartition of kinetic

TABLE 7

DISTRIBUTION OF BOLOMETRIC MAGNITUDES

M_b	A	F	G	K	M	All
Between						
− 1.0 and 0.0	.....	.....	1	.....	.....	0.2
0.0 + 1.0	14	.....	0	2	1	1.7
+ 1.0 + 2.0	21	1	3	0	0	2.5
+ 2.0 + 3.0	50	14	4	2	0	7.3
+ 3.0 + 4.0	4	49	7	2	0	12.0
+ 4.0 + 5.0	7	29	39	3	0	16.6
+ 5.0 + 6.0	4	5	36	30	1	17.9
+ 6.0 + 7.0	.....	0	8	39	24	17.8
+ 7.0 + 8.0	.....	1	2	17	35	13.3
+ 8.0 + 9.0	.....	0	.....	3	24	6.3
+ 9.0 +10.0	.....	0	.....	1	9	2.4
+10.0 +11.0	.....	0	.....	1	3	1.0
+11.0 +12.0	.....	0	.....	.....	3	0.8
+12.0 +13.0	.....	0	.....	.....	.....	0.0
+13.0 +14.0	.....	0	.....	.....	.....	0.0
+14.0 +15.0	.....	1	.....	.....	.....	0.2
Reduced numbers..	100	100	100	100	100	100.0
Actual numbers....	28	86	112	114	104	444

TABLE 8

CORRELATION BETWEEN BOLOMETRIC MAGNITUDE AND z_2

M_b	No.	$\bar{M}_b$	$\bar{z}_2$	z_2	No.	$\bar{z}_2$	$\bar{M}_b$
≤3.9	101	2.74	10.7	≤7	147	3.4	5.20
4.0 to 5.9	155	4.97	15.0	8 to 13	116	9.5	5.46
6.0 to 7.5	119	6.73	14.1	14 to 20	78	16.0	5.70
≥7.6	69	8.71	21.4	≥21	103	36.1	5.89
All	444	5.52	14.8	All	444	14.8	5.52

energy. The kinetic energy can most readily be studied in the velocity component perpendicular to the galaxy because in this component we have a well-defined origin to which the velocities can be referred. As reference frame I used a plane relative to which the sun has a velocity of 7 km/sec toward the north galactic pole, in accordance with the value of $\bar{z}$ in Table 5. Values of $z_2 = z + 7$ were then computed, and the stars were grouped according to M_b and also according to the values of z_2, with positive and negative values combined. The values thus found are given in Table 8, where all the spectral types are combined.

The data in Table 8 are shown in Figure 5, where the two regression lines are drawn. The coefficient of correlation between M_b and z_2 is equal to +0.24. The correlation between mass and motion perpendicular to the galactic plane is therefore rather small, although there can be no doubt that a positive correlation exists; hence there is only a very slight tendency toward equipartition of energy in this velocity component.

The stars were also grouped according to the size of the velocity components along the x_1-axis, which is supposed to be directed toward the center of mass of the galaxy as a whole. Among the A stars we have long had evidence of group motions along this axis,

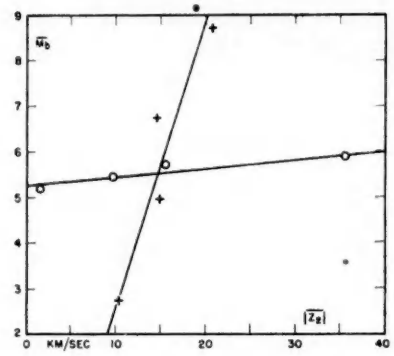

FIG. 5.—Correlation between bolometric magnitudes and the absolute values of $z_2 = z_1 + 7$. The two regression lines are shown.

TABLE 9

CORRELATION BETWEEN VELOCITIES PROJECTED ON THE x_1-AXIS AND BOLOMETRIC MAGNITUDES

x_1	No.	$\bar{x}_1$	$\bar{M}_b$	x_1	No.	$\bar{x}_1$	$\bar{M}_b$
<-46	87	−84.4	6.14	$>+13$	103	+37.9	6.18
−46 to −17	126	−31.4	5.25				
−16 to +13	128	− 1.2	4.83	All	444	−15.0	5.52

and the main groups can be identified with the generalized Taurus group and the generalized Ursa Major group. These groups are now left as the only direct evidence of Kapteyn's two star streams, the rest of these streams being engulfed in the large velocity dispersion in the x_1-axis. In the present small sample of A stars the existence of the two moving groups of stars is indicated by a minimum in the frequency of the x_1-components at +5 km/sec. It also explains the abnormally high dispersion in the x_1-components of the velocities of the A stars.

Table 9 gives the mean bolometric absolute magnitudes for the stars when grouped according to velocities projected on the x_1-axis.

The data indicate a definite maximum mass for x_1 at about +5 km/sec (Fig. 6). Such a maximum mass is to be expected on the theory, discussed later, according to which a maximum should occur for a value of the x_1-component of the velocity of a star moving in an exactly circular orbit around the center of the galaxy.

The result of a grouping of the stars according to the value of the velocity components along the y_1-axis is shown in Table 10. The data show a maximum mass for y_1 at about -9 km/sec (Fig. 7), which, according to theory, represents the difference between an exact circular motion around the center of the galaxy and that of the sun along the y_1-axis.

The sun's velocity relative to the center of the galaxy is about 300 km/sec in the approximate direction of the y_1-axis here used. The best value available at present is prob-

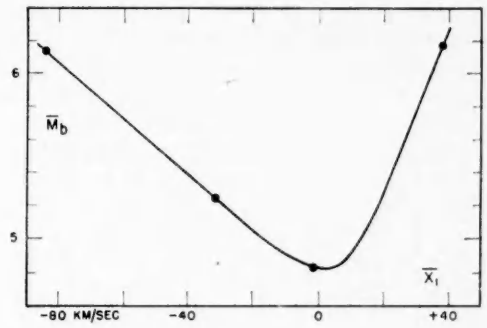

FIG. 6.—Mean bolometric magnitudes for stars grouped according to the values of x_1

TABLE 10

CORRELATION BETWEEN VELOCITIES PROJECTED ON THE y_1-AXIS AND BOLOMETRIC MAGNITUDES

y_1	No.	$\bar{y}_1$	$\bar{M}_b$	y_1	No.	$\bar{y}_1$	$\bar{M}_b$
<-40	81	-69.3	6.23	>0	78	$+12.3$	5.75
-40 to -20	100	-29.8	5.68				
-19 to 0	185	-10.0	5.02	All	444	-21.3	5.52

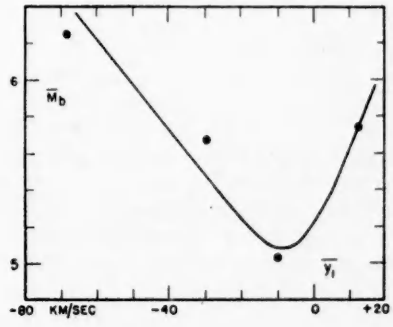

FIG. 7.—Mean bolometric magnitudes for stars grouped according to the values of y_1

ably that determined by A. H. Joy[6] from the radial velocities of the Cepheid variables. He found a value of 296 km/sec in a longitude assumed to be 55°, which is sufficiently close to the value of 69° used in this study.

I have added exactly 300 km/sec to the y_1-components of the stellar velocities when referred to the sun, in order to refer them to a nonrotating reference frame. By adding appropriate corrections, the x_1- and the z_1-components have been corrected for the deviation of the sun's orbit from an exact circle in the galactic plane. For each star I have computed a "galactic velocity," v, defined by the equation

$$v^2 = (x_1 + 17)^2 + (y_1 + 300)^2 + (z_1 + 7)^2 .$$

The stars were then grouped according to the values of v and the mean bolometric magnitudes determined. The results are given in Table 11. The results show a definite mini-

TABLE 11

CORRELATION BETWEEN GALACTIC VELOCITIES AND BOLOMETRIC MAGNITUDES

$v^2/100$	No.	$\bar{v}^2/100$	$\sqrt{\bar{v}^2}$	$\bar{M}_b$	$v^2/100$	No.	$\bar{v}^2/100$	$\sqrt{\bar{v}^2}$	$\bar{M}_b$
<700	84	586.4	242.2	6.22	>900	98	985.4	313.9	5.77
700–800	102	753.0	274.4	5.44					
800–900	160	854.8	292.4	5.04	All	444	809.5	284.5	5.52

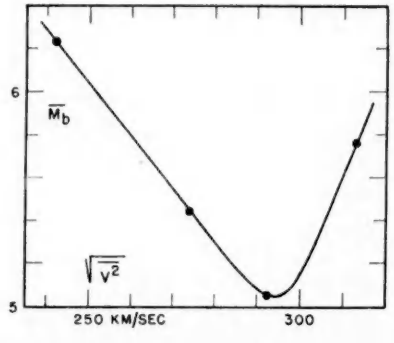

FIG. 8.—Mean bolometric magnitudes for stars grouped according to $v^2 = (x_1 + 17)^2 + (y_1 + 300)^2 + (z_1 + 7)^2$.

mum of $M_b = 5.03$ for a root-mean-square velocity of 295 km/sec, differing by 5 km/sec from the orbital velocity of the sun (Fig. 8). It should be noted that this cannot be regarded as a method of determining the circular velocity of the galaxy, which must be determined by other means. It gives, however, some data from which to study the distribution of the kinetic energy of the stars in our neighborhood.

In the correlation between mass and the velocity components, x_1 and y_1, and the galactic velocity, v, it is not practical to group the stars according to the bolometric magnitude, since the regression lines given have a minimum value of M_b for a definite value of the velocity variable. In a grouping according to M_b, values both greater and smaller than this value of the velocity variable would be mixed together, and practically the whole effect would be obliterated.

[6] *Mt. W. Contr.*, No. 607; *Ap. J.*, **89**, 356, 1939.

THE INTERPRETATION OF STELLAR MOTIONS

When the asymmetry in stellar motions was first discovered, the writer[7] showed that it could be explained formally as the combined effect of two simultaneously acting velocity restrictions, the combined effect being represented as a product of two symmetrical velocity distributions with greatly differing centers. The sun had a very small velocity, about 10 km/sec, relative to the center of one of these distributions, and a very high one, at least 250 km/sec, relative to the other center. Since the sun's velocity relative to the globular clusters is about 300 km/sec, it was natural to assume that the second restriction represented a velocity distribution centered in the galactic system as a whole. This restriction was clearly manifested by an apparently complete absence of stars of velocities greater than that of escape from the galaxy, that is, by an absence of interlopers from other galaxies. The first restriction was originally interpreted by J. H. Oort[8] as a similar effect in the local star system, for which the escape velocity was about 65 km/sec. B. Lindblad[9] found that a unitary interpretation was possible. He interpreted the asymmetry as due to a predominance of circular motions and to the fact that the frequency of stellar orbits decreases with an increase in their eccentricity. This type of distribution can be expected from kinematic considerations alone, since for circles the variation in the size of the major axis and the variation in the direction of the line of apsides disappear. A decrease in the eccentricity of the orbit of the stars with a decrease in their masses would indicate that there are now, or have been in the past, forces tending to round out the orbits of the stars about the center of the galaxy with all the stars moving in the *same direction*.

At the present time that part of the galaxy which we can survey consists mostly of well-separated stars. There are interstellar clouds, to be sure, but their effect on stellar motions is relatively small, except possibly for large stars of small density. In general, the stars are very small relative to their mutual separation, and therefore the effect of stellar encounters, and even more of actual stellar collisions, is not sufficient to produce group motions or an equipartition of energy. We know that groups of stars exist having almost exactly identical motions, and this can be explained only by assuming that the component stars have been formed from a larger system of nearly uniform mass motion.

The writer[10] has attempted to show, by a method that was probably too simplified, that the observed motions of the stars could to some extent be explained on the assumption that in the prestellar stage the motions in the matter from which the stars were formed had, to a certain extent, become systematic and had a relatively small velocity gradient. The end-result of the effect of the internal friction—which itself decreases with time but never completely disappears—was found to be a motion with uniform speed, that is, $DT/Dt = 0$, where T is the kinetic energy per unit mass and t is the time, and the differentiation is taken along the path of a moving element. The corresponding rate of change, DG/Dt, of the gravitational energy was then found to be equal to $-\varphi$, where φ is the dissipation function, which, as used in this connection, is the rate, per unit mass, at which mechanical energy is converted into heat. Since φ is always positive and approaches asymptotically a finite limit greater than zero,[11] the gravitational energy of a fluid element diminishes steadily, and the whole system therefore contracts, generally and locally. The stars gradually formed as condensations from this system would therefore, after the friction in the interstellar matter had practically disappeared, predomi-

[7] *Mt. W. Contr.*, Nos. 275 and 293; *Ap. J.*, **59**, 228, 1924, and **61**, 363, 1925.

[8] *B.A.N.*, **3**, 275, 1927; **4**, 269, 1928.

[9] *Ark. f. Mat., Astr. och Fysik*, **19A**, 27, 35, 1925, and subsequent publications. A summary is given in "Die Milchstrasse," *Handb. d. Ap.*, **5**, Part 2, 1033–1076, 1933.

[10] *Mt. W. Contr.*, Nos. 492 and 503; *Ap. J.*, **79**, 460, and **80**, 327, 1934.

[11] D. J. Korteweg, *Phil. Mag.*, **16**, 112, 1883; Rayleigh, *Phil. Mag.*, **36**, 354, 1893.

nantly move in orbits of nearly uniform speed and of approximately constant gravitational energy, and all in the same direction. In a system where there is one predominant center of attraction and where the system has an angular momentum, supposed to be produced by tidal effects sufficient to produce a definite plane of maximum density, the stars formed *after* the systematic motions had been fully established could be expected to move in circles in the plane of maximum stellar population. Since such stars were formed from a medium with relatively small internal motions and with relatively high density, they could attain great mass. Circular motions are indicated by a vanishing velocity dispersion in a particular part of the galaxy, although group motions would produce a similar effect. We should therefore expect to find a correlation between the masses of the stars and their velocity dispersion and also a correlation of the masses with the motions along the x_1- and the y_1-axes of the same type as actually found here for the stars studied. A direct correlation between the mass of a star and the time of its formation cannot be made, since we have no direct information concerning this time. The existence of such an additional correlation would, to some extent, at least, account for the lack of any detailed correlation between the mass of a star and its present motion.

The theory of the motions in a compressible, viscous fluid as outlined in *Mt. W. Contr.*, Nos. 275 and 293[7] has been criticized by T. Gustafson and H. Nordström[12] on the ground that it cannot have general validity. To the writer it seems that the investigators mentioned have not realized the specific nature of the equations. These equations were never intended to represent general equations of motion and are valid only when the internal friction is sufficiently large and has acted for a sufficiently long time to establish a stable form of motion *independent of the initial conditions*. It can be shown that the assumptions I have made are equivalent to making that term in Lagrange's equations which varies explicitly with time disappear at all points. The authors apply the theorem to the free fall of a stream of water and show that the theorem does not hold in this case; but this example represents a motion without effective friction and dependent upon the initial level of the water; obviously, the theorem cannot hold then. If, however, the jet of water is falling in a viscous fluid, like air, a constant end-velocity is reached, independent of the height from which the water drops are falling, and the loss in potential energy is balanced, not by a gain in gross kinetic energy, but by a gain in internal heat motion. This represents the final state of affairs that corresponds to the assumptions actually made.

A number of problems connected with the development of a mass of gas or dust into a system of stars should be studied by investigators more familiar with such problems than is the writer of this article. The results given here about the motions of the stars in our part of the galaxy may be useful in formulating and testing theories of the development of our own galaxy and star systems in general.

[12] *Zs. f. Ap.*, **10**, 228, 1935.

A COMPARATIVE STUDY OF THE SPECTRA OF α BOÖTIS AND 70 OPHIUCHI A

SUZANNE E. A. VAN DIJKE
Observatory of the University of Michigan
Received January 21, 1946

ABSTRACT

The weaker lines in the photographic region of the spectra of α Boötis and 70 Ophiuchi A have been compared visually and photometrically on high-dispersion coudé plates. A résumé of the behavior of the elements in the two stars is given. The relative weakness of the λ 3883 band of *CN* and several multiplets of *Ca* I in the giant and the relative strength of *La* II and the singly ionized rare earths are especially noted.

Curves of growth for the neutral iron lines have been constructed for both stars. The observed velocity and damping factor for α Boötis are 3.25 km/sec and 0.8×10^{-6}, respectively. The solar values were assumed for the dwarf.

Relative abundances are obtained, and departure from equilibrium is evident for the giant. The Adams-Russell formula provides a satisfactory correction. Values of the excitation temperatures and of the log of the relative electron pressures are 3160°, 4150°, and −3.74, −1.10 for the giant and dwarf, respectively. The results are compared to the sunspot spectrum, and the suggestion is made of a stratification of elements in the atmosphere of the giant similar to that found in the sun.

I. INTRODUCTION

In her classification of stellar spectra, Miss A. C. Maury[1] called attention to the fact that the sudden decrease of intensity in the spectrum from λ 3889 toward the ultraviolet, as well as the degree of absorption in the regions λλ 4055–4078 and λλ 4144–4216, differs for various stars within the same spectral classification. J. C. Kapteyn[2] noted that stars of small proper motion showed greater absorption in the ultraviolet than stars of large proper motion and attributed this differential absorption to interstellar scattering. W. S. Adams[3] first suggested that this difference in absorption might be connected with the intrinsic luminosity of the star. However, the outstanding differences in the spectra of giant and dwarf stars of similar spectral type were first shown by Adams and Kohlschütter.[4] They found that "the continuous spectrum of the small proper motion stars is relatively fainter in the violet as compared with the red than is the spectrum of the large proper motion stars." From a study of the spectral lines they found "systematic differences of intensity for certain lines between stars of large and stars of small proper motion" and listed the most prominent lines. The lines strengthened in the giant are λ 4077 and λ 4216 of *Sr* II; whereas λ 4325 of *Sc* II, λλ 4435, 4436, and 4455 of *Ca* I, and λ 4535 of *Ti* I are weakened in the giant. The ratios of the intensities of these crucial "absolute-magnitude lines" were then calibrated for stars of known parallax and provided a method for the determination of the absolute magnitude and hence the (spectroscopic) parallax.[5] Thus it has been possible to determine the parallaxes of stars for which no trigonometric parallaxes are available.

B. Lindblad[6] showed that the sharp decrease of intensity to the violet of λ 3883 is due not only to the differences in the energy distribution of the continuum of giants and

[1] *Harvard Ann.*, **28**, 38, 1897.

[2] *Ap. J.*, **29**, 46, 1909; *Mt. W. Contr.*, No. 31.

[3] *Ap. J.*, **39**, 89, 1914; *Mt. W. Contr.*, No. 78.

[4] *Ap. J.*, **40**, 385, 1914; *Mt. W. Contr.*, No. 89.

[5] Adams, Joy, Strömberg, and Burwell, *Ap. J.*, **53**, 13, 1921; *Mt. W. Contr.*, No. 199.

[6] *Ap. J.*, **55**, 85, 1922.

dwarfs but also to a strong cyanogen band and that the strong absorption in the giants at λ 4216 and λ 4606 is also due to cyanogen. Thus the basis for the cyanogen discriminant in the spectra of giants and dwarfs was established. W. Luyten[7] has called attention to the weakening of the sodium D lines in the late-type giants, and Miss C. G. Burwell[8] has studied the behavior of calcium in the red region of giants and dwarfs of late spectral types. She found that the lines of the neutral atom were weakened in the giants, with the exception of λ 6450, which is strengthened. More recently, Morgan, Keenan, and Miss Kellman[9] have summarized the criteria for absolute-magnitude classification for the different spectral classes in the photographic region, based on the earlier findings of Adams and Kohlschütter, Lindblad, and E. G. Williams.[10]

In general, the criteria for absolute-magnitude classification are adapted for spectra of relatively low dispersion, and on high-dispersion spectrograms many of these outstanding features are lost. The cyanogen band at λ 4216, one of the most important criteria for luminosity classification of low-dispersion spectrograms, shows very little change from dwarf to giant on high-dispersion plates, since the band is resolved into its component lines, and the net effect of the increased absorption is considerably diminished. However, on high-dispersion plates many additional lines appear and many blends are resolved, thus permitting a study of the behavior of many elements in some detail. Adams and Russell[11] have studied the behavior of a great number of lines of several dwarf, giant, and supergiant stars on high-dispersion spectrograms and, from their data for the various atoms, have calculated the relative abundances, temperatures, electron pressures, etc., with the sun as reference. In the present investigation, high-dispersion spectra of the giant and dwarf K0 stars—α Boötis and 70 Ophiuchi A—have been compared, with emphasis on the behavior of the fainter lines in the photographic region.

The star α Boötis is classified as K0 in the Draper Catalogue, at Victoria, and at Mount Wilson. The Yerkes classification is "slightly earlier than the mean for class gK2" and is given as gK2 pec. The trigonometric parallax[12] of the star is $+0''.080 \pm 0''.005$, while the spectroscopic parallaxes determined at Mount Wilson, Victoria, and Harvard are $0''.10$, $0''.10$, and $0''.21$, respectively.[13] The discrepancy has been attributed to the high-luminosity value obtained from the relative intensity of λ 4077 of ionized strontium to the neighboring iron lines, and the abnormally weak cyanogen band to the violet of λ 4215.[14] Pettit and Nicholson[15] have determined the surface temperature as 4300°; the atmospheric temperature determined by Adams and Russell[16] is 3220° (referred to the solar value of 4700°). Interferometer measurements of the diameter by F. G. Pease[17] indicate a value $0''.020$. Combined with the trigonometric parallax, this gives a radius twenty-seven times that of the sun. The mass is of the order of nine times that of the sun, and the radial velocity determined by Adams[18] is -5.621 ± 0.005 km/sec.

The system of 70 Ophiuchi consists of two dwarf K stars. The brighter component is classified K1 in the Draper Catalogue and K0 at Victoria, Mount Wilson, and Yerkes. If Kuiper's[19] values for the apparent visual magnitude, +4.19, and the parallax, $0''.196$

[7] *Pub. A.S.P.*, **35,** 175, 1923.

[8] *Pub. A.S.P.*, **42,** 352, 1930.

[9] *An Atlas of Stellar Spectra*, University of Chicago Press, 1943.

[10] *Ap. J.*, **83,** 305, 1936.

[11] *Ap. J.*, **68,** 9, 1928.

[12] *General Catalogue of Stellar Parallaxes*, New Haven, 1924.

[13] Russell, Dugan, and Stewart, *Astronomy*, **2,** 875, 1938; *Mt. W. Contr.*, No. 551.

[14] Morgan, Keenan, and Kellman, *op. cit.*

[15] *Ap. J.*, **68,** 279, 1928.

[16] *Loc. cit.*

[17] *Pub. A.S.P.*, **57,** 28, 1945.

[18] *Ap. J.*, **90,** 494, 1939; *Mt. W. Contr.*, No. 638.

[19] *Ap. J.*, **95,** 205, 1942.

± 0".004, are adopted, the absolute magnitude of the star is +5.7. The fainter component is K5, with an absolute magnitude +7.3. P. van de Kamp[20] gives a period of 87.8 years, semimajor axis of 23.3 astronomical units, and masses 0.90 and 0.73 that of the sun for the A and B components, respectively. The temperature of the brighter component is 5080° according to measures of heat-index and water-cell absorption by Pettit and Nicholson.[21]

II. DATA AND MEASUREMENTS

The plates used in the investigation were taken in the second order of the grating spectrograph at the coudé focus of the 100-inch telescope. The focal length of the camera is 114 inches, giving a dispersion of 2.9 A per millimeter. The microphotometric tracings were obtained with the Mount Wilson microphotometer at a magnification of 60.

In a preliminary survey the spectra of α Boötis and 70 Ophiuchi were compared visually on the Hartmann spectrocomparator over the entire wave-length range, and a visual scale of apparent difference of intensity from giant to dwarf was established. However, a calibration of this scale in terms of a difference of equivalent width indicated considerable scatter. The intensity scale was affected to a large extent by the complex variation in the differences of the background densities of the plates and by the degree of blending of the individual lines and, to a slighter degree, by the number of lines in the field. Accordingly, a combination of visual and photometric data was used. The spectra were reexamined visually with the corresponding high-magnification microphotometric tracings, and a new visual scale was established. In this case an attempt was made visually to account for the factors mentioned above, and subsequent calibration disclosed a remarkable consistency in the visual scale over the entire wave-length range. Photometric estimates were then made of the equivalent widths of all lines in the two stars, which apparently differed in intensity in the visual survey. These estimates were based on data obtained on similar plates and tracings of Venus for 100 relatively unblended lines in four wave-length regions in the λλ 3900–4808 interval. A double-entry table was formed, giving the equivalent width in angstrom units as a function of the central intensity and b, the width of the line at the continuum, measured in millimeters on the tracing. Equivalent widths measured by Allen[22] and those measured by the author in the *Photometric Atlas of the Solar Spectrum*[23] were used in the calibration. The probable error for an unblended line is ±0.005 for an equivalent width of 0.035 A and ±0.009 for 0.100 A. There is, of course, a large margin for error in the measurement of b, even for an unblended line; and the error increases as a function of the background density of the plate. In the case of physical and optical blends, the error is further increased because only a most probable value of b can be used. Thus the estimated equivalent width is a measure of the observed absorption—at a given wave length—which is assumed to have the true continuum as background. It should not be confused with the actual value of the equivalent width, which is a measure of the number of atoms effective in the production of a given atomic or molecular transition. The estimated value will be most seriously in error in this respect for the blend of a faint line near the core of a very strong line. It will be a measure of the number of effective atoms in the case of an unblended line arising from the undisturbed continuum, in which case the error will be solely one of measurement. The advantage of the procedure lies in the fact that they are obtained in a fraction of the time required for the measurement of accurate equivalent widths and yet make possible a preliminary quantitative discussion of the behavior of a great number of lines of various atoms.

For the great majority of lines a mean value of the differential absorption as deter-

[20] *Pub. A.S.P.*, **57**, 38, 1945. [21] *Op. cit.*

[22] *Mem. Commonwealth Obs.*, **1**, Part IV, 2, 1934.

[23] Minnaert, Mulders, and Houtgast, Amsterdam, 1940.

mined visually and photometrically was used. In cases of seriously blended lines, the visual estimate was favored in a weighted mean. To calibrate the visual scale, the differential photometric values were plotted against the visual estimates for groups of some fifty lines, covering, on the average, forty angstrom intervals. The resulting relationships were examined in sections as functions of the background density and *in toto* as functions of the degree of blending and of the strength of the lines. No systematic trends were found. However, there appeared a consistent overestimate of the increased absorption in the spectrum of 70 Ophiuchi, corresponding to one step on the visual scale of ten. This was probably due to the consistently weaker plates of the star and to the difference in the appearance of the two spectra. The latter was due, in turn, to a difference in guiding in obtaining the two spectra.

The identification of the lines was simplified by the use of the *Solar Atlas* and the latest revision of the Rowland Table. The tracings of the two stars were of magnification very similar to that of the *Atlas*. All the lines appearing on the tracings were identified, except for a very few for which the temperature effect was sufficiently great to obliterate the line in the *Atlas*.

A total of 1045 lines within the range of Rowland intensity -1 to $+4$ were found to differ in intensity between α Boötis and 70 Ophiuchi A in the wave-length interval 3900–4808. Of these, 195 lines are unidentified in the sun. The complete list of lines is too extensive to include in the present paper. However, the lines for which no solar identifications are known are of particular interest and have been included in the Appendix. The data for the section $\lambda\lambda$ 4265–4318 have been omitted because of possible errors due to slight irregularities at the cut edges of the plates. The lines are listed in the Appendix according to wave length, with disk and spot intensities from the Revised Rowland Table. The fourth column gives a measure of the relative increase of intensity between the two stars. The star in which the line appears stronger is denoted by "d" for "dwarf," i.e., 70 Ophiuchi A, and by "g" for "giant," i.e., α Boötis. An intensity difference of approximately 10–25 mA is denoted by 1; a difference of 25–40 mA by 2; a difference of 40–65 mA by 3; and a difference of 65–100 mA by 4. The lines have been classified in the fifth column, using the differential absorption between the disk and the spot spectra and between the dwarf and the giant spectra. Class A lines are those for which the increase or decrease in intensity from dwarf to giant is in the same direction as from disk to spot. Class B lines are those for which no change in intensity is given from disk to spot. Class C lines are those for which the change in intensity from dwarf to giant is reversed as from disk to spot. No classification is given to those lines for which no spot intensities are given.

In general, class A lines indicate chiefly temperature effects, class C lines are sensitive to pressure effects, and class B lines will be a combination of the two effects. For lines which strengthen in the giant in classes B and C, we can suspect *La* II, the singly ionized rare earths, faint compounds, and possibly *Sr* II and *Ba* II. For the lines which strengthen in the dwarf in classes B and C, we can suspect *Ca* I, *Na* I, *Mn* I, and possibly faint *CH*.

The fainter of the two stellar lines will, in general, be of the same order of magnitude as the solar line. Information regarding the structure and the degree of blending can thus be obtained to some extent from the *Solar Atlas*. For all faint lines of intensity difference 1, however, the classification of lines may be quite arbitrary, since the change in intensity for the stellar and solar lines may depend heavily on the background blending.

III. BEHAVIOR OF ELEMENTS

In the following section a résumé of the behavior of the various atoms is given, as shown by the weaker lines. *H*, *Ca* II, *CN*, and *CH* are included for the sake of completeness. In the descriptions the expression "unresolved line" refers to a wave length for which more than one identification is given. A "resolved line" in this manner refers to a

wave length which is attributed uniquely to a given atomic or molecular transition, regardless of the degree of physical or optical blending in the spectrum. The terms "giant" and "dwarf" are used for simplicity, although the results refer specifically to α Boötis and 70 Ophiuchi A.

H In the dwarf the lines have strong wings, whereas in the giants they are quite sharp.

Na I Only three classified lines occur in the region. The only resolved line (E.P. 2.1) is stronger in the dwarf. The behavior of the line is attributed to absolute-magnitude effect.

Mg I The single line arising from the lowest level, 3^1S, is enhanced in the giant. Lines arising from the 3^1P^o level (E.P. 4.3) are stronger in the dwarf.

K I The two classified lines occurring in the region arise from the lowest level, 4^2S (E.P. 0.0), and are strengthened in the giant.

Ca I All lines observed are stronger in the dwarf with the exception of those involved in the $4^3P^o - p^2\,{}^3P$ transition (E.P. 1.9). These lines are stronger in the giant. The decrease in the intensity of the majority of the lines from dwarf to giant is one of the outstanding absolute-magnitude effects.

Ca II The H and K lines are the strongest lines in both spectra. The double reversal of the lines is considerably more pronounced in the giant.

Sc I Lines arising from the a^2D and a^4F levels (E.P. 0.0, 1.4) are considerably strengthened in the giant.

Sc II All lines in the region arise from levels with E.P. less than 0.7, with the exception of one which arises from the b^1D level (E.P. 1.4). All are strengthened in the giant.

Ti I All lines are considerably strengthened in the giant (E.P. 0.0–2.4).

Ti II All lines are strengthened in the giant (E.P. 0.6–2.0).

V I All lines are strengthened in the giant (E.P. 0.0–2.1).

V II All lines are strengthened in the giant (E.P. 1.5–2.8).

Cr I All lines arising from levels with E.P. less than 3.2 are strengthened in the giant. At somewhat higher values the lines are strengthened in the dwarf.

Cr II The lines arising from the b^4D level (E.P. 3.1) are slightly strengthened in the giant. Those arising from the b^4F level (E.P. 4.1) are strengthened in the dwarf.

Mn I All the fainter lines occurring in the region are of E.P. 2.2 or greater and are strengthened in the dwarf.

Mn II No unresolved line was observed in the region and only one resolved line, which is of unknown classification. The behavior of the atom is indeterminate.

Fe I All lines arising from levels with E.P. less than 3.1 are strengthened in the giant, while those arising from higher levels are strengthened in the dwarf. The z^5D^o level may be somewhat enhanced in both stars. Lines arising from the lowest b levels in the giant are slightly stronger than those arising from the a and z levels of a corresponding E.P. Several multiplets of high E.P. are considerably winged in the dwarf.

Fe II Only the b^4P and b^4F multiplets (E.P. 2.6, 2.8) occur in the region. Both are strengthened in the dwarf.

Co I All the lines recorded are strengthened in the giant (E.P. 0.0–3.2).

Ni I Lines arising from levels of E.P. 0.0–1.9 are strengthened in the giant. Lines arising from levels with E.P. greater than 3.3 are somewhat strengthened in the dwarf.

Ni II Only one unresolved line was found, and it was slightly strengthened in the giant. The behavior of the atom is indeterminate.

Zn I The three classified lines occurring in the region are all of high E.P. The line λ 4722 (E.P. 4.0) is slightly strengthened in the dwarf.

Ge I Two classified lines occur in the region, one of which, λ 4686 (E.P. 2.0), is strengthened in the giant.

Sr I Of the three classified lines occurring in the region, one was strengthened in the giant.

Sr II The two ultimate lines (E.P. 0.0) in the region, λ 4078 and λ 4216, $5^2S-5^2P^o$, are strengthened in the giant. The intensities of these lines are often used for the classification of giants and dwarfs.

Y I All lines occurring in the region are weak. Those arising from the a^2D level (E.P. 0.0) are considerably strengthened in the giant.

Y II Of the ten unresolved classified lines in the region, one was observed stronger in the giant. The behavior of the atom is indeterminate.

Zr I The lines occurring in the region all arise from low-energy levels and are strengthened in the giant.

Zr II The a^2D and a^2F levels (E.P. 0.5, 0.7) are strengthened in the giant. Lines arising from higher levels show no change in intensity.

Cb I All lines occurring in the region are strongly blended or of questioned identification. The behavior of two unresolved lines suggests a strengthening in the giant.

Ru I The six classified lines occurring in the region are all very faint. The line λ 4081 is strengthened in the giant.

Rh I Only one resolved and unclassified line was noted in the region. The behavior of the atom is indeterminate.

Ba II The only line occurring in the region which arises from the lowest level, 6^2S (E.P. 0.0), λ 4554, is considerably strengthened in the giant. This line is particularly sensitive to absolute magnitude.[24] Lines belonging to the higher-energy levels (E.P. 2.5–2.7) are unresolved and probably remain constant.

La II All lines observed from E.P. 0.0 to E.P. 1.9 are strengthened in the giant. It is noted that in the spectra of the disk and spot no change of intensity is found.[25] The increase in the giant is probably due to absolute-magnitude effect.

Ce II, *Pr* II, *Nd* II, *Sm* II, *Eu* II, *Gd* II, *Dy* II, *Lu* II The rare earths are all considerably strengthened in the giant (E.P. 0.0–0.8). It is noted that the lines of these atoms remain unchanged from disk to spot.[26] Europium and then neodymium show the greatest change in intensity. The strengthening is probably due to absolute magnitude unless α Boötis is characterized by unusually strong lines of these atoms.

[24] Morgan, Keenan, and Kellman, *op. cit.*

[25] C. E. Moore, *Ap. J.*, **75**, 304, 1932.

[26] *Ibid.*

W	1	There are no resolved classified lines in the region, but there is an indication that two unresolved lines may be strengthened in the giant.
Pb	1	The only line occurring in the region is strengthened in the giant (E.P. 1.3).
CH		The $^2\Delta - {}^2\Pi$ band at λ 4300 is strengthened in the dwarf.
CN		The $^2\Sigma - {}^2\Sigma$ (0, 0) band at λ 3883 was observed visually and is somewhat strengthened in the dwarf. The $^2\Sigma - {}^2\Sigma$ (0, 1), (1, 2), (2, 3) bands are strengthened in the giant.

IV. QUANTITATIVE ANALYSIS OF THE ATOMIC SPECTRA

A. CURVES OF GROWTH FROM THE IRON SPECTRUM

1. *General considerations.*—The most complete set of data for a study of the abundance, temperature, pressure, and departures from equilibrium is afforded by the series of iron lines. The estimated equivalent widths of the resolved lines were used to determine curves of growth for α Boötis and 70 Ophiuchi. The curves were then used for the determinations of the relative abundances of the atoms other than neutral iron at different excitation potentials. From these data the temperatures and electron pressures were determined.

K. O. Wright[27] has determined an empirical curve of growth for the sun, giving log W/λ as a function of log $X_{f(\mathrm{ab})}$, where

$$\log X_{f(\mathrm{ab})} = \log \mathrm{gf} + \log \lambda - \frac{5040E}{T} = \log X_0 - 1.81 \qquad (1)$$

and gf is the laboratory intensity of the line. (Log X_0 is defined by Menzel[28] for a particular model of radiative transfer.) Let X_r be defined as follows:

$$\log X_r = 5040E\left(\frac{1}{T_\odot} - \frac{1}{T_*}\right) + \log X_\odot . \qquad (2)$$

The best excitation temperature of the star will be determined by the slope of the straight line relating log $X_r/X_\odot$ to the excitation potential. Log $X_r/X_\odot$ is determined by the shifts in log X needed to eliminate the systematic displacement of multiplets of different excitation potentials. These displacements result from a difference in temperature between the sun and the star. If the stellar equivalent widths are accurate, it is possible to construct the curve of growth directly, commencing in the manner described. However, the estimated values are but approximations and may be systematically high or low. This would lead to serious error in building up the final curve of growth, especially for a giant star whose absorbing atoms differ considerably in kinetic velocity from those of a dwarf. The effect of the velocity is inherent in the curve of growth of the star; and in practice it shows up as a vertical displacement in the log W/λ co-ordinate.

2. *Application to α Boötis.*—To establish absolute values for the curve of growth of α Boötis, 53 strong and comparatively unblended iron lines were measured on the direct-intensity tracings by Williams and Hiltner[29] in the red region of the spectrum. Eight lines arising from the a^5F level (E.P. 0.97) and 10 lines arising from the a^3F level (E.P. 1.55) were sufficiently strong to assume pure damping broadening with a curve of growth of slope ½. Log W/λ was computed for these lines in α Boötis and in the sun. The equivalent widths of the solar lines given by Allen[30] were then assumed to fall exactly on the empirical curve of growth for the sun given by Wright.

[27] *Ap. J.*, **99**, 249, 1944. [28] *Ap. J.*, **84**, 462, 1938.

[29] Unpublished data from coudé spectrograms obtained at the McDonald Observatory.

[30] *Op. cit.*

The very strong lines of the a^5F and a^3F multiplets in α Boötis were then made to coincide with the straight-line portion of the curve of growth of the sun by horizontal displacements in log $X_\odot$, giving log $X'_\odot$, let us say. The estimated values of the weak lines of these multiplets were then shifted by the corresponding amounts. A tentative straight-line relationship was assumed between the excitation potential and log $X'_\odot/X_\odot$, and the shift in log $X'_\odot/X_\odot$ was then extrapolated for the a^5D level (E.P. 0.0) and the a^3P, a^5P levels (E.P. 2.3). This was applied to both sets of data, and thus a curve of growth was tentatively constructed. The estimated values fell consistently low in the log W/λ coordinate, but the different multiplets fitted together consistently. The lines arising from the z^5D^o level (E.P. 3.2) and the z^5P^o level (E.P. 3.7) were then added and the best fit obtained.

The curve determined by the estimated values fell systematically lower in log W/λ than the direct-intensity curve, although similar slopes are indicated. The curves relating Δ log $X_\odot$ to the excitation potential fitted closely for the two sets of data. Thus the former curve was corrected for this systematic difference, amounting to 30 per cent of the estimated equivalent widths, and a common curve was derived for both sets of data. This systematic error for α Boötis was probably due to an underestimate of the continuum of the spectrum of the star.

Actually, there is no need to shift the very strong lines of the various multiplets through Δ log $X_\odot$. In this particular instance it was done to enable an extrapolation of the equivalent widths of the lines of the a^5D multiplet which were not available by direct measurement. If $+1.38$ represents Δ log $X_\odot$ at E.P. $= 0.0$, then from equation (2) we have

$$\log \frac{X'_\odot}{X_\odot} - 1.38 = 5040E\left(\frac{1}{T_\odot} - \frac{1}{T_*}\right) = \log \frac{X_r}{X_\odot}. \tag{3}$$

The curve relating log W/λ to log X_r was fitted to the family of theoretical curves of growth given by Menzel.[31] These curves give log $(c/v \cdot W/\lambda)$ as a function of log Z, where

$$Z = \frac{\Gamma}{\nu_0}\frac{c}{v}.$$

Thus the vertical coincidence of the empirical and theoretical curves yields the velocity of the atoms in the star, v_*; and the horizontal coincidence gives Γ/ν_0, the damping factor; and log $X_r -$ log X_*. The velocity and the damping factor for the star are 3.25 km/sec and 0.8×10^{-6}, respectively. The apparent velocity well exceeds that which is due solely to kinetic motion. Thus the observed value must be attributed to the combined effects of kinetic and turbulent velocities. The curves of growth for α Boötis are given in Figures 1, 2, and 3. In Figure 3 the smooth curve represents the theoretical one. The empirical curve lies above the theoretical curve where the Doppler region changes to the transition portion; and beyond log $X_* = +1.3$ it lies below the theoretical curve until the transition portion changes to the damping region. This same effect was noted to a lesser degree by Wright in his solar curve and is apparent in the curve for Sirius determined by Aller.[32] A large proportion of the departure from the theoretical curve in the present data may be due to the uncertainty in the values for the Doppler region. A small change in the horizontal displacement of the initial rise of the curve would change the length of the transition portion, and hence the damping factor. Writing the equations in X for the same line in the sun and a star and dividing, we obtain

$$\frac{X_*}{X_\odot} = \frac{N_{a*}}{N_{a\odot}}\frac{b(T_\odot)}{b(T_*)}\, e^{-E_i(1/T_*-1/T_\odot)}\,\frac{v_\odot}{v_*}. \tag{4}$$

[31] *Pop. Astr.*, **47**, 74, 1939.

[32] *Ap. J.*, **96**, 328, 1942.

Therefore,

$$\log \frac{X_*}{X_r} = \log \frac{N_{a*}}{N_{a\odot}} + \log \frac{b\,(T_\odot)}{b\,(T_*)} + \log \frac{v_\odot}{v_*}. \qquad (5)$$

Since $\log X_*/X_r$ and $\log v_*/v_\odot$ are now known, $\log N_{a*}/N_{a\odot}$ is directly obtained. Furthermore, since for a given line in the sun and the star

$$\log \frac{X_*}{X_\odot} + \log \frac{v_*}{v_\odot} = \log \frac{N_*}{N_\odot}, \qquad (6)$$

we are now in a position to obtain the relative number of atoms in the two stars for the lines of any element at any given atomic level.

3. *Application to 70 Ophiuchi.*—Only a few very strong lines are available in the photographic region for the determination of absolute values for the curve of growth for

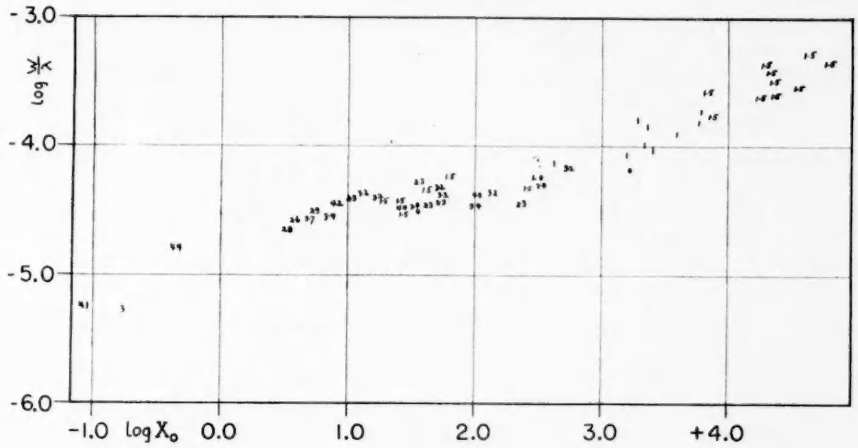

FIG. 1.—Curve of growth for the neutral iron lines in α Boötis from direct-intensity measures

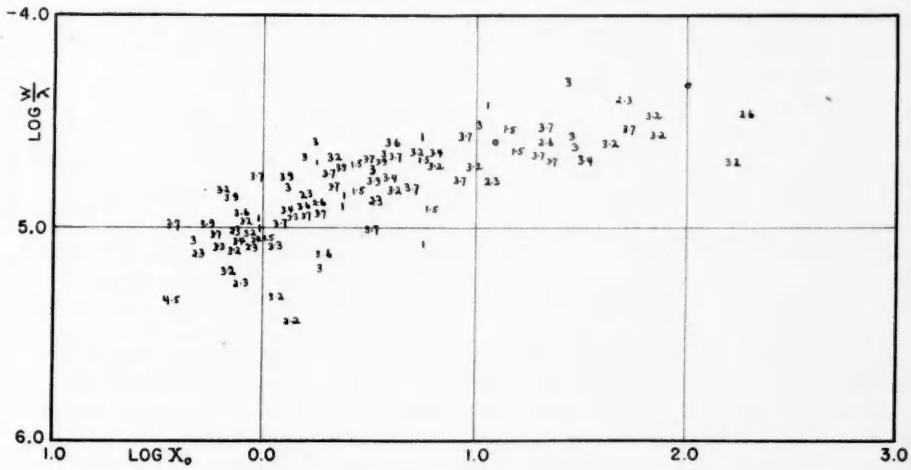

FIG. 2.—Curve of growth for the neutral iron lines in α Boötis from estimated values

70 Ophiuchi. Thus the estimated values of the equivalent widths were used to determine the curve. It was assumed (*a*) that the mean curve drawn through the scattered points maintained the same shape as the solar curve and (*b*) that log $X_*/X_\odot$ decreased linearly with increasing excitation potential. The first assumption is admissible, since we are considering a star quite comparable to the sun, and we would not expect any radical change in the turbulent velocities. The second assumption is equally admissible, since

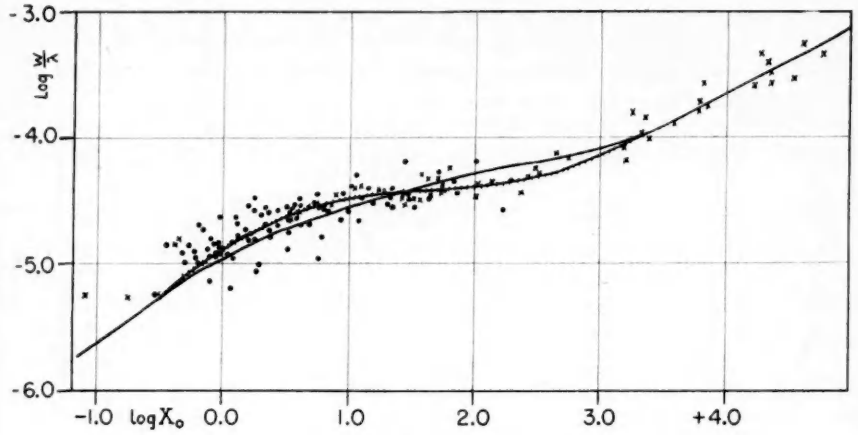

FIG. 3.—Final curve of growth adopted for α Boötis

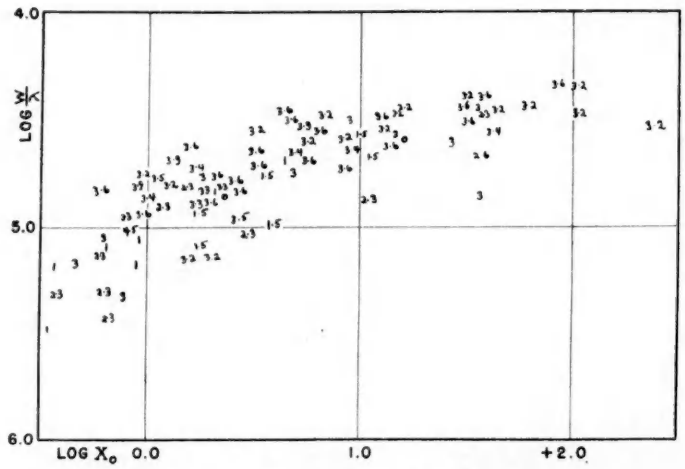

FIG. 4.—Curve of growth for 70 Ophiuchi A

we know that the K0 star is cooler than the G0 star. The assumption of linearity implies that the conditions for thermodynamic equilibrium are fulfilled in a manner similar to the sun. This may well serve for a preliminary adjustment of values. These two assumptions serve to fix the curve along the log X_0 axis but do not preclude the possibility of a systematic error in log W/λ. The final curve of growth, shown in Figure 4, represents the best over-all adjustment of values for different excitation potentials. This was obtained by

successive approximations for the relative shifts of the individual multiplets which would yield the best straight line relating log $X_*/X_\odot$ to the excitation potential. Thus the individual values of log $X_*/X_\odot$ should not be considered purely empirical; rather, the whole assemblage of values represents the best empirical determination.

Two independent checks on the reliability of the curve for 70 Ophiuchi are available. Five lines arising from the a^5F multiplet and falling on the pure damping portion of the curve are available in the photographic region. These were used to determine log $X_*/X_\odot$ at $\overline{E.P.} = 0.99$. The results agreed closely with the estimated values. Also we should expect the rare earths to remain of similar intensity in the K0 and G0 dwarfs, and thus the values of log $X_*/X_\odot$ should remain close to 0.00. We shall see later that the mean value derived is +0.10. Thus we may assume that the error in the empirical curve is not so great as to affect the analysis seriously.

B. RELATIVE ABUNDANCE OF VARIOUS ATOMS

With the curves of growth for the estimated equivalent widths of the neutral iron lines in both stars, it was possible to obtain values of log $N_*/N_\odot$ for the remaining atoms. The same preliminary procedure was followed as in the case of the iron lines. Log W/λ was computed for both the solar and the stellar lines, and the solar values were assumed to fall exactly on the curve of growth for the sun as given by Wright. The differences in log X required to bring the various multiplets to the best position on their respective curves of growth is then log $X_*/X_\odot$, and when we add log $v_*/v_\odot$ to this we immediately have log $N_*/N_\odot$. In obtaining the data for 70 Ophiuchi, it was assumed that log $v_*/v_\odot = 0$. The data are sumarized in Table 1, giving the mean excitation potential, the number of lines used, log $N_*/N_\odot = Y$ for the two stars, and the spectroscopic notations of the lower levels included in each determination. In the data for neutral iron, the starred values represent those which were used in the original determinations of the curve of growth. The other values of *Fe* I were originally interpolated or extrapolated from Figure 5, which gives log $X_\odot'/X_\odot$ as a function of the low excitation potential. The lower line of numbers under "No." of *Fe* I gives the lines measured on the direct-intensity tracings for α Boötis. Only those lines known to have a single identification were used in compiling the table.

C. DETERMINATION OF TEMPERATURES

It was pointed out earlier that "the best excitation temperature (relative to the sun) will be determined by the slope of the line relating log $X_r/X_\odot$ to the excitation potential." If the conditions for thermodynamic equilibrium are fulfilled, this relationship will be linear and

$$S' = \frac{\Delta Y}{\Delta E} = 5040\left(\frac{1}{T_\odot} - \frac{1}{T_*}\right). \tag{7}$$

This relationship appears to be quite satisfactory for 70 Ophiuchi. In the case of α Boötis, however, it is not possible to assume a simple linear relationship, and the situation becomes a trifle puzzling. It is hard to see which point on the curve should be used for the slope determination. We could determine the slope at $E = 0$ as well as at a high excitation potential and treat these slopes as the values for the minimum and maximum temperatures. From Figure 5 we find these to be 3200° and 3950°, respectively, when we use the solar value by Wright[33] of 4900° for *Fe* I. The maximum temperature was calculated at an excitation potential of 3.0 volts.

Adams and Russell[34] found that the departure from linearity was very marked for

[33] *Op. cit.*, p. 250.

[34] *Op. cit.*, p. 23.

TABLE 1

OBSERVED VALUES OF THE RELATIVE ABUNDANCES $Y = \log N_*/N_\odot$

Element	E.P.	No.	Y_g	Multiplet	Y_d
Fe I	0.00	$\left\{\begin{matrix}2\\2\end{matrix}\right\}$	+1.94	$\left\{\begin{matrix}a^5D\\a^5D\end{matrix}\right\}$	+0.60
	0.97	$\left\{\begin{matrix}8\\10\end{matrix}\right\}$	1.47*	$\left\{\begin{matrix}a^5F\\a^5F\end{matrix}\right\}$	+ .42*
	1.55	$\left\{\begin{matrix}8\\16\end{matrix}\right\}$	1.12*	$\left\{\begin{matrix}a^3F\\a^3F\end{matrix}\right\}$	+ .35*
	2.27	$\left\{\begin{matrix}8\\4\end{matrix}\right\}$	0.90*	$\left\{\begin{matrix}a^3P, a^5P, a^3H\\a^3P, a^5P, a^3H\end{matrix}\right\}$	+ .26*
	2.58	$\left\{\begin{matrix}3\\1\end{matrix}\right\}$	0.78	b^3F	+ .23
	2.87	$\left\{\begin{matrix}5\\2\end{matrix}\right\}$	0.68	z^7F^0, z^7P^0	+ .18
	2.99	$\left\{\begin{matrix}6\\1\end{matrix}\right\}$	0.66	b^3G	+ .17
	3.24	$\left\{\begin{matrix}20\\6\end{matrix}\right\}$	0.56*	z^5D^0	+ .15*
	3.27	5	0.54	a^3D	+ .14
	3.39	$\left\{\begin{matrix}5\\4\end{matrix}\right\}$	0.53	z^5F^0	+ .13
	3.56	2	0.51	a^1H	+ .10
	3.62	2	0.49	b^3D	+ .09
	3.67	$\left\{\begin{matrix}18\\1\end{matrix}\right\}$	0.56*	z^5P^0	+ .10*
	3.90	6	0.41	z^3F^0, z^3D^0	+ .07
Fe II	2.66	1	0.11	a^4H	− .18
	2.77	2	0.09	b^4P	− .19
	2.83	9	0.06	b^4F	− .20
Ti I	0.03	6	2.51	a^3F	+ .65
	0.94	15	1.76	a^5F, a^3P, a^1D	+ .65
	1.80	19	1.61	a^5P, a^3G	+ .40
	2.10	12	1.46	z^5G^0, z^5F^0	+ .50
	2.17	13	1.71	a^3H, a^3D	+ .50
	2.33	5	1.46	z^5D^0, z^3F^0	+ .45
Ti II	1.12	13	1.01	a^2G, a^2D, a^4P	+ .17
	1.23	14	1.01	a^2P, b^4F	+ .07
V I	0.03	9	2.34	a^4F	+ .60
	0.28	10	2.16	a^6D	+ .50
	1.10	9	1.86	a^4D, a^4P	+ .28
	1.99	8	1.46	a^4H, b^4F, a^4G, z^6G^0	+ .25
V II	1.84	7	1.71	a^3G, a^5P, b^3G	+ .25
Cr I	0.96	3	2.01	a^5D, a^5S	+ .65
	2.79	20	1.21	a^5G, a^5P, a^3P, z^7P^0, b^5D	+ .35
	3.23	3	0.56	z^7F^0, b^3P	+ .12
Cr II	4.06	3	0.11	b^4F	− .30
Ni I	0.20	3	1.81	a^1D, a^3F, a^3D	+ .33
	1.67	2	0.81	b^1D	− .05
	1.94	1	1.06	a^3P	+ .15
	3.51	7	0.31	z^5F^0, z^5D^0, z^5G^0	− .20
	3.70	11	0.46	z^3F^0, z^3P^0, z^3D^0, z^1F^0	+ .07
	4.08	2	0.71	y^3F^0	+ .45
Co I	0.12	6	1.96	a^4F	+ .45
	0.50	7	+1.69	b^4F	+0.35

TABLE 1—*Continued*

Element	E.P.	No.	Y_g	Multiplet	Y_d
	0.92	1	+1.86	a^2F	+0.27
	1.94	3	1.26	b^4P	+ .15
	2.71	1	1.08	b^2D	+ .30
	3.13	2	1.06	z^6D^0	+ .25
Sc I	0.01	6	1.91	a^2D	+ .67
	1.43	3	1.21	a^4F	+ .40
Sc II	0.53	4	1.23	a^1D, a^3F	+ .07
Zr I	0.04	2	1.56	a^3F	+ .45
	0.64	8	1.71	a^3P, a^1D, a^5F	+ .70
Zr II	0.67	3	0.86	a^2D, a^2F	− .10
Mn I	2.94	14	0.71	a^4D, z^6P^0	− .10
Ca I	2.50	4	0.16	3^1D, 4^1P^0, 4^3P^0, 3^3D	+ .18
La II	0.23	12	1.01	a^3D, a^3F, a^1D	+ .10
Nd II	0.15	10	1.51	a^6I, a^4I	+ .00
	0.55	3	1.01	a^6I, a^4I	+ .15
Pr II	0.12	2	1.48	a^5I^0	+ .40
Sm II	0.20	12	1.28	a^8I^0, a^6F	+ .22
	0.46	9	1.30	a^8F, a^6F	+ .00
Ce II	0.17	10	0.96	a^4H, b^4H^0, a^4H^0, a^2H, a^2G^0	+ .05
	0.61	9	1.30	b^4H^0, c^4G^0, a^4F, a^2H^0, a^2F^0	+ .15
Eu II	0.07	3	+1.66	a^7S^0, a^9S^0	+0.00

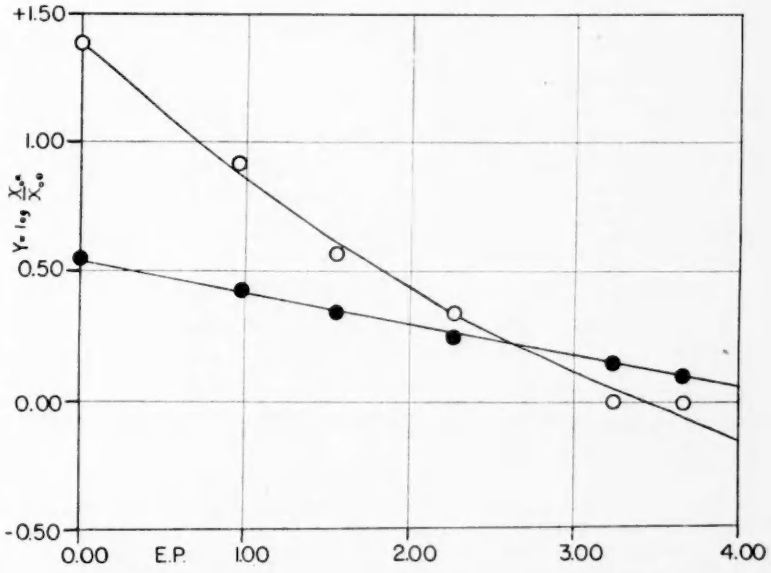

FIG. 5

α Orionis and α Scorpii and evident for α Boötis as well. They found that the curve relating $\log N_*/N_\odot$ to E for the two class-M giants could be represented by

$$Y = \log \frac{N_*}{N_\odot} = A - 1.05E + 0.087E^2 . \qquad (8)$$

A is the intercept on the axis of E for the particular curve considered. They then assumed more generally that the observed quantity Y was a linear function not of E but of a quantity X defined by

$$X = 1.05E - 0.087E^2 \tag{9}$$

such that

$$Y = Y_0 + SX\,. \tag{10}$$

Thus,

$$\frac{\Delta Y}{\Delta E} = 1.05S\,, \tag{11}$$

where S represents the slope $\Delta Y/\Delta X$, and $\Delta Y/\Delta E$ represents the initial slope of the actual curves for $E = 0$.

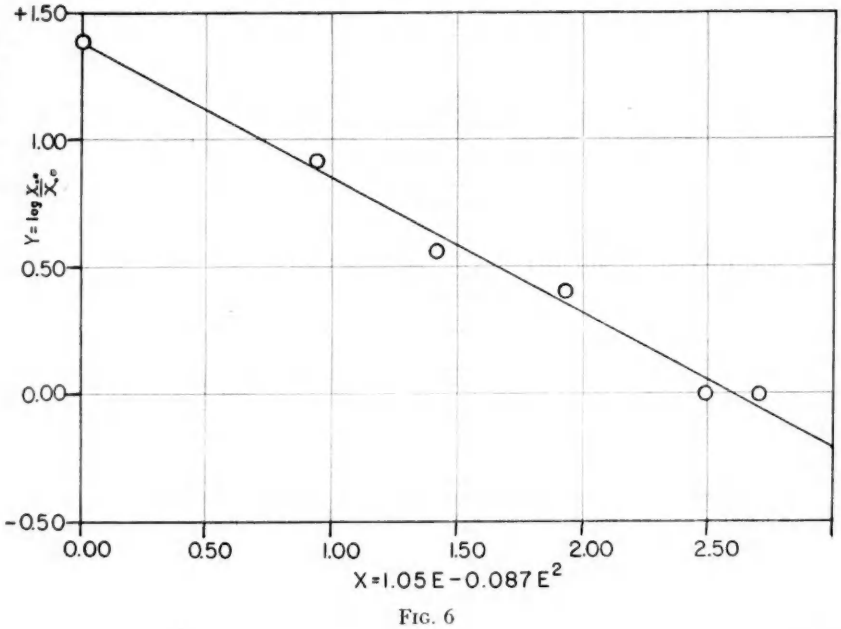

FIG. 6

When this procedure was followed for the iron lines in α Boötis, the points fell on a straight line with a slope $S = -0.520$, as shown in Figure 6. The stellar temperature was then derived by the simple equation

$$5040\left(\frac{1}{T_\odot} - \frac{1}{T_*}\right) = 1.05S\,. \tag{12}$$

In Table 2 the atoms used for the determination of the slope are listed, and the values of the slope are given for both stars. Since all these values are relative to the curve of growth for the sun by Wright, his temperature determinations have been used. He gives 4900° for *Fe* I, 4550° for *Ti* I, and 4700° as the mean value for all other atoms. The weights ascribed to each element are based on the number of lines, the range in excitation potential, and the scatter of the individual points relative to the curves of growth. The second set of values given for *Ni* I and *V* I in 70 Ophiuchi was obtained from the differential values of giant and dwarf with the temperature already computed for α Boötis.

The scatter in the original relationship is exceptionally great, while the scatter for the second set is comparatively small. In obtaining the weighted mean temperature, both values were included.

It follows that the intercept of the curve on the Y axis at E.P. = 0.00 will give log $N_{0*}/N_{0\odot}$. That is, Y_0 yields the number of atoms of a given element in their normal state above equal areas of the photosphere in the star relative to the sun. We now make the approximation that Y_0 yields the relative number of all neutral atoms of a given kind. Table 3 lists the different atoms for which sufficient data are available to afford a deter-

TABLE 2

$S = \frac{\Delta Y}{\Delta X}$ AND $S' = \frac{\Delta Y}{\Delta E}$ FOR VARIOUS ATOMS

ELEMENT	α BOÖTIS			70 OPHIUCHI		
	Wt.	S	T	Wt.	S'	T
Ti I	5	−0.537	3010°	5	−0.141	4050°
Sc I	1	.540	3080	1	.184	4010
Cr I	1	.510	3130	1	.173	4050
Ni I	3	.506	3140	2	.089	4350
				3	.137	4160
Fe I	15	.520	3200	15	.180	4170
V I	2	.480	3200	1	.195	3980
				2	.175	4040
Co I	2	−0.426	3320	2	−0.089	4350
Weighted means			3160			4150

mination of Y_0. In general, there are insufficient data for the enhanced atoms to permit an independent determination of slope. Thus the slopes of the respective neutral atoms have been applied for the extrapolation of Y_1. The differences $Y_0 - Y_1$ have been tabulated for those atoms for which two stages of ionization are given.

D. DETERMINATION OF ELECTRON PRESSURES

By comparing the number of neutral and singly ionized atoms, it is possible to determine an approximate value of the electron pressure from the ionization equation:

$$\log \frac{N_1}{N_0} = \frac{-5040I}{T} + \frac{5}{2}\log T - 6.5 - \log P_e, \qquad (13)$$

where I is the ionization potential, P_e the electron pressure, N_1/N_0 the ratio of the number of ionized to neutral atoms, and T the temperature. Strictly speaking, T should be the ionization temperature; but, in lieu of such data, the excitation temperatures have been used. If we now compare the number of neutral and ionized atoms of the same element in two stars, we have

$$\log \frac{P_{e*}}{P_{e\odot}} = \log \frac{N_{0*}}{N_{0\odot}} - \log \frac{N_{1*}}{N_{1\odot}} + \frac{5}{2}\log \frac{T_*}{T_\odot} + 5040I\left(\frac{1}{T_\odot} - \frac{1}{T_*}\right). \qquad (14)$$

The first two quantities on the right-hand side of the equation are found in Table 3, and the remaining terms are evaluated from Table 2. The resulting values of the electron pressures for α Boötis and 70 Ophiuchi relative to the sun are found in Table 4.

V. DISCUSSION

A. BEHAVIOR OF CALCIUM, THE RARE EARTHS, AND CYANOGEN

The atoms of special interest in a comparative study of the giant and dwarf stars are *H*, *Na* I, *Ca* I, *Ca* II, *Sr* II, *Ba* II, *La* II, the singly ionized rare earths, and the *CN* and

TABLE 3

RELATIVE ABUNDANCES OF VARIOUS ATOMS

$$Y_0 = \log \frac{N_{0*}}{N_{0\odot}}, \quad Y_1 = \log \frac{N_{1*}}{N_{1\odot}}$$

ELEMENT	α BOÖTIS		70 OPHIUCHI		DIFFERENCE
	$Y_{0,1}$	$Y_0 - Y_1$	$Y_{0,1}$	$Y_0 - Y_1$	
Ca I*	1.81	.....	0.54	.....	1.27
Sc I	1.93	+0.45	.67	0.29	1.26
Sc II	1.48		.38		1.10
Ti I	2.51	+ .92	.75	.30	1.76
Ti II	1.59		.45		1.14
V I	2.34	− .12	.57	.00	1.77
V II	2.46		.57		1.89
Cr I	2.23	+ .64	.83	.45	1.40
Cr II	1.59		.38		1.21
Mn I*	2.35	.....	.62	.....	1.73
Fe I	1.94	+ .70	.53	.40	1.41
Fe II	1.24		.13		1.11
Co I	1.99	.....	.43	.....	1.56
Ni I	1.84	.....	.28	.....	1.56
Zr I*	2.06	+0.76	.75	0.60	1.31
Zr II	1.30		.15		1.15
La II	1.11	.....	.10	.....	1.01
Ce II	1.13	.....	.10	.....	1.03
Pr II	1.48	.....	.40	.....	1.08
Nd II	1.76	.....	.07	.....	1.69
Sm II	1.29	.....	.11	.....	1.18
Eu II	1.66	.....	0.00	.....	1.66

* The slopes used for *Ca* I and *Mn* I in α Boötis were those determined by Adams and Russell, −0.62 and −0.70, respectively. For *Zr* I, $S = -0.50$ was assumed. The slopes assumed for these three atoms in 70 Ophiuchi were −0.20, −0.21, and −0.125.

TABLE 4

COMPUTED ELECTRON PRESSURES: $\log P_{e*}/P_{e\odot}$

Element	Wt.	α Boötis	70 Ophiuchi	Difference	Element	Wt.	α Boötis	70 Ophiuchi	Difference
Ti	2	−3.36	−0.78	−2.58	*Fe*	3	−4.04	−1.19	−2.85
Cr	1	3.39	0.84	2.55					
Sc	1	3.73	1.09	2.64	Mean		−3.74	−1.10	−2.64
V	1	−3.95	1.50	2.45					
			−1.34	−2.61					

CH molecules. In the present investigation, *Ca* I, *La* II, the rare earths, and *CN* are particularly noted.

Mention was made in Section III of the decrease in the intensity of the neutral calcium lines as we pass from dwarf to giant. Along the main sequence, the intensity of the lines increases very noticeably as we go to later spectral classes. The lower density in the atmosphere of the giant star must therefore more than compensate for the decrease in temperature. Miss Burwell found the $4^3P^o-5^3S$ transition stronger in the dwarfs, and some members of the $3^3D-dp^3F^o$, $3^3D-5^3P^o$, and $4^1P^o-p^2D$ multiplets slightly stronger in the dwarf. The strongest line in the $3^3D-dp^1D^o$ group, λ 6450, was observed to be stronger in the giant. In the present investigation, lines due to the $3^1D-6^1P^o$, $4^1P^o-6^1D$, $4^3P^o-4^3D$, and $3^3D-4^3F^o$ transitions were observed stronger in the dwarf. It is tempting to conclude that the apparent inconsistency of λ 6450 is due to the intersystem combination. However, two strong lines of the $4^3P^o-p^2\,{}^3P$ transition were observed strengthened in the giant in the present investigation, and the situation becomes puzzling.

The singly ionized rare earths and lanthanum are conspicuously strengthened in the giant. As yet, no detailed comparative study of these lines has been made in other giant and dwarf stars of late spectral type. It is thus difficult to know whether the observed strengthening is due to an absolute-magnitude effect or to a great abundance of these atoms in this giant star. It is interesting to note, however, that, with the exception of helium and hydrogen, calcium attains the greatest height for the neutral atoms in the solar atmosphere, while lanthanum and the rare earths are very low-lying. The apparent weakening of one atom and the strengthening of the others in the giant star might thus be intimately connected with an apparent stratification of the elements in stellar atmospheres.

The behavior of the *CN* band to the violet of λ 3883 in α Boötis is rather startling. The increase in the absorption of *CN* as we pass from dwarf to giant is one of the outstanding criteria for absolute-magnitude determination. The lines of the ultraviolet band are heavily blended, and the differences in the background intensities of the two stars in this region of the spectrum are great. The observed weakening of the lines in the giant might thus seem due to a large systematic error in the visual comparisons. However, lines of *Ti* I, *Fe* I, and weaker lines due to the rare earths in the same wave-length region were observed strengthened in the giant. No *CN* line in this region was observed to increase its strength in the spectrum of the giant. The abnormal weakness of the band at λ 4216 in α Boötis has already been mentioned in connection with the discrepancy of the trigonometric and spectroscopic parallax determinations, and the behavior of the λ 3883 band emphasizes this abnormality.

B. COMPARISON OF RESULTS FOR 70 OPHIUCHI AND SUNSPOTS

It is interesting to compare the results for temperature, pressure, and abundances in 70 Ophiuchi with those obtained by Mrs. Sitterly for the sunspot spectrum. A comparison of the slopes $S' = \Delta Y/\Delta E$ for *Fe* I and *Ti* I indicates an agreement within 30° for the two spectra, if we use the same solar value of the temperature. In the study of the stellar temperature, excitation temperatures were used, while in the study of the spot spectrum photospheric temperatures were used. The pressures agree within a factor of 8 if we use the mean of the individual temperature determinations for 70 Ophiuchi and within a factor of 3 if we use the mean value of the temperature for all the different atoms. However, the relative abundances disagree systematically. Log N_{spot}/N_* is positive for all neutral atoms and negative for all ionized atoms. Some of the difference in the abundance is undoubtedly due to the difference in the characteristic layers of the two K0 spectra considered. In the spot spectrum we are going down to a greater optical depth than in the K0 stellar atmosphere. Some of the difference may, of course, be intrinsic, since there is a question whether one would expect entirely similar conditions for this localized K0 region in a G0 star as for the net spectrum of a K0 star.

C. EVIDENCE SUGGESTING A STRATIFICATION OF THE ELEMENTS

From Table 2 we see that the run in temperature for the different atoms in α Boötis and 70 Ophiuchi follows closely with the exception of *V* I. Despite the uncertainty of the data for atoms of low weight, the sequence as a whole is quite similar to the sequence in the heights of the different atoms in the solar atmosphere given by Mitchell[35] with the high temperature corresponding to the low-lying element. On this basis, *V* I yields too high a temperature for α Boötis, and *Ni* I somewhat too low. The run in values of the electron pressures for the two stars also follows very closely, with the exception of *V* I. However, this apparent consistency in electron pressures is to be expected when the individual values of the temperature are used. When the mean temperatures are used, i.e., 3160° for α Boötis and 4150° for 70 Ophiuchi, we obtain the values given in Table 5. It is noted

TABLE 5

COMPUTED ELECTRON PRESSURES, log $P_{e*}/P_{e\odot}$, BASED ON MEAN TEMPERATURES

Element	Wt.	α Boötis	70 Ophiuchi	Difference	Element	Wt.	α Boötis	70 Ophiuchi	Difference
Ti	2	−3.06	−0.77	−2.29	*V*	1	−4.09	−0.78	−3.31
Cr	1	3.31	.61	2.70					
Sc	1	3.41	.74	2.67	Mean		−3.55	−0.76	−2.79
Fe	3	−3.82	− .80	−3.02					

that the pressures are very similar for the different atoms in 70 Ophiuchi. However, the sequence for α Boötis is still very similar to that found in Table 4. We may say, then, that to a first approximation the behavior of the elements in the atmosphere of the giant suggests a sequence in stratification similar to that in the solar atmosphere. The behavior of *Ca* I and the rare earths supports this view. Furthermore, it is evident from the shape of the hydrogen lines and the strong double reversal of the *Ca* II lines that these elements are at high levels, as in the sun. Adams[36] studied the wave lengths of lines of different atoms in α Boötis and concluded:

> The results found for the lines of different elements in Arcturus indicate a general arrangement of the gases in the star's atmosphere very similar to that in the sun. . . . . We know that in the sun hydrogen gas rises to very great heights, and the gases of magnesium and calcium (leaving out of consideration in the latter element the H and K lines) also attain a high level, though somewhat lower than hydrogen. Similarly, titanium is a relatively high-level element, but iron is low. In Arcturus, we find the lines of all of these elements giving wave lengths shorter than those of iron, the greatest difference being for hydrogen, the next for magnesium and calcium, and the least for titanium. It seems reasonable, therefore, to conclude that the lines of these elements are subject to less pressure than are those of iron, and consequently that the gases producing them lie at a higher average level.

VI. CONCLUSION

The preceding analysis has shown that it is possible to obtain a large amount of valuable quantitative data from the weak lines in late-type stars by the use of estimated equivalent widths. For a study of the dwarf stars, the estimated values alone suffice for a preliminary investigation. For the giant stars, however, accurate equivalent widths of very strong lines (notably those of *Fe* I) are necessary to fix the curve of growth. These values can be readily obtained from the direct-intensity tracings by Williams and Hiltner or from detailed microphotometric measures.

A comparison of the spectra of α Boötis and 70 Ophiuchi A in the photographic region has shown that:

[35] *Eclipses of the Sun*, p. 342, 4th ed., Columbia University Press, 1935.

[36] *Ap. J.*, **33**, 71, 1911; *Mt. W. Contr.*, No. 50.

APPENDIX

LINES DIFFERING IN INTENSITY BETWEEN α BOÖTIS AND 70 OPHIUCHI A FOR WHICH NO IDENTIFICATION IS GIVEN (WAVE-LENGTH REGION 3900–4808)

λ	Disk	Spot	Int. Diff.	Class	λ	Disk	Spot	Int. Diff.	Class
3899.828	0	.....	2g	.....	4181.977	2	2	2d	B
3901.600	2	2	3d	B	4184.000	4	3	1d	A
3908.276	1	.....	1d?	.....	4190.242	0	1	3g	A
3910.336	2	1	2d	A	4192.574	2	2	3d	B
3913.257	1	1	1d?	B	4194.091	−2	−1	1g	A
3914.015	1	0	1d	A	4207.409	1	0	2d	A
3915.614	3	2	1d	A	4212.978	−1	.....	2g	.....
3917.36	0	0	1g	B	4216.602	1	1	3d	B
3921.189	1	1	3g	B	4220.808	−1	.....	1g	.....
3946.555	0	0	1g	B	4221.174	−1	.....	1g	.....
3959.838	1	1	1d?	B	4221.475	1	1	2d	B
3963.442	1	1	1d	B	4223.098	1	2	3g	A
3992.253	2	2	1d	B	4223.238	−1	0	2d	C
3993.472	−1	.....	3g	.....	4228.108	−2	.....	1g?	.....
3998.475	0	0	2g	B	4228.318	−1	.....	1g?	.....
4020.277	1	1	2d	B	4231.417	−2	.....	1g	.....
4037.124	2	2	1d?	B	4244.249	0	−1	1d	A
4038.481	−1	.....	1g	.....	4245.086	0	−1	2d	A
4043.353	0	0	1d?	B	4253.006	1	1	2d	B
4048.402	−1	.....	2g	.....	4253.212	1	2	2d	C
4049.227	0	0	2g	B	4253.734	0	1	2d	C
4056.455	0	0	4g	B	4256.135	0	0	1g	B
4059.508	0	0	1d?	B	4256.608	0	0	2d	B
4092.001	−1	0	2g	A	4256.814	1	1	2d	B
4096.698	0	1	2g	A	4259.766	0	−1	2d	A
4097.462	−2	−2	2g	B	4322.833	−2	−1	1g	A
4099.056	0	1	3g	A	4324.414	2	2	2d	B
4102.623	−1	−1	1g	B	4326.922	0	−1	1g	C
4104.308	−1	0	2g	A	4328.612	0	0	2d	B
4105.830	−2	1	2g	A	4329.288	0	0	1d	B
4107.298	−1	0	2g	A	4335.275	1	1	1d	B
4114.120	−1	0	3g	A	4346.297	1	1	1d	B
4116.210	−2	.....	2g	.....	4396.067	−1	.....	1d?	.....
4117.590	−1	.....	3g	.....	.155	−1			
4119.056	−2	0	2g	A	4396.435	−1	−1	1d?	B
4125.379	−2	.....	2g	.....	4396.963	1	0	1d?	A
4132.713	1	2	1g?	A	4398.495	0	−1	1d?	A
4134.900	−1	1	1g	A	4401.027	1	1	1d	B
4136.295	−1	.....	2g	.....	4403.189	1	1	1d	B
4141.313	−2	.....	1g?	.....	4406.163	0	0	2g	B
4144.384	−1	.....	1g	.....	4406.999	−1	.....	2g	.....
4145.865	−1	.....	2g	.....	4412.704	−1	.....	1d?	.....
4146.990	2	1	2g	C	4413.123	−1	.....	1d?	.....
4147.214	−1	0	2g	A	4419.281	−1	−2	1d	A
4148.174	−1	.....	2g	.....	4420.288	1	1	2d	B
4148.396	−1	0	2g	A	4422.067	0	0	1d?	B
4148.921	−1	0	2g	A	4425.771	−1	−1	3g	B
4152.914	−1	.....	3g	.....	4430.770	0	−1	1d?	A
4155.055	−1	−1	1g	B	4431.04	−1	−1	1d?	B
4155.525	−1	.....	2g	.....	4431.850	0	0	2d	B
4162.122	−1	.....	2g	.....	4441.094	0	0	1d?	B
4162.464	1	0	1g	C	4480.828	0	0	1d	B
4162.910	−1	−1	1g	B	4499.145	1	1	2d	B
4164.787	0	1	3g	A	4509.744	1	1	1d	B
4169.618	1	1	1d	B	4518.344	1	1	3g	B
4170.147	−1	−1	1g?	B	4532.967	0	0	2d	B
4175.133	1	−1	3d	A	4533.053	0	0		

APPENDIX—*Continued*

λ	Disk	Spot	Int. Diff.	Class	λ	Disk	Spot	Int. Diff.	Class
4550.125	−1	−1	1d?	B	4658.304	0	0	1g?	B
4552.145	0	0	1d	B	4672.336	3	2	3d	A
4557.287	0	−1	2d	A	4673.791	−1	.....	1d	.....
4561.419	1	1	1d	B	4674.101	1	1	1d	B
4567.585	−2	.....	1g	.....	4678.176	3	2	2d	A
4582.313	0	−1	2g	C	4688.690	0	.....	2d	.....
4582.513	−1	.....	1g	.....	4691.601	1	0	2d	A
4584.276	−1	.....	1g	.....	4692.849	−1	.....	1d?	.....
4585.348	0	−1	1d	A	4699.342	3	2	2d	A
4597.387	0	0	1d	B	4716.510	−2	0	1g	A
4603.352	0	1	1g	A	4716.838	−1	0	1g	A
4604.247	−1	0	1g	A	4717.129	−3	.....	1g	.....
4605.596	2	2	1g	B	4751.555	−2	.....	2g	.....
4640.294	1	0	1d	A	4771.472	3	2	1d?	A
4647.960	1	1	1d	B	4783.863	−2	−1	1g	A
4655.795	−1	−1	1g	B	4793.981	−1	−2	1g	C

1. The effects of absolute magnitude are marked for the atoms of *H*, *Na* I, *Ca* I, *Ca* II, *La* II, and the singly ionized rare earths.

2. The weakness of *CN* in α Boötis indicates an unusually low abundance of the molecule and possibly accounts for the anomalous parallax determinations of the star. The relative strengthening of the λ 3883 band of *CN* in the dwarf is startling and at present unexplained.

3. The curve of growth for α Boötis corresponds to an atomic velocity of 3.25 km/sec and a damping factor of $\Gamma/\gamma_0 = 0.8 \times 10^{-6}$.

4. Departure from thermodynamic equilibrium is observed in the spectrum of the giant. The empirical correction formulated by Adams and Russell fits the data satisfactorily.

5. The weighted mean excitation temperature and the electron pressure are 3160° and −3.74 for α Boötis and 4150° and −1.10 for 70 Ophiuchi.

6. The temperatures and electron pressures for the sunspot and 70 Ophiuchi A agree closely. The relative abundances of neutral and ionized atoms disagree systematically.

7. The behavior of several atoms, as well as the data for temperature and electron pressure, suggest a stratification of the elements similar to that in the solar atmosphere.

It is a pleasure to acknowledge my gratitude to Dr. Walter S. Adams, who suggested this problem, provided me with the plates, accorded me the privileges of the Mount Wilson Observatory offices, and showed continued interest in this work. I am also very much indebted to Dr. Paul W. Merrill, who, as adviser, contributed generously in helpful discussion and criticism. I wish to thank Dr. Gerard F. W. Mulders for discussion of the calibration problems, Dr. Leo Goldberg for several suggestions regarding data for the curve of growth, Dr. Rudolph Minkowski for stimulating criticisms of the manuscript, and Drs. Robley C. Williams and W. Albert Hiltner for the use of their direct-intensity tracings prior to publication.

I am grateful to Mr. H. D. Babcock and to Mrs. Charlotte Moore Sitterly for unpublished data which provided numerous changes and additions to the identifications in the Revised Rowland Table. Mrs. Sitterly has also permitted the use of numerous, then unpublished, multiplet designations in the iron and titanium spectra.[37]

This project was made possible through the financial assistance of the Fanny Bullock Workman Fellowship offered by Wellesley College.

[37] *Multiplet Table of Astrophysical Interest*, Princeton, 1945.

THE DIAMETERS OF GLOBULAR CLUSTERS*

ALBERT G. MOWBRAY
Jet Propulsion Laboratory, California Institute of Technology
Received May 10, 1946

ABSTRACT

Estimates of the limiting diameters of sixty-nine globular clusters were made on two homogeneous series of Crossley plates, taken in blue and red light. Surface-brightness profiles and diameters at which the surface brightness falls to one-half or to one-fifth of that at the center were determined for sixty-four clusters. Diameters were determined for circles which would contain the total light of each cluster if the surface brightness were uniformly that of the center of the cluster.

For the estimated limiting diameters of clusters known to be free of interstellar absorption, a loose linear relation was found between the absolute magnitude and the logarithm of the linear diameter. The slope of the correlation line is approximately that to be expected if the clusters all have the same average light-density:

$$-M = 7.5 \log D + \text{constant} .$$

An attempt was made to use this relation for the measurement of the absorption affecting other clusters. The attempt failed, however, partly because of the low degree of correlation between M and $\log D$ and partly from errors in the estimated angular diameters arising from the absorption, from variations in the degree of central concentration of the cluster, and from variations in the richness of the surrounding star field.

No correlation between M and $\log D$ was found for the diameters determined from profiles of the clusters or for the diameters derived from measures of the total light and of the central surface brightness of the cluster. These diameters refer to a small central core of each cluster.

I. INTRODUCTION

The apparent angular diameter of a globular cluster is important in studies of its distance and linear dimensions. Shapley and his associates,[1] have published estimates of the apparent limiting diameters of most of the globular clusters based on plates of different exposure times and taken with telescopes of various apertures and focal lengths. No measures of cluster diameters have been published that made use of red light. The present paper contains estimates of the apparent limiting diameters of most of the globular clusters visible from northern latitudes, made on two homogeneous series of plates, one set in blue light and the other in red light.

The "limiting diameter" (angular or linear) of a globular cluster is a somewhat indefinite quantity, since the density of cluster stars decreases gradually in the outer regions. Attempts have been made to define and to measure more precise parameters for the angular or linear dimensions of a cluster, but no extensive results have been published. "Diameters" based on determinations of the profiles of the central parts of the clusters are included in the present paper, although they are of low precision. Estimates of the degree of concentration of stars toward the centers of the clusters are also included.

Table 1 contains the apparent angular diameters and central concentrations of the globular clusters. "Shapley's Diameter, Direct" is the diameter found by Shapley and Sawyer from eye-estimates on direct photographs,[1] "Shapley's Diameter, Micro." that found by Shapley and Sayer from estimates based on microphotometer tracings of other plates;[1] "Limiting Diameter, Blue, Red," are estimates by the author of images on Crossley plates exposed to blue and red light, respectively (see sec. II); core "0.5" and "0.2" diameters are those at which the surface brightness of the cluster falls to one-half

* *Contributions from the Lick Observatory*, Ser. II, No. 14.

[1] Shapley and Sawyer, *Harvard Bull.*, No. 852, 1927; Shapley and Sayer, *Proc. A.A.S.*, **21**, 593, 1935.

TABLE 1

DIAMETERS AND CONCENTRATIONS OF GLOBULAR CLUSTERS

Globular Cluster NGC	Shapley's Diameter		Limiting Diameter		Core Diameter		C.S.B. Diam.	Concentration	
	Direct	Micro.	Blue	Red	0.5	0.2		Shapley	A.G.M.
288	10′.0	13′.1	12′.4	.....	.....	.....	266″	10	6
1904	3.2	9.4	7.8	5′.1	13″.3	26″.9	.....	5	3
2298	1.8	3.9	4.2	.....	39	68	.....	6	5
2419	1.7	5.1	6.2	1.9	43	67	83	7	5
4147	1.7	2.8	4.1	1.5	7.3	16.2	72	9	4
4590	2.9	.....	9.8	6.5	60	106	.....	10	4½
5024	3.3	15.8	14.4	8.8	46	83	100	5	4
5053	.....	.....	8.9	.....	.....	.....	.....	11	7
5139	23	65.4	.....	.....	205	489	.....	8	.....
5272	9.8	22.1	18.6	13.7	42	80	115	6	3
5466	5.0	.....	9.2	6.7	.....	.....	191	12	7
5634	1.3	.....	3.7	.....	21	45	.....	4	4
5694	.....	.....	2.2	1.1	8.7	19.5	69	.....	3
5824	1.0	10.2	3.7	.....	9.6	17.9	58	1	1
5897	7.3	13.1	8.7	8.0	.....	.....	212	11	6
5904	12.7	25.0	19.9	14.0	49	84	116	5	3
5986	3.7	8.2	6.0	.....	53	95	93	7	3
6093	3.3	14.3	5.1	4.7	9.5	20	76	2	2½
6121	14.0:	26.3	22.8	17.9	88	168	202	9	5
6144	3.3	10.6	6.2	5.6	.....	.....	136	11	6
6171	2.2	9.6	7.8	7.6	56	101	111	10	6
6205	10.0	18.1	23.2	16.0	72	135	187	5	2½
6218	9.3	.....	12.2	10.6	64	120	178	9	5
6229	1.2	5.3	3.8	2.4	16.5	31	53	7:	1½
6235	1.9	9.1	.....	.....	.....	.....	72	10	.....
6254	8.2	21.5	12.2	12.2	73	130	157	7	4½
6266	4.3	14.4	6.3	6.0	15	39	84	4	3
6273	4.3	14.5	5.3	.....	45	89	101	8	5
6284	1.5	8.6	2.7	.....	9	21	64	9:	4
6287	1.7	6.1	2.7	.....	34	60	68	7	6
6293	1.9	8.5	3.5	.....	12	25	88	4	3
6304	1.6	9.4	3.8	.....	24	48	82	6	3
6316	1.1	6.2	2.4	.....	21	40	102	3	5
6325	.....	5.4	1.6	.....	29	47	70	4:	5
6333	2.4	12.2	5.5	4.3	32	64	93	8	4½
6341	8.3	.....	12.2	10.3	22	43	97	4	3½
6342	0.5	4.5	1.3	.....	9	22	83	4	2
6356	1.7	10.4	3.5	4.0	22	46	80	2	4
6366	4:	.....	5.8	.....	.....	.....	.....	11	7
6401	.....	.....	.....	.....	20	43	.....	.....	.....
6402	3.0	.....	6.7	6.8	68	121	121	8	5
6426	1.3	.....	2.2	.....	.....	.....	93	9:	6
6440	0.7	.....	1.7	.....	12	28	44	5	4
6441	2.3	.....	3.0	.....	17	37	65	3	1
6453	0.7	3.6	.....	.....	10	21	.....	4	1

TABLE 1—*Continued*

Globular Cluster NGC	Shapley's Diameter		Limiting Diameter		Core Diameter		C.S.B. Diam.	Concentration	
	Direct	Micro.	Blue	Red	0.5	0.2		Shapley	A. G. M.
6517	0′.4	.....	1′.0	.....	9″	19″	50″	4	3
6522	.....	.....	1.5	.....	10	24	67	6	5
6528	.....	.....	1.2	.....	15	28	79	5	6
6539	1.3	.....	3.5	.....	36	73	97	10:	6
6544	.....	.....	.....	.....	16	40	.....	.....	.....
6553	1.7	6′.6	3.2	.....	56	106	95	11	6
6569	1.4	.....	2.2	.....	32	52	72	8	6
6624	2.0	.....	2.7	.....	10	20	68	6	2
6626	4.7	15.0	.....	4′.7	20	45	84	4	3
6637	2.8	10.0	3.8	.....	32	58	83	5	4
6638	1.4	4.8	2.2	2.0	25	45	69	6	2
6652	1.7	7.4	2.3	.....	9.5	20	65	6:	1
6656	17.3	34.7	17.0	13.6	97	167	242	7	4½
6681	2.5	9.6	4.1	.....	8	16	82	5	4
6712	2.1	.....	.....	3.3	68	89	94	9:	5½
6715	2.1	13.6	5.5	.....	12	24	64	3	2
6723	5.8	12.0	7.5	7.2	67	96	141	7	4½
6760	1.9	.....	2.4	.....	42	70	88	9	6
6779	1.8	7.2	5.0	4.0	45	82	92	10	5
6809	10.0	28.7	14.8	13.8	219	382	.....	11	6
6838	.....	.....	6.1	.....	.....	.....	.....	.....	6
6864	1.9	8.7	4.6	3.1	12	22	65	1	2
6934	1.5	.....	6.2	3.7	27	46	55	8	2½
6981	2.0	8.0	5.1	3.2	39	71	95	9	5½
7006	1.1	.....	2.2	1.2	19	37	69	1	2½
7078	7.4	18.1	12.3	8.6	12	27	77	4	2
7089	8.2	16.9	11.7	12.3	31	60	85	2	2
7099	5.7	10.7	8.9	6.7	9	20	64	5	2½
7492	3.3	.....	4.3	.....	.....	.....	133	12	7

and one-fifth, respectively, of the central surface brightness, according to the author's measures (see sec. III); and "C.S.B. Diam." is the "central surface brightness diameter" discussed in section III. The "Concentration" is a classification of the cluster according to its apparent concentration toward the center (low numbers represent the most concentrated clusters) by Shapley[2] (in 12 classes) and by the author (in 7 classes, the mean of estimates from the plates used for the determination of diameters in blue and red light).

II. ESTIMATED LIMITING DIAMETERS

The plates used for the present estimates of the limiting diameters were taken with the Crossley reflector of the Lick Observatory. Those used for the "blue" diameters were taken by Mayall in 1935 and 1936, mostly on Imperial Eclipse Soft (H & D 850) plates, with exposures of 1 hour. They form a fairly uniform series and reach a limit in apparent photographic magnitude of nearly 20. A few plates[3] were of a slightly faster type; for two

[2] *Star Clusters* ("Harvard Monographs," No. 2), Appen. A, p. 224, Cambridge, 1930.

[3] For NGC 2298, 5986, 6441, 6652, 6723, Imperial H & D 1200 plates, exposed in 1940, were used.

objects—NGC 6426 and NGC 6624—photographs with 2-hour exposures, made in 1908 and 1917, respectively, were used. The "red" diameters were estimated on a series of photographs made by the author during the summer of 1942. These were 1-hour exposures on Eastman *H*-alpha plates behind a Wratten No. 16 ("Flavazine T") filter, the combination recording the wave-length region from 5200 A to 7000 A. The faintest stars on these plates have photographic magnitudes of about $18\frac{1}{2}$.

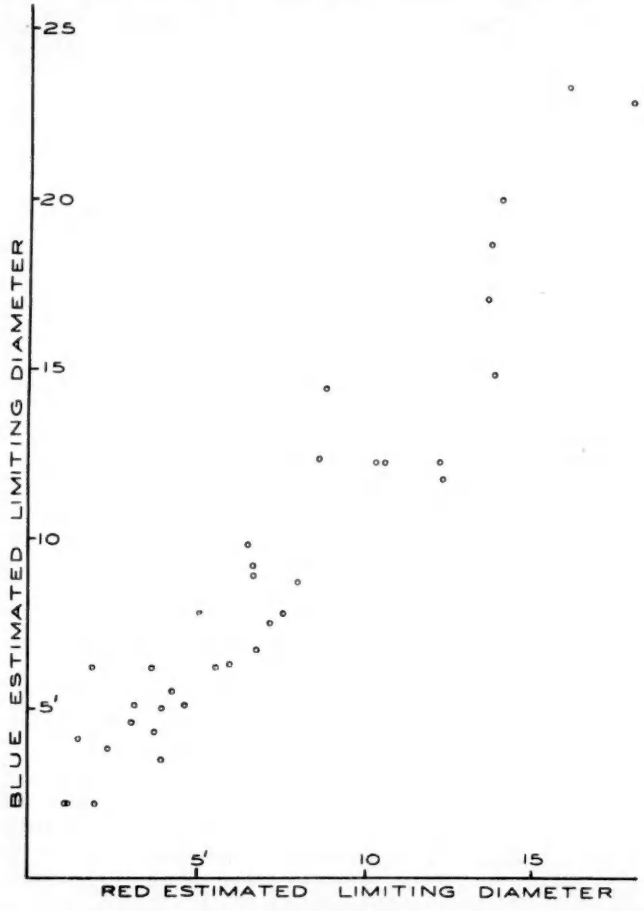

FIG. 1.—Red and blue estimated limiting diameters

In Figure 1 the present red and blue limiting-diameter estimates are plotted against each other. They are well correlated, although, with few exceptions, the red diameters are the smaller, owing mainly to the brighter limiting magnitude of their plates. The present blue estimates are usually smaller than Shapley's estimates obtained with the microphotometer but are larger than his estimates made directly on the plates.

III. PROFILE DIAMETERS

Determination of the profile of a cluster (that is, the surface brightness as a function of the distance from the center) makes possible some precise definitions of the "diameter"

of the cluster. For example, one may choose the diameter within which is included a certain fraction of the total light of the cluster—analogous to probable error in the normal error-curve. This definition has been suggested by Hertzsprung[1] and by De Sitter;[4] but no work has been published making use of it. It has the disadvantage that the outer regions of the cluster, where an intensity profile is likely to be less accurate than near the center, cover a large area and therefore have a large weight in determining the diameter

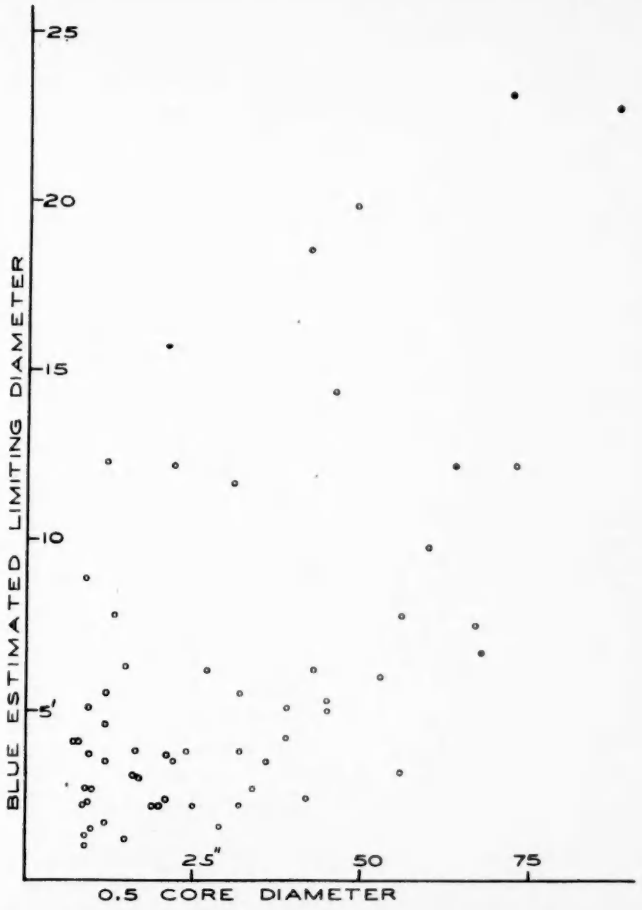

FIG. 2.—0.5 core diameters and blue estimated limiting diameters

when the total light is determined from the profile. If the total light is determined in some other way, systematic errors may easily be introduced.

Another practicable kind of diameter is that at which the surface brightness of the cluster falls to a certain fraction of that at the center. In this case the diameter does not depend on measures in the outer part of the cluster, beyond the diameter determined, but largely upon measures near the center, where the profile is less disturbed by irregularities in star distribution.

Profiles of globular clusters based on numbers of stars rather than on surface bright-

[4] A. de Sitter, *Bull. Astr. Inst. Netherlands*, **5**, 207, 1930.

ness have often been studied, but only for the outer regions of the clusters. If star counts could be carried to the centers of the clusters, profile diameters on either of the foregoing definitions could be determined from them as well as from intensity profiles. The definition proposed by Hertzsprung and by De Sitter might then be better, because it gives greater weight to the outer regions.

In an attempt to make use of the second definition involving intensity profiles, that is to say, to determine the diameter at which the surface brightness falls to a certain

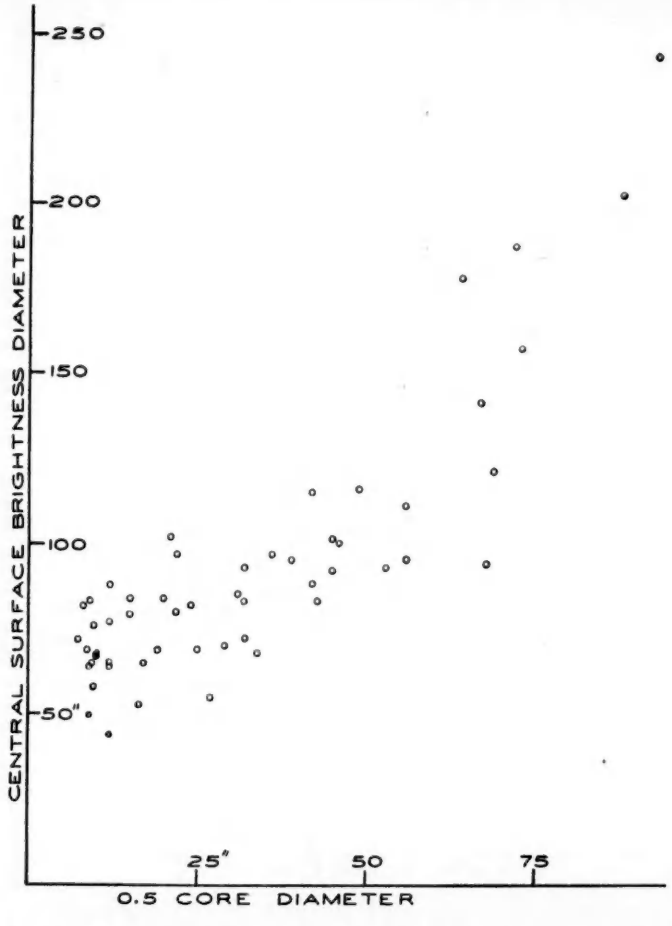

FIG. 3.—0.5 core diameters and central surface brightness diameters

fraction of that at the center, a number of globular clusters were photographed by the author with the Crossley reflector.[5] These were taken on Eastman *H*-alpha plates, with a Wratten No. 29 ("F") filter, with light from about 6000 A to 7000 A. Exposure times, ranging from 3 minutes to 3 hours, were adjusted for each object, so that the central brightness of the cluster lay on the straight-line part of the characteristic curve of the

[5] For the cluster NGC 5139 (ω Centauri), photographs were obtained at Mount Hamilton by Robert T. Smith, who used a small Wright-type flat-field Schmidt camera of his own construction (see *Pub. A.S.P.*, **52**, 355, 1940).

emulsion; some of the poorest clusters were omitted, since the required exposure times would have been too long. The plates were standardized with a tube photometer and were analyzed with a Moll self-registering microphotometer; runs across each plate were made in several position angles in order to reduce errors resulting from the irregularities of star distribution in the cluster. The clusters were assumed to be circular in outline; therefore, for a cluster having appreciable ellipticity, an average profile was found.

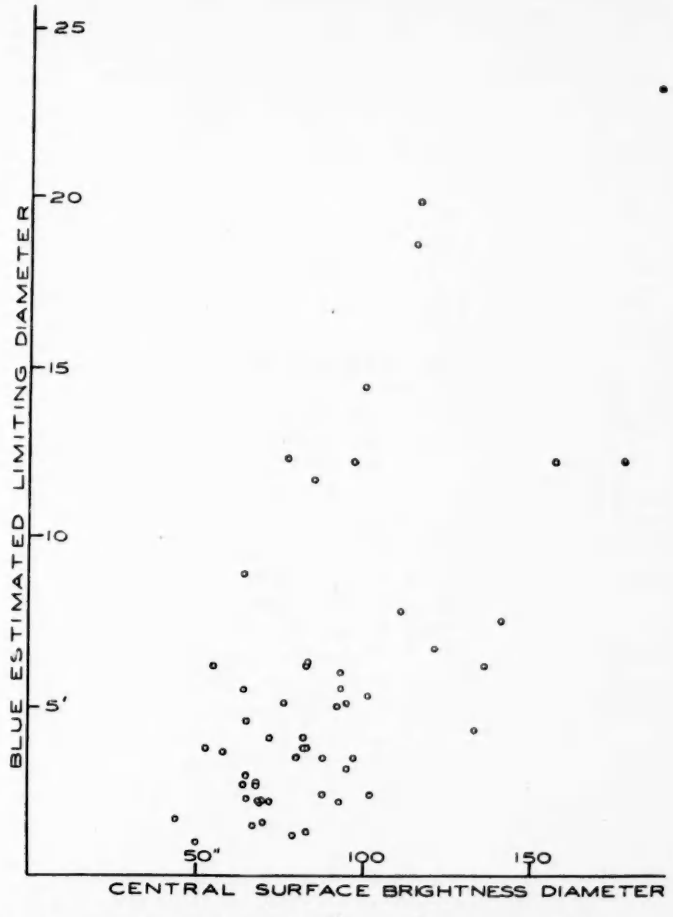

FIG. 4.—Central surface brightness diameters and blue estimated limiting diameters

The complete profiles determined in this way are not tabulated here; but the columns headed "Core 0.5" and "Core 0.2" in Table 1 give the diameters obtained from the profiles at one-half and one-fifth, respectively, of the central intensity. It is seen that these "diameters" are much smaller than the estimated limiting diameters, being measured in seconds of arc rather than in minutes. Thus they refer wholly to the central parts of the clusters and may reasonably be termed "core diameters." In Figure 2 the 0.5 core diameters are plotted against the blue estimated limiting diameters; the correlation is very poor.

Another possible definition for the diameter of a globular cluster is the diameter of a circle assumed to be uniformly as bright as the central part of the cluster and to contain the same total light as the cluster—somewhat analogous to the "equivalent width" of a spectral line. A diameter of this kind can be calculated if the total light and central surface brightness of the cluster are known. Column "C.S.B." in Table 1 gives such diameters, calculated from Christie's[6] apparent integrated magnitudes and from photoelectric measures by Stebbins and Whitford[7] of the central surface brightnesses. The

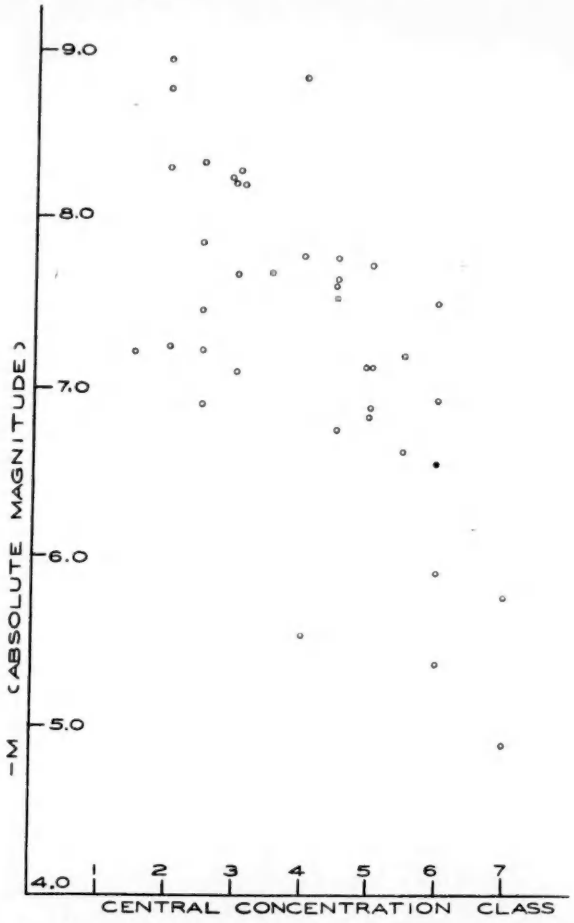

FIG. 5.—Central concentration class and absolute magnitude

latter measures, however, give the average surface brightness over a considerable central area, and hence they only approximate the true central surface brightness; therefore, the C.S.B. diameters are systematically too large for the smaller clusters, and they approach the true value only for the largest objects. This condition is indicated in Figure 3, where the C.S.B. diameters are plotted against the 0.5 core diameters. Figure 4 shows the lack of close correlation between the C.S.B. diameters and the blue estimated limiting diameters.

While neither the core diameters nor the C.S.B. diameters correlate satisfactorily

[6] *Ap. J.*, **91**, 8, 1940; *Mt. W. Contr.*, No. 620. [7] *Ap. J.*, **84**, 132, 1936; *Mt. W. Contr.*, No. 547.

with estimates of limiting diameter, they seem to be somewhat related to each other, at least among the larger objects for which the C.S.B. diameters have some significance. The core diameter will depend considerably on the height of the central peak of the cluster profile, as will the C.S.B. diameter if it is properly determined by using the surface brightness of a sufficiently small central area. The height and sharpness of this central peak of intensity vary greatly from cluster to cluster. Both C.S.B. and core diameters measure the size of a small part of the cluster around this central peak and might be expected to be more closely related with each other than with diameters of the broad outer regions, such as estimated limiting diameters. The ratio between the limiting diameter and the core diameter will be considerably affected by the degree of central concentration of the cluster and may, in fact, be used as a measure of the degree of central concentration. A good degree of correlation appears in plots of this ratio against the estimated central concentration.

It may be worth while to point out here that a fairly definite correlation appears to exist between the central concentration of a cluster and its absolute integrated magnitude, in the sense that the highly concentrated clusters are brighter (see Fig. 5).

IV. HYPOTHESIS OF CONSTANT AVERAGE LIGHT-DENSITY IN GLOBULAR CLUSTERS; AMOUNT OF ABSORPTION AFFECTING OBSCURED CLUSTERS

For a globular cluster situated so as to be free of interstellar absorption, we may observe directly the true total apparent magnitude, m; distance modulus, y; and angular diameter, d. In general, however, the observed values m', y', and d' of these quantities may be affected by interstellar absorption. If the amount of absorption is a (in magnitudes), the cluster will appear to be fainter and more distant:

$$m' = m + a \ ,$$

$$y' = y + a \ .$$

Simple eye estimates of angular diameter may be affected by interstellar absorption, since the outer parts of the cluster may be lost among foreground stars not equally obscured. But apparent diameters based on intensity profiles should be free from effects of absorption, which will lower the whole profile but will not alter its shape; for such diameters $d' = d$. However, the linear diameter D' (in parsecs) derived from this angular diameter and the observed modulus will be in error because of the effect of absorption on the modulus:

$$\log D' = \log d + 0.2\, y' + 1 \ .$$

(In this formula the angular diameter, d, is in radians; if d is expressed in minutes of arc, the numerical term is -2.54; if in seconds of arc, -4.31.) The true linear diameter, D, is given by

$$\log D = \log d + 0.2\, y + 1 \ .$$

As the true modulus is $y = y' - a$, we have

$$\log D = \log d + 0.2\,(y' - a) + 1 \ .$$

Therefore, the logarithm of the ratio of the directly determined linear diameter, D', to the true linear diameter, D, measures the amount of absorption present:

$$\log D' - \log D = \log D'/D = 0.2\, a \ .$$

The total absolute magnitude, M', of a cluster determined from the *observed* modulus and the *apparent* magnitude will *not*, however, be affected by absorption, for it is equal to the true total absolute magnitude, M:

$$M' = m' - y' = (m + a) - (y + a) = m - y = M \ .$$

TABLE 2

OBSERVATIONAL DATA FOR SELECTED GLOBULAR CLUSTERS

Globular Cluster (NGC)	Gal. Lat. (b)	App. Mag. (m')	Dist. Mod. (y')*	Abs. Mag. ($-M$)	Color Excess (E)	Number of Nebulae		Log Linear Diameter (D' in Parsecs)		
						Baade	Mayall	Blue	Red	Shapley†
288 s‡	−88°	$8^m.96$	$15^m.87$	$6^m.91$	$0^m.00$	.....	8	1.73	.....	1.75
1904 s	−28	8.39	16.61	8.22	.....	.....	30	1.68	1.49	1.76
2419 s	+23	11.51	19.32 v§	7.71	−0.15	N‖	87	2.10	1.58	2.01
4147 s	+79	11.01	16.55 v	5.54	+0.02	N	48	1.39	0.95	1.22
4590 s	+36	9.12	15.87 v	6.75	.....	.....	34	1.63	1.45	.....
5024 s	+79	8.68	16.45 v	7.77	0.00	N	65	1.91	1.70	1.95
5139	+15	5.1	14.15 v	9.05	.....	.....	.....	.....	.....	.....
5272 s	+78	7.21	15.48 v	8.27	0.05	N	50	1.82	1.69	1.90
5466 s	+72	10.39	16.16	5.77	0.05	N	25	1.66	1.52	.....
5694 s	+30	10.87	17 97	7.10	0.02	N	39	1.40	1.10	.....
5897	+29	9.61	16.16	6.55	0.05	N	4	1.63	1.60	1.81
5904 s	+46	7.04	15.26 v	8.22	0.05	N	63	1.81	1.66	1.91
6093	+18	8.39	16.24	7.85	0.10	F	6	1.42	1.39	1.87
6121	+15	7.41	14.29 v	6.88	0.22	0	1	1.67	1.57	1.73
6144	+15	10.85	16.22	5.37	0.15	.....	0	1.50	1.45	1.73
6177	+22	10.10	16.00 v	5.90	0.44	0	3	1.55	1.54	1.64
6205 s	+40	6.78	15.10 v	8.32	0.08	N	30	1.65	1.69	1.74
6218 s	+25	7.95	15.07	7.12	0.13	N	18	1.56	1.50	.....
6229 s	+40	10.29	17.46 v	7.20	0.07	N	56	1.53	1.33	1.68
6254	+22	7.64	15.17	7.53	0.19	0	0	1.58	1.58	1.83
6266	+ 7	8.16	16.37 v	8.21	0.27	0	0	1.53	1.51	1.89
6333	+10	8.92	16.70	7.78	+0.24	0	1	1.54	1.44	1.89
6341 s	+35	7.30	14.98 v	7.68	−0.02	N	43	1.55	1.48	.....
6356	+ 9	9.68	18.51	8.83	+0.32	0	0	1.71	1.76	2.18
6402	+14	9.44	16.56	7.12	0.32	0	0	1.60	1.60	.....
6626	− 7	8.48	16.14	7.66	0.29	.....	0	.....	1.37	.....
6638	− 7	10.24	17.48	7.24	0.24	.....	0	1.26	1.21	1.59
6656	− 9	6.48	14.12 v	7.64	0.19	0	0	1.51	1.42	1.82
6712	− 6	9.98	17.17	7.19	0.32	0	0	.....	1.41	.....
6723	−19	7.75	15.37 v	7.62	0.03	.....	.....	1.41	1.39	1.62
6779	+ 8	9.55	16.39	6.84	+0.07	N	.....	1.44	1.34	1.60
6809	−25	7.08	14.58	7.50	−0.02	.....	4	1.55	1.52	1.84
6864 s	−27	9.50	18.43	8.93	+0.15	N	16	1.81	1.63	2.08
6934 s	−20	10.01	16.91	6.90	0.07	N	15	1.69	1.47	.....
6981 s	−34	10.24	16.86 v	6.62	0.07	N	15	1.54	1.34	1.74
7006 s	−21	11.45	18.91 v	7.46	0.02	N	50	1.59	1.32	.....
7078 s	−28	7.33	15.63 v	8.30	0.00	N	20	1.67	1.52	1.92
7089 s	−36	7.30	16.07 v	8.77	+0.03	N	25	1.75	1.77	1.94
7099 s	−48	8.58	15.80	7.22	−0.05	N	27	1.58	1.45	1.86
7492 s	−64	12.33	17.22	4.89	−0.20	N	33	1.54	.....	.....

* Sources for the distance moduli:

NGC
2419.... Baade, *Ap. J.*, **82**, 396, 1935; *Mt. W. Contr.*, No. 529.
4147.... Baade, *A.N.*, **239**, 353, 1930.
5024.... Grosse, *A.N.*, **246**, 379, 1932.
5694.... Baade, *Pub. A.S.P.*, **46**, 52, 1934.
6171.... Oosterhoff, *Bull. Astr. Inst. Netherlands*, **8**, 273, 1938.
6229.... Baade, *Mt. W. Ann. Rept.*, 1935–36; a slightly revised value is given in *Ap. J.*, **102**, 17, 1945; *Mt. W. Contr.*, No. 706.
6341.... Nassau, *Ap. J.*, **87**, 361, 1938; and Hachenberg, *Zs. f. Ap.*, **18**, 49, 1938.
7089.... Sawyer, *Pub. Dom. Ap. Obs. Victoria*, **6**, 265, 1936.

For all others see Shapley, *Handb. d. Ap.*, **2**, 741, 1933; or *Star Clusters* ("Harvard Monographs," No. 2), p. 158, 1930.

† From microphotometer tracings.

‡ "s" = Standard object, not seriously affected by obscuration.

§ "v" = Distance modulus determined from variable stars.

‖ "N" = Normal number; "F" = few; "0" = none.

Therefore, if a relation can be found between the absolute magnitude and the linear diameter of the cluster, we can determine the true value of the linear diameter free from the effects of absorption even for the obscured clusters. Such a relation might be found through study of clusters known to be free of obscuration, for which $D' = D$; this relation could then be used to determine the true linear diameter, D, for an obscured cluster from its known M.

If the average light-density is the same for all the globular clusters, the following relation exists between the absolute magnitude, M, and the linear diameter, D, of the cluster:[8]

$$-M = \text{constant} + 7.5 \log D .$$

The various diameters given in Table 1 of the present paper have been used to test the existence of this relation. It was found to hold only in a statistical sense for the estimated limiting diameters of clusters known to be largely unaffected by absorption. Attempts by the method described above to determine the amount of absorption for obscured clusters proved fruitless however, since in a number of cases negative absorptions were obtained. For the diameters depending on profiles of the clusters or on the central surface brightness and total magnitude no correlation between M and log D was found; this negative result may be related to the fact that these diameters refer only to the extreme central parts of the clusters.

Clusters may be judged to be largely unobscured if they satisfy three criteria: (1) the galactic latitude is greater than 20°; (2) normal numbers of extra-galactic nebulae appear in the field; and (3) the cluster is not appreciably redder than other clusters. Table 2 shows the basis for the selection of unobscured objects used as standards, indicated with "s" after the NGC number for those globular clusters which satisfy the foregoing conditions. The color excesses (E) are those reported by Stebbins and Whitford[7]; the counts of nebulae according to Baade are those given in the same paper; and the numbers of nebulae according to Mayall are unpublished counts on the plates used for the estimates of limiting diameters in blue light. The distance moduli are mainly those given by Shapley in *Star Clusters* and *Handbuch der Astrophysik*, with some from other sources, as noted in the footnotes to Table 2. For 19 objects the moduli were determined from studies of variable stars in the clusters. In order to have enough objects, 21 moduli were used, which were based on studies of the magnitudes of the brightest stars in the clusters, even though such moduli are not so accurate as those based on variable stars. The apparent total magnitudes are those published by Christie,[6] who determined them at Mount Wilson with a schraffierkassette attached to a 10-inch refractor.

Table 2 also gives values for M and log D, the latter for the blue and red estimated limiting diameters, and for Shapley's determinations with the microphotometer. A plot of M against log D is given in Figure 6 for the blue estimated limiting diameters of the clusters selected as standards unaffected by serious obscuration; the plots for the red diameters and for Shapley's diameters are generally similar. Least-squares solutions were made for the best straight lines through the M versus log D plots for these diameters for the standard objects; the results are:

Blue limiting diameters : $\quad -M = -4.88 + 7.36 \log D ,$

Red limiting diameters : $\quad -M = +0.64 + 4.58 \log D ,$

Shapley (microphotometer) : $\quad -M = -2.17 + 5.43 \log D .$

[8] To derive this relation, we note that the volume of the cluster is proportional to D^3; and therefore, if the average spatial light-density is the same for all clusters, the total luminosity, L, is proportional to D^3, and the absolute magnitude, $M = -2.5 \log L$, becomes equal to $-7.5 \log D$ plus a constant.

The correlation coefficients for the three plots are 0.52, 0.70, and 0.60, respectively. The slope of the correlation line conforms fairly well to that expected from the relation for constant average light-density for the blue diameters, although these data give the smallest correlation coefficient of the three. The other two groups of data, with somewhat better correlations between M and log D, depart widely from the assumed constant average density relation. The blue diameters probably have the faintest limiting magni-

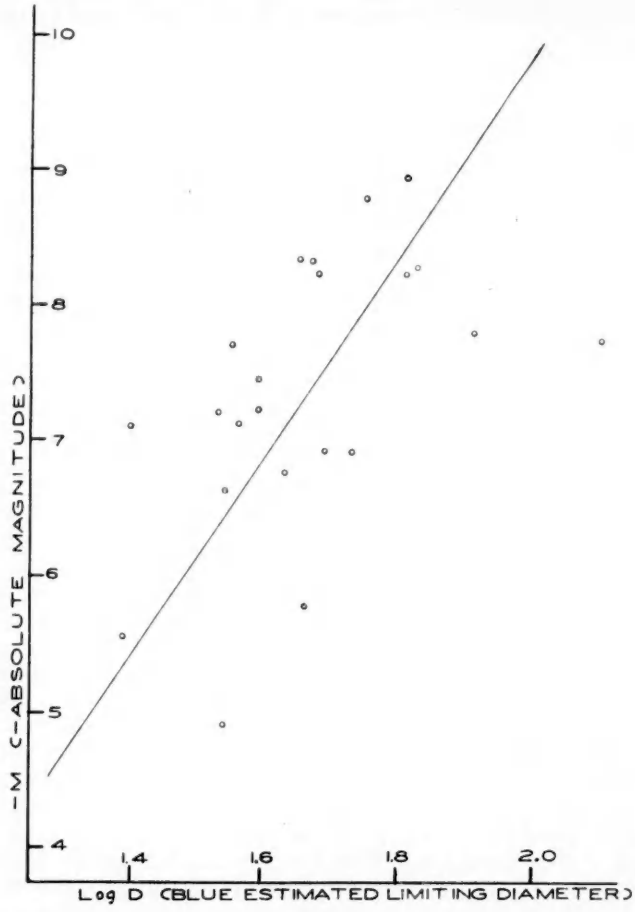

FIG. 6.—Linear diameter and absolute magnitude for blue estimated limiting diameters

tude of the three. Very poor correlation between M and log D was shown for the central surface brightness diameters or for the 0.5 or 0.2 core diameters; and no correlation lines were computed for them.

Even though the correlation line found is much different from that resulting from the hypothesis of constant average light-density, it could still be useful for a determination of the amount of absorption affecting obscured clusters, provided that the relation were sufficiently close. However, attempts to use the above relations for that purpose were not successful. When the true linear diameter, D, of an obscured cluster was obtained from the M versus log D relation, it was often larger than the value D' derived directly

from the observed distance modulus, y', and angular diameter, d', as if the cluster were affected by a *negative* absorption. This anamolous result is due largely to the looseness of the relation between M and log D and partly to the influence upon the estimated angular diameters of the rich star fields, in which a number of the obscured clusters are located. In these cases the limiting diameters are judged too small, and the resulting apparent linear diameters actually may be smaller than the true linear diameters, even though the former are calculated with distance moduli made too large by the effects of absorption. It would not be practicable to improve the situation by restricting our study to clusters in sparse star fields; for richness of star field is closely correlated with galactic latitude and therefore with amount of absorption—the clusters in rich star fields are just those for which a measure of the absorption is most needed. The variation in the degree of central concentration adds to the difficulty of obtaining correct values of angular diameters of the clusters seen among a collection of foreground stars.

V. CONCLUSIONS

It is somewhat doubtful whether estimated diameters of globular clusters will be of much use for determinations of their distances. It has sometimes been assumed that all globular clusters have the same linear dimensions, but this is actually far from the truth. For example, according to the author's estimates with blue light, the largest cluster—NGC 2419—has a linear diameter of 126 parsecs, and the next largest—NGC 5024—a diameter of 81 parsecs; while the two smallest—NGC 6638 and NGC 4147—have diameters of 18 and 25 parsecs, respectively. Average clusters, like NGC 6402 or NGC 7006, have diameters of about 40 parsecs. The ratio of the largest diameter to the smallest is 7.

If there were a close relation between absolute magnitude and linear diameter, then there would be some hope of using diameters to determine true distances. But the relation found for estimated limiting diameters is not close enough for the determination of the absorptions affecting individual clusters, and distances obtained by its use would be valid only for the average of a considerable number of clusters. Furthermore, estimated limiting diameters are much affected by such factors as central concentration of the clusters and the richness of the surrounding star fields.

Even a statistical relation between linear diameter and absolute magnitude does not appear to exist for the other types of diameters treated in this paper, and they also show a large range between extremes of size. They have therefore not proved to be useful in determining distances for obscured clusters. Progress could be made if a method were developed to obtain for a cluster a precise measure of the angular diameter which would lead to a close relation between linear diameter and integrated absolute magnitude.

An interesting by-product of the present investigation is the fact that the more highly concentrated clusters seem to be of greater luminosity, as shown in Figure 5.

The present work was done during the years 1940–1942, while the author was a graduate student and assistant at the Lick Observatory of the University of California at Mount Hamilton. The author is indebted to Dr. N. U. Mayall for much advice and assistance in the course of the work and also to Dr. J. H. Moore and Dr. R. J. Trumpler for many helpful suggestions and criticisms. I also wish to thank Dr. W. H. Wright, then director of the Lick Observatory, for making possible the use of the Crossley telescope in this investigation and for the Lick Observatory Fellowship granted during part of the time.

THE DISTRIBUTION OF BRIGHTNESS AT THE EXTREME LIMB OF THE SUN

ZDENĚK KOPAL
Harvard College Observatory
Received April 4, 1946

ABSTRACT

The distribution of brightness at the extreme limb of the sun (i.e., over the last 1 per cent of its radius) is determined from a variation of integrated luminosity of the narrow solar crescent, as observed by the Dutch solar eclipse expedition at Beloretchenskaya, U.S.S.R., on June 19, 1936, during the last minute before totality.

After a brief introduction (Sec. I) it is pointed out that a reduction of the fundamental integral equation (1) of our problem to Abel's form, as suggested previously by Heckmann and Siedentopf, is legitimate only under certain special conditions, which are unlikely to be met in practice (Sec. II). A new and more straightforward method for solving our integral equation is then developed (Sec. III) and applied to photometric data secured by the Dutch observers at the 1936 eclipse (Secs. IV and V).

The principal result of the present study is a demonstration that, in the light of effective wave length of 4540 A, the solar surface brightness remains finite and equal to approximately 21 per cent of central intensity up to the very limb of the sun. Second, the rate with which this surface brightness falls off between 99 and 99.8 per cent of solar semi-diameter turns out to be considerably less than the average decrease over the central parts of the apparent solar disk.

I

A discovery of the variation of brightness over the apparent disk of the sun followed shortly after the invention of the telescope. Luca Valerio of the Academy dei Lincei in Rome seems to have been the first man on record to have noticed that the central parts of the sun appear brighter than its limb. Curiously enough, the reality of this phenomenon was contested by Galileo Galilei in a letter to Prince Cesi on January 25, 1613.[1] Father Scheiner, however, fully admitted it and devoted some columns of his bulky *Rosa Ursina*[2] to the attempt to find its appropriate explanation. We should not scrutinize too closely his early speculations or those of Laplace, who returned to such attempts almost two hundred years later.[3] The physical theory of solar-limb darkening was not put on a solid basis until the relatively recent pioneer work of Schwarzschild[4] in 1906; and ever since this date the distribution of brightness over the apparent disk of the sun has been of primary importance for testing various consequences of the theory of radiative equilibrium of stellar atmospheres.

For the central part of the sun's disk (up to approximately 95 per cent of its radius) trustworthy information on solar darkening can be obtained by direct measurements.[5] In the early days of research the prevalent opinion derived from such measures was that solar light decreases gradually toward the limb to about 20–50 per cent of the central intensity (depending on the wave length), whereupon it abruptly drops to zero.[6] More recently, however, the measures of Moll, Burger, and Van der Bilt[7] have suggested that solar brightness increases nearly linearly from zero at the limb over at least 1 per cent of the radius, and probably longer. The same conclusion was reiterated by Kienle and

[1] *Opera*, **6**, 198.

[2] **4**, 618.

[3] *Mécanique céleste*, **10**, 323.

[4] *Göttinger Nachrichten*, No. 41, 1906.

[5] Cf., e.g., Abbot, Fowle, and Aldrich, *Ann. Ap. Obs. Smithsonian Inst.*, **4**, 221, 1922.

[6] Vogel, *Sitz.-Ber. Preuss. Akad. Wiss.*, 1877, p. 104.

[7] *B.A.N.*, **3**, 83, 1925.

Juška.[8] Nevertheless, one important circumstance is likely to cast doubt upon the results of all these investigators: namely, as we approach the limb, direct measurements are affected by scintillation due to the terrestrial atmosphere, which causes the well-known "boiling" of the solar edge and is bound to blur any fine details near the extreme limb. Fortunately, in the very region in which direct measurements seem to be destined to fail, an indirect method comes to our help. Julius[9] was the first to point out that, during a total eclipse of the sun, observations of the remaining light of a narrow solar crescent visible shortly before the beginning (or after the end) of totality can be utilized to determine the distribution of brightness over the visible lune, in a way which avoids to a large extent the disturbing effects of atmospheric scintillation Thus, direct measures over the central parts of the disk and observations during an eclipse can supplement each other in the determination of the complete variation of solar surface brightness from its center to the limb.

Minnaert[10] applied Julius' proposal to a series of thermoelectric measures of integrated sunlight secured by Julius and Moll[11] during the total eclipse in 1916, as well as to other more fragmentary pieces of available observational evidence, and he concluded that solar brightness remains finite at the limb (i.e., that a steep decrease toward zero, if real, is restricted to the last thousandth of solar semi-diameter). More recently, extensive and accurate observations of the brightness of the solar crescent near totality were obtained in two effective wave lengths by Ferwerda, Uitterdijk, and Wesselink during the eclipse in 1936 and were discussed by Wesselink.[12] This investigator has assumed the brightness in the neighborhood of the solar limb to vary as z^{α}, where z denotes the distance from the limb, and to be concentrated on the determination of the constant α. This adopted law of darkening leads a priori to a zero intensity at the limb; but it is noteworthy that Wesselink found the decrease of light over the last 5 per cent of the solar radius to be two to three times *less* rapid than the variation of light over the central part of the disk.[13]

The darkening of the sun at its extreme limb is a very important astrophysical datum, and the Dutch series of measures from 1936 represents by far the best existing piece of observational evidence from which such information can be derived. Unfortunately, the method used by Wesselink for the reduction of his data cannot be regarded as wholly satisfactory. The objection can be raised that both Minnaert and Wesselink have biased their investigations from the outset by having presumed, a priori, a certain analytical form for the variation of solar brightness near the limb and have limited themselves to a determination of constants characterizing their adopted law. Wesselink himself noticed that the O − C residuals of his investigation indeed revealed a systematic run, which suggests that a law of darkening of the form z^{α}, with α independent of z, is too simple a representation of reality.[14]

The aim of the present paper will therefore be to rediscuss the Dutch observations made during crucial phases of the total eclipse in 1936, by a new method which does not impose any initial restrictions on the form of the intensity variation that we seek to determine. We shall confine our principal attention to the extreme limb of the sun (i.e., to the region covering the last per cent of apparent solar semi-diameter), with the intention of ascertaining whether or not its surface brightness remains finite—or, in more precise terms, whether the region in which solar brightness eventually falls off to zero is of finite width or whether its width is immeasurably small. The conclusions arrived at in the course of this investigation have already been summarized in the abstract; in what follows we are merely going to substantiate them by presenting our argument in detail.

[8] *Zs. f. Phys.*, **47**, 426, 1928.

[9] *Ap. J.*, **23**, 312, 1906.

[10] *M.N.*, **89**, 197, 1929.

[11] *Ap. J.*, **37**, 225, 1913.

[12] *B.A.N.*, **9**, 81, 1940.

[13] *Ibid.*, p. 98.

[14] *Ibid.*, p. 97.

II

The basic idea of Julius' proposal to deduce solar-limb darkening from eclipse observations may be expressed in mathematical language as follows: Let r_1 and r_2 denote the apparent radii of the sun and moon, respectively; δ, the instantaneous apparent separation of centers of both components; and $J(r)$, the radially symmetrical distribution of brightness over the apparent solar disk. It follows, then, from simple geometry (cf. Fig. 1) that, during a partial eclipse, the remaining light $l(\delta)$ of the visible portion of the sun can be expressed as[15]

$$l(\delta) = 2\int_{r_2-\delta}^{r_1} J(r)\, r \cos^{-1}\frac{r_2^2 - r^2 - \delta^2}{2\delta r}\, dr\,, \qquad (1)$$

which represents an integral equation, of the Volterra type, relating the unknown function $J(r)$ with the observed light-changes $l(\delta)$. Unfortunately, no rigorous solution of

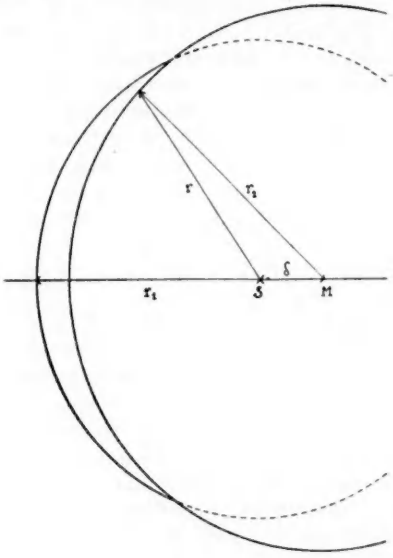

FIG. 1

equation (1) as it stands can so far be given. Heckmann and Siedentopf[16] have previously pointed out that, if certain plausible simplifications are introduced in the kernel of equation (1), this equation may be reduced to Abelian form, which admits of a formal inversion. Their procedure contains, however, a flaw which appears to render it invalid. As this flaw is not quite obvious and has so far escaped attention, it seems appropriate to point it out now and, in so doing, to demonstrate the consequent limitations of the whole procedure.

Heckmann and Siedentopf started from the premise that, during total eclipses, the apparent solar radius is only slightly smaller than that of the moon, so that $(r_2 - r_1)$

[15] Strictly speaking,we ought to add to the right-hand side of equation (1) a constant representing the light of the solar corona and such outer layers as are not eclipsed by the moon. The amount of this light is, however, so small in comparison with that of the solar crescent at almost any phase that we may safely ignore it.

[16] *Göttingen Veröff.*, No. 8, 1929.

will generally be a very small quantity. If, furthermore, we consider only phases in the neighborhood of totality, then $(r_1 - r)$ as well as δ will likewise be small (in comparison with apparent solar radius); and, neglecting the second and higher powers of all small quantities, we may replace

$$\cos^{-1} \frac{r_2^2 - \delta^2 - r^2}{2\,\delta\, r} \tag{2}$$

by

$$\cos^{-1} \frac{r_2 - r}{\delta}. \tag{3}$$

If we make this substitution in equation (1) and differentiate with respect to δ, equation (1) can readily be reduced to Abel's form.

An approximation of equation (2) by equation (3) is, unfortunately, of too restricted validity to be useful in practice. Heckmann and Siedentopf noticed, however, that the Abelian character of our equation remains unchanged if we approximate equation (2) by means of an expression of the form

$$f(r)\, g(\delta)\, \cos^{-1} \frac{r_2 - r}{\delta}, \tag{4}$$

which, by a suitable choice of f and g, can be made to simulate equation (2) over a much wider portion of the eclipse. Heckmann and Siedentopf devised a rather lengthy and elaborate process by which f and g may be determined. A simpler analysis[17] shows that, for instance,

$$f(r) = \left(\frac{r_2}{r_1}\right)^{1/2} \left(1 + \frac{r - r_1}{\pi r_1}\right), \tag{5}$$

and

$$g(\delta) = \left(1 + \frac{\delta - \delta_0}{\pi r_1}\right), \tag{6}$$

where $\delta_0 = r_2 - r_1$ offers a very satisfactory approximation.[18] If we adopt it and abbreviate

$$\frac{l(\delta)}{g(\delta)} = L(\delta)\ ,$$

and

$$rJ(r)\, f(r) = R(r)\,,$$

equation (1) may readily be re-written as

$$L(\delta) \doteq 2 \int_{r_2 - \delta}^{r_1} R(r)\, \cos^{-1} \frac{r_2 - r}{\delta}\, dr\ . \tag{7}$$

Now change over to a new independent variable, x, defined by

$$x = (r_1 - r)(2r_2 - r_1 - r)\,, \tag{8}$$

and differentiate equation (7) with respect to δ; we obtain

$$\delta \frac{\partial L}{\partial \delta} = \int_0^h \frac{R(x)\, dx}{(h - x)^{1/2}}, \tag{9}$$

[17] Based on an expansion of equation (2) in a Taylor series of two variables.

[18] In the case which we shall discuss later (Secs. IV and V), equations (5) and (6) combined with equation (4) are found to approximate equation (2), with an error not exceeding two units of the fifth place.

where

$$h = \delta^2 - \delta_0^2 = \delta^2 - (r_2 - r_1)^2 .$$

This equation is equivalent to equation (13) of the investigation by Heckmann and Siedentopf already referred to.[16] It is to be stressed, however, that equation (9) is *not* Abel's integral equation in the strict sense; for this would require that[19]

$$\delta \frac{\partial L}{\partial \delta} = 0 \qquad \text{when} \qquad h = 0 , \tag{10}$$

i.e., that the light-curve of a total solar eclipse be tangent to the δ-axis at the moment of inner contact. Physical considerations make it a very remote possibility that this condition could be met in reality.[20]

Generalized Abel's equations of the form (9), but for which condition (10) is not fulfilled, have been studied by Goursat,[21] who found that such equations possess a *discontinuous* solution of the form

$$R(x) = \frac{1}{\pi x^{1/2}} \left\{ \delta \frac{\partial L}{\partial \delta} \right\}_{\delta = \delta_0} + \frac{1}{\pi} \int_0^x \frac{\partial}{\partial h} \left\{ \delta \frac{\partial L}{\partial \delta} \right\} \frac{dh}{(x-h)^{1/2}} . \tag{11}$$

The discontinuity of $R(x)$ at $x = 0$ represents by itself no fundamental difficulty; for the actual distribution of brightness at the limb may well be so discontinuous. A very serious practical objection arises, however, from the fact that, as we approach the limb and $x \to 0$, the first term on the right-hand side of equation (11) increases beyond any limit, which means that, if the left-hand side is to remain finite, the integral in equation (11) must tend to offset the first term. In other words, as $x \to 0$, $R(x)$ will be given as a difference[22] of two steadily increasing quantities, each of which involves observational data and is affected by their uncertainty. Consider, in particular, the term factored by $x^{-\frac{1}{2}}$. The value of $\partial L/\partial\delta$ at $\delta = \delta_0$ must be inferred (or rather extrapolated) from a smooth curve drawn freely to follow the course of individual observations and will thus be known within certain empirical error. At a distance of 1 per cent from the limb, a division by $\sqrt{x}$ will magnify the absolute value of this error roughly one hundred times; at a distance of one-tenth of a per cent, a thousand times. This makes it evident that no results of any significance can be obtained in this way. The failure of the German astronomers to notice this can be directly traced back to condition (10). Heckmann and Siedentopf proceeded on the tacit assumption that, in their notations, $G(\mu^2) = 0$, without mentioning it or realizing its improbable physical implications; and when this assumption is dropped, the second part of their equation (14) becomes incomplete[23]—equation (11) of the present paper being its correct version.

III

An attempt to solve the fundamental equation (1) of our problem by means of Abel's integral theorem having ended in a failure, another way of approach must be sought. In what follows, a method will be devised which should enable us to obtain a solution of

[19] Cf., e.g., Whittaker and Watson, *Modern Analysis*, p. 229, Cambridge, 1920.

[20] The reader may notice that equation (10) would also be satisfied, regardless of the slope of the light-curve, if both the apparent disk of the sun and the moon were exactly equal in size and the eclipse were consequently central. The likelihood of such an eclipse is, however, too small; and any slightest departure from prescribed conditions would completely spoil the picture.

[21] *Acta math.*, **27**, 131, 1903.

[22] If the observed light-curve is convex with respect to the δ-axis—as it is likely to be in reality—the two terms on the right-hand side of equation (11) will be of opposite signs.

[23] It should also be pointed out that the upper limits of both integrals in this equation should read z, not δ.

equation (1) numerically. This method, which is believed to be new, provides us with a rather powerful tool for solving equation (1), as well as certain other types of Volterra integral equations of astrophysical interest with a minimum of effort, and it may be outlined as follows:

Let us return to equation (1) and change over to a new dimensionless variable, x, defined by

$$r_1 - r = D r_1 (1 - x) , \tag{12}$$

where

$$D = \frac{\delta + r_1 - r_2}{2 r_1} . \tag{13}$$

By virtue of this substitution, equation (1) readily takes the form

$$I(\delta) = 2 r_1^2 D \int_{-1}^{+1} f(\delta, x) K(\delta, x) \, dx , \tag{14}$$

where

$$K(\delta, x) = [1 - D(1 - x)] \cos^{-1} \frac{r_2^2 - \delta^2 - r^2}{2 \delta r} , \tag{15}$$

and $f(\delta, x) \equiv J(r)$. Now let us replace the integral on the right-hand side of equation (14) by a summation of a finite number of terms by means of some formula for numerical integration and write

$$I(\delta) = 2 r_1^2 D \Sigma a_j f(\delta, x_j) K(\delta, x_j) , \tag{16}$$

where the weights a_j and ordinates x_j are constants chosen so as to insure the best representation of the integral. Their choice depends, naturally, on the type of the quadrature formula that we propose to employ. It is known that the best representation with a minimum number of terms is obtained if the ordinates are spaced unequally in a manner investigated by Gauss.[24] Gauss's well-known quadrature formula, is unfortunately, one of the "open type"—i.e., it does not involve ordinates at the limit of the interval of integration. If we were to use it, equation (16) would not contain explicitly the surface brightness at the limb of the sun (where $x = 1$)—a quantity we are most interested in.

A quadrature formula of the "closed type" of accuracy equal to Gauss's has been derived by Radau,[25] who found that if the integrand in equation (14) is a function of order not in excess of $2n - 1$, a representation of equation (14) by equation (16) becomes exact if the sum in equation (16) is extended over all roots of the equation

$$P_{n+1}(x) - P_{n-1}(x) = 0 , \tag{17}$$

with weights

$$a_j = \frac{2}{n(n+1)} \{P_n(x_j)\}^{-2} , \tag{18}$$

where $P_n(x)$ denotes the Legendre polynomial of order n. Equation (17) admits of $n + 1$ roots, which are ± 1 plus roots of $P_n'(x) = 0$.[26] This shows that Radau's formula will ordinarily call for one more ordinate than Gauss's to attain the same accuracy; but, as the kernel (15) of our fundamental equation vanishes for $x = -1$, the sum on the right-hand side of equation (16) will actually consist of the same number of terms, regardless of

[24] "Methodus nova integralium valores per approximationes inveniendi," *Coll. Works*, **3**, 163.

[25] *J. math.*, 3d ser., **6**, 283, 1880.

[26] This immediately becomes obvious if we remember that

$$n(n+1)[P_{n-1}(x) + P_{n+1}(x)] = (2n+1)(1-x^2) P_n'(x) ,$$

where P' denotes the derivative with respect to x.

whether Gauss's or Radau's formula is employed. Since, however, the latter involves explicitly $f(\delta, 1)$, we shall hereafter adopt it for the purpose of this investigation.[27]

In passing from equation (14) to equation (16) by means of Radau's summation formula, we have replaced the integral on the right-hand side of equation (14) by a weighted sum of particular values of $f(\delta, x)$, corresponding to n discrete values of its argument x, which should represent the integral exactly if its integrand is a function of degree not in excess of $2n - 1$, and very approximately so if its degree is higher. An equation of the form (16) can be set up for every individual observation or normal point of solar light-curve during an eclipse. If f were a function of x alone and were independent of δ, the discrete values of f occurring in each such equation would be identical, and their magnitudes could therefore be obtained by the solution of a set of equations of condition of the form (16)—provided that the number of such equations (i.e., the number of the observed normals) were equal to, or greater than, n. Such cases have already been considered.[28] Our present problem turns out, however, to be inherently more difficult. Since the original limits of integration in equation (12) involve δ, the discrete values of $f(\delta, x)$ in the individual equations of condition will *not* correspond to the same distances from solar limb for equal values of x (except for $x = 1$, which always corresponds to $r = r_1$)—and if we regard the f's as unknown, a set of m such equations would represent a diophantine system containing $m(n - 1) + 1$ unknowns.

This apparent indeterminacy can, however, be resolved in the following manner. A representation of the integral in equation (14) by a weighted sum of n unequally spaced ordinates tacitly presumes its integrand to be a function of degree not in excess of $2n - 1$; and is the (known) degree of the kernel (15) is p, the degree of the unknown function f is thereby limited not to exceed $2n - p - 1$ if the representation of our integral equation by an equivalent system of linear algebraic equations is to be exact. Suppose now that, out of the array of $m(n - 1) + 1$ ordinates of the diophantine system, *we single out* $2n - p$ *of them as unknowns, while expressing all others in terms of these unknowns by means of an interpolation polynomial of* $(2n - p - 1)$*th degree.* This is indeed admissible: for, though the magnitude of each ordinate is unknown, its position with respect to any other one is specified as soon as the elements of the eclipse are fixed.

Let $f(\delta, x)$ be such a polynomial of degree $2n - p - 1$, which for arbitrarily spaced values $x_1, x_2, x_3, \ldots, x_{2n-p}$ of argument x admits of the values $f(\delta, x_1), f(\delta, x_2), \ldots, f(\delta, x_{2n-p})$. A value of $f(\delta, x)$ appropriate for any particular value of x may then be found, for instance, from Lagrange's interpolation formula,[29]

$$\left.\begin{aligned}\frac{f(\delta,x)}{(x-x_1)(x-x_2)\ldots(x-x_{2n-p})} &= \frac{f(\delta,x_1)}{(x-x_1)(x_1-x_2)(x_1-x_3)\ldots(x_1-x_{2n-p})} \\ &+ \frac{f(\delta,x_2)}{(x-x_2)(x_2-x_1)(x_2-x_3)\ldots(x_2-x_{2n-p})} + \ldots \\ &+ \frac{f(\delta,x_{2n-p})}{(x-x_{2n-p})(x_{2n-p}-x_1)(x_{2n-p}-x_2)\ldots(x_{2n-p}-x_{2n-p-1})},\end{aligned}\right\} \quad (19)$$

which is of a form suitable for computation and which will permit us to reduce the originally indeterminate system to a set of m linear equations containing $2n - p$ discrete values of f, which correspond to known distances from the limb of the sun. If $m = 2n - p$ the system will possess a unique solution; if $m > 2n - p$, the system becomes overdeterminate and may be solved by the method of least squares. When values of f so ob-

[27] It may be noticed that if $n = 1$, Radau's formula reduces to the well-known trapezoidal rule; for $n = 2$, it gives Simpson's rule.

[28] Nyström, *Acta math.*, **54**, 185, 1930; or Reisz, *Arkiv f. Math., Astr., och Fysik*, Vol. **29** A, No. 29, 1943.

[29] *Œuvres*, **7**, 286, cf. also Whittaker and Robinson, *The Calculus of Observations*, p. 29, London, 1944.

tained are inserted back in the interpolation polynomial (19), the latter will represent an nth approximation to f—and therefore to $J(r)$—whose accuracy may be arbitrarily increased by taking n sufficiently large.

The above-described method for solving the fundamental equation of our problem consists, in brief, in replacing the original integral equation by an equivalent system of linear algebraic equations by means of a convenient summation formula and in reducing subsequently the number of the unknowns by expressing $(m - 2)\ n + p - m + 1$ of them as interpolates in terms of $2n - p$ pivotal points. This procedure requires the unknown function $J(r)$ to be continuous for $r < r_{r_1}$; for, if so, both approximate steps represented by equations (16) and (19) are easily justified, and the process can be shown to lead to a rigorous solution of our fundamental integral equation when n is allowed to increase beyond any limit. In practice, however, even a moderate number of terms (i.e., a low value of n) should, as a rule, yield a good approximation; for the method has been so adjusted as to give the best possible fit with the smallest number of terms.

IV

The observations which we are going to analyze will include twenty-five normal points (Nos. 105–129) of Table 5*a* of Wesselink's paper,[12] which cover a time interval of approximately 18 seconds; for these are of relatively greatest weight for determining the distribution of light at the extreme limb of the sun. We are, moreover, going to discuss observations in the blue ($\lambda_{\text{eff}} = 4540$ A) only; for, since according to the Dutch observers the color index of the narrow solar crescent proves to be constant (in the interval considered) within one- or two-hundredths of a magnitude, the solar surface brightnesses in the blue and in the red would obviously differ by a mere multiplication constant.

Table 1 summarizes the data which will form the basis of the present investigation. The first and second columns indicate the number of the respective normal (after Wesselink) and the difference in time between the instant of observation (t) and that of mid-totality (t_0), both reckoned from an arbitrary zero point (which turns out to be 123.6 seconds before second contact). The apparent separation, δ, of centers of the sun and moon can be conveniently written as

$$\delta^2 = (t - t_0)^2 + \delta_0^2$$

and expressed in terms of an angular distance which the moon traverses with respect to the sun in 1 sidereal second. In this unit $\delta = 10.0$ sid. seconds; and the individual values of δ corresponding to the observed times, t, are listed in the third column.

The speed of the relative motions of the sun and moon at the time of the eclipse can be deduced from the ephemeris. The observations which we propose to discuss were made 58 ± 9 seconds before the mid-eclipse, which took place at $3^h59^m48^s$, G.M.T. The observations were therefore made at $3^h58^m50 \pm 9^{sec}$, during which time the geocentric angular speed of the moon relative to the sun (as obtained by differentiation of positions given in the *Nautical Almanac* for 1936) was 0".5479 per sid. second. This corresponds to a topocentric speed, at the site and time of observations ($\lambda = 39°\ 54'.7$ east of Greenwich; $\beta = +44°\ 44'.5$), of 0".5158 per sidereal second; this latter value being constant to $\pm 0''.0002$ within 18 seconds, during which the observations were carried out. The geocentric apparent radius of the sun was $944''.27L$, its topocentric value being augmented by 0".01. The apparent geocentric radius of the moon (as derived from stellar occultations[30]) was 932".63[31] for the mean horizontal parallax of 3422".70.[32] At the time and site of ob-

[30] Cf. Comrie, *A.J.*, **46**, 61, 1937.

[31] The apparent lunar semi-diameter (for the same mean parallax) of 931".87, as given in the *Nautical Almanac* and also in Michailov's ephemeris (*Total Eclipse of the Sun, June 19, 1936, in USSR*, Moscow: Sternberg State Astronomical Institute, 1935) refers to the valleys of the profile of the lunar limb and is significantly smaller (by 0".75) than the radius derived from the occultations—which must be used in this connection.

[32] At the time of observation the equatorial horizontal parallax of the moon was 3532".86.

servation the augmentation of geocentric lunar semi-diameter amounted to $6''.40 \pm 0''.01$, so that the apparent topocentric radii of the sun and moon were $944''.28$ and $968''.99$, respectively. The last digits of these figures may be in error by a few units, which is also the order of magnitude of effects of the differential refraction upon the true figures of the sun and moon at an altitude of approximately 23° above the horizon, at which the total eclipse was observed.

When the values of δ as given in the third column of Table 1 are multiplied by $0''.5158$, the instantaneous angular distances of the centers of the sun and moon can be converted to seconds of arc. We shall hereafter find it convenient to adopt the apparent solar radius of $944''.28$ as our unit of length; and the fourth column of Table 1 then gives the δ's expressed in this unit. The fifth column contains the quantity D, as defined by equation

TABLE 1

No.	$t-t_0$	δ^{sec}	δ/r_1	D	Δm	$(\pi k/D)I(\delta)/I(0)$
105.....	−66.8 sec	68.1 sec	0.03720	0.00552	$6^m.51$	0.463
106.....	66.1	67.3	.03676	.00530	6.69	.447
107.....	65.4	66.8	.03649	.00516	6.73	.443
108.....	64.6	66.0	.03605	.00494	6.81	.430
109.....	63.8	65.1	.03556	.00470	6.89	.420
110.....	63.0	64.1	.03501	.00442	6.98	.411
111.....	62.3	63.1	.03447	.00415	7.08	.399
112.....	61.5	62.3	.03403	.00393	7.14	.399
113.....	60.8	61.6	.03365	.00374	7.21	.393
114.....	60.1	60.9	.03326	.00355	7.29	.385
115.....	59.4	60.2	.03288	.00336	7.39	.371
116.....	58.8	59.6	.03255	.00319	7.48	.359
117.....	58.2	59.1	.03228	.00306	7.57	.345
118.....	57.6	58.4	.03190	.00287	7.66	.338
119.....	56.8	57.7	.03152	.00268	7.78	.324
120.....	56.0	56.9	.03108	.00246	7.78	.325
121.....	55.3	56.2	.03070	.00227	8.00	.313
122.....	54.6	55.5	.03031	.00207	8.17	.293
123.....	53.7	54.6	.02982	.00183	8.36	.278
124.....	52.9	53.8	.02939	.00161	8.54	.268
125.....	52.1	53.1	.02900	.00142	8.78	.244
126.....	51.3	52.3	.02857	.00120	9.04	.227
127.....	50.6	51.6	.02818	.00101	9.35	.203
128.....	49.8	50.8	.02775	.00079	9.75	.179
129.....	−49.1	50.1	0.02736	0.00060	10.28	0.145

(13), computed with the aid of the preceding δ's and with $r_2 - r_1 = 24''.71 = 0.02617\, r_1$. The sixth column of the same table then indicates the difference, in stellar magnitudes, between the light of the uneclipsed sun and the crescent visible at the respective phase. The Dutch observers actually measured the difference between the crescent and their standard lamp, C. This lamp was later found to be 13 mag. fainter than the uneclipsed sun (at $\lambda_{eff} = 4540$ A); so that values listed in the sixth column of Table 1 are equal to 13 minus the "brightness" as given by Wesselink in the third column of his Table 5*a*. These data may easily be systematically in error, as the calibration of lamp C relative to full sunlight was characterized as "rather rough"; later (Sec. V) we shall find a way for improving upon it. It may be added that the light of the solar corona turned out to be about 4 mag. (or approximately forty times) fainter than the faintest observation made outside of totality. The neglect of an additive constant on the right-hand side of equations (1) or (14) (cf. n. 15) is therefore fully justified.

The magnitude differences as given in the sixth column specify (within the above res-

ervation) the fractional luminosity of the remaining solar crescent expressed in terms of the full luminosity of the uneclipsed sun. The latter can evidently be defined as

$$l(0) = 2\pi \int^{r} J(r)\, r\, dr\,, \tag{20}$$

where $J(r)$ denotes, as before, the distribution of brightness over the apparent solar disk. The form of this function near the extreme limb of the sun is the object of the present investigation; but, because the contribution to total sunlight of the narrow outer fringe of the apparent solar disk is relatively minute, no sensible error is committed if we insert in equation (20) a distribution of brightness deduced from direct measurements over the central portion of the sun and extrapolate it to the limb. Busbridge[33] found that the measures of Moll, Burger, and Van der Bilt[7]—the relatively best observational data in existence—can be well represented by an empirical formula of the form

$$J(r) = J(0)\ (m \sec\theta + 1 - m)^{-a}\,, \qquad \sin\theta = \frac{r}{r_1}, \tag{21}$$

where, for $\lambda = 4540$ A, $a = 0.787$ and $m = 0.699$.[34] If we write

$$l(0) = 2\pi J(0)\, r_1^2\, k\,, \tag{22}$$

then

$$k = \int_0^{\pi/2} (m \sec\theta + 1 - m)^{-a} \sin\theta \cos\theta\, d\theta = 0.3851\ldots,$$

as can be verified by quadratures. Dividing equation (14) by equation (22), we ultimately obtain

$$\frac{\pi k}{D}\frac{l(\delta)}{l(0)} = \int_{-1}^{+1} f(\delta,x)\, K(\delta,x)\, dx\,, \tag{23}$$

where $f(\delta, x) = J(r)$ will now be expressed in terms of solar intensity, $J(0)$, at the center of its apparent disk taken as unity. The quantity on the left-hand side of equation (23) has been evaluated for every observed normal and is given in the last column of Table 1.

V

The solution of the integral equation (23) for f may now proceed as outlined in Section III. As the first step, we split up the integral on the right-hand side of equation (23) in a summation using Radau's formula with seven ordinates. This number is found to reproduce the true values of the integral for uniformly bright disks ($f = 1$), as well as for those completely darkened at the limb ($f = \cos\theta$), correctly to one unit of the fifth decimal place—an accuracy wholly sufficient for our present purpose. The seven roots of equation (17) for $n = 6$ are (cf. the appendix)

$$x_{1,7} = \pm 1\,, \qquad x_{3,5} = \pm 0.4688\ldots,$$
$$x_{2,6} = \pm 0.8302\ldots, \qquad x_4 = 0\,;$$

and the fractional distances, r, from the sun's center corresponding to these roots for the first normal (Wesselink's No. 105) listed in Table 1 are

$$r_1 = 1.00000\,, \qquad r_4 = 0.99448\,,$$
$$r_2 = 0.99906\,, \qquad r_5 = 0.99189\,,$$
$$r_3 = 0.99707\,, \qquad r_6 = 0.98990\,,$$
$$r_7 = 0.98897\,.$$

[33] *M.N.*, **101**, 26, 1941.

[34] These values were obtained by interpolation of the data compiled by Busbridge in Table VII of her paper, referred to above. It may be mentioned that the first line of this table contains a misprint; namely, in the column for m, the first entry should read "0.694" instead of "0.649."

Let us now select the values of $J(r)$ corresponding to these distances as our fundamental set of unknowns and express all other $f(\delta, x)$'s in terms of these unknowns by means of the interpolation polynominal (19). The material compiled in Table 1 will then furnish us with a system of twenty-five equations for seven unknowns, a solution of which should supply the key for determining the variation of apparent brightness near the extreme limb of the sun.

The actual computations at this stage become rather tedious; but, as the method is new, it seems worth while to illustrate it on at least one of the twenty-five normals underlying our investigation—say, the normal No. 115, for which $\delta = 0.03288$ and $D = 0.00336$. Table 2 summarizes the relevant data. Its successive columns indicate (1) the

TABLE 2

x	r	$K(\delta, x)$	$2a$	$2aK$
1.....	1.00000	0.6603	0.0952	0.0629
0.8302....	0.99943	.6303	.5537	.3490
0.4688....	0.99822	.5623	.8635	.4855
0.....	0.99664	.4610	.9752	.4496
−0.4688....	0.99506	.3333	.8635	.2878
−0.8302....	0.99385	.1872	.5537	.1037
−1.....	0.99329	0.0000	0.0952	0.0000

respective root of equation (17) for $n = 6$; (2) the corresponding fractional distance from the sun's center as computed from equation (12); (3) the numerical values of the kernel $K(0.03288, x)$ as defined by equation (15); (4) the weight $2a$ of the respective ordinate in Radau's formula as defined by equation (16) (cf. also the appendix); and (5) the product $2aK$. Note that the sum of all entries in the fourth column must reduce to four; and that D times the sum of all entries in the last column is equal to π times the fractional area of the solar crescent visible at this phase.

Now let $f(0.03720, r_{1,2,3,\ldots,7})$ or simply $f_{1,2,3,\ldots,7}$ denote our master-set of unknowns, and $f(0.03288, r_{a,b,c,\ldots,g})$ or simply $f_{a,b,c,\ldots,g}$ denote values of the unknown function for distances r given in the second column of Table 2. An application of equation (19) then shows that the latter f's can be expressed in terms of the former as[35]

$$\left.\begin{aligned}
f_a &= 1.000 f_1 ;\\
f_b &= 0.237 f_1 + 0.882 f_2 - 0.173 f_3 + 0.087 f_4 - 0.054 f_5 + 0.034 f_6 - 0.013 f_7 ;\\
f_c &= -0.129 f_1 + 0.659 f_2 + 0.599 f_3 - 0.196 f_4 + 0.109 f_5 - 0.067 f_6 + 0.025 f_7 ;\\
f_d &= 0.041 f_1 - 0.136 f_2 + 0.940 f_3 + 0.201 f_4 + 0.086 f_5 + 0.049 f_6 - 0.018 f_7 ;\\
f_e &= 0.034 f_1 - 0.102 f_2 + 0.251 f_3 + 0.925 f_4 - 0.159 f_5 + 0.079 f_6 - 0.028 f_7 ;\\
f_f &= -0.029 f_1 + 0.087 f_2 - 0.168 f_3 + 0.908 f_4 + 0.275 f_5 - 0.110 f_6 + 0.037 f_7 ,
\end{aligned}\right\} \quad (24)$$

f_g being of no concern, since $K(\delta, -1) = 0$. In the order of accuracy at which we are working (i.e., within the scheme of our seven-ordinate approximation), equation (16) for $\delta = 0.03288$ then takes the explicit form

$$\left.\begin{aligned}
0.108 f_1 + 0.546 f_2 + 0.712 f_3 + 0.386 f_4 - 0.022 f_5 \\
+ 0.013 f_6 - 0.005 f_7 = 1.862 ,
\end{aligned}\right\} \quad (25)$$

[35] Note that the algebraic sum of coefficients in each row must reduce to unity.

where coefficients of the individual f's are obtained by a multiplication of the matrix of coefficients on the right-hand side of equations (24) by the fifth column of Table 2—i.e.,

$$0.108 = 1.000 \times 0.0629 + 0.237 \times 0.3490 - 0.129 \times 0.4855 + 0.041 \times 0.4496 + 0.034 \times 0.2878 - 0.029 \times 0.1037 ,$$

and similarly for other coefficients.

This work was repeated for each of the remaining twenty-four normal points listed in Table 1, and it yielded an equal number of equations of condition of the form (25). An inspection of their coefficients reveals, however, that f_7 enters everywhere with such a small weight as to render its determination well-nigh impossible. An assumption was therefore made that $f_6 = f_7$ on grounds that these ordinates are nearly isotopic. A least-squares solution of our twenty-five equations of condition was then carried out and led to the following result:

$$f_1 = 0.334 \pm 0.010 \text{ (p.e.)}, \qquad f_5 = 0.432 \pm 0.004 ,$$
$$f_2 = 0.390 \pm 0.004 , \qquad f_6 = 0.44 \pm 0.01 ,$$
$$f_3 = 0.417 \pm 0.003 , \qquad f_7 = 0.44 .$$
$$f_4 = 0.426 \pm 0.002 ,$$

A glance at these values reveals that the computed brightnesses appear to be systematically too high; and the reason is perhaps not too hard to suspect. The values of solar brightness just obtained depend on the correctness of the comparison of the luminosities of lamp C employed by the Dutch observers with the uneclipsed sun. The latter was found to be approximately 13 mag. brighter than the lamp—a determination characterized by Wesselink as "rather rough." A better way for calibrating the computed surface brightnesses seems to be a comparison with direct measures. Moll, Burger, and Van der Bilt claimed that their measurements of the distribution of brightness over the apparent solar disk were reliable up to $r = 0.99r_1$,[36] where, according to equation (21) which is based largely on their measures, $J(r) = 0.271$, the central brightness of the apparent solar disk being taken as unity. If our computed surface brightnesses are to agree at $r = 0.99$ with this determination, the difference, in magnitudes, between uneclipsed sun and lamp C must have been 13.52 mag. Since this appears to be well within the limits of possibilities, we conclude that the best approximation to the distribution of brightness near the extreme limb of the sun is obtained if values (26) are multiplied by 0.622, which leads to the following values as the final result of our investigation:

r/r_1	$J(r)/J(0)$
1.00000	0.207±0.006
0.99906	.243± .003
0.99707	.259± .002
0.99448	.265± .001
0.99189	.269± .003
0.98990	.275±0.005
0.98897	(0.27)

The probable errors of computed solar brightnesses faithfully reflect the dispersion of observed normal points around the mean light-curve but do *not* take account of systematic errors, such as may arise from inexact calibration at $r = 0.99$ or from errors in adopted semi-diameters of the sun and moon, from irregularities of lunar profile, or from imperfect knowledge of the circumstances of the eclipse. The true uncertainty of

[36] *Op. cit.*, p. 89.

computed solar surface brightnesses is therefore likely to be higher (though probably of the same order of magnitude) than its values given above. The computed intensity distribution, together with the observed light-changes, is diagrammatically shown in Figure 2; while Figure 3 shows the mean surface brightness of the solar crescent at each phase (obtained by dividing the light of the crescent by its area) as plotted against the instantaneous distance of the crescent's center of light from the center of the apparent solar disk.

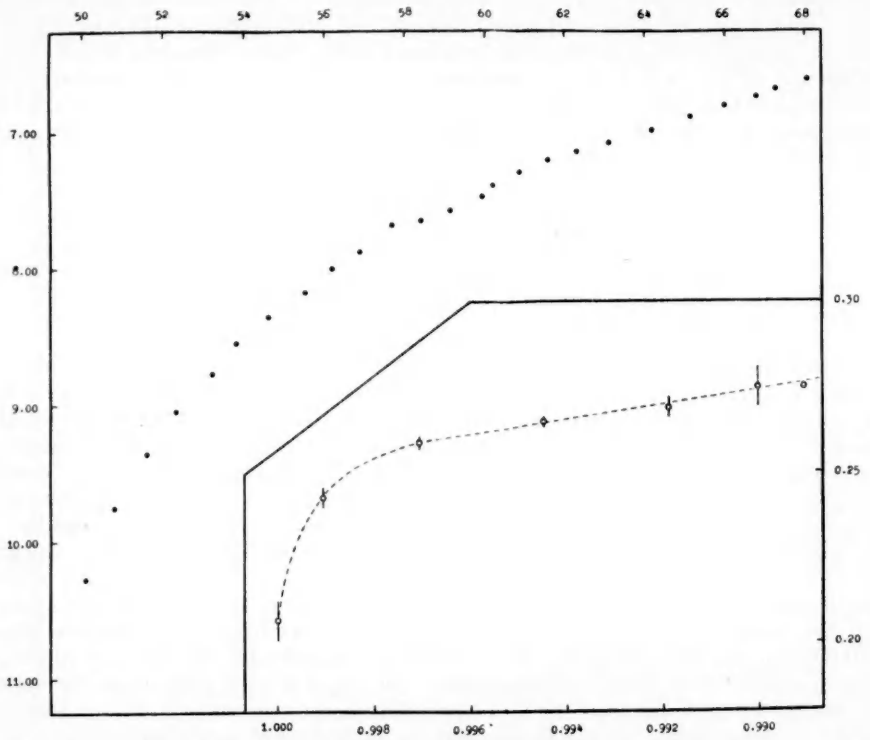

FIG. 2.—*Upper (left)*: The observed light-curve of total solar eclipse of June 19, 1936, some 20 seconds before the inner contact. *Abscissae:* the differences, in magnitudes, between full brightness of the uneclipsed sun and that of its crescent visible at the respective phase. *Ordinates:* time, in seconds, reckoned backward from mid-totality. The inner contact, on this scale, occurred at 46.8 seconds.

Lower (right): The distribution of surface brightness over the last per cent of the apparent solar radius, as determined in the present invest gation. *Abscissae:* $J(r)/J(0)$; ordinates: r/r_1.

The outstanding feature borne out by the foregoing results is a proof that *solar surface brightness remains finite and equal* (at $\lambda_{\text{eff}} = 4540$ A) *to approximately 21 per cent of central brightness up to the very limb of the sun*. The "resolving power" of our method[37] permits us to restrict the region where solar brightness will eventually drop to zero to a width of the order of 0".1, which is to be expected from purely theoretical considerations.[38] Our result is therefore in excellent agreement with the view advocated earlier by Minnaert.[10] Extensive and accurate data secured by the Dutch observers during the 1936

[37] I.e., the limits of uncertainty within which the positions of our ordinates can be located on the apparent solar disk.

[38] Cf. Unsöld, *Physik der Sternatmosphären*, pp. 394–396, Berlin, 1938.

eclipse, treated by a more powerful method, permit us, however, to reassert the same conclusions with much greater weight.

The second point which can be drawn from the above results is that *the gradient of solar surface brightness between* $0.99 < r < 0.998$ *turns out to be remarkably small.* We have already mentioned that Wesselink, in analyzing the light-changes between $0.95 < r < 0.99$, found that, in this region, dJ/dr was approximately one-third the average decrease observed over the central portions of the apparent solar disk; and our present outcome bears out the theory that, between $0.99 < r < 0.998$, dJ/dr is less than one-half of

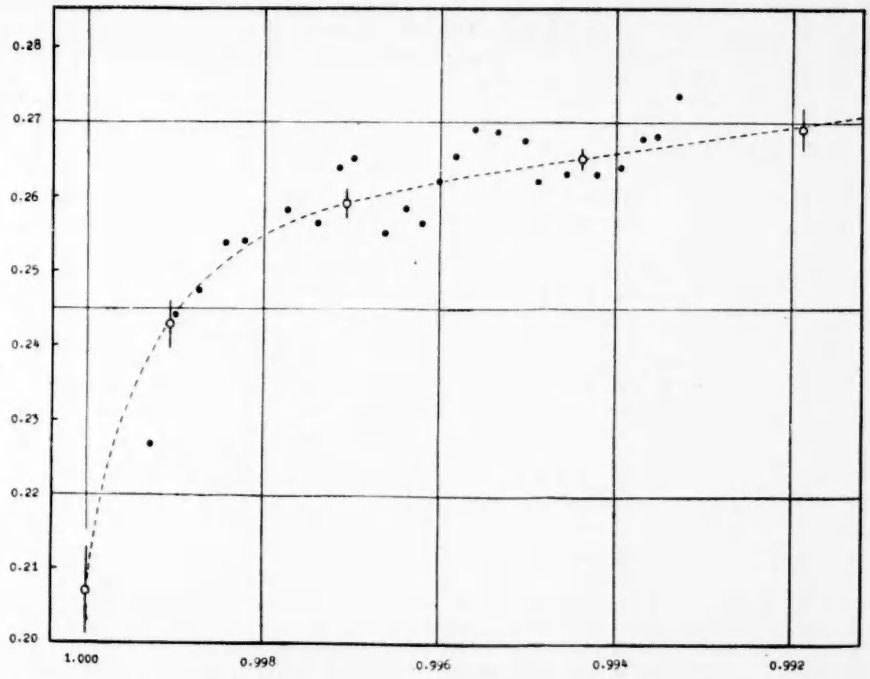

FIG. 3.—The dots represent the mean surface brightness of the solar crescent at the respective phase (obtained by dividing the light of the crescent by its area; *abscissae*), plotted against the instantaneous distance of the crescent's center of light from the center of apparent solar disk (*ordinates*). The broken line indicates the most probable distribution of apparent solar brightness near the limb. The open circles represent the values of $J(r)J(0)$ actually computed; the vertical bars indicate their probable errors.

Wesselink's value. The rate with which the surface brightness of the sun, as inferred from the eclipse observations, falls off from center to limb appears thus to diminish progressively as we approach the limb, up to roughly 99.8 per cent of the solar semi-diameter.

In conclusion, the writer expresses a hope that photometric measures of the light emitted by the narrow solar crescent in advanced partial phases will be included on programs of future eclipse expeditions. Several possible improvements of the observational technique have been pointed out by Wesselink in the appendix to his paper, frequently referred to. From the theoretical standpoint, the ultimate limit to the precision with which solar surface brightness can be determined in this way is imposed only by irregularities of lunar profile.

APPENDIX

Throughout the foregoing investigation, extensive use has been made of Radau's formula for numerical integration. This formula asserts that, if $f(x)$ is a function of degree less than $2n - 1$, then

$$\int_{-1}^{+1} f(x)\, dx = \Sigma a_j f(x_j)\,, \qquad (a)$$

where the sum on the right-hand side is to be extended over $n + 1$ roots of equation (17) and the weights a_j are defined by equation (18) of Section III. The fact that Radau's formula represents an "open-type" analogy of Gauss's method for numerical integration renders the former very useful in many astronomical applications. As the roots of equation (17), as well as the weights a, have, to the writer's knowledge, never been systematically evaluated before, their summary for $n = 1$ to $n = 8$ is given below:

$n=1$:	$x_{1,2} = \pm 1$	$a_{1,2} = 1$
$n=2$:	$x_{1,3} = \pm 1$ $x_2 = 0$	$a_{1,3} = 1/3$ $a_2 = 4/3$
$n=3$:	$x_{1,4} = \pm 1$ $x_{2,3} = \pm\sqrt{1/5}$	$a_{1,4} = 1/6$ $a_{2,3} = 5/6$
$n=4$:	$x_{1,5} = \pm 1$ $x_{2,4} = \pm\sqrt{3/7}$ $x_3 = 0$	$a_{1,5} = 1/10$ $a_{2,4} = 49/90$ $a_3 = 32/45$
$n=5$:	$x_{1,6} = \pm 1$ $x_{2,5} = \pm 0.7650553\ldots.$ $x_{3,4} = \pm 0.0813570\ldots.$	$a_{1,6} = 1/15$ $a_{2,5} = 0.3784750\ldots.$ $a_{3,4} = 0.5548584\ldots.$
$n=6$:	$x_{1,7} = \pm 1$ $x_{2,6} = \pm 0.8302239\ldots.$ $x_{3,5} = \pm 0.4688488\ldots.$ $x_4 = 0$	$a_{1,7} = 1/21$ $a_{2,6} = 0.2768260\ldots.$ $a_{3,5} = 0.4317454\ldots.$ $a_4 = 256/525$
$n=7$:	$x_{1,8} = \pm 1$ $x_{2,7} = \pm 0.8717401\ldots.$ $x_{3,6} = \pm 0.5917002\ldots.$ $x_{4,5} = \pm 0.2092992\ldots.$	$a_{1,8} = 1/28$ $a_{2,7} = 0.2107042\ldots.$ $a_{3,6} = 0.3411227\ldots.$ $a_{4,5} = 0.4124591\ldots.$
$n=8$:	$x_{1,9} = \pm 1$ $x_{2,8} = \pm 0.8997580\ldots.$ $x_{3,7} = \pm 0.6771863\ldots.$ $x_{4,6} = \pm 0.3631175\ldots.$ $x_5 = 0$	$a_{1,9} = 1/36$ $a_{2,8} = 0.1654953\ldots.$ $a_{3,7} = 0.2745387\ldots.$ $a_{4,6} = 0.3464284\ldots.$ $a_5 = 4096/11025$

It may be noticed that, for $n = 1$, Radau's formula reduces to the well-known trapezoidal rule; for $n = 2$, it gives Simpson's rule. The summation on the right-hand side of (a) will always contain one ordinate more than Gauss's method would call for if the same accuracy is to be attained; but, as equation (17) admits of the roots ± 1 regardless of n, this summation will always include ordinates at both borders of the interval of integration—which is frequently of distinct advantage.

THE PHOTOGRAPHIC LIGHT-CURVE OF T CORONAE BOREALIS

CECILIA PAYNE-GAPOSCHKIN AND FRANCES W. WRIGHT
Harvard College Observatory
Received June 5, 1946

ABSTRACT

Analysis of 1334 photographic estimates, on Harvard plates made before the maximum of February, 1946, shows that T Coronae Borealis had displayed a series of minor outbursts during the preceding six thousand days.

The changes of brightness and of color index are closely related to the observed spectral changes.

The recurrent nova, T Coronae Borealis, is never fainter photographically than the twelfth magnitude and can therefore be successfully studied on the Harvard patrol plates. Variations in photographic brightness were noted by Miss Walker.[1] Because of

TABLE 1

COMPARISON STARS

BD	HD	Spectrum	I Pg
+26°2767	143707	F2	7.97
+26 2769	143808	F5	8.67
+26 2763	143352	F2	9.52
+26 2768	.....	.....	10.00
+26 2764	.....	.....	10.93
.....	.....	.....	11.50
+26 2759	.....	.....	11.87

TABLE 2

T CORONAE BOREALIS, PHOTOGRAPHIC SEASONAL MEANS BEFORE JD 2427000

JD	I Pg	No.	Weight	JD	I Pg	No.	Weight
2413240	11.60	4	4	2420615	11.36	16	16
14742	11.46	4	4	21012	11.33	20	19
15098	11.48	5	5	305	11.20	12	12
562	11.30	10	10	750	11.48	17	17
862	11.42	19	19	22090	11.39	15	15
16260	11.32	13	13	360	11.41	14	12
16638	11.40	12	12	790	11.29	8	8
982	11.47	23	23	23143	11.28	9	6
17352	11.40	12	12	552	11.41	10	7
702	11.48	13	13	24250	11.16	7	7
18160	11.45	6	6	648	11.39	7	6
428	11.44	19	19	25040	11.22	13	12
806	11.45	16	16	414	11.38	32	32
19254	11.48	5	5	729	11.38	36	35
518	11.34	12	12	26112	11.39	27	27
894	11.28	19	19	478	11.30	18	18
20290	11.20	28	28	833	11.34	26	26

[1] *Harvard Ann.*, **84**, 151, 1920.

the possibility that the star might prove to be a recurrent nova,[2] it was placed on the program for the systematic study of the brighter variable stars, which is supported by a grant from the Milton Fund of Harvard University.

The present study makes use of 1334 estimates made on Harvard plates by Mrs. Helen Trueblood and Miss Frances Wright. Photographic magnitudes of comparison stars were determined by Miss Wright from series plates; they are based directly on the North Polar Sequence. The magnitudes of the comparison stars are given in Table 1. The photographic estimates of T Coronae Borealis are summarized in Tables 2 and 3.

Table 2 gives seasonal means before JD 2427000, and Table 3, 10-day means after this date. They contain, in successive columns: the average JD, the photographic magnitude, the number of plates, and the weight. Plates made from all series except the AI and FA received unit weight; estimates from AI and FA plates received half-weight because of the poorer quality of the material.

The photographic observations, from JD 2427000 up to the recent outburst, are shown in Figure 1 by dots, graduated according to weight. Figure 1 also shows the visual estimates by Peltier[3] and by Steavenson.[4] The figure shows that the star brightened photographically by more than a magnitude, while the visual magnitude changed by very little. Just before the major outburst of JD 2431861, the photographic brightness again fell below the eleventh magnitude.

The photographic changes of brightness are exactly similar to those determined from plates taken at German observatories by Hachenberg and Wellmann,[5] who were the first to call attention to them.

A rough idea of the changes of red and blue components is obtained on the assumption that they correspond, respectively, to objects of color index 1^m6 and 0^m0. The resulting magnitudes are plotted in Figure 2 and given in Table 4. The red component appears to remain constant, while the blue component brightens in irregular spurts, apparently falling again to its minimum brightness just before the major outburst.

The spectrum of T Coronae Borealis has long been known to be of interest, because it was basically of type M, whereas "without exception, other novae which have been observed are now blue stars."[6] It should be mentioned that RS Ophiuchi, another recurrent nova, is now known to show a late-type spectrum at minimum.

A survey of spectroscopic behavior of T Coronae Borealis is given in Table 5. The strong bright lines noted by Adams and Joy at JD 2422700 precede the interval covered by our diagram. They coincided with a very slight brightening of the photographic curve (see Table 2); however, the spectrum classified by Miss Cannon, which showed no bright lines, occurred when the star was slightly brighter than it had been earlier.

The times of the spectra are marked on Figure 2. Wellmann and also Swings, Elvey, and Struve remarked that the two components were about equal in photographic magnitude at the times of their observations, and this is confirmed in Figure 2. Minkowski noted a fall in the intensity of the blue continuum from JD 2429138 to JD 2429198, and this fall is seen in the light-curve of the blue component in Figure 2.

It seems that T Coronae underwent several minor outbursts of nova-like character before the major explosion of February, 1946. The P Cygni nature of the spectrum at the small maxima and the increase in excitation as the brightness gradually declined are in harmony with this picture. So far as we know, this is the first detailed evidence of the occurrence of a series of minor nova-like disturbances as a prelude to the outburst of a nova.

[2] See C. Payne-Gaposchkin and S. Gaposchkin, *Variable Stars*, p. 264, Cambridge, 1938.

[3] Contributed to the AAVSO.

[4] *M.N.*, **95**, 640, 1935; **97**, 657, 1937; **99**, 697, 1939.

[5] *Zs. f. Ap.*, **17**, 246, 1939.

[6] M. L. Humason, *Ap. J.*, **88**, 234, 1938.

TABLE 3

T CORONAE BOREALIS, PHOTOGRAPHIC 10-DAY MEANS AFTER JD 2427000

JD	I Pg	No.	Weight	JD	I Pg	No.	Weight
2427100	11.07	2	2	2428250	11.22	2	2
120	11.45	2	1½	260	11.21	2	2
130	11.50	1	1	270	11.42	3	3
140	11.50	2	2	280	11.42	16	15
160	11.56	7	5½	290	11.44	6	6
170	11.45	3	3	310	11.33	12	11
180	11.50	1	1	320	11.28	2	2
190	11.56	7	6	330	11.43	2	2
200	11.50	2	2	340	11.21	7	5½
210	11.40	4	3½	350	11.21	1	1
220	11.43	2	2	360	11.07	6	6
230	11.21	2	2	400	11.10	3	2
240	11.28	2	2	570	11.21	2	1
250	11.36	1	1	600	11.06	1	1
270	11.60	1	1	610	11.21	1	1
330	11.36	1	1	620	11.21	2	2
340	11.70	1	½	630	10.93	1	1
350	11.43	1	1	640	11.21	4	4
410	11.50	1	½	650	11.21	1	1
460	11.21	1	1	660	11.28	6	5½
470	11.50	1	1	670	11.07	4	3
480	11.42	4	3½	680	10.84	2	2
490	11.58	3	2½	690	11.20	5	3
510	11.48	6	5½	700	11.01	4	2½
520	11.32	3	2½	710	10.93	1	1
530	11.36	1	1	720	11.09	7	4½
540	11.34	3	2	730	10.93	1	½
550	11.31	5	4½	740	10.96	3	2½
560	11.43	6	6	750	10.93	1	½
570	11.55	9	8½	780	11.14	2	2
580	11.49	3	3	810	10.93	1	1
590	11.74	2	2	930	11.14	2	2
600	11.65	4	3	940	11.21	2	1½
630	11.50	1	1	950	10.93	1	½
650	11.36	1	1	960	11.00	2	1½
660	11.43	2	2	980	10.98	4	3½
670	11.36	1	1	990	10.82	6	5
680	11.28	1	½	2429000	10.62	2	1½
840	11.52	3	3	010	10.56	1	1
860	11.47	2	1½	020	10.45	3	2½
870	11.21	3	2½	040	10.19	3	2½
880	11.50	1	1	050	10.30	10	7½
890	11.26	2	1½	060	10.29	2	2
900	11.38	5	4½	070	10.51	10	7½
920	11.26	6	6	080	10.58	4	2½
930	11.36	1	1	090	11.14	1	½
940	11.27	5	4½	130	10.20	1	½
950	11.41	8	7½	150	9.80	1	½
960	11.28	8	8	160	9.85	2	1
980	11.15	6	5½	170	10.56	1	½
990	11.21	2	2	320	10.60	3	2½
2428010	11.46	4	4	330	10.45	3	2½
020	11.54	3	2½	340	10.11	7	6
030	11.48	4	4	350	10.00	1	1
040	11.21	1	1	360	10.20	1	1
060	11.50	1	1	370	10.08	3	2
080	11.50	1	½	380	10.08	3	2½
200	11.36	1	1	390	10.23	5	4
220	11.26	7	6	400	10.32	6	4
230	11.21	6	6	410	10.38	5	3½
240	11.33	3	3	420	10.48	8	6

TABLE 3—*Continued*

JD	I Pg	No.	Weight	JD	I Pg	No.	Weight
2429430	10.27	9	5½	2430490	10.45	4	2½
440	10.66	2	1	500	10.56	1	1
450	10.53	10	7½	510	10.10	2	1
460	10.55	14	8½	520	10.39	11	6½
470	10.38	5	3½	530	10.43	5	3½
480	10.00	2	1½	540	10.38	1	½
490	10.52	7	4	550	10.72	7	4
510	10.56	1	½	560	10.71	4	2½
520	10.80	2	1	580	10.43	5	2½
570	10.38	1	1	600	10.24	3	2
680	10.20	1	1	630	10.56	1	½
690	10.29	3	2	790	10.47	2	2
700	10.56	1	½	810	10.29	2	1
720	10.34	3	2½	820	10.66	2	1
730	10.13	6	5	830	10.30	6	4
750	10.11	6	5½	840	10.40	5	4
760	10.14	17	11	850	10.36	5	3
770	10.10	1	½	870	10.00	2	1
780	10.22	10	8	880	10.26	4	2½
790	10.23	8	5	890	10.38	1	½
800	10.25	6	4	900	10.51	7	4
810	10.36	7	4½	910	10.66	3	2
820	10.02	11	7½	920	10.29	2	2
840	10.60	3	2½	930	10.64	5	2½
850	10.70	4	2	940	10.42	4	2
860	10.38	1	1	960	10.81	3	1½
870	10.19	5	2½	970	10.75	1	½
900	10.20	1	½	2431110	10.56	1	1
970	10.15	2	2	140	10.62	2	1½
2430010	9.96	1	½	150	10.38	1	1
030	10.56	1	1	160	10.75	1	½
050	9.85	1	½	170	10.93	3	2
060	10.38	4	3½	180	10.75	1	½
070	10.25	3	3	190	10.38	2	1
080	10.08	9	6	200	10.32	2	1½
090	10.22	3	1½	210	10.39	4	3½
100	10.00	1	½	230	10.65	10	6½
110	10.47	5	3	240	10.96	9	6½
120	10.41	3	1½	250	10.38	2	2
130	10.07	4	2	260	10.67	3	1½
140	10.19	6	3½	290	10.75	1	½
150	10.00	2	1	510	10.81	3	3
160	10.35	8	4½	530	10.93	1	1
170	10.29	12	7½	540	11.22	2	2
175	10.56	1	½	550	11.21	1	1
180	10.32	6	4½	560	11.06	1	1
190	10.41	6	3	570	10.93	2	1½
220	10.51	2	2	580	11.36	1	1
230	10.56	1	½	590	11.22	2	1½
240	10.20	1	½	610	11.28	2	2
250	10.14	3	2½	620	11.15	3	2½
370	10.38	1	½	630	11.36	1	1
410	10.51	2	1	640	11.02	3	1½
420	10.93	1	½	650	11.06	1	½
430	10.62	2	1½	670	11.18	3	2½
440	10.37	8	6	680	11.36	1	½
450	10.38	1	½	820	11.36	1	1
460	10.47	3	2	830	11.36	2	2
470	10.59	6	7	855	11.21	1	½
480	10.37	2	1½				

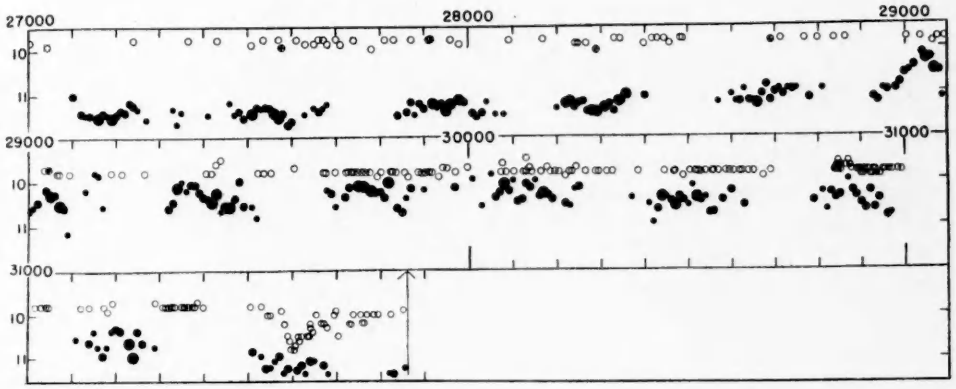

FIG. 1.—Photographic (*dots*) and visual (*circles*) light-curves of T Coronae Borealis. Circled crosses denote Steavenson's observations.

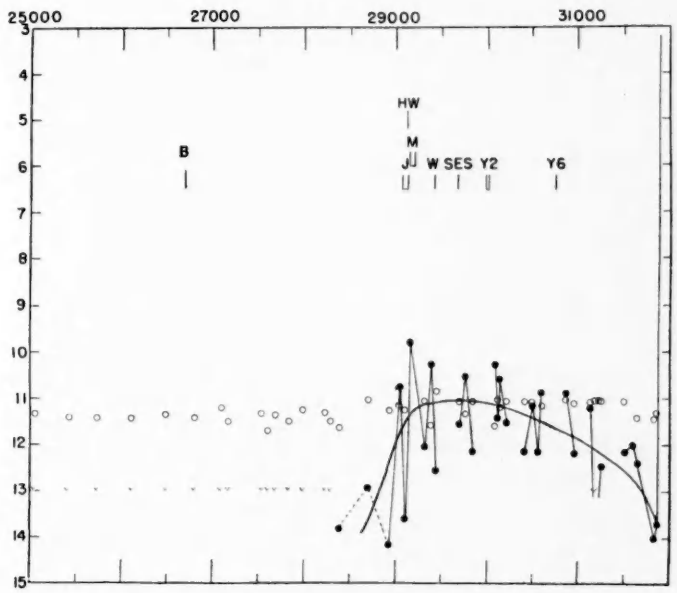

FIG. 2.—Resolution of light-curves of T Coronae Borealis into red (*circles*) and blue (*dots*) components

TABLE 4

VARIATIONS OF THE PHOTOGRAPHIC MAGNITUDES OF THE COMPONENTS OF T CORONAE BOREALIS

JD	Blue Component	Red Component
2425040	Fainter than 13	11.35
414	Fainter than 14	11.44
729	Fainter than 14	11.44
2426112	Fainter than 14	11.45
478	Fainter than 14	11.39
833	Fainter than 14	11.42
2427100	Fainter than 13	11.22
170	Fainter than 14	11.51
530	Fainter than 14	11.35
600	Fainter than 14	11.71
680	Fainter than 14	11.39
840	Fainter than 14	11.51
980	Fainter than 14	11.26
2428230	Fainter than 14	11.31
290	Fainter than 14	11.50
370	13.83	11.63
700	12.92	11.02
935	14.17	11.27
2429040	10.77	11.17
100	13.61	11.21
150	9.81	.....
320	12.02	11.02
370	10.29	11.59:
440	12.51	10.81
700	11.53	11.03
760	10.52	11.32
850	12.14	11.04
2430080	10.29	11.59
110	11.42	11.02
140	10.59	11.19
220	11.53	11.03
420	12.14	11.04
500	11.15	11.05
560	12.14	11.04
600	10.88	11.13
860	10.90	11.00
960	12.19	11.09
2431130	11.22	11.06
170	14.1:	11.02
200	11.15	11.05
250	12.46	11.06
510	12.16	11.06
600	12.00	12.10
650	12.41	11.41
830	14.04	11.44
855	13.71	11.31

TABLE 5

SUMMARY OF SPECTROSCOPIC OBSERVATIONS

JD	Symbol	Observer	Remarks
2420245		A. J. Cannon (*HD Catalogue*)	K0; no bright lines
22700		W. S. Adams and A. H. Joy (*Pub. A.S.P.*, **33**, 263, 1921)	Bright lines of *H*, *He* II
26700	B	L. Berman (*Pub. A.S.P.*, **44**, 318, 1932)	gM3; emission almost gone; *Hβ* has bright edge
29102	HW	O. Hachenberg and P. Wellmann (*Zs. f. Ap.*, **17**, 246, 1939)	Bright lines of *H*, *He* II, *N* III, [*O* II]; spectrophotometric gradient corresponds to $T=6000°$
29056–117	J	A. H. Joy (*Pub. A.S.P.* **50**, 300, 1938)	Continuum superimposed on M-type spectrum; decreased in intensity from 29138 to 29198
29138–198	M	R. Minkowski (*Pub. A.S.P.*, **51**, 54, 1939; *Pub. A.S.P.*, **50**, 300, 1938)	Bright lines of *H*, *He* I, *He* II, *Ca* II, [*Ne* III]
29417	W	P. Wellmann (*Zs. f. Ap.*, **19**, 16, 1939)	Continuums corresponding to stars of $T=3000°$ and $16000°$ about equal in photographic magnitude
29671–744	SES	P. Swings, C. T. Elvey, and O. Struve (*Pub. A.S.P.*, **52**, 199, 1940)	Strong continuum of early-type star, superimposed on M star of about same photographic magnitude. *Hα*, *Hβ* have P Cygni absorption components; bright lines of *H*, *He* I, *He* II, *Ca* II, [*O* II], [*O* III], *O* III, *N* III, [*Ne* III]; N_1, N_2, stronger than 4363; no [*Ne* V] or [*Fe* VII]
29995–30026	Y2	Yerkes II (P. Swings and O. Struve, *Ap. J.*, **94**, 295, 1941)	Excitation of emission layers increased; P Cygni absorption components decrease; increase of *He* II, *He* I, *O* III, *N* III, since 29744 and from 29995 to 30026; red component visible; relatively more luminous than in AX Persei, CI Cygni, or Z Andromedae
29620–30630	Y4	Yerkes IV (P. Swings and O. Struve, *Ap. J.*, **96**, 257, 1942)	Balmer lines in emission; shows *Fe* II but no [*Ne* V]
30753–754	Y6	Yerkes VI (P. Swings and O. Struve, *Ap. J.*, **98**, 91, 1943)	Balmer lines have violet and red emission components separated by absorption; violet component stronger; bright lines: *H*, *He* II, [*O* II], [*O* III], *O* III, *N* III, [*Ne* III], *Fe* II, [*Fe* II]?, trace of [*Ne* V], [*Fe* VII]; excitation has increased

THE INTERNAL TEMPERATURE-DENSITY DISTRIBUTION OF MAIN SEQUENCE STARS BUILT ON THE POINT-CONVECTIVE MODEL. II. SIRIUS A[1]

R. E. MARSHAK AND G. BLANCH
University of Rochester and Mathematical Tables Project
Received April 15, 1946

ABSTRACT

Following the procedure adopted for the sun, the equations of stellar equilibrium, are integrated for Sirius A. Expressed in solar units, the mass, luminosity, and radius of Sirius A are 2.34, 38.9, and 1.78, respectively. The point-convective model is used as before, but Morse's improved tables of the opacity replace Strömgren's. Account is taken of electron scattering which becomes as much as 17 per cent of the total opacity at the boundary of the convective core. A hydrogen content of 37 per cent by weight gives fitting of the radiative envelope to the convective core and leads to a central temperature of 30.7×10^6 degrees C., and a central density of 43 gm/cm^3. In agreement with the solar calculation the hydrogen content does not differ from the value found with the Eddington standard model, whereas the central temperature and density are considerably higher than the corresponding Eddington values. This agreement between the calculations for the sun and for Sirius A is especially striking, since Morse's values of the opacity are uniformly lower than Strömgren's—sometimes as much as 50 per cent. It is probable that both the sun and Sirius A contain appreciable amounts of helium.

The first main-sequence star investigated in detail on the basis of the point-convective model was the sun.[2] The equations of stellar equilibrium were numerically integrated, using Strömgren's tables of the opacity. The helium content was chosen as zero, and the hydrogen concentration was adjusted to secure a fit of radiative envelope onto convective core. It turned out that the predicted luminosity of the sun was about one hundred times as large as the observed luminosity. We thereupon pointed out in Paper I that the discrepancy could be removed either by (1) the use of Morse's improved tables,[3] which had just been published and which gave lower opacities than Strömgren's, or (2) the taking into account of the variation of the effective molecular weight (equation of state) throughout the star, or, finally, (3) the assumption of an appreciable admixture of helium (30–40 per cent by weight). The discrepancy could also be explained by lowering the carbon-nitrogen concentration by a factor of one hundred. However, this is an observational question (the evidence at present is against a reduction[4]) in contrast to the other three possibilities, which can be decided on theoretical grounds.

In order to throw further light on the first alternative mentioned above and, at the same time, to obtain accurate information on the internal constitution of another interesting star of the main sequence, the equations of equilibrium have been integrated for Sirius A on the basis of the point-convective model. Again, as in the sun, the molecular weight is taken as constant throughout the star, and the helium content is assumed zero. However, Morse's opacity tables are used instead of Strömgren's. Otherwise, the procedure is identical with that adopted for the sun (for details see Paper I).

[1] The results presented here are based on computations carried out by Miss E. Godefray and Mr. W. Horenstein, of the Mathematical Tables Project, with Dr. A. N. Lowan as technical director and under the immediate supervision of Dr. G. Blanch. At the time the computations were performed, in 1941, the Mathematical Tables Project was sponsored by the National Bureau of Standards, with Dr. L. J. Briggs as director, and was operated by the Work Projects Administration, New York City. These results were first reported at a meeting of the American Physical Society (cf. *Phys. Rev.*, **61**, 543(A), 1942).

[2] Cf. G. Blanch, A. N. Lowan, R. E. Marshak, and H. A. Bethe, *Ap. J.*, **94**, 37, 1941 (this paper will be referred to as "Paper I").

[3] P. Morse, *Ap. J.*, **92**, 27, 1940.

[4] Cf. H. A. Bethe, *Ap. J.*, **91**, 362, 1940; and H. N. Russell, *Scientific American*, September, 1942.

Applied to Sirius A, the equations for the radiative envelope become (cf. Paper I):

$$\frac{dp_R}{dr} = -\frac{\kappa \rho L}{4\pi r^2 c}, \tag{1}$$

$$\frac{dP}{dr} = -\frac{GM_r}{r^2}\rho, \tag{2}$$

$$\frac{dM_r}{dr} = 4\pi r^2 \rho, \tag{3}$$

$$P = p_G + p_R = \frac{\Re}{\mu}\rho T + \tfrac{1}{3}aT^4, \tag{4}$$

and

$$\kappa = \kappa_a + 1.5\kappa_s = \frac{\kappa_a'}{\tau}\frac{\rho}{T^{3.5}} + 1.5\kappa_s. \tag{5}$$

In these equations a, c, G, and $\Re$ have their usual significance; their definitions and numerical values are given in Chandrasekhar's book, *An Introduction to the Study of Stellar Structure*, page 487. The quantity M_r is the mass contained within a sphere of radius r. The total pressure P consists of two parts, the gas pressure p_G and the radiation pressure p_R; in the expression for p_G, μ is the average molecular weight and equal to $1/[2X_H + 0.52(1 - X_H)]$, where 0.52 is the average number of free electrons plus nuclei per proton.[5] The opacity κ_a from photoelectric ionizations contains the guillotine factor τ and a constant κ_a', depending on X_H, which may be written as

$$\kappa_a' = 7.65 \times 10^{25} \times (1 - X_H)[X_H + 0.48(1 - X_H)].^{6}$$

The opacity arising from electron scattering is given by

$$\kappa_S = 0.385[X_H + 0.48(1 - X_H)].$$

If a change of variable is made as in Paper I, equations (1)–(3) become

$$\frac{d\bar{T}}{dt} = \frac{A_0\rho^2}{\tau \bar{T}^{6.5}} + \frac{A_1\rho}{\bar{T}^3}, \tag{6}$$

$$\frac{d\rho}{dt} = \frac{A_2\rho\mu}{\bar{T}} - \frac{d\log\sigma\bar{T}}{dt}(\rho + A_3\bar{T}^3), \tag{7}$$

and

$$\frac{du}{dt} = -\frac{A_4\rho}{t^4}, \tag{8}$$

where

$$T = 10^6\bar{T}, \qquad t = \frac{R}{r}, \qquad u = \frac{M_r}{M},$$

$$A_0 = \frac{3\kappa_a' L}{16\pi a c R} \times 10^{-45}, \qquad A_1 = \frac{4.5\kappa_S L}{16\pi a c R} \times 10^{-24},$$

$$A_2 = \frac{\mu G M}{\Re R} \times 10^{-6}, \qquad A_3 = \frac{4a\mu}{3\Re} \times 10^{18}, \qquad A_4 = \frac{4\pi R^3}{M}.$$

[5] This number (0.52), in contrast to 0.46 for the sun, was obtained in the usual way by finding the state of ionization at the point in the star where $T \approx \frac{2}{3}T_c$ (T_c is the central temperature) (cf. Strömgren, *Zs. f. Ap.*, **7**, 229, 1932; and Paper I).

[6] Only the electrons contribute to the opacity, so that 0.48 is the average number of free electrons per proton and is chosen in the same manner as 0.52 (cf. n. 5).

If the values of L, M, and R for Sirius A are inserted—namely, $M = 2.34M_\odot$, $R = 1.78R_\odot$, $L = 38.9L_\odot$—and if, e.g., we choose $X_H = 0.35$ (i.e., $\mu = 0.96339$), we get

$$A_0 = 1.0308 \times 10^7 , \qquad A_1 = 119.55 ,$$

$$A_2 = 29.276 , \qquad A_3 = 1.1769 \times 10^{-4} , \qquad A_4 = 5.1243 .$$

As before, Strömgren's method[7] was used to obtain initial values of t and ρ for $T = 1.00 \times 10^6$, and the integration was continued at sufficiently small intervals in t so that the final results are probably correct to three significant figures.

TABLE 1

TEMPERATURE-DENSITY DISTRIBUTION OF SIRIUS A WITH $X_H = 0.35$

t	$T \times 10^{-6}$	ρ	$u = \frac{M_r}{M}$	τ	$n = \frac{d \log \rho}{d \log T}$
1.1435	1.000	0.00082	0.9998	1.57	5.42
1.154	1.045	0.00102	.9998	1.57	4.62
1.162	1.093	0.00122	.9998	1.56	4.07
1.170	1.140	0.00144	.9997	1.54	3.70
1.21	1.40	0.00288	.9995	1.43	3.20
1.25	1.68	0.00506	.9992	1.36	3.14
1.32	2.15	0.0112	.9982	1.35	3.22
1.40	2.69	0.0231	.9962	1.34	3.22
1.48	3.24	0.0416	.9932	1.28	3.12
1.56	3.79	0.0679	.989	1.23	3.12
1.64	4.33	0.104	.984	1.30	3.39
1.72	4.83	0.152	.977	1.41	3.50
1.80	5.32	0.215	.970	1.51	3.52
2.00	6.53	0.444	.945	1.82	3.68
2.20	7.66	0.809	.913	2.33	3.87
2.40	8.71	1.34	.874	2.93	3.91
2.70	10.2	2.48	.807	3.70	3.72
3.10	12.2	4.58	.708	4.35	3.36
3.50	14.0	7.14	.608	4.68	3.05
3.90	15.6	9.93	.515	5.16	2.94
4.30	17.0	12.7	.432	5.78	2.87
4.70	18.2	15.4	.362	6.25	2.68
5.10	19.3	17.9	.302	6.57	2.45
5.50	20.2	20.0	.253	6.79	2.22
5.90	21.1	21.9	.212	6.93	1.99
6.30	21.9	23.4	.178	7.01	1.78
6.70	22.6	24.7	.151	7.11	1.59
6.9111	22.912	25.277	0.1380	7.15	1.50

Two independent integrations were performed for Sirius A, namel , for $X_H = 0.35$ and $X_H = 0.40$. The results are given in Tables 1 and 2, respectively, at intervals at least four times as large as those used in the actual computations. The integrations are carried along until $n \equiv d \log \rho / d \log T$ becomes equal to 1.5. At this point, radiative equilibrium gives way to convective equilibrium, and one must try to fit the radiative envelope onto an incomplete Emden polytrope of index $n = 1.5$.[8] For the case $X_H =$

[7] Cf. *Zs. f. Ap.*, **2**, 350, 1931, and Paper I.

[8] The value of n is altered if the radiation pressure becomes large; for Sirius A the radiation pressure was taken into account in the integration, but its effect on n is inappreciable.

0.35, $\Delta\xi \equiv \xi(U) - \xi(V) = 0.068$,[9] where U and V are the two associated Emden functions of polytropic index 1.5 (defined in Paper I). For the case $X_H = 0.40$, $\Delta\xi \equiv \xi(U) - \xi(V) = -0.113$.[9] It follows that $X_H = 0.369$ would lead to $\Delta\xi = 0$[10] and, would therefore, fit the radiative envelope onto the convective core. To obtain the corresponding central temperature and density, we must interpolate between the two cases which have been integrated. From footnote 9 we see that $\xi_{av} = 1.225$ for the first case; this leads to $T_c = 29.5_5 \times 10^6$ and $\rho_c = 36.9$. For the second case, $\xi_{av} = 1.001$, which

TABLE 2

TEMPERATURE-DENSITY DISTRIBUTION OF SIRIUS A WITH $X_H = 0.40$

l	$T \times 10^{-6}$	ρ	$u = \frac{M_r}{M}$	τ	$n = \frac{d \log \rho}{d \log T}$
1.1624	1.000	0.00081	0.9997	1.69	5.88
1.166	1.015	0.00088	.9997	1.59	4.98
1.174	1.05	0.00104	.9997	1.57	4.37
1.182	1.09	0.00122	.9997	1.55	3.95
1.190	1.14	0.00142	.9997	1.53	3.67
1.198	1.19	0.00164	.9996	1.51	3.48
1.206	1.23	0.00188	.9996	1.49	3.36
1.23	1.38	0.00272	.9995	1.43	3.20
1.27	1.64	0.00465	.9992	1.36	3.13
1.34	2.08	0.0100	.9983	1.35	3.20
1.42	2.59	0.0201	.9967	1.35	3.24
1.50	3.10	0.0357	.994	1.30	3.17
1.58	3.61	0.0577	.991	1.24	3.10
1.75	4.67	0.133	.981	1.37	3.49
1.95	5.82	0.289	.963	1.61	3.55
2.15	6.92	0.544	.940	1.98	3.77
2.35	7.96	0.928	.911	2.50	3.93
2.55	8.94	1.47	.878	3.05	3.91
2.75	9.89	2.17	.841	3.55	3.80
3.10	11.5	3.80	.769	4.17	3.51
3.50	13.3	6.20	.684	4.60	3.23
3.90	15.0	9.01	.601	5.02	3.11
4.30	16.5	12.1	.525	5.62	3.09
4.70	17.8	15.2	.457	6.20	2.99
5.10	19.0	18.4	.397	6.62	2.82
5.50	20.1	21.3	.345	6.90	2.63
5.90	21.0	24.1	.301	7.12	2.46
6.30	21.9	26.6	.264	7.32	2.31
6.70	22.8	28.9	.232	7.47	2.16
7.10	23.5	31.0	.204	7.57	2.02
7.50	24.2	32.8	.181	7.63	1.88
7.90	24.9	34.4	.162	7.67	1.76
8.30	25.5	35.9	.145	7.95	1.72
8.70	26.0	37.2	.130	8.23	1.67
9.40	26.9	39.2	.110	8.76	1.59
10.00	27.5	40.7	0.096	9.16	1.50

[9] For $X_H = 0.35$,

$$\xi(U) = \xi(1.9211) = 1.259\,,$$
$$\xi(V) = \xi(1.2186) = 1.191\,;$$

for $X_H = 0.40$,

$$\xi(U) = \xi(0.68513) = 0.94457\,,$$
$$\xi(V) = \xi(0.95291) = 1.05757\,.$$

[10] Linear interpolation was used; this is adequate (cf. Paper I).

yields $T_c = 32.5_5 \times 10^6$ and $\rho_c = 52.5$. Using linear interpolation,[11] we get, corresponding to $X_H = 0.369$, $T_c = 30.7 \times 10^6$, and $\rho_c = 42.8$. These values are to be compared with those derived for the same μ (i.e., $\mu = 0.94$) on the Eddington standard model, namely, $T_c = 24.4 \times 10^6$ and $\rho_c = 31.5$, or with the point-convective values (assuming constant guillotine factor), namely, $T_c = 25.2 \times 10^6$ and $\rho_c = 21$.

If the temperature-density distributions obtained for the cases $X_H = 0.35$ and $X_H = 0.40$ (cf. Tables 1 and 2) are inserted into the expression for the energy production due to the carbon cycle,[12] one finds for the luminosities:

$$L = \int_0^R 4\pi r^2 \epsilon \rho \, dr = \begin{cases} 1100 L_\odot & \text{for} \quad X_H = 0.35 \\ 8200 L_\odot & \text{for} \quad X_H = 0.40 \, . \end{cases} \tag{9}$$

These values are to be compared with an observed value of $38.9 L_\odot$ and are, therefore, 28 and 210 times too large, respectively. For $X_H = 0.369$ it is necessary to interpolate between the above two luminosities. Because of the sensitive dependence of the luminosity on the temperature, linear interpolation is too crude. Therefore, we resort to the following device: roughly, $L \backsim \rho_c^2 T_c^n$. We fix n so that the ratio of $L(X_H = 0.40)$ to $L(X_H = 0.35)$ is correctly given when the appropriate values of ρ_c and T_c are inserted. This leads to $n = 13.5$. We then substitute the values of ρ_c and T_c corresponding to $X_H = 0.369$ and obtain $L(X_H = 0.369) = 2400 L_\odot$. This is about sixty times the observed luminosity.

In agreement with the solar calculations, the theoretical luminosity turns out to be much larger than the observed value. The discrepancy is especially striking for Sirius A, since Morse's tables of the opacity were used—in contrast to Strömgren's tables for the sun—and Morse's opacities are uniformly lower than Strömgren's, sometimes as much as 50 per cent. The source of the discrepancy is, therefore, not to be found in the opacity tables used. Nor is it likely that the use of constant molecular weight in the integrations is responsible, although this point should ultimately be checked. Furthermore, considerations of the sort given by Sen and Burman[13] do not really resolve the difficulty. These authors show that they can reconcile the observed luminosity and mass of the sun with a hydrogen content of 36 per cent (zero helium content) and a central temperature of 20×10^6. However, the radius turns out to be 15 per cent larger than the sun's. This discrepancy appears small but actually contains the source of the trouble. The central temperature varies roughly as the inverse power of the radius, and the luminosity as the seventeenth power of the central temperature; also a 15 per cent decrease in radius increases the density by 50 per cent. The combination of these two factors leads to almost as serious a discrepancy as that found previously for the sun.

The most plausible conclusion to be drawn from the evidence obtained thus far is that helium is present in appreciable amounts in both the sun and Sirius A. It is not expected that the helium content would be the same in all stars of the main sequence. As a matter of fact, it would be interesting to discover whether there is a systematic variation of the helium content among main-sequence stars from the point of view of the theory of stellar interiors.

[11] In the case of the sun (cf. Paper I) linear interpolation between the $X_H = 0.30$ and $X_H = 0.40$ solutions in accordance with the above procedure leads to $T_c = 26.2 \times 10^6$ and $\rho_c = 123$, as compared with the correct values, $T_c = 25.7 \times 10^6$ and $\rho_c = 110$ (for $X_H = 0.35$). This is quite good and will be even better for Sirius A where the range covered is smaller.

[12] The carbon cycle gives $\epsilon = 3 \times 10^{21} X_H \zeta^2 e^{-\zeta}$, where $\zeta = 152/T^{1/3}$ and T is expressed in millions of degrees (cf. Paper I).

[13] *Ap. J.*, **100**, 347, 1944.

THE EFFECT OF THE ABSORPTION LINES ON THE TEMPERATURE DISTRIBUTION OF THE SOLAR ATMOSPHERE

GUIDO MÜNCH[1]
Yerkes Observatory
Received March 30, 1946

ABSTRACT

In this paper the influence of the absorption lines on the temperature distribution of a stellar atmosphere is reconsidered, using the new methods in the theory of radiative equilibrium. The analysis is carried out by solving simultaneously the appropriate equations of transfer for the continuous and the line spectra, under the condition of a constant net flux and on the assumption that the probability of occurrence of an absorption line at a frequency ν is governed by a distribution function $w_2(\nu)$. When $w_2(\nu)$ is independent of frequency, several cases are investigated according to whether the lines arise in absorption and/or scattering. When $w_2(\nu)$ is not constant throughout the spectrum, only the case of pure local thermodynamical equilibrium is considered. For the various cases considered, numerical models are computed in the first two approximations. These models are characterized by an emergent flux in the lines of the same order of magnitude as that observed in the solar spectrum. From the discussion of the different models, a value for the boundary temperature of the sun near 4600° K is derived. Further, it is shown that the darkening in integrated light of the solar disk is accounted for in terms of the combined darkening in the lines and in the continuum of one of the models considered. Finally, some remarks on the phenomenon of monochromatic darkening are also made.

1. *Introduction.*—The effect of the absorption lines on the temperature distribution in a stellar atmosphere has been studied in the past, mainly with the purpose of explaining the observed features of the continuous spectrum of the sun which could not be explained by the simple theory of radiative transfer in a gray atmosphere. As the writer has recently shown,[2] the dependence on wave length of the continuous absorption coefficient of the negative hydrogen ion, together with the theory of a nongray stellar atmosphere (disregarding, however, the presence of lines), accounts for the main features of the departures from grayness of the solar continuum, except in the ultraviolet part of the spectrum. In the latter region the problem is complicated by the overcrowding of the Fraunhofer lines, which produces a total absorption of an unknown amount. Nevertheless, when the darkening in the nongray atmosphere is computed and the comparison with the observed darkening is carried out, small systematic differences are found, in the sense that the computed center-limb contrast is higher than the observed one. It would seem that, to account for these differences, we should allow for the presence of absorption lines in determining the temperature distribution. In this connection we may recall that earlier treatments of this "blanketing effect" by E. A. Milne[3] and S. Chandrasekhar[4] have shown that the modifications of the temperature distribution in a gray atmosphere are not inappreciable.

The present paper presents some further developments relating to the effect produced by the absorption lines on the temperature distribution of a stellar atmosphere in radiative equilibrium, on the basis of the methods recently developed by S. Chandrasekhar,[5] in connection with a variety of problems of radiative transfer. These methods

[1] Fellow of the John Simon Guggenheim Memorial Foundation at the Yerkes Observatory.

[2] *Ap. J.*, **102**, 385, 1945.

[3] *Phil. Trans. R. Soc.*, A, **223**, 201–255, 1922: *Observatory*, **51**, 88, 1928.

[4] *M.N.*, **96**, 21, 1936. This paper will be referred to hereafter as "paper B." See also V. Ambarzumian, *Pub. Astr. Obs. U. Leningrad*, new ser., **1**, 7, 1936.

[5] *Ap. J.*, **100**, 76, 1944, and **101**, 328, 1945. These papers will be referred to as papers "II" and "VII," respectively.

enable us to treat the problem not only in a more exact fashion but also under less restrictive conditions.

2. *The equations of transfer and their approximate forms.*—The basic idea involved in the precise formulation of the problem was given first in paper B. Let $I_\nu(x, \mu)$ denote, as usual, the intensity of radiation of frequency ν and in a direction forming an angle ϑ $(= \cos^{-1}\mu)$ with the positive normal, $B_\nu(T_x)$ the Planck function for the temperature T_x prevailing at the depth x, and κ_ν the continuous absorption coefficient. The equation of transfer for the continuous spectrum, on the hypothesis of local thermodynamic equilibrium, is

$$\mu \frac{dI_\nu}{\rho dx} = -\kappa_\nu (I_\nu - B_\nu) . \tag{1}$$

On the other hand, for points within the line spectrum (assuming that for our purposes all lines can be treated in the same way as resonance lines), the appropriate equation of transfer is

$$\mu \frac{dI_\nu}{\rho dx} = -(\kappa_\nu + a_\nu) I_\nu + (1 - \epsilon_\nu) a_\nu J_\nu + (\kappa_\nu + \epsilon_\nu a_\nu) B_\nu \tag{2}$$

where

$$J_\nu = \frac{1}{2} \int_{-1}^{+1} I_\nu (x, \mu)\, d\mu , \tag{3}$$

and, further, where a_ν is the mean coefficient of scattering in the line and ϵ_ν the probability that the radiation of frequency ν is lost by photoelectric ionizations and collisions of the second kind. If we remember that a_ν and ϵ_ν in a stellar spectrum are highly singular functions of frequency, it would seem that the adoption of constant values a and ϵ for them, in the domain covered by the line spectrum, is likely to have a statistical significance. Without restricting the generality of the analysis as much as might appear at first sight, we can also suppose κ_ν to be a constant independent of frequency. In this context we may recall that, in paper VII, Chandrasekhar found that the temperature distribution in a gray atmosphere coincides with the temperature distribution in a nongray atmosphere "up to a second approximation," provided that the optical depth is measured in terms of a certain appropriately defined mean $\bar{\kappa}$.

We now introduce two distribution functions $w_1(\nu)$ and $w_2(\nu) = 1 - w_1(\nu)$, that govern the probability of our finding at the frequency ν the continuous and the line spectra, respectively. The integration of equations (1) and (2) over all frequencies then gives

$$\mu \frac{dI^{(1)}}{d\tau} = I^{(1)} - \int_0^\infty w_1 (\nu) B_\nu d\nu \tag{4}$$

and

$$\mu \frac{dI^{(2)}}{d\tau} = (1 + \xi) I^{(2)} - (1 - \epsilon) \xi J^{(2)} - (1 + \epsilon\xi) \int_0^\infty w_2 (\nu) B_\nu d\nu , \tag{5}$$

where τ is the optical depth measured in terms of the constant coefficient of continuous absorption and $\xi = a/\kappa$. It is to be noticed that in equations (4) and (5) we have introduced the superscripts (1) and (2) to distinguish the quantities related to the continuous and to the line spectra, respectively.

Equations (4) and (5) must be solved simultaneously under the condition of constant flux, expressed by the relation

$$J^{(1)} + (1 + \epsilon\xi) J^{(2)} = \int_0^\infty [w_1 (\nu) + (1 + \epsilon\xi) w_2 (\nu)] B_\nu d\nu . \tag{6}$$

In the following sections we shall be concerned with the solution of the system of equations (4), (5), and (6) under different conditions: First, we shall consider the cases

when $w_1(\nu)$ and $w_2(\nu)$ are independent of frequency, that is, when the lines can be considered uniformly distributed throughout the spectrum. In this case, equations (4), (5), and (6) reduce to

$$\mu \frac{dI^{(1)}}{d\tau} = I^{(1)} - w_1 B , \tag{7}$$

$$\mu \frac{dI^{(2)}}{d\tau} = (1+\xi) I^{(2)} - (1-\epsilon) \xi J^{(2)} - (1+\epsilon\xi) w_2 B , \tag{8}$$

and

$$J^{(1)} + (1+\epsilon\xi) J^{(2)} = [w_1 + (1+\epsilon\xi) w_2] B . \tag{9}$$

These equations have been solved by Chandrasekhar in paper B, following a Milne-Eddington type of approximation.

3.1. *The absorption lines formed in pure local thermodynamic equilibrium.*—When the Fraunhofer lines arise in a process of pure absorption, $\epsilon = 1$ and equations (7) and (8) become

$$\left.\begin{aligned} \mu \frac{dI^{(1)}}{d\tau} &= I^{(1)} - w_1 B , \\ \frac{\mu}{\gamma} \frac{dI^{(2)}}{d\tau} &= I^{(2)} - w_2 B , \end{aligned}\right\} \tag{10}$$

where $\gamma = 1 + \xi$. An important contribution to the study of this case has been given by E. Hopf,[6] who was able to evaluate the exact value of the integrated Planck function $B(\tau)$ at $\tau = 0$. Following this latter work, we shall formally generalize equations (10) to the system

$$\frac{\mu}{\gamma_a} \frac{dI^{(a)}}{d\tau} = I^{(a)} - w_a B \qquad (a = 1, 2, \ldots, m), \tag{11}$$

which represents the situation when the spectrum is divided into m parts, each characterized by a parameter γ_a, supposed to be independent of depth, and a relative density w_a. The condition of radiative equilibrium, under these more general circumstances, is

$$B(\tau) \Sigma \gamma_a w_a = \Sigma \gamma_a J^{(a)} = \Sigma \gamma_a \frac{1}{2} \int_{-1}^{+1} I^{(a)}(\tau, \mu)\, d\mu . \tag{12}$$

Using the foregoing relation, we can re-write equations (11) in the form

$$\frac{\mu}{\gamma_a} \frac{dI^{(a)}}{d\tau} = I^{(a)} - w_a \frac{\Sigma \gamma_\beta J^{(\beta)}}{\Sigma \gamma_\beta w_\beta} \qquad (a = 1, 2, \ldots, m). \tag{13}$$

Following the method developed in paper II, this system is replaced in the nth approximation by $2nm$ linear equations obtained by expressing $J^{(\beta)}$ in terms of Gauss's quadrature formula, involving the zeros μ_i of the $2n$th Legendre polynomial and the associated weights a_i. Thus we get

$$\frac{\mu_i}{\gamma_a} \frac{dI_i^{(a)}}{d\tau} = I_i^{(a)} - \frac{w_a}{\Sigma \gamma_\beta w_\beta} \sum_{\beta=1}^{m} \gamma_\beta \frac{1}{2} \sum_{j=-n}^{n} a_j I_j^{(\beta)} \qquad \begin{pmatrix} i = \pm 1, \ldots, \pm n \\ a = 1, 2, \ldots, m \end{pmatrix}, \tag{14}$$

where $I_i^{(a)} = I^{(a)}(\tau, \mu_i)$. This system of linear equations admits solutions of the form

$$I_i^{(a)} = \text{constant} \frac{e^{-k\tau}}{1 + k\mu_i/\gamma_a}, \tag{15}$$

[6] *M.N.*, **96**, 522, 1936.

where k_α is any of the $(2nm-2)$ nonvanishing roots of the equation

$$2\sum_{\alpha=1}^{m}\gamma_\alpha^2 w_\alpha = \sum_{\alpha=1}^{m}\gamma_\alpha w_\alpha \sum_{j=-n}^{n}\frac{a_j}{1+k\mu_j/\gamma_\alpha}. \tag{16}$$

Equations (14) also admit a solution of the form

$$I_i^{(\alpha)} = bw_\alpha\left(\tau+\frac{\mu_i}{\gamma_\alpha}+Q\right), \tag{17}$$

where b and Q are constants. Therefore, the general solution is

$$\left.\begin{aligned} I_i^{(\alpha)} = bw_\alpha\left\{\tau+\frac{\mu_i}{\gamma_\alpha}+Q+\sum_{\beta=1}^{nm-1}\frac{L_\beta e^{-k_\beta\tau}}{1+k_\beta\mu_i/\gamma_\alpha}+\sum_{\beta=1}^{nm-1}\frac{L_{-\beta}e^{k_\beta\tau}}{1-k_\beta\mu_i/\gamma_\alpha}\right\} \\ (\alpha=1,2,\ldots,m\ ;\ i=\pm1,\pm2,\ldots,\pm n). \end{aligned}\right\} \tag{18}$$

The integration constants L_β and $L_{-\beta}$ $(\beta=1,\ldots,nm-1)$, b and Q, are fixed by the boundary conditions. First, we require that the solution be asymptotically linear in τ as $\tau\to\infty$; and, second, we make use of the fact that there is no radiation incident at $\tau=0$. The first condition implies that $L_{-\beta}=0$ for every β, while the second condition gives $I_{-i}^{(\alpha)}(0)=0$, for every α and i. Thus

$$\sum_{\beta=1}^{nm-1}\frac{L_\beta}{1-k_\beta\mu_i/\gamma_\alpha}+Q=\frac{\mu_i}{\gamma_\alpha}\qquad\begin{pmatrix} i=1,\ldots,n \\ \alpha=1,\ldots,m\end{pmatrix}. \tag{19}$$

These are the nm equations which determine the $(nm-1)$ L_β's, and Q. The further integration constant, b, is readily found to be related to the constant net flux, according to

$$b=\tfrac{3}{4}F\frac{1}{\Sigma w_\alpha/\gamma_\alpha}. \tag{20}$$

The solution which satisfies the boundary conditions must, accordingly, be of the form

$$I_i^{(\alpha)}=\frac{3}{4}\frac{Fw_\alpha}{\Sigma w_\alpha/\gamma_\alpha}\left\{\tau+\frac{\mu_i}{\gamma_\alpha}+Q+\sum_{\beta=1}^{nm-1}\frac{L_\beta e^{-k_\beta\tau}}{1+k_\beta\mu_i/\gamma_\alpha}\right\}. \tag{21}$$

Using the foregoing solution, we can find $J^{(\alpha)}$ and $F^{(\alpha)}$ by representing the integrals by the corresponding Gaussian sums. Thus

$$J^{(\alpha)}=\frac{3}{4}\frac{Fw_\alpha}{\Sigma w_\alpha/\gamma_\alpha}\left\{\tau+Q+\sum_{\beta=1}^{nm-1}L_\beta e^{-k_\beta\tau}\sum_{j=1}^{n}\frac{a_j}{1-\mu_j^2k_\beta^2/\gamma_\alpha^2}\right\}, \tag{22}$$

and

$$F^{(\alpha)}=\frac{3}{2}\frac{Fw_\alpha}{\Sigma w_\alpha/\gamma_\alpha}\left\{\frac{2}{3}\frac{1}{\gamma_\alpha}+2\gamma_\alpha\sum_{\beta=1}^{nm-1}\frac{L_\beta}{k_\beta}e^{-k_\beta\tau}\left(1-\sum_{j=1}^{n}\frac{a_j}{1-\mu_j^2k_\beta^2/\gamma_\alpha^2}\right)\right\}. \tag{23}$$

The integrated Planck function is then obtained by substituting equation (22) in equation (12). We find

$$B(\tau)=\frac{3}{4}\frac{F}{\Sigma w_\alpha/\gamma_\alpha}\left\{\tau+Q+\sum_{\beta=1}^{nm-1}L_\beta e^{-k_\beta\tau}\right\}. \tag{24}$$

3.2. *The value of the boundary temperature.*—We shall now show how the value of $B(\tau)$ at $\tau = 0$ can be evaluated explicitly. Consider the function

$$S(\mu) = \sum_{\beta=1}^{nm-1} \frac{L_\beta}{1-\mu k_\beta} + Q - \mu . \tag{25}$$

According to equation (19), $S(\mu_i/\gamma_\alpha) = 0$ for every α and i. Hence, multiplying equation (25) by

$$R(\mu) = \prod_{\beta=1}^{nm-1} (1-\mu k_\beta) , \tag{26}$$

we obtain a polynomial of degree nm in μ, which vanishes for $\mu = \mu_i/\gamma_\alpha$ ($i = 1, 2, \ldots, n$; $\alpha = 1, 2, \ldots, m$). Accordingly, $S(\mu)R(\mu)$ cannot differ from the polynomial

$$P(\mu) = \prod_{\beta=1}^{m} \prod_{i=1}^{n} \left(\mu - \frac{\mu_i}{k_\beta}\right) \tag{27}$$

by more than a constant factor. This factor can be determined by comparing the coefficients of μ^{nm} in the expressions for $R(\mu)S(\mu)$ and $P(\mu)$. In the former it is $(-1)^{nm} k_1 k_2 \ldots k_{nm-1}$, while in the latter it is unity. Hence

$$S(\mu) = (-1)^{nm} k_1 k_2 \ldots k_{nm-1} \frac{P(\mu)}{R(\mu)} . \tag{28}$$

Setting $\mu = 0$ in the foregoing equation, we obtain

$$S(0) = k_1 k_2 \ldots k_{nm-1} \frac{(\mu_1 \mu_2 \ldots \mu_n)^m}{(\gamma_1 \gamma_2 \ldots \gamma_m)^n} . \tag{29}$$

In this expression the product of the characteristic roots appears; this can be evaluated by writing down the characteristic equation (16) in the form of a polymomial in k^2. We find

$$k_1 k_2 \ldots k_{nm-1} = \frac{(\gamma_1 \gamma_2 \ldots \gamma_m)^n}{(\mu_1 \mu_2 \ldots \mu_n)^m} \left(\frac{\Sigma w_\alpha/\gamma_\alpha}{3\Sigma w_\alpha \gamma_\alpha}\right)^{\frac{1}{2}} , \tag{30}$$

and equation (29) becomes

$$S(0) = \left(\frac{\Sigma w_\alpha/\gamma_\alpha}{3\Sigma w_\alpha \gamma_\alpha}\right)^{\frac{1}{2}} . \tag{31}$$

On the other hand, according to equations (24) and (25),

$$B(0) = \tfrac{3}{4} F \frac{S(0)}{\Sigma w_\alpha/\gamma_\alpha} ; \tag{32}$$

or, using equation (31), we have

$$B(0) = \frac{\sqrt{3}}{4} \frac{F}{[(\Sigma w_\alpha \gamma_\alpha)(\Sigma w_\alpha/\gamma_\alpha)]^{\frac{1}{2}}} . \tag{33}$$

It is clear from equations (11) and (12) that, without loss of generality, we can impose on the γ_α's a condition of the form

$$\sum_{\alpha=1}^{m} w_\alpha/\gamma_\alpha = 1 . \tag{34}$$

With such a "normalization," equation (33) becomes identical with the result first proved by Hopf.[7]

An explicit expression for the constants L_α occurring in our solution (21) can be obtained from equations (25) and (28); for, defining

$$R_\beta(\mu) = \prod_{\alpha \neq \beta} (1 - \mu k_\alpha) \tag{35}$$

and multiplying equation (25) by $R(\mu)$, we get

$$\sum_{\beta=1}^{nm-1} L_\beta R_\beta(\mu) + (Q - \mu) R(\mu) = (-1)^{nm} k_1 k_2 \ldots k_{nm-1} P(\mu). \tag{36}$$

If we now set $\mu = 1/k_\beta$ in equation (36), we find

$$L_\beta = (-1)^{nm} k_1 k_2 \ldots k_{nm-1} \frac{P(1/k_\beta)}{R_\beta(1/k_\beta)}. \tag{37}$$

The function $S(\mu)$ given by expression (28) also gives a closed expression for the emergent radiation in the different parts into which the spectrum has been divided. Thus, introducing equation (24) in the expression

$$I^{(\alpha)}(0, \mu) = w_\alpha \int_0^\infty B(t)\, e^{-t/\mu} \frac{dt}{\mu} \tag{38}$$

and making use of the definition (25), we obtain

$$I^{(\alpha)}(0, \mu) = \tfrac{3}{4} F \frac{w_\alpha}{\Sigma w_\alpha/\gamma_\alpha} S\left(-\frac{\mu}{\gamma_\alpha}\right). \tag{39}$$

Thus we complete the description of the radiation field for the case of pure absorption.

3.3. *Numerical examples.*—We shall now give the numerical solutions in the first two approximations for the models considered in paper B.

Example a: $$w_1 = 0.8\,, \qquad w_2 = 0.2\,, \qquad \gamma = 5\,. \tag{40}$$

In the first approximation the characteristic root is $k_1 = \sqrt{35} = 5.91608$, and the integrated Planck function is given by

$$B(\tau) = \frac{3}{4} \frac{F}{0.84} (\tau + 0.52379 - 0.12938\, e^{-k_1 \tau}). \tag{41}$$

In the second approximation the characteristic roots are

$$k_1 = 1.91751\,, \qquad k_2 = 5.00488\,, \qquad k_3 = 11.98673\,, \tag{42}$$

and the expression for the source function is

$$\left.\begin{aligned} B(\tau) = \frac{3}{4} \frac{F}{0.84} (\tau + 0.63660 - 0.13287\, e^{-k_1 \tau} - 0.04505\, e^{-k_2 \tau} \\ - 0.06427\, e^{-k_3 \tau}). \end{aligned}\right\} \tag{43}$$

The corresponding relation between boundary and effective temperatures is

$$T_0 = 0.76034 T_e\,. \tag{44}$$

[7] *Ibid.*, eq. (51).

The values of $B(\tau)$ given by expressions (41) and (43) are tabulated in Table 1 and further illustrated in Figure 1.

Example b: $w_1 = 0.8\,, \quad w_2 = 0.2\,, \quad \gamma = 10\,. \tag{45}$

First approximation:

$$k_1 = 9.37321\,, \tag{46}$$

$$B(\tau) = \frac{3}{4}\frac{F}{0.82}(\tau + 0.52840 - 0.21596\,e^{-k_1\tau})\,. \tag{47}$$

TABLE 1

THE INTEGRATED PLANCK FUNCTION B(τ) FOR THE VARIOUS MODELS

τ	$\gamma=\lambda=5$		$\gamma=\lambda=10$		$\gamma=5,\ \lambda=1$		$\gamma=10,\ \lambda=1$		$\gamma=10,\ \lambda=1$ $\tau<1/6$ $\gamma=\lambda=1$ $\tau>1/6$	
	I*	II	I	II	I	II	I	II	I	II
0.00	0.3522	0.3522	0.2858	0.2858	0.4330	0.4097	0.4330	0.4308	0.4330	0.4362
0.02	0.3829	0.3905	0.3378	0.3526	0.4538	0.4348	0.4572	0.4603	0.4650	0.4724
0.05	0.4264	0.4424	0.4054	0.4335	0.4845	0.4712	0.4923	0.5019	0.5126	0.5236
0.10	0.4930	0.5180	0.4974	0.5379	0.5349	0.5295	0.5487	0.5664	0.5921	0.6045
0.20	0.6109	0.6462	0.6359	0.6942	0.6330	0.6400	0.6549	0.6856	0.7266	0.7364
0.30	0.7159	0.7590	0.7458	0.8203	0.7285	0.7454	0.7553	0.7972	0.8016	0.8209
0.40	0.8140	0.8645	0.8445	0.9328	0.8222	0.8475	0.8522	0.9039	0.8766	0.9037
0.50	0.9081	0.9659	0.9388	1.0380	0.9145	0.9472	0.9470	1.0072	0.9516	0.9851
0.60	1.0001	1.0645	1.0314	1.1391	1.0059	1.0450	1.0405	1.1079	1.0266	1.0654
0.80	1.1809	1.2564	1.2149	1.3343	1.1871	1.2364	1.2254	1.3041	1.1766	1.2233
1.00	1.3602	1.4435	1.3979	1.5246	1.3669	1.4238	1.4091	1.4956	1.3266	1.3786
1.40	1.7176	1.8103	1.7638	1.8981	1.7250	1.7910	1.7753	1.8709	1.6266	1.6846
1.60	1.8962	1.9914	1.9467	2.0829	1.9036	1.9726	1.9583	2.0564	1.7766	1.8362
2.00	2.2534	2.3515	2.3125	2.4508	2.2609	2.3331	2.3241	2.4251	2.0766	2.1380
3.00	3.1462	3.2466	3.2272	3.3668	3.1538	3.2287	3.2388	3.3418	2.8266	2.8893
4.00	4.0391	4.1398	4.1418	4.2815	4.0467	4.1220	4.1534	4.2568	3.5766	3.6395

* "I" and "II" refer to the first and second approximations, respectively.

Second approximation:

$$k_1 = 2.16772\,, \quad k_2 = 7.43277\,, \quad k_3 = 22.62302\,, \tag{48}$$

$$B(\tau) = \frac{3}{4}\frac{F}{0.82}(\tau + 0.68117 - 0.12370\,e^{-k_1\tau} - 0.18300\,e^{-k_2\tau} - 0.06205\,e^{-k_3\tau})\,. \tag{49}$$

The boundary value of the temperature in this example is

$$T_0 = 0.72114\,T_e\,. \tag{50}$$

The numerical values of $B(\tau)$ determined by equations (47) and (49) are given in Table 1 and are graphically represented in Figure 1.

4.1. *Absorption lines formed in a process involving scattering as well as absorption.*— When $\epsilon \neq 1$, equations (7) and (8) can be written in the form

$$\left.\begin{aligned} \mu\frac{dI^{(1)}}{d\tau} &= I^{(1)} - w_1 B\,, \\ \mu\frac{dI^{(2)}}{d\tau} &= \gamma I^{(2)} - (\gamma - \lambda)J^{(2)} - w_2\lambda B\,, \end{aligned}\right\} \tag{51}$$

where

$$\gamma = 1 + \xi \qquad \text{and} \qquad \lambda = 1 + \epsilon\xi \,. \tag{52}$$

The condition (9) for a constant net flux is

$$B = \frac{J^{(1)} + \lambda J^{(2)}}{w_1 + \lambda w_2} = \sigma\,(J^{(1)} + \lambda J^{(2)})\,, \tag{53}$$

and the system of equations to be solved becomes

$$\left.\begin{aligned} \mu\,\frac{dI^{(1)}}{d\tau} &= I^{(1)} - w_1\sigma J^{(1)} - w_1\lambda\sigma J^{(2)}\,, \\ \mu\,\frac{dI^{(2)}}{d\tau} &= \gamma I^{(2)} - (\gamma - w_1\lambda\sigma)\,J^{(2)} - w_2\lambda\sigma J^{(2)}\,. \end{aligned}\right\} \tag{54}$$

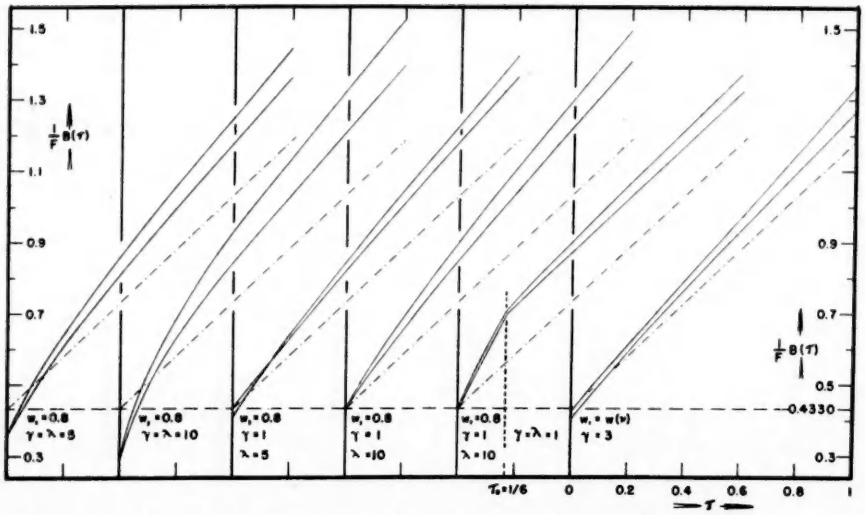

FIG. 1.—Comparison of the integrated Planck function in the various models for the first two approximations (*solid lines*) with the first approximation of the standard case (*broken line*). The scale of the abscissae is displaced by 0.4 units for each case considered. (The value of γ and λ in this diagram should be interchanged in every case but that on the extreme right.)

Again following the method developed in paper II, we find that the general solution of this system in the nth approximation is

$$\left.\begin{aligned} I_i^{(1)} &= \frac{3}{4}\,\frac{Fw_1}{w_1 + w_2/\gamma}\left[\tau + \mu_i + Q + \frac{1}{w_1}\sum_{a=1}^{2n-1}\left(\frac{L_a e^{-k_a\tau}}{1 + k_a\mu_i} + \frac{L_{-a}e^{k_a\tau}}{1 - k_a\mu_i}\right)\frac{1}{1 - G_a}\right], \\ I_i^{(2)} &= \frac{3}{4}\,\frac{Fw_2}{w_1 + w_2/\gamma}\left[\tau + \frac{\mu_i}{\gamma} + Q + \frac{1}{w_2\gamma}\sum_{a=1}^{2n-1}\left(\frac{L_a e^{-k_a\tau}}{1 + k_a\mu_i/\gamma}\right.\right. \\ &\qquad \left.\left. + \frac{L_{-a}e^{k_a\tau}}{1 - k_a\mu_i/\gamma}\right)\frac{1}{H_a - 1}\right] \qquad (i = \pm 1, \pm 2, \ldots, \pm n)\,, \end{aligned}\right\} \tag{55}$$

where L_a, $L_{-a}(a = 1, 2, \ldots, 2n-1)$, and Q are $4n - 1$ constants of integration, the k_a's are the $2n - 1$ positive roots of the characteristic equation

$$1 - w_1\sigma G - \left(1 - \frac{w_1\lambda\sigma}{\gamma}\right)H + w_1\sigma\left(1 - \frac{\lambda}{\gamma}\right)GH = 0\,, \tag{56}$$

and where, furthermore,

$$G=\frac{1}{2}\sum_{i=-n}^{n}\frac{a_i}{1+k\mu_i} \qquad \text{and} \qquad H=\frac{1}{2}\sum_{i=-n}^{n}\frac{a_i}{1+k\mu_i/\gamma}. \tag{57}$$

If the solution has to be asymptotically linear as $\tau\to\infty$, $L_{-a}=0$ for every a, and equations (55) become

$$\left.\begin{aligned} I_i^{(1)}&=\frac{3}{4}\frac{Fw_1}{w_1+w_2/\gamma}\left[\tau+\mu_i+Q+\frac{1}{w_1}\sum_{a=1}^{2n-1}\frac{L_a}{1-G_a}\frac{e^{-k_a\tau}}{1+k_a\mu_i}\right],\\ I_i^{(2)}&=\frac{3}{4}\frac{Fw_2}{w_1+w_2/\gamma}\left[\tau+\frac{\mu_i}{\gamma}+Q+\frac{1}{w_2\gamma}\sum_{a=1}^{2n-1}\frac{L_a}{H_a-1}\frac{e^{-k_a\tau}}{1+k_a\mu_i/\gamma}\right]. \end{aligned}\right\} \tag{58}$$

The $2n$ constants that appear in these equations are determined by the condition of vanishing incident radiation:

$$\left.\begin{aligned} &\frac{1}{w_1}\sum_{a=1}^{2n-1}\frac{L_a}{1-G_a}\frac{1}{1-k_a\mu_i}+Q=\mu_i,\\ &\frac{1}{w_2\gamma}\sum_{a=1}^{2n-1}\frac{L_a}{H_a-1}\frac{1}{1-k_a\mu_i/\gamma}+Q=\frac{\mu_i}{\gamma} \end{aligned}\right\} \quad (i=1,\ldots,n). \tag{59}$$

The source function $B(\tau)$ in this case is given by

$$B(\tau)=\frac{3}{4}\frac{F}{w_1+w_2/\gamma}\left[\tau+Q+\sum_{a=1}^{2n-1}L_a e^{-k_a\tau}\left(\frac{G_a}{1-G_a}+\frac{\lambda}{\gamma}\frac{H_a}{H_a-1}\right)\sigma\right]. \tag{60}$$

It has not been possible to evaluate explicitly the value of $B(\tau)$ at $\tau=0$. It is perhaps of interest, however, to mention that in the case of pure scattering ($\lambda=1$), the first approximation always gives for the boundary temperature the exact value obtained in the standard case, independently of the values that w_1, w_2, and γ might have. However, this situation no longer holds in a higher approximation, because the value of $B(0)$ obtained then is smaller than the one given in the first approximation, as can be seen from the numerical examples given below.

4.2. *Numerical examples.*—Again we shall consider the two models given in paper B. Both refer to the extreme case in which the lines arise as a pure scattering phenomenon, i.e., $\epsilon=0$ and $\lambda=1$.

Example a: $$w_1=0.8\,,\qquad w_2=0.2\,,\qquad \gamma=5\,,\qquad \lambda=1\,. \tag{61}$$

First approximation:
$$\left.\begin{aligned} &k_1=3.54965\,,\qquad Q=0.53228\,,\\ &G_1=-0.31250\,,\qquad H_1=1.201923\,,\qquad L_1=-0.049666\,, \end{aligned}\right\} \tag{62}$$

$$B(\tau)=\frac{3}{4}\frac{F}{0.84}(\tau+0.53228-0.04730\,e^{-k_1\tau}), \tag{63}$$

and

$$T_0=0.80119\,T_e\,. \tag{64}$$

Second approximation:

$$\left.\begin{aligned} &k_1 = 1.81355\,, && k_2 = 3.43621\,, && k_3 = 10.55209\,,\\ &G_1 = 0.915925\,, && G_2 = -1.83255\,, && G_3 = -0.059204\,,\\ &H_1 = 1.053002\,, && H_2 = 1.22516\,, && H_3 = 1.14460\,,\\ &L_1 = -0.0089599\,, && L_2 = -0.024963\,, && L_3 = -0.0115666\,,\\ & && Q = 0.61668\,, \end{aligned}\right\} \tag{65}$$

$$\left.\begin{aligned} B(\tau) = \frac{3}{4}\frac{F}{0.84}(\tau + 0.61668 - 0.13321\,e^{-k_1\tau} - 0.01102\,e^{-k_2\tau}\\ - 0.01359\,e^{-k_3\tau})\,, \end{aligned}\right\} \tag{66}$$

and

$$T_0 = 0.80004\,T_e\,. \tag{67}$$

Example b: $w_1 = 0.8\,,\quad w_2 = 0.2\,,\quad \gamma = 10\,,\quad \lambda = 1\,.$ (68)

First approximation: $k_1 = 4.95984\,,\quad Q = 0.54106\,,$

$$G_1 = -0.13889\,,\quad H_1 = 1.08932\,,\quad L_1 = -0.061620\,, \tag{69}$$

$$B(\tau) = \frac{3}{4}\frac{F}{0.82}(\tau + 0.54106 - 0.06763\,e^{-k_1\tau})\,, \tag{70}$$

and

$$T_0 = 0.80119\,T_e\,. \tag{71}$$

Second approximation:

$$\left.\begin{aligned} &k_1 = 1.94284\,, && k_2 = 4.87106\,, && k_3 = 20.38105\,,\\ &G_1 = 0.96358\,, && G_2 = -0.39521\,, && G_3 = -0.01500\,,\\ &H_1 = 1.01288\,, && H_2 = 1.09266\,, && H_3 = 1.08723\,,\\ &L_1 = -0.0037807\,, && L_2 = -0.048638\,, && L_3 = -0.0079513\,,\\ & && Q = 0.65413\,, \end{aligned}\right\} \tag{72}$$

$$\left.\begin{aligned} B(\tau) = \frac{3}{4}\frac{F}{0.82}(\tau + 0.65413 - 0.12976\,e^{-k_1\tau} - 0.04358\,e^{-k_2\tau}\\ - 0.00979\,e^{-k_3\tau})\,, \end{aligned}\right\} \tag{73}$$

and

$$T_0 = 0.80015\,T_e\,. \tag{74}$$

The values of $B(\tau)$, determined on the two approximations of the two examples considered for different values of τ, are given in Table 1 and illustrated in Figure 1.

5.1. *The layer model.*—We shall consider now the case when the parameters that describe the radiation field are not constant throughout the atmosphere but have different values above and below a certain optical depth τ_0 (for continuous absorption). We shall suppose that in the higher layer ($\tau < \tau_0$) the process in which the lines arise is characterized by certain parameters (γ_a, λ_a), while in the bottom layer ($\tau > \tau_0$) these contants are (γ_b, λ_b). We shall further assume that w_2 is the same in both layers. According to the results of the preceding paragraph, the solution of the equations of transfer for $\tau < \tau_0$ will have the form (55); this involves $4n - 1$ constants of integration. Moreover, for $\tau > \tau_0$, the solution will be of the form (58), since it must be asymptotically linear as $\tau \to \infty$ and will therefore involve $2n$ further constants of integration. Consequently, we have a total of

$6n - 1$ constants of integration, which have to be determined from the boundary conditions. These conditions are the vanishing of the incident radiation at $\tau = 0$.

$$I^{(1)}_{-i}(\tau = 0) = 0\,, \qquad I^{(2)}_{-i}(\tau = 0) = 0 \qquad (i = 1, 2, \ldots, n)\,, \quad (75)$$

and the continuity of the solution at $\tau = \tau_0$,

$$I^{(1)}_i(\tau_0^-) = I^{(1)}_i(\tau_0^+)\,, \qquad I^{(2)}_i(\tau_0^-) = I^{(2)}_i(\tau_0^+) \qquad (i = \pm 1, \ldots, \pm n)\,. \quad (76)$$

Of the $4n$ equations represented in relations (76), only $4n - 1$ are linearly independent, since our solution in the two regions satisfies the condition of constant net flux:

$$F = 2\sum_{i=-n}^{n} a_i \mu_i (I_i^{(1)} + I_i^{(2)})\, \tau_0^- = 2\sum_{i=-n}^{n} a_i \mu_i (I_i^{(1)} + I_i^{(2)})\, \tau_0^+\,. \quad (77)$$

Hence, the system of $6n$ linear equations, represented by equations (75) and (76), is of rank $6n - 1$ and determines uniquely the $6n - 1$ constants of integration which describe the solution of the problem. For the numerical solution of this system it is convenient to write down equations (76) in the alternative form

$$\left.\begin{aligned} \sum_{i=-n}^{n} a_i \mu_i^m I_i^{(1)}(\tau_0^-) &= \sum_{i=-n}^{n} a_i \mu_i^m I_i^{(1)}(\tau_0^+)\,, \\ \sum_{i=-n}^{n} a_i \mu_i^m I_i^{(2)}(\tau_0^-) &= \sum_{i=-n}^{n} a_i \mu_i I_i^{(2)}(\tau_0^+) \end{aligned}\right\} \quad (m = 0, 1, \ldots, 2n - 1)\,. \quad (78)$$

For $m = 0$ these equations give

$$J^{(1)}(\tau_0^-) = J^{(1)}(\tau_0^+)\,, \qquad J^{(2)}(\tau_0^-) = J^{(2)}(\tau_0^+)\,. \quad (79)$$

From the expression (53) for the integrated Planck function,

$$B(\tau) = \frac{J^{(1)} + \lambda J^{(2)}}{w_1 + \lambda w_2}\,, \quad (80)$$

we conclude that the continuity of $B(\tau)$ at τ_0 implies

$$\lambda_a = \lambda_b \qquad \text{or} \qquad (\epsilon\xi)_a = (\epsilon\xi)_b\,. \quad (81)$$

Thus we have proved that the temperature will be continuous at $\tau = \tau_0$ only when relation (81) is satisfied, a condition which was stated by Chandrasekhar in paper B for the Milne approximation.

A. Unsöld in his recent treatment of the subject[8] has questioned the use made by Chandrasekhar in paper B of equation (81) as one of the conditions of the problem, on the grounds that the quantity $\epsilon\xi$ has nothing to do with the formulation of the problem of radiative equilibrium. Although this argument is formally correct, it should be pointed out that a model atmosphere with a discontinuity in its temperature distribution would not seem to have a physical basis.

5.2. *Layer model with pure scattering for $\tau < \tau_0$ and only continuous absorption for $\tau > \tau_0$.*—The discussion of a layer model for which $\lambda_a = 1$, $\gamma_a = \gamma$, and $\lambda_b = \gamma_b = \eta$ is of interest, since in our picture of the problem for $\eta = 1$ we approach the original "blanketing model" first considered by Milne[9] and Lindblad.[10] According to the general method outlined in the preceding paragraph, the solution for $\tau < \tau_0$ will have the form

[8] *Zs. f. Ap.*, **22**, 356, 1943.

[9] *Op. cit.*, p. 225.

[10] *Nova Acta Reg. Soc. Sci., Upsala*, **6**, No. 1, 17, 1923.

$$I_i^{(1)} = \frac{3}{4}\frac{Fw_1}{w_1+w_2/\gamma}\left\{\tau+\mu_i+Q+\frac{1}{w_1}\sum_{a=1}^{2n-1}\left(\frac{L_a e^{-k_a\tau}}{1+\mu_i k_a}+\frac{L_{-a}e^{k_a\tau}}{1-\mu_i k_a}\right)\frac{1}{1-G_a}\right\},$$

$$I_i^{(2)} = \frac{3}{4}\frac{Fw_2}{w_1+w_2/\gamma}\left\{\tau+\frac{\mu_i}{\gamma}+Q+\frac{1}{w_2\gamma}\sum_{a=1}^{2n-1}\left(\frac{L_a e^{-k_a\tau}}{1+\mu_i k_a/\gamma}+\frac{L_{-a}e^{k_a\tau}}{1-\mu_i k_a/\gamma}\right)\frac{1}{H_a-1}\right\} \qquad (i=\pm 1,\ldots,\pm n), \tag{82}$$

and for $\tau > \tau_0$

$$I_i^{(1)} = \frac{3}{4}\frac{Fw_1}{w_1+w_2/\gamma}\left\{\tau+\mu_i+R+\sum_{a=1}^{2n-1}\frac{M_a e^{-q_a\tau}}{1+\mu_i q_a}\right\},$$

$$I_i^{(2)} = \frac{3}{4}\frac{Fw_2}{w_1+w_2/\gamma}\left\{\tau+\frac{\mu_i}{\gamma}+R+\sum_{a=1}^{2n-1}\frac{M_a e^{-q_a\tau}}{1+\mu_i q_a/\gamma}\right\}. \tag{83}$$

The k_a's appearing in equation (82) are the roots of equation (56), while the q_a's occurring in equation (83) are the roots of the equation

$$w_1\sum_{i=1}^{n}\frac{a_i}{1-\mu_i^2q^2}+w_2\eta\sum_{i=1}^{n}\frac{a_i}{1-\mu_i^2q^2/\eta^2}=w_1+w_2\eta\,. \tag{84}$$

The boundary conditions (75) and (78), which determine the $6n-1$ constants of integration, are readily written down and solved numerically without difficulty. However, if we let $\eta\to 1$, the solution of these equations is not straightforward, and some care must be taken in the limiting process. If we introduce the definitions

$$D_{m,a}=\sum_{i=1}^{n}\frac{a_i\mu_i^m}{1-\mu_i^2q_a^2}, \qquad E_{m,a}=\sum_{i=1}^{n}\frac{a_i\mu_i^m}{1-\mu_i^2q_a^2/\eta^2}, \tag{85}$$

the boundary conditions (78), with their right-hand sides in explicit form, can be written in the following fashion:

$$\sum_{i=-n}^{n}a_i\mu_i^{2j}I_i^{(1)}(\tau_0^-)=\frac{3}{2}\frac{Fw_1}{w_1+w_2/\eta}\left\{\frac{\tau_0+R}{2j+1}+\sum_{a=1}^{2n-1}M_a e^{-q_a\tau_0}D_{2j,a}\right\},$$

$$\sum_{i=-n}^{n}a_i\mu_i^{2j}I_i^{(2)}(\tau_0^-)=\frac{3}{2}\frac{Fw_2}{w_1+w_2/\eta}\left\{\frac{\tau_0+R}{2j+1}+\sum_{a=1}^{2n-1}M_a e^{-q_a\tau_0}E_{2j,a}\right\},$$

$$\sum_{i=-n}^{n}a_i\mu_i^{2j+1}I_i^{(1)}(\tau_0^-)=\frac{3}{2}\frac{Fw_1}{w_1+w_2/\eta}\left\{\frac{1}{2j+3}+\sum_{a=1}^{2n-1}M_a e^{-q_a\tau_0}D_{2j+1,a}\right\},$$

$$\sum_{i=-n}^{n}a_i\mu_i^{2j+1}I_i^{(2)}(\tau_0^-)=\frac{3}{2}\frac{Fw_2}{w_1+w_2/\eta}\left\{\frac{1/\eta}{2j+3}+\sum_{a=1}^{2n-1}M_a e^{-q_a\tau_0}E_{2j+1,a}\right\}. \tag{86}$$

If we now write the characteristic equation (84) in the form of a polynomial in q^2 and then let $\eta\to 1$, we find that $n-1$ of its roots tend to the characteristic roots of the "standard case," i.e., the positive roots of the equation

$$\sum_{i=1}^{n}\frac{a_i}{1-\mu_i^2q^2}=1\,, \tag{87}$$

while the other n roots tend to the reciprocals $1/\mu_i$ of the n-positive zeros of the $2n$th Legendre polynomial. On the other hand, from definitions (85) it is a simple matter[11] to obtain the following recursion formula:

$$\left.\begin{aligned}
D_{2j-1,a} &= \frac{1}{(2j-1)\,q_a} + \frac{1}{(2j-3)\,q_a^3} + \cdots + \frac{1-D_{0,a}}{q_a^{2j-1}}, \\
D_{2j,a} &= -\frac{1}{(2j-1)\,q_a^2} - \frac{1}{(2j-3)\,q_a^4} - \cdots - \frac{1-D_{0,a}}{q_a^{2j}}, \\
E_{2j-1,a} &= \frac{\eta}{(2j-1)\,q_a} + \frac{\eta^3}{(2j-3)\,q_a^3} + \cdots + \frac{1-E_{0,a}}{q_a^{2j-1}}\,\eta^{2j-1}, \\
E_{2j,a} &= -\frac{\eta^2}{(2j-1)\,q_a^2} - \frac{\eta^4}{(2j-3)\,q_a^4} - \cdots - \frac{1-E_{0,a}}{q_a^{2j}}\,\eta^{2j} \\
&\qquad (j = 1, 2, \ldots, n-1).
\end{aligned}\right\} \tag{88}$$

Making use of these expressions and letting $\eta \to 1$ in equations (86), we see that for the q_a's that tend to $1/\mu_i$, the corresponding values of $D_{0,i}$ and $E_{0,i}$ will diverge to infinity, and equations (86) can be satisfied only if the corresponding values of M_i tend to zero in such a way that the limits,

$$\lim_{\eta \to 1} M_i D_{0,i} = \frac{\mathfrak{R}_i}{w_1} \quad \text{and} \quad \lim_{\eta \to 1} M_i E_{0,i} = \frac{\mathfrak{R}'_i}{w_2}, \tag{89}$$

are finite for every i. Furthermore, the condition of constant net flux requires that these limits $\mathfrak{R}_i$ and $\mathfrak{R}'_i$ satisfy the relation

$$\frac{\mathfrak{R}_i}{\mathfrak{R}'_i} = -1 \qquad (i = 1, 2, \ldots, n). \tag{90}$$

As a result of this limiting process, we can write the complete boundary conditions in the form

$$\left.\begin{aligned}
I^{(1)}_{-i}(\tau = 0) &= 0, \\
I^{(2)}_{-i}(\tau = 0) &= 0
\end{aligned}\right\} \qquad (i = 1, 2, \ldots, n), \tag{91}$$

and

$$\left.\begin{aligned}
\sum_{i=-n}^{n} a_i \mu_i^{2j} I_i^{(1)}(\tau_0^-) &= \tfrac{3}{2} F w_1 \left\{ \frac{\tau_0 + R}{2j+1} + \sum_{a=1}^{n-1} M_a D_{2j,a} e^{-q_a \tau_0} + \frac{1}{w_1} \sum_{i=1}^{n} \mu_i^{2j} \mathfrak{R}_i \right\}, \\
\sum_{i=-n}^{n} a_i \mu_i^{2j} I_i^{(2)}(\tau_0^-) &= \tfrac{3}{2} F w_2 \left\{ \frac{\tau_0 + R}{2j+1} + \sum_{a=1}^{n-1} M_a D_{2j,a} e^{-q_a \tau_0} - \frac{1}{w_2} \sum_{i=1}^{n} \mu_i^{2j} \mathfrak{R}_i \right\}, \\
\sum_{i=-n}^{n} a_i \mu_i^{2j+1} I_i^{(1)}(\tau_0^-) &= \tfrac{3}{2} F w_1 \left\{ \frac{1}{2j+3} + \sum_{a=1}^{n-1} M_a D_{2j+1,a} e^{-q_a \tau_0} - \frac{1}{w_1} \sum_{i=1}^{n} \mu_i^{2j+1} \mathfrak{R}_i \right\}, \\
\sum_{i=-n}^{n} a_i \mu_i^{2j+1} I_i^{(2)}(\tau_0^-) &= \tfrac{3}{2} F w_2 \left\{ \frac{1}{2j+3} + \sum_{a=1}^{n-1} M_a D_{2j+1,a} e^{-q_a \tau_0} + \frac{1}{w_2} \sum_{i=1}^{n} \mu_i^{2j+1} \mathfrak{R}_i \right\} \\
&\qquad (j = 0, 1, \ldots, n-1).
\end{aligned}\right\} \tag{92}$$

[11] Cf. Paper VII, pp. 335–336.

If we introduce the values of $I_i^{(1)}$ and $I_i^{(2)}$ given by the relations (82) in the left-hand sides of equations (91) and (92), the determination of the constants is immediate.

The source function, $B(\tau)$, then takes the form

$$\left.\begin{aligned} B(\tau) &= \frac{3}{4}\frac{F}{w_1+w_2/\gamma}\left\{\tau+Q+\sum_{a=1}^{2n-1} c_a\left(L_a e^{-k_a\tau}+L_{-a}e^{k_a\tau}\right)\right\} && (\tau \leqslant \tau_0), \\ B(\tau) &= \tfrac{3}{4}F\left\{\tau+R+\sum_{a=1}^{n-1} M_a e^{-q_a\tau}\right\} && (\tau \geqslant \tau_0), \end{aligned}\right\} \tag{93}$$

where

$$c_a = \frac{G_a}{1-G_a}+\frac{1}{\gamma}\frac{H_a}{H_a-1}. \tag{94}$$

If equations (93) are introduced into the expression for the emergent intensity in the continuum,

$$I^{(1)}(0,\mu) = w_1\int_0^\infty B(\tau)\, e^{-\tau/\mu}\frac{d\tau}{\mu}, \tag{95}$$

we find that

$$\left.\begin{aligned} I^{(1)}(0,\mu) = \tfrac{3}{4}Fw_1\Bigg\{&\frac{1}{w_1+w_2/\gamma}\Bigg[\mu+Q-(\tau_0+\mu+Q)\,e^{-\tau_0/\mu} \\ &-\sum_{a=1}^{2n-1} c_a\left(L_a\frac{e^{-(1+k_a\mu)\tau_0/\mu}-1}{1+k_a\mu}+L_{-a}\frac{e^{-(1-k_a\mu)\tau_0/\mu}-1}{1-k_a\mu}\right)\Bigg] \\ &+e^{-\tau_0/\mu}\Bigg[\tau_0+\mu+R+\sum_{a=1}^{n-1} M_a\frac{e^{-\tau_0 q_a}}{1+q_a\mu}\Bigg]\Bigg\}. \end{aligned}\right\} \tag{96}$$

The expression for the emergent intensity in the lines $I^{(2)}(0,\mu)$ is obtained if in equation (96) we substitute, throughout, μ/γ for μ and change the factor w_1 in front of the bracket by w_2.

The expression for the total emergent intensity, $I(0,\mu)$, is then given by

$$I(0,\mu) = I^{(1)}(0,\mu)+I^{(2)}(0,\mu), \tag{97}$$

and the resulting law of darkening is

$$\phi(\mu) = \frac{I(0,\mu)}{I(0,1)}. \tag{98}$$

5.3. *Numerical example.*—We have computed the example

$$w_1 = 0.8\,, \quad w_2 = 0.2\,, \quad \tau_0 = \tfrac{1}{6}\,, \quad \gamma = 10\,, \quad \lambda = 1\,, \quad \eta = 1\,, \tag{99}$$

considered in paper B.

The characteristic roots for $\tau < \tau_0$ have been computed already in example *b* of section 4.2, while the characteristic roots for $\tau > \tau_0$ are taken from paper II.

First approximation:

$$\left.\begin{aligned} k_1 &= 4.95984\,, & G_1 &= -0.13889\,, & H_1 &= 1.0893246\,, \\ L_1 &= -0.086740\,, & L_{-1} &= 0.052080\,, & Q &= 0.51147\,, \\ & & R &= 0.76886\,, & q_1 &= -0.131976\,, \end{aligned}\right\} \tag{100}$$

$$\left.\begin{aligned} B(\tau) &= \frac{3}{4}\frac{F}{0.82}(\tau+0.51147-0.09520\,e^{-k_1\tau}+0.05716\,e^{k_1\tau}) && (\tau \leqslant \tau_0), \\ B(\tau) &= \tfrac{3}{4}F(\tau+0.76886) && (\tau \geqslant \tau_0). \end{aligned}\right\} \tag{101}$$

The dependence on τ of $B(\tau)$ is given in Table 1 and illustrated in Figure 1. We may notice that the value of $B(\tau)$ at $\tau = 0$ is now the same as that in the standard model,

$$B(0) = 0.43301\,F\,. \tag{102}$$

Second approximation:

$$\left.\begin{array}{lll} k_1 = 1.94285\,, & k_2 = 4.87104\,, & k_3 = 20.38105\,, \\ G_1 = 0.9635599\,, & G_2 = -0.3952121\,, & G_3 = -0.0150044\,, \\ H_1 = 1.0128751\,, & H_2 = 1.0926626\,, & H_3 = 1.0872368\,, \\ L_1 = -0.0039855\,, & L_2 = -0.064554\,, & L_3 = -0.010949\,, \\ L_{-1} = 0.0009266\,, & L_{-2} = 0.036146\,, & L_{-3} = -0.0001520\,, \\ M_1 = -0.10505\,, & \mathfrak{P}_1 = -0.062414\,, & \mathfrak{P}_2 = -0.0022012\,, \\ q_1 = 1.97203\,, & R = 0.85271\,, & Q = 0.62098\,. \end{array}\right\} \tag{103}$$

The values of $B(\tau)$ obtained with these constants are given in Table 1 and are plotted in Figure 1. We have computed for this model the darkening in the continuum and in the lines, as well as the total darkening. The resulting values are given in Table 2 for

TABLE 2

LIMB DARKENING IN THE LAYER MODEL

μ	$\frac{1}{F}I^{(1)}(0,\mu)$		$\frac{1}{F}I^{(2)}(0,\mu)$		$\frac{1}{F}I(0,\mu)$		$\phi(\mu)$	
	I*	II	I	II	I	II	I	II
0.0	0.3464	0.3490	0.0866	0.0872	0.4330	0.4362	0.3749	0.3633
0.1	0.4617	0.4702	.0898	.0909	0.5515	0.5611	0.4774	0.4673
0.2	0.5436	0.5553	.0930	.0943	0.6365	0.6497	0.5511	0.5411
0.3	0.6142	0.6298	.0962	.0977	0.7104	0.7274	0.6059	0.6150
0.4	0.6801	0.6990	.0994	.1009	0.7794	0.8000	0.6748	0.6663
0.5	0.7439	0.7654	.1023	.1041	0.8461	0.8695	0.7354	0.7245
0.6	0.8064	0.8308	.1051	.1067	0.9116	0.9375	0.7892	0.7809
0.7	0.8684	0.8948	.1079	.1098	0.9763	1.0046	0.8453	0.8376
0.8	0.9300	0.9583	.1105	.1125	1.0405	1.0708	0.9008	0.8919
0.9	0.9911	1.0207	.1130	.1151	1.1041	1.1358	0.9559	0.9460
1.0	1.0397	1.0830	0.1154	0.1176	1.1551	1.2006	1.0000	1.0000

* "I" and "II" refer to the first and the second approximations, respectively.

the first two approximations. The results for the second approximation are shown in Figure 2, where we have also exhibited the values of the observed limb darkening for integrated light in the sun, as reduced by Minnaert,[12] using Abbot's measures of the monochromatic darkening and Mulders' intensity distribution with wave length at the center of the solar disk. The agreement between the observed values and the computed total darkening is seen to be very satisfactory down to a distance of 0.05 from the limb, in units of the solar radius. The significance of this agreement will be considered in the last section of this article, in connection with the general discussion of the phenomenon of darkening.

6.1. *Absorption lines not uniformly distributed throughout the spectrum.*—In the preceding sections we have assumed that the distribution function of the lines is independent of frequency. We shall now construct an iteration method for solving the equations of radiative transfer in an atmosphere in which the lines arise in pure local thermodynamical

[12] *Zs. f. Ap.*, **13**, 196, 1937.

equilibrium, on the assumption that the probability distribution of the lines along the spectrum is a given function of frequency. The hypothesis that the lines arise in pure absorption is introduced not only for the sake of simplicity in the calculations, but also because, as Unsöld has pointed out,[13] the true process in which the majority of nonresonance lines arise must have, to a great extent, the character of an absorption process. Accordingly, we shall write the equations of transfer (4) and (5) in the form

$$\left.\begin{aligned} \mu \frac{dI^{(1)}}{d\tau} &= I^{(1)} - \int_0^\infty w_1(\nu) B_\nu d\nu , \\ \frac{\mu}{\gamma} \frac{dI^{(2)}}{d\tau} &= I^{(2)} - \int_0^\infty w_2(\nu) B_\nu d\nu . \end{aligned}\right\} \tag{104}$$

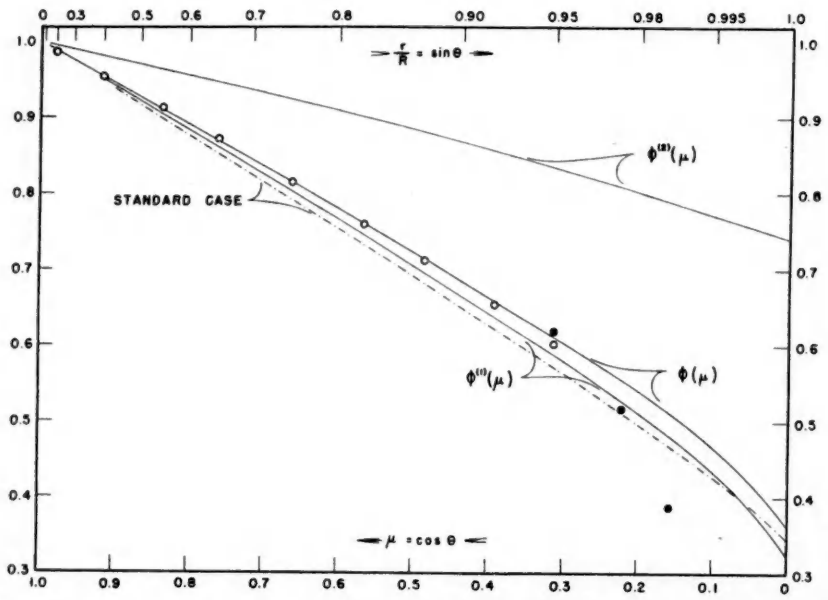

FIG. 2.—Comparison between the total darkening in the layer model and the observed integrated darkening in the solar disk. Open circles are points obtained from Abbot's observations of monochromatic darkening, and filled circles represent values reduced from measurements by Moll, Burger, and van der Bilt.

where $\gamma = 1 + \xi$ is supposed to be independent of depth and frequency. If we now define the averages

$$\left.\begin{aligned} \bar{w}_1(\tau) &= \frac{1}{B(T_\tau)} \int_0^\infty w_1(\nu) B_\nu(T_\tau)\, d\nu , \\ \bar{w}_2(\tau) &= \frac{1}{B(T_\tau)} \int_0^\infty w_2(\nu) B_\nu(T_\tau)\, d\nu , \end{aligned}\right\} \tag{105}$$

we can write

$$\bar{w}_1(\tau) = \omega_1 - \delta(\tau) \qquad \text{and} \qquad w_2(\tau) = \omega_2 + \delta(\tau) , \tag{106}$$

with

$$\omega_1 + \omega_2 = 1 . \tag{107}$$

[13] Cf. *op. cit.*, p. 369.

In equation (106) ω_1 is a constant to be chosen appropriately. We can now write equations (104) in the form

$$\left.\begin{aligned} \mu \frac{dI^{(1)}}{d\tau} &= I^{(1)} - \omega_1 B(\tau) + \delta(\tau) B(\tau), \\ \frac{\mu}{\gamma} \frac{dI^{(2)}}{d\tau} &= I^{(2)} - \omega_2 B(\tau) - \delta(\tau) B(\tau). \end{aligned}\right\} \tag{108}$$

These equations have to be solved under the condition of constant net flux, expressed by the relation

$$J^{(1)} + \gamma J^{(2)} = (\omega_1 + \gamma\omega_2) B(\tau) + (\gamma - 1)\, \delta(\tau) B(\tau). \tag{109}$$

The iteration process that will be devised for the solution of equations (108) is entirely similar to the methods used by Chandrasekhar in paper VII and by Miss Tuberg[14] in her discussion of the formation of absorption lines. The fundamental idea of the process is the following: If the solution of the equations

$$\left.\begin{aligned} \mu \frac{dI^{(1)}}{d\tau} &= I^{(1)} - \omega_1 B, \\ \frac{\mu}{\gamma} \frac{dI^{(2)}}{d\tau} &= I^{(2)} - \omega_2 B, \end{aligned}\right\} \tag{110}$$

under the condition

$$J^{(1)} + \gamma J^{(2)} = (\omega_1 + \gamma\omega_2) B, \tag{111}$$

gives a first approximation $B_1(\tau)$ to the source function $B(\tau)$, then the second approximation $B_2(\tau)$ will be given by the solution of the system

$$\left.\begin{aligned} \mu \frac{dI^{(1)}}{d\tau} &= I^{(1)} - \omega_1 B_2(\tau) + \delta(\tau) B_1(\tau), \\ \frac{\mu}{\gamma} \frac{dI^{(2)}}{d\tau} &= I^{(2)} - \omega_2 B_2(\tau) - \delta(\tau) B_1(\tau), \end{aligned}\right\} \tag{112}$$

with

$$J^{(1)} + \gamma J^{(2)} - (\gamma - 1)\, \delta(\tau) B_1(\tau) = (\omega_1 + \gamma\omega_2) B_2(\tau). \tag{113}$$

However, in order to compute the integrals appearing in the averages (105), we must have a knowledge of a zero-order approximation for the Planck function. We shall suppose that such a zero-order approximation is given by the distribution of temperature in the gray atmosphere. This assumption is justified by the fact that in practical cases the small uncertainty arising from the use of an approximate temperature distribution is negligible when compared with the errors caused by the uncertainty with which we can define numerically the function $w_2(\nu)$.

The formal generalizations that are necessary to define the nth iteration are easily written down; but we do not wish to go into these refinements of the theory, since we shall restrict our numerical computations to the first iteration, defined by equations (110)–(113).

The solution of equations (110), as we have seen, is

$$\left.\begin{aligned} I_i^{(1)} &= \frac{3}{4} \frac{F\omega_1}{\omega_1 + \omega_2/\gamma} \left\{ \tau + \mu_i + Q + \sum_{a=1}^{2n-1} \frac{L_a e^{-k_a\tau}}{1 + \mu_i k_a} \right\}, \\ I_i^{(2)} &= \frac{3}{4} \frac{F\omega_2}{\omega_1 + \omega_2/\gamma} \left\{ \tau + \frac{\mu_i}{\gamma} + Q + \sum_{a=1}^{2n-1} \frac{L_a e^{-k_a\tau}}{1 + \mu_i k_a/\gamma} \right\} \\ & \qquad (i = \pm 1, \ldots, \pm n), \end{aligned}\right\} \tag{114}$$

[14] *Ap. J.*, **103**, 145, 1946.

where the k_a's are the $2n-1$ positive roots of the equation

$$\omega_1+\omega_2\gamma=\omega_1\sum_{i=1}^{n}\frac{a_i}{1-\mu_i^2k^2}+\omega_2\gamma\sum_{i=1}^{n}\frac{a_i}{1-\mu_i^2k^2/\gamma^2} \tag{115}$$

and the L_a's and Q are given by the boundary conditions. The corresponding integrated Planck function is

$$B_1(\tau)=\frac{3}{4}\frac{F}{w_1+w_2/\gamma}\left(\tau+Q+\sum_{a=1}^{2n-1}L_a e^{-k_a\tau}\right). \tag{116}$$

The system that we have to solve is obtained by combining equations (112) and (113) in the form

$$\left.\begin{aligned}\mu\frac{dI^{(1)}}{d\tau}&=I^{(1)}-\omega_1\frac{J^{(1)}+\gamma J^{(2)}}{\omega_1+\gamma\omega_2}+\gamma\frac{\delta(\tau)B_1(\tau)}{\omega_1+\gamma\omega_2},\\ \frac{\mu}{\gamma}\frac{dI^{(2)}}{d\tau}&=I^{(2)}-\omega_2\frac{J^{(1)}+\gamma J^{(2)}}{\omega_1+\gamma\omega_2}-\gamma\frac{\delta(\tau)B_1(\tau)}{\omega_1+\gamma\omega_2}.\end{aligned}\right\} \tag{117}$$

Since the homogeneous part of these equations has the form of system (110), we seek for equations (118) a solution of the form

$$\left.\begin{aligned}I_i^{(1)}&=\frac{3}{4}\frac{F\omega_1}{\omega_1+\omega_2/\gamma}\left\{\tau+\mu_i+\mathcal{Q}(\tau)+\sum_{a=1}^{2n-1}\left[\frac{\mathcal{L}_a(\tau)\,e^{-k_a\tau}}{1+\mu_ik_a}+\frac{\mathcal{L}_{-a}(\tau)\,e^{k_a\tau}}{1-\mu_ik_a}\right]\right\},\\ I_i^{(2)}&=\frac{3}{4}\frac{F\omega_2}{\omega_1+\omega_2/\gamma}\left\{\tau+\frac{\mu_i}{\gamma}+\mathcal{Q}(\tau)+\sum_{a=1}^{2n-1}\left[\frac{\mathcal{L}_a(\tau)\,e^{-k_a\tau}}{1+\mu_ik_a/\gamma}+\frac{\mathcal{L}_{-a}(\tau)\,e^{k_a\tau}}{1-\mu_ik_a/\gamma}\right]\right\}\\ &\qquad(i=\pm1,\pm2,\ldots,\pm n).\end{aligned}\right\} \tag{118}$$

Substituting these equations in system (117), written for the points μ_i, we readily find that the variational equations for the determination of the $4n-1$ functions $\mathcal{L}_a(\tau)$, $\mathcal{L}_{-a}(\tau)$, and $\mathcal{Q}(\tau)$ are:

$$\left.\begin{aligned}\mu_i\left\{\frac{d\mathcal{Q}}{d\tau}+\sum_{a=1}^{2n-1}\left[\frac{e^{-k_a\tau}}{1+\mu_ik_a}\frac{d\mathcal{L}_a}{d\tau}+\frac{e^{k_a\tau}}{1-\mu_ik_a}\frac{d\mathcal{L}_{-a}}{d\tau}\right]\right\}&=\frac{\Delta(\tau)}{w_1},\\ \mu_i\left\{\frac{d\mathcal{Q}}{d\tau}+\sum_{a=1}^{2n-1}\left[\frac{e^{-k_a\tau}}{1+\mu_ik_a/\gamma}\frac{d\mathcal{L}_a}{d\tau}+\frac{e^{k_a\tau}}{1-\mu_ik_a/\gamma}\frac{d\mathcal{L}_{-a}}{d\tau}\right]\right\}&=-\frac{\Delta(\tau)}{w_2},\end{aligned}\right\} \tag{119}$$

where

$$\Delta(\tau)=\frac{\omega_1+\omega_2/\gamma}{\omega_1+\gamma\omega_2}\frac{4}{3F}\gamma\delta(\tau)B_1(\tau). \tag{120}$$

It is possible to write down explicitly the solution of the $2n$ variational equations (119) by following a procedure entirely similar to that followed by Chandrasekhar in paper VII. But again, since we shall restrict our numerical calculations to the case $n=1$, we do not wish to go into these developments. For the case $n=1$, equations (119) give immediately

$$\frac{d\mathcal{Q}}{d\tau}=0, \tag{121}$$

$$e^{-k\tau}\frac{d\mathcal{L}_1}{d\tau}=\frac{k}{2}\frac{1-1/\gamma^2}{w_1+w_2/\gamma}\Delta(\tau), \tag{122}$$

and

$$e^{k\tau}\frac{d\mathfrak{L}_{-1}}{d\tau} = -\frac{k}{2}\frac{1-1/\gamma^2}{w_1+w_2/\gamma}\Delta(\tau)\,, \tag{123}$$

from which the solution for $\mathfrak{Q}$, $\mathfrak{L}_1(\tau)$, and $\mathfrak{L}_{-1}(\tau)$ follows. We have

$$\mathfrak{Q} = \text{constant} = Q + \Delta Q\,, \tag{124}$$

$$\mathfrak{L}_1(\tau) = \frac{k}{2}\frac{1-1/\gamma^2}{w_1+w_2/\gamma}\int_0^\tau e^{k\tau}\Delta(\tau)\,d\tau + L_1 + \Delta L_1\,, \tag{125}$$

and

$$\mathfrak{L}_{-1}(\tau) = \frac{k}{2}\frac{1-1/\gamma^2}{w_1+w_2/\gamma}\int_\tau^\infty e^{-k\tau}\Delta(\tau)\,d\tau\,, \tag{126}$$

where ΔQ and ΔL_1 are constants of integration. It is to be noticed, however, that, in integrating equation (123) in the form (126), the constant of integration has been so chosen as to satisfy the requirement that the values of $I_i^{(1)}$ and $I_i^{(2)}$ given by equations (118) do not increase exponentially as $\tau \to \infty$.

Finally, the constants of integration, ΔL_1 and ΔQ, are to be determined from the condition of vanishing incident radiation,

$$\left.\begin{aligned} \frac{L_1+\Delta L_1}{1-\mu_1 k} + \frac{\mathfrak{L}_{-1}(0)}{1+\mu_1 k} + Q + \Delta Q &= \mu_1\,, \\ \frac{L_1+\Delta L_1}{1-\mu_1 k/\gamma} + \frac{\mathfrak{L}_{-1}(0)}{1+\mu_1 k/\gamma} + Q + \Delta Q &= \frac{\mu_i}{\gamma}\,, \end{aligned}\right\} \tag{127}$$

or, since L_1 and Q are so chosen as to satisfy

$$\left.\begin{aligned} \frac{L_1}{1-\mu_1 k} + Q &= \mu_1\,, \\ \frac{L_1}{1-\mu_1 k/\gamma} + Q &= \frac{\mu_1}{\gamma}\,, \end{aligned}\right\} \tag{128}$$

we are left with

$$\left.\begin{aligned} \frac{\Delta L_1}{1-\mu_1 k} + \Delta Q &= -\frac{\mathfrak{L}_{-1}(0)}{1+\mu_1 k}\,, \\ \frac{\Delta L_1}{1-\mu_1 k/\gamma} + \Delta Q &= -\frac{\mathfrak{L}_{-1}(0)}{1+\mu_1 k/\gamma}\,, \end{aligned}\right\} \tag{129}$$

for the determination of ΔQ and ΔL_1.

On the other hand, since the constant ω_2 has been left unspecified up to the present, we now determine it by the condition that $\mathfrak{L}_{-1}(0)$ vanish, i.e.,

$$\int_0^\infty e^{-k\tau}\Delta(\tau)\,d\tau = 0\,. \tag{130}$$

Equations (106) and (120), together with equation (130), give

$$\omega_0 = \frac{\int_0^\infty e^{-k\tau}B_1(\tau)\bar{w}_2(\tau)\,d\tau}{\int_0^\infty e^{-k\tau}B_1(\tau)\,d\tau}\,. \tag{131}$$

If in this equation we express the integrals by numerical quadrature formulas, in terms of the zeros of the Laguerre polynomials and the associated Christoffel numbers λ_i, we obtain

$$\omega_2 = \frac{\sum_{i=1}^{n} \lambda_i B_1(\tau_i/k)\bar{w}_2(\tau_i/k)}{\sum_{i=1}^{n} \lambda_i B_1(\tau_i/k)}. \tag{132}$$

It is seen that ω_2 is a weighted average of $\bar{w}_2(\tau)$. However, it should be noticed that the weights depend on ω_2 and that, therefore, the value of ω_2 has to be found by a method of trial and error.

When equation (130) is satisfied, the integration constants ΔL_1 and ΔQ, according to equation (129), have the values

$$\Delta Q = 0 \qquad \text{and} \qquad \Delta L_1 = 0\ ; \tag{133}$$

and our solution (118) takes the form

$$\left.\begin{aligned} I_i^{(1)} &= \frac{3}{4}\frac{F\omega_1}{\omega_1+\omega_2/\gamma}\left(\tau+\mu_i+Q+\frac{\mathfrak{L}_1(\tau)\,e^{-k\tau}}{1+\mu_i\kappa}+\frac{\mathfrak{L}_{-1}(\tau)\,e^{k\tau}}{1-\mu_i k}\right), \\ I_i^{(2)} &= \frac{3}{4}\frac{F\omega_2}{\omega_1+\omega_2/\gamma}\left(\tau+\frac{\mu_i}{\gamma}+Q+\frac{\mathfrak{L}_1(\tau)\,e^{-k\tau}}{1+\mu_i k/\gamma}+\frac{\mathfrak{L}_{-1}(\tau)\,e^{k\tau}}{1-\mu_i k/\gamma}\right) \\ &\qquad\qquad (i=\pm 1). \end{aligned}\right\} \tag{134}$$

Finally, the integrated Planck function takes the form

$$B(\tau) = B_1(\tau)\left[1-\frac{\gamma-1}{\omega_1+\gamma\omega_2}\,\delta(\tau)\right]+\tfrac{3}{4}F\frac{\Psi(\tau)}{\omega_1+\omega_2/\gamma}, \tag{135}$$

where

$$\Psi(\tau) = \frac{k}{2}\frac{1-1/\gamma^2}{\omega_1+\omega_2/\gamma}\int_0^\infty e^{-k|t-\tau|}\Delta(t)\,dt. \tag{136}$$

It may be further noticed that, as a consequence of the procedure followed to determine the constants of integration, the emergent fluxes $F^{(1)}$ and $F^{(2)}$ in this (2, 1) approximation retain the values given by the (1, 1) approximation.

6.2. *Application to the solar atmosphere.*—In order to apply the theory developed in the preceding paragraph to the case of the sun, we need, first, to define numerically the distribution function of the lines $w_2(\nu)$. We shall take as a measure of the probability distribution of the lines the distribution with frequency of the total absorption $A(\nu)$ produced by the Fraunhofer lines in the solar spectrum. The dependence on frequency of this total absorption, as determined by Mulders,[15] is shown graphically in Figure 3, together with the smooth curve adopted for $A(\nu)$. It should be pointed out that, although his values are uncertain below λ 3900 A, this uncertainty is not significant in our calculation, since the values for λ 3000 A have to be arbitrarily extrapolated. We have, therefore, set

$$\left.\begin{aligned} w_2(\nu) &= \Gamma A(\nu) \qquad \text{for} \quad \Gamma A(\nu) < 1 \\ &= 1 \qquad\quad \text{for} \quad \Gamma A(\nu) > 1\ , \end{aligned}\right\} \tag{137}$$

Γ being a constant factor that takes into account the finite residual intensity of the lines. An inspection of the Utrecht *Atlas of the Solar Spectrum* indicates that the adop-

[15] *Zs. f. Ap.*, **11**, 132, Table 2, 1935.

tion of the value $\Gamma = 2.5$ is reasonable. Once $w_2(\nu)$ is defined in numerical form, we can evaluate $\bar{w}_2(\tau)$ according to equation (105). For this purpose we have used tables of the function $B_\nu(T_\tau)/B(T_\tau)$ computed with the temperature distribution of a gray atmosphere in the fourth approximation, which were kindly provided by Dr. Chandrasekhar. The integrations were carried out graphically, and the resulting values of $\bar{w}_2(\tau)$ are given for small values of τ in Table 3. Two further constants have still to be fixed,

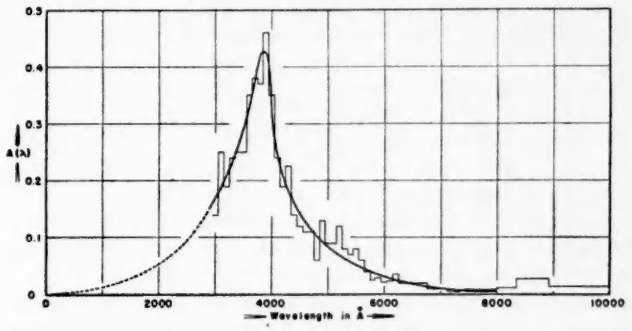

FIG. 3.—The distribution with wave length of the total absorption produced by the Fraunhofer lines in the solar spectrum.

TABLE 3

THE INTEGRATED PLANCK FUNCTION WHEN THE DISTRIBUTION OF THE LINES DEPENDS ON FREQUENCY

τ	$\bar{w}_2(\tau)$	$\delta(\tau)$	$\frac{1}{F}B_1(\tau)$	$\Psi(\tau)$	$\frac{1}{F}B_2(\tau)$
0.00	0.0906	−0.0411	0.4034	0.00000	0.4296
0.05	.0998	− .0319	0.4530	.00028	0.4773
0.10	.1086	− .0231	0.5010	.00081	0.5235
0.15	.1167	− .0150	0.5477	.00155	0.5686
0.20	.1242	− .0075	0.5932	.00260	0.6136
0.30	.1372	+ .0055	0.6818	.00548	0.7039
0.40	.1405	+ .0178	0.7682	.00909	0.7929
0.50	.1602	+ .0285	0.8530	.01319	0.8819
0.60	.1690	+ .0373	0.9370	.01768	0.9719
0.80	.1842	+ .0525	1.1032	.02798	1.1544
1.00	.1979	+ .0662	1.2684	.03980	1.3388
1.40	.2213	+ .0896	1.5977	.06578	1.7070
1.80	.2404	+ .1087	1.9266	.09497	2.0802
2.20	.2543	+ .1226	2.2555	.12583	2.4831
3.00	0.2760	+0.1443	2.9133	0.19135	3.2252

namely, γ and ω_2. Both of them can be fixed by trial and error in such a way that in the (1, 1) approximation we obtain the observed emergent flux in the lines and, at the same time, satisfy equation (131). We have found that the values $\omega_2 = 0.1317$ and $\gamma = 3$ satisfy these conditions. Actually, for the emergent flux we obtain $F^{(2)} = 0.0855\ F$, against the observed value of $0.083\ F$. Further, equation (132) is satisfied within 0.00003. The first approximation is therefore described by the constants

$$\omega_1 = 0.8683\,, \qquad \omega_2 = 0.1317\,, \qquad \gamma = 3\,, \tag{138}$$

which give for the temperature distribution

$$B_1(\tau) = 0.82219\,(\tau + 0.54331 - 0.05273\,e^{-k\tau}), \tag{139}$$

with

$$k = 4.41526\,. \tag{140}$$

The values of $B_1(\tau)$ for some values of τ are given in Table 3 and in Figure 1. We are now in a position to compute $B_2(\tau)$ according to formula (135), since, once ω_2 is known, the function $\delta(\tau)$ is fixed by equation (106). (Some of the values of $\delta(\tau)$ obtained in this manner are given in Table 3.) The definite integral appearing in expression (136) is then numerically evaluated, and the resulting values of $\Psi(\tau)$ are given in Table 3. Finally, the calculation of $B_2(\tau)$ according to equation (125) readily follows, and the values obtained are given in the last column of Table 3 and further illustrated in Figure 1.

How nearly the temperature distribution derived in this fashion represents the actual distribution of temperature in the outer layers of the sun is a question that depends more on the reliability of the data of observational character that we have used than on the approximations made to solve the problem of radiative equilibrium. In this context we may point out that if Mulders has underestimated the absorption caused by the lines to the violet of λ 4000 A (and there is evidence to believe that such is the case) and if the absorption immediately to the violet of λ 3000 A does not follow the course indicated in Figure 3, the values adopted for $w_2(\tau)$ would be systematically too low. An immediate consequence of higher values of ω_2 would be the lowering of the obtained boundary temperature, followed by a steeper temperature gradient. It would seem that with a further refinement of the theory, considering the dependence of the distribution function of the lines on depth, the temperature gradient for $\tau < 0.2$ will be steeper and will approach a situation similar to that described by the layer model. Nevertheless, we can consider that the boundary temperature provided by the model analyzed in this section gives an upper limit to the actual one. With $T_e = 5713°$ K, the boundary temperature in the first approximation is 4550° K and 4630° K in the second—values which have to be compared with 4656° K given by the standard model.

7. *The distribution of temperature in the outer layers of the sun and the limb-darkening phenomenon.*—With the solution of the transfer problem completed in the preceding sections, we can now answer the question raised in the introductory section, namely, as to how the temperature distribution in the outer layers of the solar atmosphere is modified by the formation of absorption lines.

From an inspection of Figure 1, we can say, in the first place, that the effect of the Fraunhofer lines on the boundary temperature T_0 cannot be expected to increase the value given by the standard model. On the contrary, it is likely that the value of T_0 is somewhat lower than 4600° K, as was shown at the end of the preceding paragraph. This result is in substantial agreement with determinations of the "effective excitation temperature of the solar reversing layers" made by K. O. Wright[16] and other authors.[17] This shows clearly the misleading results given by the Milne blanketing model, which gives $T_0 = 5050°$ K.[18] In the layers in which the lines arise, that is, in the range $0 < \tau < 0.2$, the temperature increases rather fast compared to the standard model; but, for optical depths larger than 0.2, the temperature gradient has essentially the same value as in the standard case, the temperature itself being higher. Finally, around $\tau = 2$, where the convective equilibrium sets in, all our models will give a temperature gradient which is too high as compared with the real one. However, for a discussion of the emergent radiation, the existence of this zone of convective equilibrium can be disregarded, as Keenan[19] has shown.

[16] *Ap. J.*, **99**, 249, 1944.

[17] R. B. King, *Ap. J.*, **87**, 40, 1938; Menzel, Baker, and Goldberg, *Ap. J.*, **87**, 81, 1938.

[18] Cf. Mulders, *op. cit.*

[19] *Ap. J.*, **87**, 45, 1938.

From the foregoing remarks it is now apparent that the temperature distribution in the solar atmosphere does not deviate greatly from the one obtained in the layer model considered in section 5.3 and that, therefore, the comparison of total darkening in this model with observations in integrated light on the solar disk is justified. From the comparison, carried out in Figure 2, we see that the agreement between observed and computed darkening is entirely satisfactory up to a distance of 0.95 (in units of the radius of the disk) from the center. However, for points still nearer the limb, the theoretical values are larger than the observed ones, as we should expect from the fact that the boundary temperature of the sun is lower than the one given by the layer model. Finally, this agreement between observed and theoretical integrated darkening suggests immediately the origin of the systematic departures found by the writer[20] between observed and computed monochromatic darkening. For, as we have seen, the darkening given by the gray atmosphere is too low, compared with the observed one, for two reasons: first, the temperature distribution of the sun differs from that of the gray body, and, second, the darkening measures have been made over wave-length intervals which include not only continuous spectrum but also some Fraunhofer lines. From the publications containing the original darkening measures by Abbot,[21] it is not possible to find out how wide the wave-length regions were which were isolated by the spectrobolometer used to make the measurements; but there can be hardly any doubt that the measures for wave lengths below λ 6702 A are affected by this cause.

From this discussion we may conclude that a definitive comparison between theoretical and observed monochromatic darkening in the sun can be made only when, on the theoretical side, we use a temperature distribution which takes into account the presence of absorption lines and the nongrayness of the atmosphere[22] and when, on the observational side, observations made with higher resolving power are available.

I gratefully acknowledge the valuable suggestions I have received from Dr. S. Chandrasekhar in connection with the present work. I am also deeply indebted to Dr. Otto Struve for the facilities made available to me during my stay at the Yerkes Observatory.

[20] *Op. cit.*, see p. 391, Fig. 3.

[21] *Ann. Smithsonian Inst.*, **3**, 153, 1913.

[22] Cf. Paper VII, No. 6, p. 345.

ON THE RADIATIVE EQUILIBRIUM OF A STELLAR ATMOSPHERE. XI

S. CHANDRASEKHAR
Yerkes Observatory
Received May 13, 1946

ABSTRACT

In this paper the general equations of transfer allowing for the polarization of the scattered radiation in accordance with Rayleigh's law are formulated. It is shown that, for a general, partially plane-polarized radiation field, equations of transfer are required not only for the intensities I_l and I_r in two directions at right angles to each other in the plane of the electric and the magnetic vectors but also for a third quantity, $U = (I_l - I_r) \tan 2\chi$, where χ denotes the inclination of the plane of polarization to the direction to which I_l refers. This last quantity allows for the turning of the plane of polarization on scattering. It is further shown that, when partially plane-polarized light is scattered by an element of gas, the scattered radiation in any given direction can be analyzed as a mixture of *independent* plane-polarized streams: and the law of composition of such streams is formulated, following an early investigation of Stokes.

The equations of transfer appropriate to the problem of diffuse reflection of a parallel unpolarized beam by a semi-infinite plane-parallel atmosphere are solved in a general nth approximation, and explicit formulae are derived for the characterization of the state of polarization and the angular distribution of the reflected radiation. Tables of the necessary functions (four of them) are provided in the second and the third approximations.

1. *Introduction.*—In Paper X[1] of this series the theory of radiative transfer in a semi-infinite plane-parallel atmosphere, allowing for the polarization of the scattered radiation in accordance with Rayleigh's law,[2] has been worked out. However, under the circumstances in which the problem was formulated, there was an essential simplification arising from the axial symmetry of the radiation field at each point about the normal to the plane of stratification. For, under conditions of axial symmetry, the radiation field can be characterized completely by the specification of the intensities I_l and I_r referring, respectively, to the two states of polarization in which the electric vector vibrates in the meridian plane and at right angles to it. There is, however, a large class of problems in the theory of radiative transfer, as, for example, in the theory of diffuse reflection,[3] in which the axial symmetry of the radiation field is not present. The intensities I_l and I_r will not then completely suffice to characterize the radiation field. The question, therefore, arises as to how best we can characterize the radiation field under these more general conditions, in order that the relevant equations of transfer may be most conveniently formulated. This is a fundamental question; for on its answer will depend the solution of a variety of problems, including the important one of the illumination and the polarization of the sunlit sky. Indeed, it is somewhat surprising to find that even the basic equations of the problem have not so far been written down, though their necessity has been recognized since Lord Rayleigh[4] accounted in a general way for the color and polarization of the light from the sky.[5] In this paper we shall accordingly formulate the basic principles

[1] *Ap. J.*, **103,** 351, 1946. This paper will be referred to as "Paper X."

[2] Here and in the sequel we shall include under "Rayleigh's law" only that part of it which pertains to the state of polarization and the angular distribution of the scattered radiation. Therefore, the scattering by free electrons (in which context the problem was specifically formulated in paper X) also comes under the general scope of Rayleigh's law in this sense.

[3] *Ap. J.*, **103,** 165, 1946. This Paper will be referred to as "Paper IX."

[4] *Phil. Mag.*, **41,** 107, 274, 447, 1871; also *Scientific Papers of Lord Rayleigh*, **1,** 87, 104, 518, Cambridge, England, 1899. In this connection see also C. V. Raman, *Molecular Diffraction of Light*, chap. iii, University of Calcutta, 1922.

[5] E.g., L. V. King in his classic work, "On the Scattering and Absorption of Light in Gaseous Media with Applications to the Sky Radiation" (*Phil. Trans. Roy. Soc.*, A, **212,** 375, 1913), remarks:
"That portion of the sky radiation due to self-illumination is largely unpolarized and may to a large extent account for this deficiency from complete polarization: this point is mentioned by Rayleigh in his

on which the theory will have to be developed and then establish the equations of transfer which are valid for an atmosphere scattering radiation in accordance with Rayleigh's law. These equations will then be solved appropriately for the problem of diffuse reflection of a parallel beam of unpolarized radiation by a semi-infinite plane-parallel atmosphere. It may be stated here that for this latter problem simple closed expressions for the solution can be found in a general nth approximation. To reduce these solutions to their numerical forms it is only necessary to solve certain algebraic equations for characteristic roots.[6]

Applications of the theory developed in this paper to the interpretation of Lyot's observations[7] on the polarization of the light reflected from the various planets, particularly Venus, will be found in a forthcoming paper.

2. *The parametric representation of partially plane-polarized light and the composition of plane-polarized streams with no mutual phase relationships.*—The composition and resolution of streams of polarized light with no mutual phase relationships and the most convenient characterization of an arbitrarily polarized light was first considered by Sir George Stokes in a paper published in 1852.[8] This paper of Stokes is basic for our further considerations. However, the extreme generality of Stokes's considerations[9] are not essential for our purposes. It may, therefore, be useful to have them presented under the simplified conditions of our problem in which, as we shall see, only partially plane-polarized light need be considered.

Consider, then, a partially plane-polarized beam with the plane of polarization inclined at an angle χ to a certain fixed direction[10] l (say) and with intensities I_χ and $I_{\chi+\pi/2}$ in the directions[10] of maximum and minimum intensity. The intensity $I(\psi)$ in a direction inclined at an angle ψ to the direction of l is clearly

$$I(\psi) = I_\chi \cos^2(\psi - \chi) + I_{\chi+\pi/2} \sin^2(\psi - \chi). \tag{1}$$

After some elementary transformations, the foregoing equation can be reduced to the form

$$\left.\begin{aligned} I(\psi) = \tfrac{1}{2}(I_\chi + I_{\chi+\pi/2}) + \tfrac{1}{2}(I_\chi - I_{\chi+\pi/2}) \cos 2\chi \cos 2\psi \\ + \tfrac{1}{2}(I_\chi - I_{\chi+\pi/2}) \sin 2\chi \sin 2\psi . \end{aligned}\right\} \tag{2}$$

On the other hand, if I_l and I_r denote the intensities in the direction l and in the direction r at right angles to it, we have

$$I_l = I_\chi \cos^2\chi + I_{\chi+\pi/2} \sin^2\chi \tag{3}$$

and

$$I_r = I_\chi \sin^2\chi + I_{\chi+\pi/2} \cos^2\chi . \tag{4}$$

1871 paper. . . . . The complete solution of the problem from this aspect would require us to split up the incident radiation into two components, one of which is polarized in the principal plane, the other at right angles to it: the effect of self-illumination would lead to two simultaneous integral equations in three variables, the solutions of which would be much too complicated to be useful."

Actually, the problem requires the solution of three simultaneous integral equations (and not two, as King mentions); but, even so, there is no difficulty in solving these equations in a manner appropriate to any problem and to any desired degree of accuracy.

[6] The degree of these equations depends on the order of the approximation in which the solutions are sought.

[7] *Ann. Obs. Meudon* (Paris), Vol. **8**, 1926.

[8] *Trans. Cambridge Phil. Soc.*, **9**, 399, 1852; or *Mathematical and Physical Papers of Sir George Stokes*, **1**, 233, Cambridge, England, 1901.

[9] It is surprising that these fundamental considerations of Stokes are not to be found in any of the standard books on physical optics. The only book which I have been able to discover in which the matter is considered is J. Walker, *The Analytical Theory of Light*, §§ 20–22, pp. 28–32, Cambridge, England, 1904.

[10] These directions are referred in the plane containing the electric and the magnetic vectors.

From these equations we conclude that

$$I_l + I_r = I_\chi + I_{\chi+\pi/2} \tag{5}$$

and

$$(I_l - I_r) = (I_\chi - I_{\chi+\pi/2}) \cos 2\chi \,. \tag{6}$$

Using these relations, we can re-write equation (2) in the form

$$I(\psi) = \tfrac{1}{2}(I_l + I_r) + \tfrac{1}{2}(I_l - I_r) \cos 2\psi + \tfrac{1}{2}(I_l - I_r) \tan 2\chi \sin 2\psi \,. \tag{7}$$

From equation (7) it follows that *optically equivalent*,[11] partially plane-polarized beams can be described completely in terms of the intensities I_l and I_r in two directions at right angles to each other and the further quantity,

$$U = (I_l - I_r) \tan 2\chi \,. \tag{8}$$

Conversely, whenever the intensity in a direction ψ of a polarized beam can be expressed in the form

$$I(\psi) = A + B \cos 2\psi + \tfrac{1}{2} U \sin 2\psi \,, \tag{9}$$

it represents a partially plane-polarized beam with intensities $A + B$ and $A - B$ in the directions l and r and with the plane of polarization inclined at an angle

$$\chi = \tfrac{1}{2} \tan^{-1} \frac{U}{2B} \tag{10}$$

to the direction of l.

We shall next examine what the result of composition of a number of streams of *plane*-polarized light with no mutual phase relationships is. Let $I^{(n)}$ denote the intensity of a typical stream and χ_n the inclination of its plane of polarization to the direction l. Further, let $I(\psi)$ denote the intensity of the mixture in the direction ψ. Since the different streams are assumed to have no phase relationships, it is evident that[12]

$$I(\psi) = \Sigma I^{(n)}(\psi) \,, \tag{11}$$

where $I^{(n)}(\psi)$ denotes the intensity of the stream $I^{(n)}$ in the direction ψ. Accordingly,

$$I(\psi) = \Sigma I^{(n)} \cos^2(\psi - \chi_n) \,, \tag{12}$$

or, after some minor reductions,

$$I(\psi) = \tfrac{1}{2}\Sigma I^{(n)} + \tfrac{1}{2}\Sigma I^{(n)} (\cos^2 \chi_n - \sin^2 \chi_n) \cos 2\psi + \tfrac{1}{2}\Sigma I^{(n)} \sin 2\chi_n \sin 2\psi \,, \tag{13}$$

Comparing this with equations (7) and (9), we conclude that the mixture of a number of independent plane-polarized streams is a partially plane-polarized beam. Further,

$$I_l = \Sigma I^{(n)} \cos^2 \chi_n \,; \qquad I_r = \Sigma I^{(n)} \sin^2 \chi_n \,; \tag{14}$$

and

$$U = (I_l - I_r) \tan 2\chi = \Sigma I^{(n)} \sin 2\chi_n \,. \tag{15}$$

In other words, the intensities I_l and I_r of the mixture are simply the sum of the intensities of the component streams in the directions l and r, while the plane of polarization of the resultant is determined by U, according to equation (15).

3. *The laws of scattering.*—We shall suppose that the laws of scattering as they pertain to the angular distribution and the state of polarization of the scattered radiation

[11] For a discussion of the concept of optical equivalence see Stokes (*op. cit.*).

[12] However, for an explicit demonstration see *ibid.*

are those of Rayleigh. For our purposes we may formulate them in the following manner (cf. Paper X, eqs. [1]–[3]):

If I denotes the intensity of a plane-polarized beam incident on an element of gas, then the amount of radiation scattered in a direction inclined at an angle Θ to the direction of incidence and confined to an element of solid angle $d\omega$ and per unit mass of the scattering material will be given by

$$\tfrac{3}{2}\sigma I \frac{d\omega}{4\pi} \quad \text{or} \quad \tfrac{3}{2}\sigma I \cos^2\Theta \frac{d\omega}{4\pi}, \tag{16}$$

depending on whether the incident radiation is polarized with the electric vector perpendicular or parallel to the plane of scattering[13] and where σ denotes the mass-scattering coefficient. More generally, if I_α denotes the intensity of an incident plane-polarized beam in which the electric vector is inclined at an angle α to the plane of scattering, we may resolve the incident amplitude[14] into its components

$$\xi_\alpha \sin\alpha \quad \text{and} \quad \xi_\alpha \cos\alpha \tag{17}$$

perpendicular and, respectively, parallel to the plane of scattering. According to equation (16), these incident amplitudes will give rise to scattered amplitudes proportional to $\xi_\alpha \sin\alpha$ and $\xi_\alpha \cos\alpha \cos\Theta$, which are perpendicular and parallel, respectively, to the plane of scattering. However, since the incident beam is plane-polarized, the scattered amplitudes in the two directions will be in phase. The resultant will therefore represent a plane-polarized beam with the electric vector inclined to the plane of scattering by an angle

$$\chi = \tan^{-1}(\tan\alpha \sec\Theta). \tag{18}$$

Further, the scattered intensity will be given by

$$\tfrac{3}{2}\sigma I_\alpha (\sin^2\alpha + \cos^2\alpha \cos^2\Theta) \frac{d\omega}{4\pi}. \tag{19}$$

4. *The source functions* $\mathfrak{J}_l, \mathfrak{J}_r,$ *and* $\mathfrak{J}_U$.—We shall now show how, with the laws of scattering formulated in § 3 and with the rule of composition of plane-polarized beams given in § 2, we can obtain the equations of transfer valid under conditions when the radiation field is characterized by no special symmetry properties.

First, we may observe that, since on Rayleigh's laws of scattering a plane-polarized beam remains plane-polarized also after being scattered, it follows that the radiation scattered by an element of gas exposed to a partially plane-polarized radiation field will again be partially plane-polarized. For, under the circumstances, the radiation scattered in any given direction can be regarded as a mixture of several independent plane-polarized components, and this, according to our remarks in §2, can lead only to a partially plane-polarized beam. Hence, under conditions in which the diffuse reflection of an initially unpolarized radiation is the most that is contemplated, we need not consider a state of polarization more general than partial plane-polarization. Accordingly, we may characterize the radiation field at each point by the three quantities $I_l(\vartheta, \varphi)$, $I_r(\vartheta, \varphi)$, and $U(\vartheta, \varphi)$, where ϑ and φ are the polar angles referred to an appropriately chosen coordinate system through the point under consideration (see Fig. 1 in Paper X) and I_l and I_r are the intensities in the beam in the direction of the meridian plane through (ϑ, φ) and at right angles to it, respectively. And, finally, the quantity U is related to I_l and I_r according to equation (8), χ now denoting the inclination of the plane of maximum amplitude of the electric vector with the meridian plane.

[13] This is the plane which contains the direction of the incident and the scattered light.

[14] As in Paper X, we shall mean by "amplitude" a quantity whose square is the intensity.

It is now apparent that equations of transfer for I_l, I_r, and U must be expressible in the forms

$$\frac{dI_l(s, \vartheta, \varphi)}{\rho\sigma ds} = -I_l(s, \vartheta, \varphi) + \mathfrak{J}_l(s, \vartheta, \varphi), \tag{20}$$

$$\frac{dI_r(s, \vartheta, \varphi)}{\rho\sigma ds} = -I_r(s, \vartheta, \varphi) + \mathfrak{J}_r(s, \vartheta, \varphi), \tag{21}$$

$$\frac{dU(s, \vartheta, \varphi)}{\rho\sigma ds} = -U(s, \vartheta, \varphi) + \mathfrak{J}_U(s, \vartheta, \varphi), \tag{22}$$

where s measures the linear distance in the direction of (ϑ, φ), and $\mathfrak{J}_l$, $\mathfrak{J}_r$, and $\mathfrak{J}_U$ are the source functions for the respective quantities.

To evaluate $\mathfrak{J}_l(\vartheta, \varphi)$, $\mathfrak{J}_r(\vartheta, \varphi)$, and $\mathfrak{J}_U(\vartheta, \varphi)$ appropriate to any point of the atmosphere, we shall first consider the contributions to these source functions for the radiation in the direction (ϑ, φ) arising from the scattering of the radiation in the direction (ϑ', φ').

The radiation in the direction (ϑ', φ') is characterized by the intensities $I_l(\vartheta', \varphi')$, $I_r(\vartheta', \varphi')$, and $U(\vartheta', \varphi')$. Equivalently, we may, of course, also characterize it by the intensities $I_\chi(\vartheta', \varphi')$ and $I_{\chi+\pi/2}(\vartheta', \varphi')$ in the directions of maximum and minimum intensity, and the inclination χ of the direction of maximum amplitude of the electric vector to the meridian plane through (ϑ', φ'). The intensities I_χ and $I_{\chi+\pi/2}$ are related to I_l and I_r according to the equations

$$I_\chi + I_{\chi+\pi/2} = I_l + I_r \qquad \text{and} \qquad I_\chi - I_{\chi+\pi/2} = (I_l - I_r)\sec 2\chi\,. \tag{23}$$

Now a partially plane-polarized beam characterized by the maximum and minimum intensities I_χ and $I_{\chi+\pi/2}$ is optically equivalent to two plane-polarized beams of intensities, I_χ and $I_{\chi+\pi/2}$, with no correlation in their phases. We may, accordingly, consider the scattering of the radiation in the direction (ϑ', φ') as the result of scattering of the two plane-polarized components. According to the laws of scattering formulated in § 3, each of these components will give rise to plane-polarized scattered beams, which will again have no correlation in phases. In other words, the radiation scattered in the direction (ϑ, φ) from other directions can be considered as a mixture of a very large number of independent plane-polarized streams and can therefore be combined according to the laws of composition given in § 2.

Consider, then, the scattering of a plane-polarized beam of intensity $I_\chi(\vartheta', \varphi')$ in the direction (ϑ', φ') and confined to an element of solid angle, $d\omega'$, into the direction (ϑ, φ). Let ξ_χ denote the corresponding amplitude. The components of this amplitude parallel, respectively, perpendicular to the meridian plane through (ϑ', φ') are

$$\xi_\chi \cos\chi \qquad \text{and} \qquad \xi_\chi \sin\chi\,. \tag{24}$$

The amplitude $\xi_\chi \cos\chi$ has components parallel, respectively, perpendicular, to the plane of scattering, which are

$$\xi_\chi \cos\chi \cos i_1 \qquad \text{and} \qquad \xi_\chi \cos\chi \sin i_1 \tag{25}$$

where i_1 denotes the angle between the meridian plane through (ϑ', φ') and the plane of scattering (see Fig. 1 of Paper X). When this radiation is scattered in the direction (ϑ, φ), the components of the scattered amplitude that are parallel, respectively, perpendicular to the plane of scattering are proportional to

$$\xi_\chi \cos\chi \cos i_1 \cos\Theta \qquad \text{and} \qquad \xi_\chi \cos\chi \sin i_1\,. \tag{26}$$

The corresponding amplitudes in the meridian plane through (ϑ, φ) and at right angles to it are proportional (cf. Paper X, eqs. [12] and [13]) to

$$\left.\begin{aligned}\xi_\chi \cos\chi\,(\sin i_1 \sin i_2 - \cos i_1 \cos i_2 \cos\Theta)\\ = \xi_\chi \cos\chi\,(\sin\vartheta \sin\vartheta' + \cos\vartheta \cos\vartheta' \cos[\varphi' - \varphi])\,,\end{aligned}\right\} \quad (27)$$

and

$$-\xi_\chi \cos\chi\,(\sin i_1 \cos i_2 + \sin i_2 \cos i_1 \cos\Theta) = -\xi_\chi \cos\chi \cos\vartheta' \sin(\varphi' - \varphi)\,, \quad (28)$$

where i_2 denotes the angle between the meridian plane through (ϑ, φ) and the scattering plane.

Similarly, the amplitude $\xi_\chi \sin\chi$, when scattered in the direction (ϑ, φ), leads to amplitudes in the meridian plane through (ϑ, φ) and at right angles to it which are proportional, respectively, to (cf. Paper X, eqs. [27] and [28]),

$$\xi_\chi \sin\chi\,(\sin i_1 \cos i_2 \cos\Theta + \cos i_1 \sin i_2) = \xi_\chi \sin\chi \cos\vartheta \sin(\varphi' - \varphi) \quad (29)$$

and

$$\xi_\chi \sin\chi\,(\sin i_1 \sin i_2 \cos\Theta - \cos i_1 \cos i_2) = \xi_\chi \sin\chi \cos(\varphi' - \varphi)\,. \quad (30)$$

Since the original amplitudes, $\xi_\chi \cos\chi$ and $\xi_\chi \sin\chi$, were derived from a plane-polarized beam, the scattered amplitudes represented by equations (27)–(30) are all in phase and should therefore be added as amplitudes, vectorially. Thus, the plane-polarized component $I_\chi(\vartheta', \varphi')$ of the radiation in the direction (ϑ', φ'), when scattered in the direction (ϑ, φ), leads to a plane-polarized beam, the amplitudes of which in the meridian plane and at right angles to it are proportional, respectively, to

$$\xi_\chi [\,(l, l)\cos\chi + (r, l)\sin\chi\,], \quad (31)$$

and

$$\xi_\chi [\,(l, r)\cos\chi + (r, r)\sin\chi\,], \quad (32)$$

where, for the sake of brevity, we have written

$$\left.\begin{aligned}(l, l) &= \sin\vartheta \sin\vartheta' + \cos\vartheta \cos\vartheta' \cos(\varphi' - \varphi)\,,\\ (r, l) &= +\cos\vartheta \sin(\varphi' - \varphi)\,,\\ (l, r) &= -\cos\vartheta' \sin(\varphi' - \varphi)\,,\\ (r, r) &= \cos(\varphi' - \varphi)\,.\end{aligned}\right\} \quad (33)$$

Writing the amplitudes (31) and (32) as

$$A_\chi \xi_\chi \quad \text{and} \quad B_\chi \xi_\chi\,, \quad (34)$$

we observe that the intensity of scattered plane-polarized beam is proportional to

$$I_\chi(\vartheta', \varphi')\,(A_\chi^2 + B_\chi^2)\,, \quad (35)$$

while its plane of vibration of the electric vector is inclined to the meridian plane through (ϑ, φ) by an angle

$$\tan^{-1}\frac{B_\chi}{A_\chi}\,. \quad (36)$$

Hence, the contributions $d\mathfrak{J}_{l,\chi}(\vartheta, \varphi; \vartheta', \varphi')$, $d\mathfrak{J}_{r,\chi}(\vartheta, \varphi; \vartheta,' \varphi')$, and $d\mathfrak{J}_{U,\chi}(\vartheta, \varphi; \vartheta', \varphi')$ to the source functions $\mathfrak{J}_l(\vartheta, \varphi)$, $\mathfrak{J}_r(\vartheta, \varphi)$, and $\mathfrak{J}_U(\vartheta, \varphi)$, arising from the scattering of

the plane-polarized component $I_\chi(\vartheta', \varphi')$ of the radiation in the direction (ϑ', φ') and confined to an element of solid angle $d\omega'$, are

$$d\mathfrak{I}_{l,\chi}(\vartheta, \varphi; \vartheta', \varphi') = \frac{3}{8\pi} A_\chi^2 I_\chi(\vartheta', \varphi')\, d\omega', \tag{37}$$

$$d\mathfrak{I}_{r,\chi}(\vartheta, \varphi; \vartheta', \varphi') = \frac{3}{8\pi} B_\chi^2 I_\chi(\vartheta', \varphi')\, d\omega', \tag{38}$$

and

$$\left.\begin{aligned} d\mathfrak{I}_{U,\chi}(\vartheta, \varphi; \vartheta', \varphi') &= \frac{3}{8\pi} I_\chi(\vartheta', \varphi')(A_\chi^2 + B_\chi^2) \sin 2\left(\tan^{-1}\frac{B_\chi}{A_\chi}\right) d\omega' \\ &= \frac{3}{4\pi} A_\chi B_\chi I_\chi(\vartheta', \varphi')\, d\omega'. \end{aligned}\right\} \tag{39}$$

Substituting for A_χ and B_χ, we have

$$d\mathfrak{I}_{l,\chi}(\vartheta, \varphi; \vartheta', \varphi') = \frac{3}{8\pi} I_\chi(\vartheta', \varphi')[(l, l)\cos\chi + (r, l)\sin\chi]^2 d\omega', \tag{40}$$

$$d\mathfrak{I}_{r,\chi}(\vartheta, \varphi; \vartheta', \varphi') = \frac{3}{8\pi} I_\chi(\vartheta', \varphi')[(l, r)\cos\chi + (r, r)\sin\chi]^2 d\omega', \tag{41}$$

and

$$\left.\begin{aligned} d\mathfrak{I}_{U,\chi}(\vartheta, \varphi; \vartheta'\, \varphi') = \frac{3}{4\pi} I_\chi(\vartheta', \varphi')&[(l, l)\cos\chi + (r, l)\sin\chi] \\ &\times [(l, r)\cos\chi + (r, r)\sin\chi]\, d\omega'. \end{aligned}\right\} \tag{42}$$

The contributions to the source functions for the radiation in the direction (ϑ, φ) arising from the scattering of the other plane-polarized component $I_{\chi+\pi/2}(\vartheta', \varphi')$ in the direction (ϑ', φ') can be readily obtained from equations (40)–(42) by simply replacing χ by $\chi+\pi/2$. In this manner we obtain

$$d\mathfrak{I}_{l,\chi+\pi/2}(\vartheta, \varphi; \vartheta'\ \varphi') = \frac{3}{8\pi} I_{\chi+\pi/2}(\vartheta', \varphi')[-(l, l)\sin\chi + (r, l)\cos\chi]^2 d\omega', \tag{43}$$

$$d\mathfrak{I}_{r,\chi+\pi/2}(\vartheta, \varphi; \vartheta', \varphi') = \frac{3}{8\pi} I_{\chi+\pi/2}(\vartheta', \varphi')[-(l, r)\sin\chi + (r, r)\cos\chi]^2 d\omega', \tag{44}$$

and

$$\left.\begin{aligned} d\mathfrak{I}_{U,\chi+\pi/2}(\vartheta, \varphi; \vartheta', \varphi') = \frac{3}{4\pi} I_{\chi+\pi/2}(\vartheta', \varphi')&[-(l, l)\sin\chi + (r, l)\cos\chi] \\ &\times [-(l, r)\sin\chi + (r, r)\cos\chi]\, d\omega'. \end{aligned}\right\} \tag{45}$$

Adding the respective equations of the two foregoing sets of equations and making use of the relations (23), we obtain for the contributions $d\mathfrak{I}_l(\vartheta, \varphi; \vartheta', \varphi')$, $d\mathfrak{I}_r(\vartheta, \varphi; \vartheta', \varphi')$, and $d\mathfrak{I}_U(\vartheta, \varphi; \vartheta', \varphi')$ to the source functions $\mathfrak{I}_l(\vartheta, \varphi)$, $\mathfrak{I}_r(\vartheta, \varphi)$, and $\mathfrak{I}_U(\vartheta, \varphi)$ arising from the scattering of the radiation in the direction (ϑ, φ),

$$\left.\begin{aligned} d\mathfrak{I}_l(\vartheta, \varphi; \vartheta', \varphi') = \frac{3}{8\pi}\{&(l, l)^2 I_l(\vartheta', \varphi') + (r, l)^2 I_r(\vartheta', \varphi') \\ &+ (l, l)(r, l)\, U(\vartheta', \varphi')\}\, d\omega', \end{aligned}\right\} \tag{46}$$

$$\left.\begin{aligned} d\mathfrak{I}_r(\vartheta, \varphi; \vartheta', \varphi') = \frac{3}{8\pi}\{&(l, r)^2 I_l(\vartheta', \varphi') + (r, r)^2 I_r(\vartheta', \varphi') \\ &+ (l, r)(r, r)\, U(\vartheta', \varphi')\}\, d\omega', \end{aligned}\right\} \tag{47}$$

and

$$d\mathfrak{J}_U(\vartheta, \varphi; \vartheta', \varphi') = \frac{3}{8\pi}\{2(l, l)(l, r) I_l(\vartheta', \varphi') + 2(r, l)(r, r) I_r(\vartheta', \varphi') + [(l, l)(r, r) + (r, l)(l, r)] U(\vartheta', \varphi')\} d\omega' . \quad (48)$$

It is to be particularly noted that the foregoing equations involve only the intensities $I_l(\vartheta', \varphi')$, $I_r(\vartheta', \varphi')$, and $U(\vartheta', \varphi')$, in terms of which we agreed to characterize the radiation field.

Finally, integrating equations (46), (47), and (48) over the unit sphere, we obtain the required source functions. We have

$$\mathfrak{J}_l(\mu, \varphi) = \frac{3}{8\pi}\int_{-1}^{+1}\int_0^{2\pi}\{(l, l)^2 I_l(\mu', \varphi') + (r, l)^2 I_r(\mu', \varphi') + (l, l)(r, l) U(\mu', \varphi')\} d\mu' d\varphi' , \quad (49)$$

$$\mathfrak{J}_r(\mu, \varphi) = \frac{3}{8\pi}\int_{-1}^{+1}\int_0^{2\pi}\{(l, r)^2 I_l(\mu', \varphi') + (r, r)^2 I_r(\mu', \varphi') + (l, r)(r, r) U(\mu', \varphi')\} d\mu' d\varphi' , \quad (50)$$

and

$$\mathfrak{J}_U(\mu, \varphi) = \frac{3}{8\pi}\int_{-1}^{+1}\int_0^{2\pi}\{2(l, l)(l, r) I_l(\mu', \varphi') + 2(r, l)(r, r) I_r(\mu', \varphi') + [(l, l)(r, r) + (r, l)(l, r)] U(\mu', \varphi')\} d\mu' d\varphi' , \quad (51)$$

where the direction cosines μ and μ' have been used in place of $\cos\vartheta$ and $\cos\vartheta'$. We may further note that, according to equation (33), we have

$$\begin{aligned}
&(l, l)^2 = \tfrac{1}{2}[2(1-\mu'^2) + \mu^2(3\mu'^2 - 2)] \\
&\qquad + 2\mu\mu'(1-\mu^2)^{\frac{1}{2}}(1-\mu'^2)^{\frac{1}{2}}\cos(\varphi'-\varphi) + \tfrac{1}{2}\mu^2\mu'^2\cos 2(\varphi'-\varphi) , \\
&(r, l)^2 = \tfrac{1}{2}\mu^2[1-\cos 2(\varphi'-\varphi)] ; \qquad (l, r)^2 = \tfrac{1}{2}\mu'^2[1-\cos 2(\varphi'-\varphi)] , \\
&(r, r)^2 = \tfrac{1}{2}[1+\cos 2(\varphi'-\varphi)] , \\
&(l, l)(r, l) = \mu(1-\mu^2)^{\frac{1}{2}}(1-\mu'^2)^{\frac{1}{2}}\sin(\varphi'-\varphi) + \tfrac{1}{2}\mu^2\mu'\sin 2(\varphi'-\varphi) , \\
&(l, r)(r, r) = -\tfrac{1}{2}\mu'\sin 2(\varphi'-\varphi) ; \qquad (r, l)(r, r) = \tfrac{1}{2}\mu\sin 2(\varphi'-\varphi) , \\
&(l, l)(l, r) = -\mu'(1-\mu^2)^{\frac{1}{2}}(1-\mu'^2)^{\frac{1}{2}}\sin(\varphi'-\varphi) - \tfrac{1}{2}\mu\mu'^2\sin 2(\varphi'-\varphi) , \\
&(l, l)(r, r) + (r, l)(l, r) = (1-\mu^2)^{\frac{1}{2}}(1-\mu'^2)^{\frac{1}{2}}\cos(\varphi'-\varphi) \\
&\qquad + \mu\mu'\cos 2(\varphi'-\varphi) .
\end{aligned} \quad (52)$$

5. *The reduction of the equations of transfer for the problem of diffuse reflection of a parallel beam of unpolarized radiation by a plane-parallel atmosphere.*—For the problem of diffuse reflection, it is convenient to distinguish between the incident radiation which penetrates to various depths, unaffected by any scattering or absorbing mechanisms, and the diffuse scattered radiation. Thus, if a parallel beam of unpolarized radiation of flux πF per unit area normal to itself is incident on a plane-parallel atmosphere at an angle β normal to the boundary, then at a level which is at an optical depth τ (measured in terms of the mass-scattering coefficient σ) below the surface, a fraction $e^{-\tau\sec\beta}$ of the incident radiation would not have suffered any scattering process and will, accordingly, be unpolarized: it is this unpolarized part of the radiation field which we wish to distinguish from the rest. With this understanding we may also distinguish

between the contributions to the various source functions arising from the unpolarized incident radiation field and the partially polarized diffuse radiation field. As in § 4, we shall now characterize the diffuse radiation field by the intensities $I_l(\tau, \vartheta, \varphi)$, $I_r(\tau, \vartheta, \varphi)$, and $U(\tau, \vartheta, \varphi)$, where ϑ and φ may now be chosen as the polar angles in a co-ordinate system in which the Z-axis is normal to the plane of stratification and the direction of the incident flux is $(\pi - \beta, 0)$.

The equations of transfer may now be written in the forms

$$\mu \frac{dI_l(\tau, \mu, \varphi)}{d\tau} = I_l(\tau, \mu, \varphi) - \mathfrak{J}_l(\tau, \mu, \varphi) - \mathfrak{J}_l^{(i)}(\tau, \mu, \varphi), \tag{53}$$

$$\mu \frac{dI_r(\tau, \mu, \varphi)}{d\tau} = I_r(\tau, \mu, \varphi) - \mathfrak{J}_r(\tau, \mu, \varphi) - \mathfrak{J}_r^{(i)}(\tau, \mu, \varphi), \tag{54}$$

and

$$\mu \frac{dU(\tau, \mu, \varphi)}{d\tau} = U(\tau, \mu, \varphi) - \mathfrak{J}_U(\tau, \mu, \varphi) - \mathfrak{J}_U^{(i)}(\tau, \mu, \varphi), \tag{55}$$

where $\mathfrak{J}_l(\tau, \mu, \varphi)$, $\mathfrak{J}_r(\tau, \mu, \varphi)$, and $\mathfrak{J}_U(\tau, \mu, \varphi)$ are the contributions to the respective source functions for the radiation at τ and in the direction (μ, φ), arising from the scattering of the diffuse radiation from all other directions, while $\mathfrak{J}_l^{(i)}(\tau, \mu, \varphi)$, $\mathfrak{J}_r^{(i)}(\tau, \mu, \varphi)$, and $\mathfrak{J}_U^{(i)}(\tau, \mu, \varphi)$ are those arising from the scattering of the unpolarized radiation of flux $\pi F e^{-\tau \sec\beta}$, which prevails at τ. By arguments similar to those used to establish formulae (46)–(48) it can readily be shown that

$$\left.\begin{aligned}\mathfrak{J}_l^{(i)}(\tau, \mu, \varphi) = {}&\tfrac{3}{16} F e^{-\tau \sec\beta} \{ \tfrac{1}{2} [\, 2 \sin^2\beta + \mu^2 (3 \cos^2\beta - 1)\,] \\ &- 2\mu (1 - \mu^2)^{\frac{1}{2}} \cos\beta \sin\beta \cos\varphi - \tfrac{1}{2}\mu^2 \sin^2\beta \cos 2\varphi \},\end{aligned}\right\} \tag{56}$$

$$\mathfrak{J}_r^{(i)}(\tau, \mu, \varphi) = \tfrac{3}{32} F e^{-\tau \sec\beta} \{ (1 + \cos^2\beta) + \sin^2\beta \cos 2\varphi \}, \tag{57}$$

and

$$\mathfrak{J}_U^{(i)}(\tau, \mu, \varphi) = -\tfrac{3}{16} F e^{-\tau \sec\beta} \{ 2(1 - \mu^2)^{\frac{1}{2}} \sin\beta \cos\beta \sin\varphi + \mu \sin^2\beta \sin 2\varphi \}. \tag{58}$$

Combining equations (49)–(58), we have the required equations of transfer. An examination of these equations indicates that the solutions for $I_l(\tau, \mu\, \varphi)$, $I_r(\tau, \mu, \varphi)$, and $U(\tau, \mu, \varphi)$ must be expressible in the forms

$$I_l(\tau, \mu, \varphi) = I_l^{(0)}(\tau, \mu) + I_l^{(1)}(\tau, \mu) \cos\varphi + I_l^{(2)}(\tau, \mu) \cos 2\varphi, \tag{59}$$

$$I_r(\tau, \mu, \varphi) = I_r^{(0)}(\tau, \mu) + I_r^{(2)}(\tau, \mu) \cos 2\varphi, \tag{60}$$

and

$$U(\tau, \mu, \varphi) = U^{(1)}(\tau, \mu) \sin\varphi + U^{(2)}(\tau, \mu) \sin 2\varphi. \tag{61}$$

As the notation indicates, $I_l^{(0)}$, $I_l^{(1)}$, etc., are all functions of τ and μ only. Substituting the foregoing forms for the solution in the equations of transfer, we find that they break up into three sets of equations, which are

$$\left.\begin{aligned}\mu \frac{dI_l^{(0)}}{d\tau} = {}& I_l^{(0)} - \frac{3}{8}\Big[\int_{-1}^{+1} I_l^{(0)}(\tau, \mu') \{\!\{ 2(1 - \mu'^2) + \mu^2 (3\mu'^2 - 2) \}\!\} \, d\mu' \\ &+ \mu^2 \int_{-1}^{+1} I_r^{(0)}(\tau, \mu')\, d\mu'\Big] - \tfrac{3}{32} F e^{-\tau \sec\beta} [\, 2 \sin^2\beta + \mu^2 (3 \cos^2\beta - 1)\,], \\ \mu \frac{dI_r^{(0)}}{d\tau} = {}& I_r^{(0)} - \frac{3}{8}\Big[\int_{-1}^{+1} I_l^{(0)}(\tau, \mu')\, \mu'^2 d\mu' + \int_{-1}^{+1} I_r^{(0)}(\tau, \mu')\, d\mu'\Big] \\ &- \tfrac{3}{32} F e^{-\tau \sec\beta} (1 + \cos^2\beta);\end{aligned}\right\} \quad \text{(I)}$$

$$\left.\begin{aligned}
&\mu\frac{dI_l^{(1)}}{d\tau}=I_l^{(1)}-\tfrac{3}{4}\mu(1-\mu^2)^{\frac{1}{2}}\int_{-1}^{+1}I_l^{(1)}(\tau,\mu')\,\mu'(1-\mu'^2)^{\frac{1}{2}}d\mu'\\
&-\tfrac{3}{8}\mu(1-\mu^2)^{\frac{1}{2}}\int_{-1}^{+1}U^{(1)}(\tau,\mu')(1-\mu'^2)^{\frac{1}{2}}d\mu'+\tfrac{3}{8}Fe^{-\tau\sec\beta}\mu(1-\mu^2)^{\frac{1}{2}}\cos\beta\sin\beta\,,\\
&\mu\frac{dU^{(1)}}{d\tau}=U^{(1)}-\tfrac{3}{4}(1-\mu^2)^{\frac{1}{2}}\int_{-1}^{+1}I_l^{(1)}(\tau,\mu')\,\mu'(1-\mu'^2)^{\frac{1}{2}}d\mu'\\
&-\tfrac{3}{8}(1-\mu^2)^{\frac{1}{2}}\int_{-1}^{+1}U^{(1)}(\tau,\mu')(1-\mu'^2)^{\frac{1}{2}}d\mu'+\tfrac{3}{8}Fe^{-\tau\sec\beta}(1-\mu^2)^{\frac{1}{2}}\cos\beta\sin\beta\,;
\end{aligned}\right\}\quad\text{(II)}$$

$$\left.\begin{aligned}
&\mu\frac{dI_l^{(2)}}{d\tau}=I_l^{(2)}-\tfrac{3}{16}\mu^2\int_{-1}^{+1}I_l^{(2)}(\tau,\mu')\,\mu'^2d\mu'+\tfrac{3}{16}\mu^2\int_{-1}^{+1}I_r^{(2)}(\tau,\mu')\,d\mu'\\
&\qquad-\tfrac{3}{16}\mu^2\int_{-1}^{+1}U^{(2)}(\tau,\mu')\,\mu'd\mu'+\tfrac{3}{32}Fe^{-\tau\sec\beta}\mu^2\sin^2\beta\,,\\
&\mu\frac{dI_r^{(2)}}{d\tau}=I_r^{(2)}+\frac{3}{16}\int_{-1}^{+1}I_l^{(2)}(\tau,\mu')\,\mu'^2d\mu'-\tfrac{3}{16}\int_{-1}^{+1}I_r^{(2)}(\tau,\mu')\,d\mu'\\
&\qquad+\tfrac{3}{16}\int_{-1}^{+1}U^{(2)}(\tau,\mu')\,\mu'd\mu'-\tfrac{3}{32}Fe^{-\tau\sec\beta}\sin^2\beta\,,\\
&\mu\frac{dU^{(2)}}{d\tau}=U^{(2)}-\tfrac{3}{8}\mu\int_{-1}^{+1}I_l^{(2)}(\tau,\mu')\,\mu'^2d\mu'+\tfrac{3}{8}\mu\int_{-1}^{+1}I_r^{(2)}(\tau,\mu')\,d\mu'\\
&\qquad-\tfrac{3}{8}\mu\int_{-1}^{+1}U^{(2)}(\tau,\mu')\,\mu'd\mu'+\tfrac{3}{16}Fe^{-\tau\sec\beta}\mu\sin^2\beta\,.
\end{aligned}\right\}\quad\text{(III)}$$

We now proceed to the solution of these equations appropriately for the problem of diffuse reflection from a semi-infinite plane-parallel atmosphere.

6. *The solutions of the equations for* $\mathrm{I}_l^{(0)}$ *and* $\mathrm{I}_r^{(0)}$.—Considering the equations of the first of the three systems to which we reduced our problem in § 5, we replace it in the nth approximation by the following system of $4n$ linear equations:

$$\left.\begin{aligned}
\mu_i\frac{dI_{l,i}^{(0)}}{d\tau}&=I_{l,i}^{(0)}-\tfrac{3}{8}\left[2\Sigma a_jI_{l,j}^{(0)}(1-\mu_j^2)+\mu_i^2\{\Sigma a_jI_{l,j}^{(0)}(3\mu_j^2-2)+\Sigma a_jI_{r,j}^{(0)}\}\right]\\
&\quad-\tfrac{3}{32}Fe^{-\tau\sec\beta}\left[2\sin^2\beta+\mu_i^2(3\cos^2\beta-1)\right]\qquad(i=\pm1\,,\ldots..\,,\pm n)\,,
\end{aligned}\right\}\quad(62)$$

and

$$\left.\begin{aligned}
\mu_i\frac{dI_{r,i}^{(0)}}{d\tau}&=I_{r,i}^{(0)}-\tfrac{3}{8}\left[\Sigma a_jI_{l,j}^{(0)}\mu_j^2+\Sigma a_jI_{r,j}^{(0)}\right]-\tfrac{3}{32}Fe^{-\tau\sec\beta}(1+\cos^2\beta)\\
&\qquad(i=\pm1\,,\ldots..\,,\pm n)\,,
\end{aligned}\right\}\quad(63)$$

where the various symbols have their usual meanings.

It is now seen that the homogeneous system associated with equations (62) and (63) is the same as that considered in Paper X, §§ 3–6. The complementary functions for $I_{l,i}^{(0)}$ and $I_{r,i}^{(0)}$ are therefore the same as those derived in the general solution (Paper X, eqs. [85] and [86]) of the homogeneous system. To complete the solution we therefore need only certain particular integrals for $I_{l,i}^{(0)}$ and $I_{r,i}^{(0)}$; and these can be found in the following manner:

Setting

$$I_{l,i}^{(0)}=\tfrac{3}{32}Fg_ie^{-\tau\sec\beta}\qquad\text{and}\qquad I_{r,i}^{(0)}=\tfrac{3}{32}Fh_ie^{-\tau\sec\beta}\qquad(i=\pm1\,,\ldots..\,,\pm n)\quad(64)$$

in equations (62) and (63), we readily verify that the constants g_i and h_i must be expressible in the forms

$$g_i = \frac{\alpha\mu_i^2 + \delta}{1 + \mu_i \sec\beta} \quad \text{and} \quad h_i = \frac{\gamma}{1 + \mu_i \sec\beta} \qquad (i = \pm 1, \ldots, \pm n), \tag{65}$$

where α, δ, and γ are certain constants which are determined in accordance with the relations

$$\left.\begin{aligned} \alpha\mu_i^2 + \delta = \tfrac{3}{8}\,[\,2\alpha\,(E_2 - E_4) + 2\delta\,(E_0 - E_2) + \mu_i^2\{\alpha\,(3E_4 - 2E_2) \\ + \delta\,(3E_2 - 2E_0) + \gamma E_0\}\,] + 2\sin^2\beta + \mu_i^2\,(3\cos^2\beta - 1), \end{aligned}\right\} \tag{66}$$

and

$$\gamma = \tfrac{3}{8}\,[\,\alpha E_4 + \delta E_2 + \gamma E_0\,] + 1 + \cos^2\beta, \tag{67}$$

where we have used E_m to denote

$$E_m = \Sigma\,\frac{a_j\mu_j^m}{1 + \mu_j \sec\beta}. \tag{68}$$

Since equations (66) and (67) must be valid for all i, we must require that

$$\tfrac{8}{3}\,\alpha = \alpha\,(3E_4 - 2E_2) + \delta\,(3E_2 - 2E_0) + \gamma E_0 + \tfrac{8}{3}\,(3\cos^2\beta - 1), \tag{69}$$

$$\tfrac{4}{3}\,\delta = \alpha\,(E_2 - E_4) + \delta\,(E_0 - E_2) + \tfrac{8}{3}\sin^2\beta, \tag{70}$$

and

$$\tfrac{8}{3}\,\gamma = \alpha E_4 + \delta E_2 + \gamma E_0 + \tfrac{8}{3}\,(1 + \cos^2\beta). \tag{71}$$

These equations determine α, δ, and γ. We find

$$\alpha = +\frac{1}{1 - \tfrac{3}{8}\,(E_0 - E_2)} - \frac{2}{1 - \tfrac{3}{4}\,(E_0 - E_2)}, \tag{72}$$

$$\delta = -\frac{\cos^2\beta}{1 - \tfrac{3}{8}\,(E_0 - E_2)} + \frac{2}{1 - \tfrac{3}{4}\,(E_0 - E_2)}, \tag{73}$$

and

$$\gamma = +\frac{\sin^2\beta}{1 - \tfrac{3}{8}\,(E_0 - E_2)}. \tag{74}$$

In reducing the solutions for α, δ, and γ to the foregoing forms, repeated use has been made of the recursion formula (Paper IX, eq. [42]),

$$E_m = \cos\beta\left(\frac{2}{m}\,\epsilon_{m,\,\mathrm{odd}} - E_{m-1}\right) \qquad (m \leqslant 4n), \tag{75}$$

which the E's satisfy. In terms of the quantities

$$C = \frac{1}{1 - \tfrac{3}{8}\,(E_0 - E_2)} = \frac{1}{1 - \dfrac{3}{4}\displaystyle\sum_{j=1}^{n}\frac{a_j(1 - \mu_j^2)}{1 - \mu_j^2\sec^2\beta}} \tag{76}$$

and

$$\Gamma = \frac{1}{1 - \tfrac{3}{4}\,(E_0 - E_2)} = \frac{1}{1 - \dfrac{3}{2}\displaystyle\sum_{j=1}^{n}\frac{a_j(1 - \mu_j^2)}{1 - \mu_j^2\sec^2\beta}}, \tag{77}$$

we can express α, δ, and γ more conveniently in the forms

$$\alpha = C - 2\Gamma\,; \qquad \delta = -C\cos^2\beta + 2\Gamma\,; \qquad \gamma = C\sin^2\beta\,. \tag{78}$$

We now observe that C and Γ, as defined in equations (76) and (77), bear the same relations to the characteristic equations (Paper X, eqs. [72] and [73])

$$1 = \frac{3}{4}\sum_{j=1}^{n}\frac{a_j(1-\mu_j^2)}{1-\mu_j^2k^2} \qquad \text{and} \qquad 1 = \frac{3}{2}\sum_{j=1}^{n}\frac{a_j(1-\mu_j^2)}{1-\mu_j^2k^2}\,, \tag{79}$$

as γ, defined in Paper VIII, equation (40), bears to the corresponding characteristic equation (Paper VIII, eq. [10]). We can therefore express C and Γ in the forms (cf. also Paper IX, eqs. [52], [123], and [166])

$$C = \frac{1}{\mu_1^2\ldots.\,\mu_n^2}\frac{P(\cos\beta)P(-\cos\beta)}{R(\cos\beta)R(-\cos\beta)}\,, \tag{80}$$

and

$$\Gamma = \frac{1}{\mu_1^2\ldots.\,\mu_n^2}\frac{P(\cos\beta)P(-\cos\beta)}{\rho(\cos\beta)\,\rho(-\cos\beta)}\,, \tag{81}$$

where the functions R, ρ, and P have the same meanings as in paper X, equations (129), (130), and (132).

Returning to equation (64), we can now express the particular integrals for $I_{l,i}^{(0)}$ and $I_{r,i}^{(0)}$ in the forms

$$\left.\begin{aligned} I_{l,i}^{(0)} = {}_3^3F\,e^{-\tau\sec\beta}\left[\frac{2(1-\mu_i^2)\,\Gamma}{1+\mu_i\sec\beta} - C(1-\mu_i\sec\beta)\cos^2\beta\right] \\ (i=\pm1\,,\ldots.\,,\pm n)\end{aligned}\right\} \tag{82}$$

and

$$I_{r,i}^{(0)} = {}_3^3F\,e^{-\tau\sec\beta}\frac{C\sin^2\beta}{1+\mu_i\sec\beta} \qquad (i=\pm1\,,\ldots.\,,\pm n)\,. \tag{83}$$

Adding these particular integrals for $I_{l,i}^{(0)}$ and $I_{r,i}^{(0)}$ to the corresponding solutions (Paper X, eqs. [87] and [88]) derived from the homogeneous equations and which are further compatible with our present requirement of the boundedness of the solutions for $\tau\to\infty$, we have

$$\left.\begin{aligned} I_{l,i}^{(0)} = {}_3^3F\Bigg[(1-\mu_i^2)\sum_{\beta=1}^{n-1}\frac{L_\beta e^{-\kappa_\beta\tau}}{1+\mu_i\kappa_\beta} + \sum_{\alpha=1}^{n}M_\alpha(1-k_\alpha\mu_i)\,e^{-k_\alpha\tau} + Q \\ + e^{-\tau\sec\beta}\left\{\frac{2(1-\mu_i^2)\,\Gamma}{1+\mu_i\sec\beta} - C(1-\mu_i\sec\beta)\cos^2\beta\right\}\Bigg] \qquad (i=\pm1\,,\ldots.\,,\pm n)\end{aligned}\right\} \tag{84}$$

and

$$\left.\begin{aligned} I_{r,i}^{(0)} = {}_3^3F\left[Q - \sum_{\alpha=1}^{n}\frac{M_\alpha(k_\alpha^2-1)\,e^{-k_\alpha\tau}}{1+\mu_ik_\alpha} + \frac{C\sin^2\beta}{1+\mu_i\sec\beta}\,e^{-\tau\sec\beta}\right] \\ (i=\pm1\,,\ldots.\,,\pm n)\,,\end{aligned}\right\} \tag{85}$$

where $L_\beta(\beta=1,\ldots.\,,n-1)$, $M_\alpha(\alpha=1,\ldots.\,,n)$, and Q are $2n$ constants of integration to be determined by the boundary conditions

$$I_{l,i}^{(0)} = I_{r,i}^{(0)} = 0 \qquad (i=-1\,,\ldots.\,,-n)\,. \tag{86}$$

In terms of the functions

$$\left.\begin{aligned} S_l(\mu) = (1-\mu^2)\sum_{\beta=1}^{n-1}\frac{L_\beta}{1-\mu\kappa_\beta} + \sum_{a=1}^{n} M_a(1+k_a\mu) + Q \\ + (1-\mu^2)\frac{2\Gamma}{1-\mu\sec\beta} - C(1+\mu\sec\beta)\cos^2\beta \end{aligned}\right\} \quad (87)$$

and

$$S_r(\mu) = Q - \sum_{a=1}^{n}\frac{M_a(k_a^2-1)}{1-\mu k_a} + \frac{C\sin^2\beta}{1-\mu\sec\beta}, \quad (88)$$

the boundary conditions are

$$S_l(\mu_i) = S_r(\mu_i) = 0 \qquad (i = 1, \ldots, n). \quad (89)$$

The angular distribution of the reflected radiation, corresponding to the parts $I_l^{(0)}$ and $I_r^{(0)}$ of the emergent intensities are also expressible in terms of the functions $S_l(\mu)$ and $S_r(\mu)$. We have

$$I_l^{(0)}(0, \mu) = {}_3^3FS_l(-\mu) \quad \text{and} \quad I_r^{(0)}(0, \mu) = {}_3^3FS_r(-\mu). \quad (90)$$

We shall now show how explicit formulae for $S_l(\mu)$ and $S_r(\mu)$ can be found without having the necessity of solving for the constants L_β, M_a, and Q.

Consider the function

$$(1-\mu\sec\beta)\,\rho(\mu)\,S_l(\mu) = (1-\mu\sec\beta)\prod_{\beta=1}^{n-1}(1-\kappa_\beta\mu)\,S_l(\mu). \quad (91)$$

This is a polynomial of degree $(n+1)$ in μ, which vanishes for $\mu = \mu_i\,(i = 1, \ldots, n)$. There must, therefore, exist a relation of the form

$$S_l(\mu) = X\frac{P(\mu)(\mu+a)}{(1-\mu\sec\beta)\,\rho(\mu)}, \quad (92)$$

where X and a are certain constants. Of these two constants, X is readily determined; for, from equations (87) and (92), it follows that

$$\lim_{\mu\to\cos\beta}(1-\mu\sec\beta)\,S_l(\mu) = X\frac{P(\cos\beta)}{\rho(\cos\beta)}(\cos\beta+a) = 2\Gamma\sin^2\beta, \quad (93)$$

and, substituting for Γ from equation (81), we obtain

$$X = \frac{2\sin^2\beta}{\mu_1^2\ldots\mu_n^2}\frac{P(-\cos\beta)}{\rho(-\cos\beta)(\cos\beta+a)}. \quad (94)$$

Hence,

$$S_l(\mu) = \frac{2\sin^2\beta}{\mu_1^2\ldots\mu_n^2}\frac{P(-\cos\beta)P(\mu)}{\rho(-\cos\beta)\,\rho(\mu)}\frac{\mu+a}{(\cos\beta+a)(1-\mu\sec\beta)}. \quad (95)$$

Similarly, it can be shown that

$$S_r(\mu) = \frac{\sin^2\beta}{\mu_1^2\ldots\mu_n^2}\frac{P(-\cos\beta)P(\mu)}{R(-\cos\beta)R(\mu)}\frac{\mu+b}{(\cos\beta+b)(1-\mu\sec\beta)}, \quad (96)$$

where b is another constant. It now remains to determine the constants a and b. For this purpose we proceed as follows:

Setting $\mu = +1$, respectively -1, in equation (87), we have

$$\sum_{a=1}^{n} M_a (1 + k_a) + Q - C (\cos \beta + 1) \cos \beta = S_l (+1) \tag{97}$$

and

$$\sum_{a=1}^{n} M_a (1 - k_a) + Q - C (\cos \beta - 1) \cos \beta = S_l (-1) . \tag{98}$$

Adding and subtracting these two equations, we obtain

$$\sum_{a=1}^{n} M_a + Q - C \cos^2 \beta = \tfrac{1}{2} [S_l (+1) + S_l (-1)] \tag{99}$$

and

$$\sum_{a=1}^{n} M_a k_a - C \cos \beta = \tfrac{1}{2} [S_l (+1) - S_l (-1)] . \tag{100}$$

Next, setting $\mu = 0$ in equation (88), we have

$$Q - \sum_{a=1}^{n} M_a (k_a^2 - 1) + C \sin^2 \beta = S_r (0) , \tag{101}$$

and, subtracting this equation from equation (99), we obtain

$$\sum_{a=1}^{n} M_a k_a^2 - C = \tfrac{1}{2} [S_l (+1) + S_l (-1)] - S_r (0) . \tag{102}$$

We shall now show how the constants a and b can be determined from equations (100) and (102).

First, substituting for $S_l(+1)$, $S_l(-1)$, and $S_r(0)$ according to equations (95) and (96) in equations (100) and (102), we find, after some minor reductions, that

$$\left.\begin{aligned} \sum_{a=1}^{n} M_a k_a - C \cos \beta = & - \frac{\cos \beta \; P (- \cos \beta)}{\mu_1^2 \cdots \mu_n^2 \rho (- \cos \beta) (a + \cos \beta)} \\ & \times \left[(a+1)(1+\cos\beta) \frac{P(1)}{\rho(1)} + (a-1)(1-\cos\beta) \frac{P(-1)}{\rho(-1)} \right] \end{aligned}\right\} \tag{103}$$

and

$$\left.\begin{aligned} \sum_{a=1}^{n} M_a k_a^2 - C + & \frac{\sin^2 \beta \quad P (- \cos \beta)}{\mu_1^2 \cdots \mu_n^2 R (- \cos \beta)} \; \frac{(-1)^n \mu_1 \cdots \mu_n b}{b + \cos \beta} \\ & = \frac{\cos \beta \; P (- \cos \beta)}{\mu_1^2 \cdots \mu_n^2 \rho (- \cos \beta) (a + \cos \beta)} \left[- (a+1)(1+\cos\beta) \frac{P(1)}{\rho(1)} \right. \\ & \qquad \left. + (a-1)(1-\cos\beta) \frac{P(-1)}{\rho(-1)} \right] . \end{aligned}\right\} \tag{104}$$

On the other hand, from equations (88) and (96) it follows that

$$\left.\begin{aligned} M_a &= -\frac{1}{(k_a^2-1)} \lim_{\mu \to k_a^{-1}} (1-\mu k_a) S_r(\mu) \\ &= \frac{\sin^2\beta \cos\beta}{\mu_1^2 \ldots \mu_n^2} \frac{P(-\cos\beta)}{R(-\cos\beta)(b+\cos\beta)} \frac{(1+bk_a)P(1/k_a)}{(k_a^2-1)(1-k_a\cos\beta)R_a(1/k_a)}, \end{aligned}\right\} \quad (105)$$

where $R_a(x)$ has the same meaning as in Paper X, equation (129). Substituting the foregoing expression for M_a in equations (103) and (104), we find that they can be reduced to the forms

$$\left.\begin{aligned} &\frac{(\zeta_1+b\zeta_2)\sin^2\beta}{R(-\cos\beta)(b+\cos\beta)} - \frac{P(\cos\beta)}{R(\cos\beta)R(-\cos\beta)} \\ &= \frac{-1}{\rho(-\cos\beta)(a+\cos\beta)}\left[(a+1)(1+\cos\beta)\frac{P(1)}{\rho(1)} + (a-1)(1-\cos\beta)\frac{P(-1)}{\rho(-1)}\right], \end{aligned}\right\} \quad (106)$$

$$\left.\begin{aligned} &\frac{\sin^2\beta}{R(-\cos\beta)(b+\cos\beta)}\left[(\zeta_2+b\zeta_3)\cos\beta + (-1)^n\mu_1 \ldots \mu_n b\right] \\ &- \frac{P(\cos\beta)}{R(\cos\beta)R(-\cos\beta)} = \frac{\cos\beta}{\rho(-\cos\beta)(a+\cos\beta)}\left[-(a+1)(1+\cos\beta)\frac{P(1)}{\rho(1)}\right. \\ &\qquad \left. + (a-1)(1-\cos\beta)\frac{P(-1)}{\rho(-1)}\right], \end{aligned}\right\} \quad (107)$$

where

$$\zeta_m = \sum_{a=1}^{n} \frac{k_a^m}{(k_a^2-1)(1-k_a\cos\beta)} \frac{P(1/k_a)}{R_a(1/k_a)} \qquad (m=1, 2, 3). \quad (108)$$

To evaluate the sum occurring on the right side of equation (108), we introduce the function

$$f_m(x) = \sum_{a=1}^{n} \frac{P(1/k_a)\, k_a^m}{(k_a^2-1)R_a(1/k_a)} R_a(x) \quad (109)$$

and express ζ_m in terms of it. Thus

$$\zeta_m = \frac{f_m(\cos\beta)}{R(\cos\beta)}. \quad (110)$$

Now $f_m(x)$, defined as in equation (109), is a polynomial of degree $(n-1)$ in x, which takes the values

$$\frac{P(1/k_a)\, k_a^m}{(k_a^2-1)} \quad (111)$$

for $x = 1/k_a$, $(a = 1, \ldots, n)$. In other words,

$$(1-x^2) f_m(x) - x^{2-m} P(x) \quad (112)$$

vanishes for $x = 1/k_\alpha$, ($\alpha = 1, \ldots, n$). It must accordingly divide $R(x)$. This fact enables us to determine $f_m(x)$. To illustrate this, we shall consider the case $m = 3$. In this case there must exist a relation of the form

$$x(1-x^2)\,f_3(x) - P(x) = R(x)(Ax^2 + Bx + D), \tag{113}$$

since the polynomial on the right-hand side is of degree $n+2$ in x and vanishes for $x = 1/k_\alpha$, $\alpha = 1, \ldots, n$. To determine the constants A, B, and D, we first set $x = 0$ and find at once that

$$D = (-1)^{n+1}\mu_1 \ldots \mu_n . \tag{114}$$

Next, setting $x = +1$, respectively -1, we have

$$A + B + D = -\frac{P(1)}{R(1)} \tag{115}$$

and

$$A - B + D = -\frac{P(-1)}{R(-1)} . \tag{116}$$

These equations determine A and B and make $f_3(x)$ determinate; ζ_3 then follows according to equation (110). In this manner we find that

$$\left.\begin{aligned}\zeta_3 = \frac{1}{\cos\beta \sin^2\beta}\Big\{&\frac{P(\cos\beta)}{R(\cos\beta)} - \frac{1}{2}\Big[\frac{P(1)}{R(1)} + \frac{P(-1)}{R(-1)}\Big]\cos^2\beta \\ &- \frac{1}{2}\Big[\frac{P(1)}{R(1)} - \frac{P(-1)}{R(-1)}\Big]\cos\beta + (-1)^{n+1}\mu_1 \ldots \mu_n \sin^2\beta\Big\} .\end{aligned}\right\} \tag{117}$$

Similarly,

$$\left.\begin{aligned}\zeta_1 = \frac{1}{\sin^2\beta}\Big\{&\frac{P(\cos\beta)}{R(\cos\beta)}\cos\beta - \frac{1}{2}\Big[\frac{P(1)}{R(1)} + \frac{P(-1)}{R(-1)}\Big]\cos\beta \\ &- \frac{1}{2}\Big[\frac{P(1)}{R(1)} - \frac{P(-1)}{R(-1)}\Big]\Big\} ,\end{aligned}\right\} \tag{118}$$

and

$$\left.\begin{aligned}\zeta_2 = \frac{1}{\sin^2\beta}\Big\{&\frac{P(\cos\beta)}{R(\cos\beta)} - \frac{1}{2}\Big[\frac{P(1)}{R(1)} - \frac{P(-1)}{R(-1)}\Big]\cos\beta \\ &- \frac{1}{2}\Big[\frac{P(1)}{R(1)} + \frac{P(-1)}{R(-1)}\Big]\Big\} .\end{aligned}\right\} \tag{119}$$

Substituting these expressions for ζ_1, ζ_2, and ζ_3 in equations (106) and (107) we obtain, after some further reductions, the equations

$$\frac{1}{R(1)R(-\cos\beta)}\,\frac{b+1}{b+\cos\beta} = \frac{2}{\rho(1)\,\rho(-\cos\beta)}\,\frac{a+1}{a+\cos\beta} \tag{120}$$

and

$$\frac{1}{R(-1)R(-\cos\beta)}\,\frac{b-1}{b+\cos\beta} = \frac{2}{\rho(-1)\,\rho(-\cos\beta)}\,\frac{a-1}{a+\cos\beta} . \tag{121}$$

Finally, solving these equations for a and b, we find

$$a = \frac{xy\cos\beta - (x\eta + y\xi)\cos\beta + (x\eta - y\xi)}{(x\eta + y\xi) - xy - (x\eta - y\xi)\cos\beta}$$

and

$$b = \frac{4\xi\eta\cos\beta - (x\eta + y\xi)\cos\beta - (x\eta - y\xi)}{(x\eta + y\xi) - 4\xi\eta + (x\eta - y\xi)\cos\beta},$$

where we have used the abbreviations

$$x = \frac{1}{R(1)R(-\cos\beta)}; \qquad y = \frac{1}{R(-1)R(-\cos\beta)}, \tag{124}$$

and

$$\xi = \frac{1}{\rho(1)\,\rho(-\cos\beta)}; \qquad \eta = \frac{1}{\rho(-1)\,\rho(-\cos\beta)}. \tag{125}$$

With the solutions (122) and (123) for a and b, we find that (cf. eqs. 95] and [96]),

$$\frac{a+\mu}{a+\cos\beta}\sin^2\beta = 1 - \mu\cos\beta + \frac{x\eta + y\xi - xy}{x\eta - y\xi}(\mu - \cos\beta, \tag{126}$$

and

$$\frac{b+\mu}{b+\cos\beta}\sin^2\beta = 1 - \mu\cos\beta - \frac{x\eta + y\xi - 4\xi\eta}{x\eta - y\xi}(\mu - \cos\beta \text{ling} \tag{127}$$

Using these formulae in equations (95) and (96), we have

$$S_l(\mu) = \frac{2}{\mu_1^2 \cdots \mu_n^2}\frac{P(-\cos\beta)P(\mu)}{\rho(-\cos\beta)\,\rho(\mu)}\Big[1 - \mu\cos\beta + \frac{x\eta + y\xi - xy}{x\eta - y\xi}(\mu - \cos\beta)\Big]\frac{1}{1 - \mu\sec\beta}, \tag{128}$$

and

$$S_r(\mu) = \frac{1}{\mu_1^2 \cdots \mu_n^2}\frac{P(-\cos\beta)P(\mu)}{R(-\cos\beta)R(\mu)}\Big[1 - \mu\cos\beta - \frac{x\eta + y\xi - 4\xi\eta}{x\eta - y\xi}(\mu - \cos\beta)\Big]\frac{1}{1 - \mu\sec\beta}. \tag{129}$$

Now, using our definitions of x, y, ξ, and η, we readily verify that

$$\frac{x\eta + y\xi}{x\eta - y\xi} = \frac{R(-1)\,\rho(1) + R(1)\,\rho(-1)}{R(-1)\,\rho(1) - R(1)\,\rho(-1)} = c \text{ (say)}, \tag{130}$$[15]

$$\frac{xy}{x\eta - y\xi} = \frac{\rho(-\cos\beta)}{R(-\cos\beta)}\frac{\rho(1)\,\rho(-1)}{R(-1)\,\rho(1) - R(1)\,\rho(-1)}, \tag{131}$$

and

$$\frac{4\xi\eta}{x\eta - y\xi} = \frac{R(-\cos\beta)}{\rho(-\cos\beta)}\frac{4R(1)R(-1)}{R(-1)\,\rho(1) - R(1)\,\rho(-1)}. \tag{132}$$

[15] It may be further verified that this is the same as the quantity $(\alpha a - \beta b)/(ab - \beta a)$, which has already occurred in our analysis in Paper X (eq. [167]).

can be shown that

$$R(1)R(-1) = -\tfrac{1}{2}\rho(1)\,\rho(-1). \tag{133}$$ [16]

in terms of the quantity

$$q = \frac{2\rho(1)\,\rho(-1)}{R(-1)\,\rho(1) - R(1)\,\rho(-1)}, \tag{134}$$ [17]

we can write

$$\frac{xy}{x\eta - y\xi} = \tfrac{1}{2}q\,\frac{\rho(-\cos\beta)}{R(-\cos\beta)} \tag{135}$$

and

$$\frac{4\xi\eta}{x\eta - y\xi} = -q\,\frac{R(-\cos\beta)}{\rho(-\cos\beta)}. \tag{136}$$

In terms of c and q we can re-write equations (128) and (129) in the forms

$$S(\mu) = \frac{1}{\mu_1^2 \ldots \mu_n^2}\,\frac{P(\mu)}{\rho(\mu)}\left\{2\,\frac{P(-\cos\beta)}{\rho(-\cos\beta)}\,[\,1 - \mu\cos\beta + c\,(\mu - \cos\beta)\,] - q\,\frac{P(-\cos\beta)}{R(-\cos\beta)}\,(\mu - \cos\beta)\right\}\frac{1}{1 - \mu\sec\beta} \tag{137}$$

[16] This rela[illegible]ollows, for example, from the identities

$$1 - \tfrac{3}{4}\sum_{j=1}^{n}\frac{a_j(1-\mu_j^2)}{1-\mu_j^2 x} \equiv (-1)^n\mu_1^2 \ldots \mu_n^2\,\frac{\prod_{a=1}^{n}(x - k_a^2)}{\prod_{j=1}^{n}(1-\mu_j^2 x)}$$

and

$$1 - \tfrac{3}{2}\sum_{j=1}^{n}\frac{a_j(1-\mu_j^2)}{1-\mu_j^2 x} \equiv (-1)^n\mu_1^2 \ldots \mu_n^2\,\frac{x\prod_{\beta=1}^{n-1}(x - \kappa_\beta^2)}{\prod_{j=1}^{n}(1-\mu_j^2 x)},$$

which can be readily established (cf. Paper VIII, eqs. [41] – [46]). Thus putting $x = 1$ in these identities, we find that

$$(-1)^n\mu_1^2 \ldots \mu_n^2\,\frac{R(1)\,R(-1)}{\prod_{j=1}^{n}(1-\mu_j^2)} = \tfrac{1}{4}$$

and

$$(-1)^n\mu_1^2 \ldots \mu_n^2\,\frac{\rho(1)\,\rho(-1)}{\prod_{j=1}^{n}(1-\mu_j^2)} = -\tfrac{1}{2},$$

from which the relation in question follows immediately.

[17] Again, it may be verified that this is the same as the quantity $(a^2 - b^2)/(ab - \beta a)$, which occurred in Paper X (eq. [168]).

and

$$S_r(\mu) = \frac{1}{\mu_1^2 \ldots \mu_n^2} \frac{P(\mu)}{R(\mu)} \left\{ \frac{P(-\cos\beta)}{R(-\cos\beta)} [1 - \mu\cos\beta - c(\mu - \cos\beta)] - q \frac{P(-\cos\beta)}{\rho(-\cos\beta)} (\mu - \cos\beta) \right\} \frac{1}{1 - \mu\sec\beta}, \tag{138}$$

which are the required expressions for $S_l(\mu)$ and $S_r(\mu)$.

According to equation (90), we can now express the angular distributions $I_l^{(0)}(0, \mu)$ and $I_r^{(0)}(0, \mu)$ in the forms

$$I_l^{(0)}(0, \mu) = {}_3^3F\{2H_l(\cos\beta) H_l(\mu) [1 + \mu\cos\beta - c(\mu + \cos\beta)] + qH_r(\cos\beta) H_l(\mu)(\mu + \cos\beta)\} \frac{\cos\beta}{\cos\beta + \mu} \tag{139}$$

and

$$I_r^{(0)}(0, \mu) = {}_3^3F\{H_r(\cos\beta) H_r(\mu) [1 + \mu\cos\beta + c(\mu + \cos\beta)] + qH_l(\cos\beta) H_r(\mu)(\mu + \cos\beta)\} \frac{\cos\beta}{\cos\beta + \mu}, \tag{140}$$

where we have introduced the functions $H_l(\mu)$ and $H_r(\mu)$, defined accor[illegible] to

$$H_l(\mu) = \frac{(-1)^n}{\mu_1 \ldots \mu_n} \frac{P(-\mu)}{\rho(-\mu)} = \frac{1}{\mu_1 \ldots \mu_n} \frac{\prod_{i=1}^{n} (\mu + \mu_i)}{\prod_{\beta=1}^{n-1} (1 + \kappa_\beta \mu)} \tag{141}$$

and

$$H_r(\mu) = \frac{(-1)^n}{\mu_1 \ldots \mu_n} \frac{P(-\mu)}{R(-\mu)} = \frac{1}{\mu_1 \ldots \mu_n} \frac{\prod_{i=1}^{n} (\mu + \mu_i)}{\prod_{a=1}^{n} (1 + k_a \mu)}. \tag{142}$$

This completes the solution of system (I).

7. *The solution of the equations for* $I_l^{(1)}$ *and* $U^{(1)}$.—Considering, next, the equations of the second system (p. 119), we first observe that there must exist a simple proportionality between the functions $I_l^{(1)}(\tau, \mu)$ and $U^{(1)}(\tau, \mu)$. For, from the two equations belonging to this system, it immediately follows that

$$\mu \frac{d}{d\tau} [I_l^{(1)} - \mu U^{(1)}] = I_l^{(1)} - \mu U^{(1)}. \tag{143}$$

The boundedness of the solutions for $\tau \to \infty$ now requires that

$$I_l^{(1)}(\tau, \mu) \equiv \mu U^{(1)}(\tau, \mu). \tag{144}$$

Using this identity in the equation for $U^{(1)}$, we find

$$\left.\begin{aligned}\mu\frac{dU^{(1)}}{d\tau} = U^{(1)} - \tfrac{3}{8}(1-\mu^2)^{\frac{1}{2}}\int_{-1}^{+1} U^{(1)}(\tau,\mu')(1-\mu'^2)^{\frac{1}{2}}(1+2\mu'^2)\,a\,\mu \\ + \tfrac{3}{8}Fe^{-\tau\sec\beta}(1-\mu^2)^{\frac{1}{2}}\sin\beta\cos\beta\,.\end{aligned}\right\} \quad (145)$$

Now, writing

$$U^{(1)}(\tau,\mu) = \tfrac{3}{8}F(1-\mu^2)^{\frac{1}{2}}\sin\beta\cos\beta\;\phi(\tau,\mu)\,, \quad (146)$$

we obtain for ϕ the integrodifferential equation

$$\mu\frac{d\phi}{d\tau} = \phi - \frac{3}{8}\int_{-1}^{+1}\phi(\tau,\mu')(1-\mu'^2)(1+2\mu'^2)\,d\mu' + e^{-\tau\sec\beta}\,. \quad (147)$$

Equation (147) can be solved in a general nth approximation by following a procedure exactly similar to that described for the solution of a class of integrodifferential equations in Paper IX, § 4. In our present context, we are, however, most interested only in the angular distribution of ϕ at $\tau = 0$. For this we have (cf. Paper IX, eq. [136])

$$\phi(0,\mu) = -H^{(1)}(\cos\beta)\,H^{(1)}(\mu)\frac{\cos\beta}{\cos\beta+\mu}\,, \quad (148)$$

where, in the nth approximation,

$$H^{(1)}(\mu) = \frac{1}{\mu_1\ldots\mu_n}\frac{\prod_{i=1}^{n}(\mu+\mu_i)}{\prod_{\alpha=1}^{n}(1+k_\alpha^{(1)}\mu)}\,, \quad (149)$$

the $k_\alpha^{(1)}$'s being the n positive roots of the characteristic equation (cf. Paper X, eq. [117])

$$1 = \frac{3}{4}\sum_{j=1}^{n}\frac{a_j(1-\mu_j^2)(1+2\mu_j^2)}{1-\mu_j^2k^2}\,. \quad (150)$$

For the angular distributions $I_l^{(1)}(0,\mu)$ and $U^{(1)}(0,\mu)$ we therefore have

$$I_l^{(1)}(0,\mu) = -\tfrac{3}{8}F\mu(1-\mu^2)^{\frac{1}{2}}\sin\beta\cos\beta\,H^{(1)}(\cos\beta)\,H^{(1)}(\mu)\frac{\cos\beta}{\cos\beta+\mu} \quad (151)$$

and

$$U^{(1)}(0,\mu) = -\tfrac{3}{8}F(1-\mu^2)^{\frac{1}{2}}\sin\beta\cos\beta\,H^{(1)}(\cos\beta)\,H^{(1)}(\mu)\frac{\cos\beta}{\cos\beta+\mu}\,. \quad (152)$$

8. *The solution of the equations for* $I_l^{(2)}$, $I_l^{(2)}$, *and* $U^{(2)}$.—As in the case of system (II), a simple inspection of the three equations belonging to the third system (p. 119) shows that we must identically require

$$I_l^{(2)}(\tau,\mu) \equiv -\mu^2 I_r^{(2)}(\tau,\mu) \quad (153)$$

and

$$U^{(2)}(\tau,\mu) \equiv -2\mu I_r^{(2)}(\tau,\mu)\,. \quad (154)$$

Using these identities in the equation for $I_r^{(2)}$, we obtain

$$\mu \frac{dI_r^{(2)}}{d\tau} = I_r^{(2)} - \frac{3}{16}\int_{-1}^{+1} I_r^{(2)}(\tau, \mu')(1+\mu'^2)^2 d\mu' - \tfrac{3}{8}\sqrt{2}Fe^{-\tau\sec\beta}\sin^2\beta\,. \quad (155)$$

Equation (155) can again be solved quite readily by our standard procedures. In the nth approximation the characteristic equation is

$$1 = \frac{3}{8}\sum_{j=1}^{n} \frac{a_j(1+\mu_j^2)^2}{1-\mu_j^2 k^2}; \quad (156)$$

and the solution for the angular distributions of the various functions at $\tau = 0$ can all be expressed in terms of the function

$$H^{(2)}(\mu) = \frac{1}{\mu_1 \cdot \cdots \cdot \mu_n} \frac{\prod_{i=1}^{n}(\mu+\mu_i)}{\prod_{\alpha=1}^{n}(1+k_\alpha^{(2)}\mu)}, \quad (157)$$

where the $k_\alpha^{(2)}$'s are the n positive characteristic roots. Thus,

$$I_l^{(2)}(0, \mu) = -\tfrac{3}{8}\sqrt{2}F\mu^2\sin^2\beta\, H^{(2)}(\cos\beta)\, H^{(2)}(\mu)\frac{\cos\beta}{\cos\beta+\mu} \quad (158)$$

and

$$I_r^{(2)}(0, \mu) = +\tfrac{3}{8}\sqrt{2}F\sin^2\beta\, H^{(2)}(\cos\beta)\, H^{(2)}(\mu)\frac{\cos\beta}{\cos\beta+\mu} \quad (159)$$

and

$$U^{(2)}(0, \mu) = -\tfrac{3}{16}F\mu\sin^2\beta\, H^{(2)}(\cos\beta)\, H^{(2)}(\mu)\frac{\cos\beta}{\cos\beta+\mu}. \quad (160)$$

9. *The polarization and the angular distribution of the reflected radiation: tables of the necessary functions.*—Combining the solutions (139), (140), (151), (152), and (158)–(160) in accordance with equations (59)–(61), we obtain the equations which determine the polarization and the angular distribution of the radiation diffusely reflected by a semi-infinite plane-parallel atmosphere. We have

$$\left.\begin{aligned} I_l(0, \mu) = {} & \tfrac{3}{8}\sqrt{2}F\{2H_l(\mu)H_l(\mu')[1+\mu\mu'-c(\mu+\mu')] \\ & + qH_l(\mu)H_r(\mu')(\mu+\mu') - 4\mu\mu'(1-\mu^2)^{\frac{1}{2}}(1-\mu'^2)^{\frac{1}{2}}H^{(1)}(\mu)\,H^{(1)}(\mu')\cos\varphi \\ & - \mu^2(1-\mu'^2)\,H^{(2)}(\mu)\,H^{(2)}(\mu')\cos 2\varphi\}\frac{\mu'}{\mu+\mu'}, \end{aligned}\right\} \quad (161)$$

$$\left.\begin{aligned} I_r(0, \mu) = {} & \tfrac{3}{8}\sqrt{2}F\{H_r(\mu)H_r(\mu')[1+\mu\mu'+c(\mu+\mu')] \\ & + qH_r(\mu)\,H_l(\mu')(\mu+\mu') + (1-\mu'^2)\,H^{(2)}(\mu)\,H^{(2)}(\mu')\cos 2\varphi\}\frac{\mu'}{\mu+\mu'}, \end{aligned}\right\} \quad (162)$$

and

$$\left.\begin{aligned} U(0, \mu) = {} & -\tfrac{3}{16}F\{2(1-\mu^2)^{\frac{1}{2}}(1-\mu'^2)^{\frac{1}{2}}\mu' H^{(1)}(\mu)\,H^{(1)}(\mu')\sin\varphi \\ & + \mu(1-\mu'^2)\,H^{(2)}(\mu)\,H^{(2)}(\mu')\sin 2\varphi\}\frac{\mu'}{\mu+\mu'}, \end{aligned}\right\} \quad (163)$$

where we have written μ' for $\cos\beta$.

In Table 1 we have collected the various constants which occur in the foregoing solution in the second and the third approximations. In Tables 2 and 3 the functions $H_l(\mu)$,

TABLE 1

THE CONSTANTS OCCURRING IN THE SOLUTION FOR THE DIFFUSELY REFLECTED RADIATION

Second Approximation	Third Approximation
$k_1=2.23607$	$k_1=3.45859$
$k_2=1.08012$	$k_2=1.32757$
	$k_3=1.04677$
$\kappa_1=1.52753$	$\kappa_1=2.71838$
	$\kappa_2=1.11822$
$c=0.86830$	$c=0.87134$
$q=0.70151$	$q=0.69392$
$k_1^{(1)}=2.08921$	$k_1^{(1)}=3.39756$
$k_2^{(1)}=0.89547$	$k_2^{(1)}=1.20271$
	$k_3^{(1)}=0.91108$
$k_1^{(2)}=2.50512$	$k_1^{(2)}=3.78851$
$k_2^{(2)}=0.74680$	$k_2^{(2)}=1.32582$
	$k_3^{(2)}=0.74119$

TABLE 2

THE FUNCTIONS $H_l(\mu)$, $H_r(\mu)$, $H^{(1)}(\mu)$, AND $H^{(2)}(\mu)$ IN THE SECOND APPROXIMATION

μ	SECOND APPROXIMATION			
	H_l	H_r	$H^{(1)}$	$H^{(2)}$
0	1.000	1.000	1.000	1.000
0.10	1.253	1.065	1.097	1.075
0.20	1.499	1.112	1.171	1.134
0.30	1.741	1.147	1.230	1.184
0.40	1.979	1.175	1.278	1.226
0.50	2.214	1.197	1.319	1.262
0.60	2.448	1.216	1.354	1.294
0.70	2.680	1.231	1.384	1.323
0.80	2.911	1.244	1.411	1.348
0.90	3.141	1.256	1.434	1.371
1.00	3.370	1.265	1.455	1.391

$H_r(\mu)$, $H^{(1)}(\mu)$, and $H^{(2)}(\mu)$ are all tabulated in the second and the third approximations.[18]

An inspection of these tables reveals that the accuracy of the third approximation is probably within 1 per cent over the entire range in which the functions are defined.

TABLE 3

THE FUNCTIONS $H_l(\mu)$, $H_r(\mu)$, $H^{(1)}(\mu)$, AND $H^{(2)}(\mu)$ IN THE THIRD APPROXIMATION

μ	THIRD APPROXIMATION			
	H_l	H_r	$H^{(1)}$	$H^{(2)}$
0	1.000	1.000	1.000	1.000
0.05	1.143	1.041	1.057	1.042
0.10	1.279	1.074	1.105	1.078
0.15	1.411	1.101	1.145	1.110
0.20	1.539	1.123	1.180	1.139
0.25	1.665	1.142	1.212	1.165
0.30	1.789	1.158	1.240	1.188
0.35	1.911	1.173	1.265	1.210
0.40	2.032	1.186	1.288	1.230
0.45	2.152	1.197	1.308	1.249
0.50	2.270	1.207	1.328	1.266
0.55	2.389	1.216	1.345	1.282
0.60	2.506	1.225	1.362	1.298
0.65	2.623	1.233	1.377	1.312
0.70	2.739	1.240	1.391	1.326
0.75	2.856	1.246	1.404	1.338
0.80	2.971	1.252	1.417	1.351
0.85	3.087	1.258	1.429	1.362
0.90	3.202	1.263	1.440	1.373
0.95	3.317	1.268	1.450	1.384
1.00	3.431	1.272	1.460	1.394

As stated in the introduction, applications of the theory developed in this paper to an interpretation of Lyot's polarization measurements on the planets will be found in a forthcoming paper.

[18] I am indebted to Mrs. Frances H. Breen for assistance with these calculations.

CURVE OF GROWTH OF γ CYGNI*

JORGE SAHADE AND CARLOS U. CESCO
Yerkes and McDonald Observatories
Received April 23, 1946

ABSTRACT

The curve of growth of γ Cygni from one coudé spectrogram covering the region $\lambda\lambda$ 4029–4755 indicates for *Fe* I, an excitation temperature of 4600° and a turbulent velocity of 7.5 km/sec.

In connection with a general investigation of high-dispersion spectra of supergiants, a coudé plate (Cd 435; dispersion 3.8 A/mm at λ 4405) of γ Cygni (SP F8I*b*[1]) was taken on May 28, 1943, by Dr. W. A. Hiltner with the 82-inch reflecting telescope of the McDonald Observatory. The exposure time was 113 minutes on Eastman 103*a*-0 emulsion. The spectrogram, covering the region $\lambda\lambda$ 4029–4755, was calibrated by means of a wedge slit, and tracings were made by Hiltner with the direct-intensity microphotometer of the University of Michigan. For the determination of the curve of growth of γ Cygni this material was turned over to the writers.

The identification of the stellar lines on the tracings was made with the help of Roach's[2] list of wave lengths for γ Cygni and Dunham's[3] list for α Persei. The latter was used for the lines in the region $\lambda\lambda$ 4405–4754. Equivalent widths were determined for all lines which are practically unblended, by measuring with a planimeter the areas between their profiles and the continuum. These measurements were made independently by both writers, and the means of the two measures were used in this paper. The results, listed in Table 1, have been arranged according to the increasing atomic number of the elements. Some of the values for the excitation potential of the lower level of the line considered, namely, those with two decimal figures, were taken from Miss Moore's *Revised Multiplet Table*,[4] which was also used to check a few of the identifications.

The great majority of the lines correspond to *Fe* I. In the usual way, we plotted log W/λ against log X_r using Menzel and Goldberg's solar log X_0' values, for different assumed excitation temperatures, namely, 5600°, 4800°, 4600°, 4400°, and 4200°. The least scatter of points was that obtained for 4600°, a value which agrees with the temperature usually assigned to supergiants of type F. An excitation temperature of 4400° had been found previously[5] for γ Cygni from the *Fe* I lines.

Figure 1 shows our plot and the theoretical curve of growth computed with the expressions given by Menzel.[6] This theoretical curve agrees fairly well with the empirical curve suggested by the plotted points for *Fe* I. The vertical shift necessary for the superposition of the two curves gives $v = 7.6$ km/sec, which implies a turbulent velocity of 7.5 km/sec, if we remove the contribution of the thermal motion which corresponds to the effective temperature of the star, namely, 5500°, according to Kuiper.[7] The values corresponding to the other neutral elements were fitted to the theoretical curve after shifts, arbitrary for each element, had been made along the log X_0 axis.

* *Contributions from the McDonald Observatory, University of Texas*, No. 123.

[1] Morgan, Keenan, and Kellman, *An Atlas of Stellar Spectra*, Chicago: University of Chicago Press, 1943.

[2] *Ap. J.*, **96**, 272, 1942; *McDonald Contr.*, No. 57.

[3] *Contr. Princeton U. Obs.*, No. 9, 1929.

[4] *Contr. Princeton U. Obs.*, No. 20, 1945.

[5] K. O. Wright, *Pub. A.A.S.*, **10**, 338, 1944.

[6] *Ap. J.*, **84**, 462, 1936.

[7] *Ap. J.*, **88**, 429, 1938.

TABLE 1

EQUIVALENT WIDTHS IN THE SPECTRUM OF γ CYGNI

λ	Lower E.P.	$-\log W/\lambda$
	Mg I	
4167.26	4.327	4.14
4571.09	0.000	4.29
4702.97	4.327	4.03
	Ca I	
4094.96	2.512	4.25
4283.03	1.878	4.12
4302.55	1.891	3.97
4318.67	1.891	4.01
4425.45	1.871	4.15
4455.89	1.891	4.15
4578.56	2.510	4.42
4585.92	2.515	4.24
	Sc II	
4374.40	0.616	3.80
4400.46	0.603	3.74
4415.49	0.593	3.95
4420.63	0.616	4.20
4431.37	0.603	4.24
	Ti I	
4287.44	0.832	4.48
4453.31	1.424	4.53
4465.81	1.732	4.67
4512.79	0.832	4.69
4533.16	0.845	4.12
4534.81	0.832	4.31
4617.26	1.741	4.67
4623.09	1.732	4.80
	Ti II	
4056.22	0.605	3.97
4163.63	2.579	3.93
4287.95	1.075	3.90
4290.29	1.160	3.89
4301.95	1.156	3.86
4312.86	1.175	3.89
4316.80	2.039	4.03
4330.24	2.039	3.92
4330.71	1.175	3.92
4337.88	1.075	3.65
4350.88	2.052	3.99
4386.79	2.586	3.95
4394.05	1.216	3.98
4395.02	1.079	3.81
4395.86	1.238	3.96
4399.76	1.230	3.83
4411.94	1.219	4.01
4417.71	1.160	3.82
4418.34	1.232	3.89
4421.95	2.052	4.06
4443.81	1.075	3.80
4444.55	1.111	3.94
4450.49	1.079	3.89
4464.50	1.156	3.89
4468.49	1.126	3.84
4470.84	1.160	3.85
4488.30	3.110	4.16
4493.53	1.075	4.25
4501.29	1.111	3.99
4506.75	1.126	4.38
4524.72	1.226	4.10
4529.49	1.565	3.98
4544.02	1.238	4.10
4568.30	1.219	4.17
4589.96	1.232	3.98
4636.35	1.160	4.29
4708.73	1.232	3.97
	V I	
4379.24	0.299	4.39
4389.98	0.274	4.33
4406.72	0.299	4.50
4577.13	0.000	4.86
	V II	
4035.63	1.785	4.00
4036.77	1.470	4.21
4234.24	1.68	4.29
	Cr I	
4254.34	0.000	3.94
4274.77	0.000	3.90
4371.31	0.999	4.24
4500.40	3.07	4.38
4545.97	0.937	4.42
4591.33	0.964	4.39
4600.85	0.999	4.29
4626.07	0.964	4.29
4646.19	1.026	4.10
4651.29	0.979	4.44
4652.19	0.999	4.31
4665.81	3.54	4.46
4718.41	3.181	4.58

Ti II—*Continued*

TABLE 1—*Continued*

λ	Lower E.P.	−log W/λ
	Cr II	
4252.58	3.842	4.08
4261.91	3.848	3.98
4555.00	4.054	4.08
4558.66	4.056	3.91
4588.18	4.054	3.98
4592.01	4.057	4.04
4616.66	4.055	4.06
4634.08	4.055	4.07
	Mn I	
4034.48	0.000	3.95
4055.55	2.133	4.25
4059.40	3.060	4.84
4265.89	2.928	4.71
4502.25	2.907	4.90
4754.03	2.272	4.27
	Fe I	
4043.92	2.716	4.16
4044.60	2.819	4.11
4047.22	2.269	4.57
4052.55	3.034	4.05
4059.74	3.53	4.36
4062.43	2.833	3.98
4065.39	3.415	4.32
4067.02	2.819	3.95
4067.98	3.197	4.09
4074.77	3.034	4.16
4076.69	3.197	3.97
4080.91	3.28	4.55
4082.12	3.402	4.42
4083.65	3.402	4.05
4084.49	3.318	4.14
4085.03	2.833	4.20
4089.24	2.936	4.37
4091.57	2.819	4.44
4097.08	3.269	4.09
4098.17	3.227	3.96
4109.83	2.833	3.87
4112.36	3.382	4.47
4112.99	4.16	4.21
4114.47	2.819	4.26
4117.00	3.227	4.51
4118.58	3.56	3.86
4120.22	2.98	4.32
4121.82	2.819	4.19
4125.64	4.20	4.28
4126.21	3.318	4.25
4132.09	1.601	3.93
4132.92	1.601	4.14
4134.65	2.819	4.09
4136.52	3.354	4.53
4136.99	3.40	4.14
4139.92	0.986	4.43
4143.88	1.551	3.94
4147.67	1.478	4.11
4150.26	3.415	4.20
4153.92	3.382	4.06
4154.50	2.819	4.04
4154.78	3.354	4.21
4156.78	3.819	4.11
4157.76	3.402	4.17
4158.81	3.415	4.24
4168.97	3.40	4.59
4169.84	3.382	4.19
4170.93	3.004	4.08
4174.91	0.911	4.20
4175.64	2.833	4.06
4181.75	2.819	3.97
4182.38	3.004	4.26
4184.91	2.819	4.18
4187.05	2.439	3.83
4191.49	2.458	3.90
4196.26	3.382	4.14
4198.21	2.389	3.80
4200.01	0.087	4.49
4200.93	3.382	4.23
4206.70	0.051	4.08
4208.61	3.382	4.10
4213.62	2.83	4.28
4216.17	0.000	4.09
4220.33	3.06	4.16
4222.20	2.439	3.99
4224.19	3.354	4.01
4225.95	3.034	4.32
4227.41	3.318	3.77
4230.55	3.004	5.15
4233.56	2.471	4.00
4238.03	3.402	4.23
4238.81	3.382	4.09
4245.38	2.846	4.21
4245.99	3.26	4.18
4248.24	3.058	4.21
4250.78	1.551	3.91
4255.49	3.00	4.57
4260.51	2.389	3.88
4264.23	3.354	4.36
4264.81	3.943	4.66
4265.22	3.912	4.53
4266.97	2.716	4.31
4276.73	3.865	4.45
4291.50	0.051	4.27
4298.06	3.03	4.33
4346.54	3.29	4.15
4347.80	3.587	4.32
4352.72	2.213	4.07
4365.88	2.977	4.65
4369.78	3.03	4.12
4375.93	0.000	4.05
4383.52	1.478	3.81
4387.91	3.06	4.20
4388.42	3.59	4.22

TABLE 1—*Continued*

λ	Lower E.P.	−log W/λ
	Fe I—*Continued*	
4389.25	0.051	4.41
4392.60	3.865	4.75
4404.76	1.551	3.84
4408.46	2.188	3.97
4415.16	1.601	3.80
4427.29	0.051	3.91
4430.61	2.213	4.08
4432.65	3.56	4.53
4433.20	3.005	4.23
4436.91	3.03	4.63
4438.40	3.671	4.58
4442.38	2.188	4.02
4447.76	2.213	4.15
4454.47	2.819	3.83
4466.56	2.819	4.05
4476.05	2.833	4.11
4482.83	3.638	4.54
4525.12	5.39	4.08
4528.62	2.167	3.94
4547.89	3.53	4.40
4587.13	3.56	4.62
4598.05	3.269	4.15
4601.98	1.601	4.49
4602.97	1.478	4.08
4607.63	3.252	4.19
4611.28	0.911	4.17
4625.02	3.227	4.22
4630.11	2.269	4.47
4637.50	3.269	4.23
4638.03	3.59	4.40
4643.52	3.64	4.42
4647.41	2.936	4.17
4668.14	3.252	4.17
4678.89	3.59	4.12
4683.54	2.82	4.65
4690.17	3.67	4.58
4691.44	2.977	4.19
4704.91	3.67	4.65
4705.59	3.53	4.65
4721.13	2.977	4.77
4728.50	3.64	4.32
4735.84	4.06	4.68
4736.82	3.197	4.07
4741.62	2.82	4.51
4745.81	4.086	4.42
	Fe II	
4128.78	2.572	3.97
4296.60	2.693	3.91
4303.17	2.693	3.82
4369.43	2.766	4.10
4416.84	2.766	3.93
4489.19	2.816	4.04
4491.43	2.843	4.11
4508.29	2.843	4.04
4515.34	2.832	4.08
4520.23	2.795	4.07
4522.63	2.832	3.77
4555.96	2.816	3.82
4576.36	2.832	3.99
4582.82	2.832	3.84
4601.40	2.879	4.45
4620.53	2.816	4.04
4635.35	5.93	4.41
4663.74	2.879	4.10
4666.75	2.816	3.95
4731.48	2.879	3.98
	Ni I	
4115.99	4.136	4.91
4331.66	1.669	4.21
4605.01	3.465	4.27
4648.74	3.405	4.09
4686.13	3.582	4.58
4703.81	3.592	4.52
4714.41	3.365	4.08
4715.81	3.528	4.40
4732.50	4.088	4.81
	Co I	
4212.33	0.919	4.16
4693.09	3.217	4.95
	V II	
4309.56	0.179	3.85
4682.24	0.407	4.01
	Zr II	
4071.06	0.995	4.31
4090.54	0.754	4.18
4149.24	0.798	3.91
4179.81	1.658	4.43
4209.00	0.710	4.10
4211.88	0.524	4.09
4317.33	0.710	4.26
4333.25	2.40	4.25
4359.68	1.231	4.02
4370.95	1.203	4.21
4414.47	1.231	4.34
4496.95	0.710	4.08
4613.92	0.968	4.33
	La II	
4086.73	0.000	4.08
4123.29	0.320	4.00
4333.75	0.172	3.94
	Sm II	
4467.43	0.66	4.34

In a recent investigation of the curve of growth for α Persei,[8] Wright found that the neutral and ionized elements give curves of growth of different shapes, the one derived from the neutral elements agreeing with the theoretical curve. A similar effect was suspected by us in γ Cygni. Hence a separate plot was made for *Ti* II, for which a large number of lines had been measured. This plot (Fig. 2) gives a curve of growth which agrees approximately with the one for neutral elements after an appropriate horizontal shift. However, a slight difference is possible, because the number of lines was not

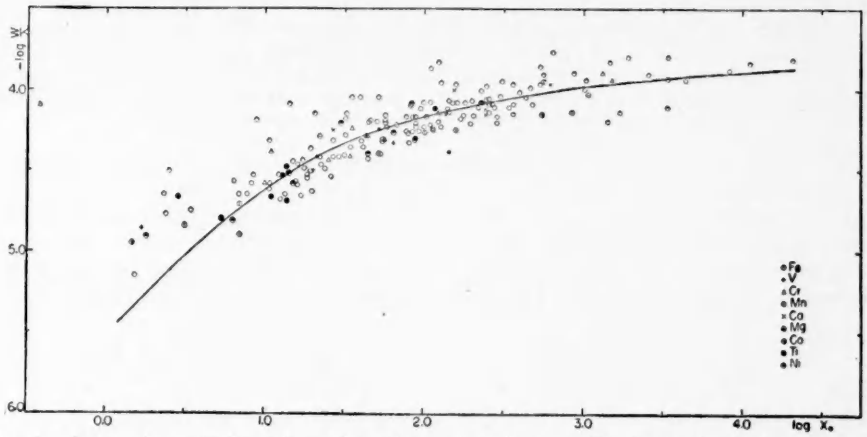

FIG. 1.—Curve of growth for γ Cygni from the neutral elements. The line is the theoretical curve

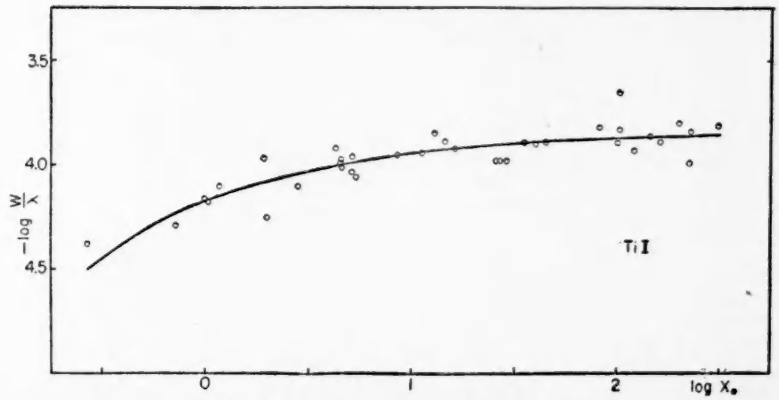

FIG. 2.—Curve of growth from *Ti* II

sufficient for an accurate test. In making the plot for *Ti* II an excitation temperature equal to the one derived for *Fe* I, namely, 4600°, was adopted. Trials, assuming excitation temperatures of 4400° and 5600°, did not show appreciable changes in the shape of the curve.

We are indebted to Dr. O. Struve for suggesting this investigation and for helpful discussions, and to Dr. W. A. Hiltner for allowing us to use his valuable material.

[8] Unpublished. Presented at the New York meeting of the American Astronomical Society, February, 1946.

AN INTERESTING PHENOMENON IN STELLAR SPECTROSCOPY*

OTTO STRUVE
Yerkes Observatory and McDonald Observatory
Received May 20, 1946

ABSTRACT

Measurements of several line contours in δ CMa show that they are produced by turbulent motions of the order of $v_0' = 30$km/sec. This is not consistent with the value of $v_0' = 5.1$ km/sec derived from the conventional curve of growth. It is suggested that v_0' is an increasing function of the equivalent width. This concept requires a far-reaching modification of the theory of curves of growth.

The purpose of this note is to call attention to a remarkable discordance between the result of Miss Steel's recent investigation of the curve of growth of δ Canis Majoris[1] and a direct study of the line contours in this supergiant F8 spectrum. Miss Steel found from a plot of the measured equivalent widths of a considerable number of *Fe* I lines as functions of the relative numbers of absorbing atoms that the most frequent turbulent velocity $v_0 = 4.9$ km/sec and that the effective velocity, consisting of the turbulent and the

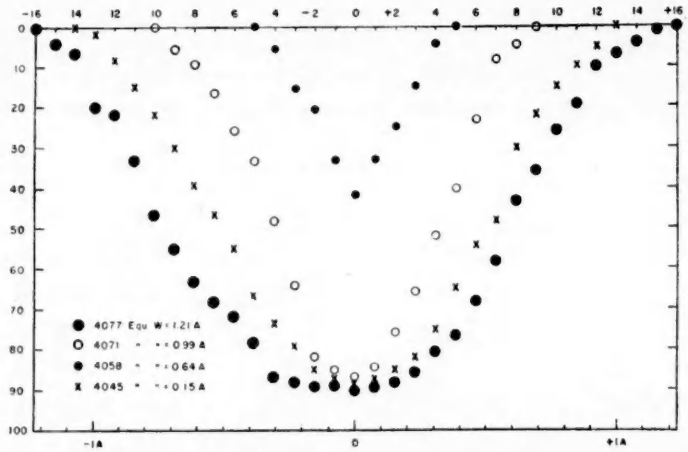

Fig. 1.—Contours of four lines in δ Canis Majoris. The abscissae are given in Angstrom units (*bottom*) and in millimeters on the tracing (*top*).

thermal distributions, is $v_0' = 5.1$ km/sec. There seems to be no doubt that the slope of the curve of growth is consistent only with a value of this order of magnitude. In Figure 1, I have shown several contours measured on a coudé spectrogram of δ CMa having a linear dispersion of 2.3 A/mm at about λ 4060. The original tracing, with its sensitometer marks labeled in magnitudes, is shown in Plate I. Finally, Plate II is a reproduction of the original spectrogram, together with spectrograms of α Persei and α Canis Minoris.

It will be seen from the fainter comparison lines of the *Fe* I arc spectrum and from the fainter absorption lines of α CMi, that the instrumental contour is exceedingly narrow, even when compared to the contours of the faintest absorption lines of δ CMa. Hence

* *Contributions from the McDonald Observatory, University of Texas*, No. 125.

[1] *Ap. J.*, **102**, 429, 1945.

PLATE I

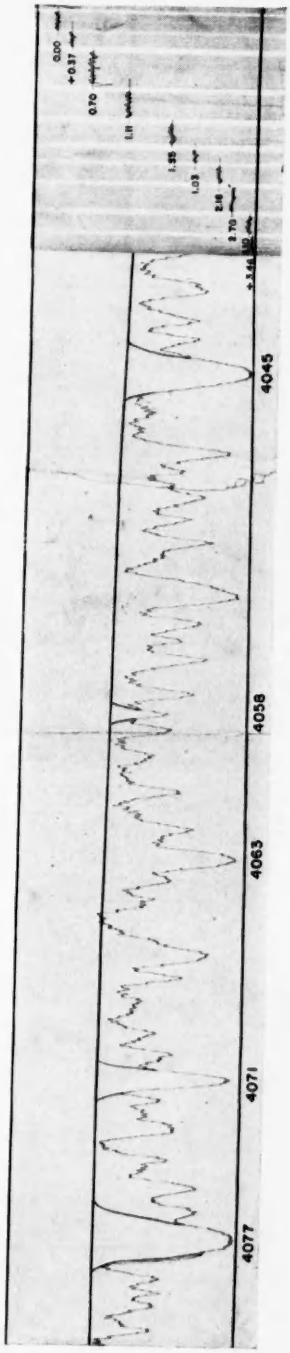

PLATE II

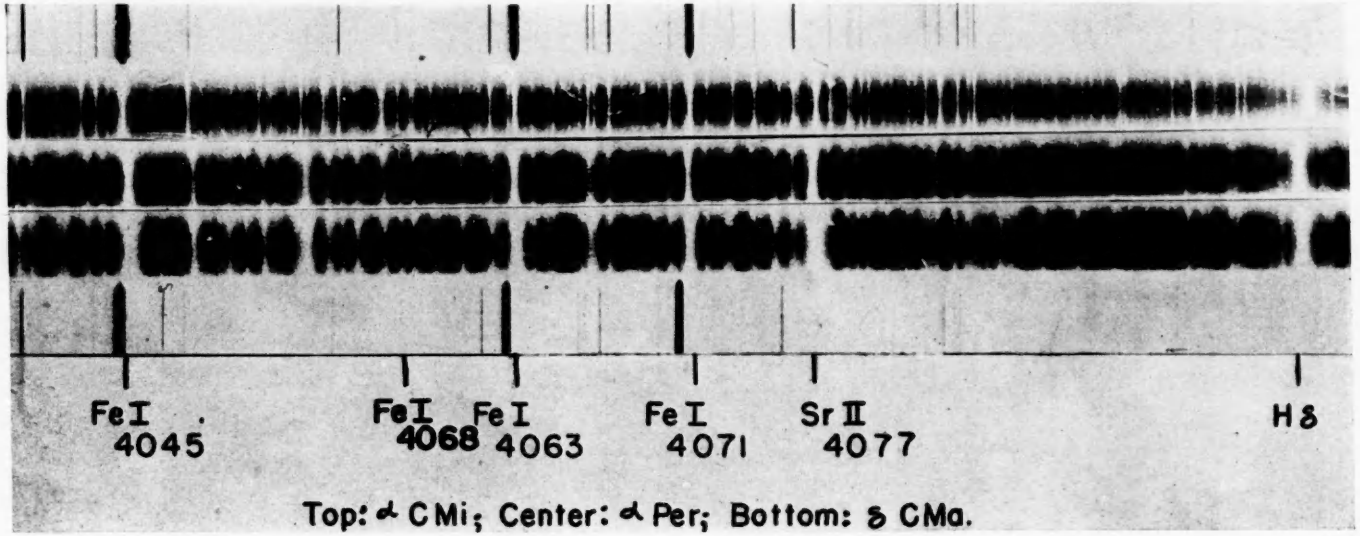

Top: α CMi; Center: α Per; Bottom: δ CMa.

I have not attempted to correct the measured contours in Figure 1. If such corrections had been introduced, the conclusions of this paper would be still further enhanced. From an inspection of Plate II and the two figures we draw the following conclusions:

1. All lines of δ CMa and α Per are appreciably broadened.

2. The character of this broadening is that produced by turbulence and does not resemble broadening by rotation or by other forms of mass-motion which leave the absorption coefficient unaffected.

3. The strongest and broadest lines of δ CMa shown in the region $\lambda\lambda$ 4000–4100 have contours of the type produced by turbulence and show no indication of wings produced by radiation damping or by collisional damping. Such wings have a very characteristic appearance and cannot be missed by an experienced observer. They are, for example, present in the stronger lines of *Fe* I in the spectrum of the sun.

4. The central intensities of the strong lines are so small that saturation is nearly complete, but the faintest lines of δ CMa are certainly not saturated in the centers.

5. We should then expect that the curve of growth of δ CMa would include an appreciable portion of the $A \backsim N$, straight-line section and would extend into the region where A is very little dependent on N. In other words, the curve should show a marked degree of curvature. In reality, no such curvature can be detected in the curve of growth published by Miss Steel.

6. Since we are certain that radiation damping is not effective in producing the observed contours and since this conclusion also agrees with Miss Steel's work, we shall use for the absorption coefficient within the line the expression

$$\kappa = \frac{\sqrt{\pi}\, e^2\lambda^2}{m\, c^2 \Delta\lambda_0} \mathrm{N} f e^{-(\Delta\lambda/\Delta\lambda_0)^2} \approx 10^{-13} \frac{Nf}{\Delta\lambda_0} e^{-(\Delta\lambda/\Delta\lambda_0)^2}.$$

Here the constant

$$\Delta\lambda_0 = \frac{\lambda v_0'}{c} \approx 0.07\mathrm{A}$$

if we use Miss Steel's value $v_0' = 5.1$ km/sec. For the intensity within the line we can use, with ample precision, the expression

$$\frac{I}{I_0} = \left(\frac{1}{\kappa H} + \frac{1}{R_c}\right)^{-1},$$

which was first proposed by Minnaert and later extensively used by Unsöld. It is clear that values of the order of $NHf \approx 10^{12}$ will produce lines whose central intensities are of the order of $0.5\, I_0$. The broader lines of Figure 1 have contours which reach $I = 0.5\, I_0$ at about $\Delta\lambda = 0.7$ A. This would require values[2] of the order of $NHf \approx 10^{55}$ in order to compensate for the extremely small value of

$$e^{-(\Delta\lambda/\Delta\lambda_0)^2} = 4 \times 10^{-44} \qquad \text{at} \qquad \Delta\lambda = 0.7\mathrm{A}\,.$$

Since we are quite certain that such large values of NHf are impossible, we can conclude that the simple theory of the curve of growth does not apply to δ CMa.

7. The contours of the strongest lines suggest a turbulent velocity of the order of $v_0' = 30$ km/sec. This result is not compatible with Miss Steel's curve of growth.

8. A clue to the solution of this problem is presented by the remarkable fact that the fainter lines of δ CMa in Plate II are no wider than the corresponding lines of α Per. But the strong lines of δ CMa are two or three times broader than those of α Per. This

[2] Reference may here be made to the pure Doppler contours illustrated in Fig. 8 of a paper by Struve and Elvey, *Ap.J.*, **79**, 433, 1934; or in Fig. 54*b* of the book by Goldberg and Aller, *Atoms, Stars, and Nebulae*, Philadelphia: Blakiston Co., 1943.

result is physically significant, because in both stars even the faintest perceptible lines are several times broader than the instrumental contours of the faint comparison lines.

9. We can explain this phenomenon by assuming that v_0' is an increasing function of the equivalent width.[3] It is easily shown that for the case of

$$v_0' = a + bA \ ,$$

where A is the equivalent width and a and b are constants, the resulting curve of growth may well be an approximately straight line with a slope intermediate between the $A \sim N$ branch and zero. This seems to be the character of the curve of growth in δ CMa and perhaps also of one or two other supergiants, notably of α Cygni. Since the average equivalent widths of the lines used by Miss Steel was about $A = 0.2$ A, and the strongest lines measured by me are of the order of $A = 1.0$ A, we find $a = -1$ and $b = 31$. The small negative value of a is probably of no physical significance. In order to construct the complete curve of growth we must now think of a family of curves, characterized by different parameters of v_0'. To each observed value of A there corresponds a separate curve. The actual curve of growth must be interpreted as resulting from a series of points located upon these curves at appropriate intervals. The linear approximation is, of course, only an illustration; the observations do not yet suffice to derive the form of the function.

10. It is more difficult to find a physical interpretation of the purely formal assumption made in the preceding paragraph. The degree of turbulence may increase with height in a supergiant stellar atmosphere. Or the distribution of the velocities may, in the first place, not be of the Maxwellian type. For example, the motions may be predominately radial in character, in which case the geometry of the problem will influence the observed distribution.

11. The recognition of the phenomenon described in the preceding sections represents, I believe, an important extension to the theory of turbulence first proposed by Elvey and me in 1934[4] and promises to yield significant results. In this connection it may be pointed out that recent efforts to perfect the theory of the curve of growth over that presented by us in 1934 have remained largely sterile, in view of the enormous discordances which we have found in δ CMa. As long as a curve of growth fails to detect a range of from 5 to 30 km/sec in the turbulent velocity, there is little use in being concerned with the exact mathematical form of the absorption coefficient in the region of transition between Doppler broadening and natural damping. Nor is it important whether we use the Minnaert-Unsöld form of the transfer problem or the pure exponential expression. But I believe that the study of the actual contours has often been seriously neglected. After all, it is useful to realize that the method of curves of growth represents only a necessary, but by no means an entirely satisfactory, means of determining certain properties of the original contours of stellar absorption lines which are not directly measurable because of the finite resolving power of the spectrograph.

I wish to acknowledge that my interest in the problems of curves of growth has been recently revived by the stimulating contributions on this subject by Dr. K. O. Wright, of the Dominion Astrophysical Observatory.

[3] This is analogous to a problem encountered in the discussion of the curves of growth of interstellar lines, where a linear effect due to galactic rotation is superposed upon natural damping and turbulence.

[4] *Ap. J.*, 79, 409, 1934.

THE REFLECTION EFFECT IN ECLIPSING BINARY STARS

PARIS PIŞMIŞ
Princeton University Observatory
Received June 3, 1946

ABSTRACT

Using 24 eclipsing binaries with well-determined elements, it is shown that the differences between the observed reflection effect and that computed for integrated light give a systematic trend with the ratio of luminous efficiencies of the two components. This systematic trend is removed by the application of the bolometric corrections; this result indicates that the mechanism underlying the reflection effect is very probably absorption and re-emission of the incident light.

This paper presents a discussion of the differences between the observed and the theoretically computed "reflection" effects in eclipsing binaries. Eddington[1] for the first time developed a theoretical expression for the "reflection" effect. The application of his formula, however, gave systematically larger values for the reflection effect than for the observed ones. Both Eddington's formula and the more refined expression worked out later by Milne[2] give the total intensity of the reflected (re-radiated) light—that is, the intensity of light integrated over all wave lengths.

If the process of "reflection" is that of absorption and re-emission, the re-emitted light will have a spectral distribution, in general, different from that of the body responsible for the reflection—which may be called the "primary." To a first approximation it may be assumed to be the same as that of the total light of the secondary. Expressed otherwise, the luminous efficiency of the incident radiation will be different from the luminous efficiency of the reflected radiation. But if the process underlying "reflection" is scattering by free electrons of the secondary, the spectral distribution of the re-radiated light will be the same as that of the incident light.

The introduction of the corrections necessary to reduce the reflected light to the spectral range in which the observations are made was first suggested by Kopal.[3] A simplified manner of applying these bolometric corrections is given in a recent paper by H. N. Russell[4] on the assumption of black-body radiation for both components. When these corrections are introduced, Milne's formula gives, for the reflection coefficient,

$$A_1^{\lambda} = 0.347 \left(\frac{E_f}{E_b} L_b r_f^2 - \frac{E_b}{E_f} L_f r_b^2 \right) \sin i \ . \qquad (1)$$

Here r_b, r_f are the radii, L_b, L_f the luminosities, and E_b, E_f the luminous efficiencies of the bright and the faint components, respectively. Obviously, formula (1) with $E_b/E_f = 1$ will give the reflection constant for total radiation:

$$A_1^{T} = 0.347 \, (L_b r_f^2 - L_f r_b^2) \sin i \ . \qquad (2)$$

For the present discussion, 24 eclipsing binaries with well-determined elements are used. These are given in Table 1. Column 1 is self-explanatory; column 2 gives the luminosity of the brighter star, where r_b and r_f are the geometric means of the minor equatorial and polar semi-axes, thus correcting for the ellipticity of the figure; column 5 gives the character of the eclipse and the assumed limb darkening; column 6 gives the observed spectrum of the brighter component and the computed spectrum of the secondary from the ratio of surface brightnesses of the brightened sides of the components (in par-

[1] *M.N.*, **86**, 320, 1926. [2] *M.N.*, **87**, 43, 1927.

[3] *Ap. J.*, **89**, 323, 1939; the numerical coefficient of the exponential in formulae (2) in this article should read "0.92" in place of "0.15."

[4] *Ap. J.*, **102**, 1, 1945.

entheses); column 7 gives the reflection effect observed in the light-curve, that is, twice the coefficient A_1 in the expression

$$l = A_0 - A_1 \cos\theta + A_2 \cos 2\theta .$$

With these data the reflection effect for the listed stars is computed. The results appear in Table 2. Column 2 gives the reflection effect for integrated light (using formula

TABLE 1

(1) Star	(2) L_b	(3) r_b	(4) r_f	(5) Eclipse	(6) Sp b	(6) Sp f	(7) $2A_1$	(8) E_b/E_f	(9) Authority
R CMa...	0.936	0.268	0.248	Partial u.	F0	(dK1)	0.013	0.53	F. B. Wood; to appear shortly as a *Princeton Contr.*
RW CrB ...	.972	.395	.235	Partial d.	F0	(dK4)	.026	0.63	Pierce, *Princeton Contr.*, No. 18
ZZ Aur....	.978	.437	.299	Ann. d.	A7	(dK1)	.020	0.73	Pierce, *A. J.*, No. 1086
Z Dra....	.911	.212	.264	Partial u.	A5	(dK2)	.032	0.74	Dugan, *Princeton Contr.*, No. 2
RT Per....	.863	.274	.274	Partial u.	F2	(dK0)	.022	0.76	Dugan, *Princeton Contr.*, No. 1
TW And ...	.829	.160	.236	Total d.	A5	(dG8)	.005	0.84	Dugan, *Princeton Contr.*, No. 14
δ Lib.....	.917	.291	.302	Partial d.	A0	(dG3)	.046	0.87	
		.273	.296	Partial ½d.		(dG3)	.....	0.89	Krat, *NNVS*, **4**, 236, 1933; **4**, 281, 1933.
		.257	.289	Partial u.		(dG2)	.....	0.86	
		.288	.312	Partial u.		(dG2)	.....	0.94	Stebbins, *Washburn Pub.* Vol. 15
TT Her....	.990	.442	.238	Partial d.	A0	(dK1)	.020	0.96	Baldwin, *A. J.*, No. 1101
X Tri	.867	.255	.292	Total ⅓d.	A3	(dG5)	.018	1.01	Dugan, *Princeton Contr.*, No. 8
RV Oph ...	.825	.126	.202	Total u.	A2	(dG6)	.036	1.04	Dugan, *Princeton Contr.*, No. 4
β Per....	.925	.207	.244	Partial u.	B8	(dG5)	.030	1.12	Stebbins, *Ap. J.*, **53**, 105, 1921
SZ Her....	.800	.314	.327	Partial u.	A3	(F7)	.030	1.14	Dugan, *Princeton Contr.*, No. 6
U Cep....	.838	.193	.311	Total ⅓d.	A0	(dG5)	.043	1.17	Dugan, *Princeton Contr.*, No. 5
RZ Cas....	.877	.223	.290	Partial u.	A2	(dG7)	.057	1.24	Dugan, *Princeton Contr.*, No. 4
		.272	.285	Partial d.		(dG5)	.....	1.30	
W UMi...	.890	.352	.307	Partial d.	A0	(F7)	.038	1.32	Dugan, *Princeton Contr.*, No. 10
		.410	.298	Gr. ann. d.		(F5)	.....	1.34	
μ′ Sco....	.568	.303	.336	Partial u.	B3	(B5)	.035	1.36	Rudnick and Elvey, *Ap. J.*, **87**, 533, 1938
VV Ori....	.888	.353	.173	Annular u.	B2	(B5)	.028	1.41	Wood, to appear shortly as a *Princeton Contr.*
		.365	.169	.4d		(B5)	.....	1.40	
TT Aur....	.66	.30	.25	Gr. ann. u.	B3	(B4)	.050	1.42	Joy and Sitterly, *Ap. J.*, **73**, 77, 1931.
U Oph ...	.637	.299	.245	Gr. ann. u.	B8	(dG4)	.013	1.46	Shapley, *Princeton Contr.*, No. 3
TV Cas....	.859	.278	.293	Partial u.	B9	(F5)	.074	1.48	McDiarmid, *Princeton Contr.*, No. 7
GO Cyg ...	.940	.437	.248	Partial d.	B9n	(F5)	.056	1.59	Pierce, *A. J.*, No. 1112
u Her....	.713	.282	.282	Partial u.	B3	(B7)	.018	1.63	Baker, *L.O.B.*, **12**, 130, 1926.
XX Cas....	.796	.329	.230	Partial d.	B4n	(B7)	.076	1.63	Pierce, *Princeton Contr.*, No. 18
RS Vul....	0.804	0.201	0.262	Partial u.	B8	(dG5)	0.078	1.63	Dugan, *Princeton Contr.*, No. 6

[2]). Column 3 is that for the wave length λ, in which the observations were made (using formula [1]); columns 4 and 5 give the differences between the observed and the computed reflection effects for total radiation and for radiation in wave length λ, respectively; and, finally, column 6 gives the ratio of the luminous efficiencies of the bright sides of the two components. For visual and for photographic observations E_b and E_f are estimated with the help of Table 1 in *Ap. J.*, **102**, 5. For λ 4500 the luminous efficiencies are calculated from the temperatures of the brighter faces of the components. The remaining columns—6, 7, 8, and 9—will be treated later.

TABLE 2

	Using Formulae (1), (2)				Using Formulae (1'), (2')				
(1) Star	(2) $2A_1^T$	(3) $2A_1^\lambda$	(4) $2A_1-2A_1^T$	(5) $2A_1-2A_1^\lambda$	(6) $2A_1^T$	(7) $2A_1^\lambda$	(8) $2A_1-2A_1^T$	(9) $2A_1-2A_1^\lambda$	(10) λ eff.
R CMa	0.037	0.015	−0.024	−0.002	0.042	0.017	−0.029	−0.004	4500A
RW CrB	.034	.019	− .008	+ .007	.038	.020	− .012	+ .006	5290
ZZ Aur	.039	.026	− .019	− .006	.045	.029	− .025	− .009	5290
Z Dra	.041	.029	− .009	+ .003	.048	.034	− .016	− .002	5290
RT Per	.043	.028	− .021	− .006	.043	.028	− .021	− .006	5290
TW And	.028	.023	− .023	− .018	.032	.026	− .027	− .021	5290
δ Lib	.055	.046	− .009	.000	.055	.054	− .009	− .008	4500
	.052	.044	− .006	+ .002	.062	.054	− .016	− .008	4500
	.050	.042	− .004	+ .004	.059	.049	− .013	− .003	4500
	.055	.044	− .009	+ .002	.065	.061	− .019	− .015	4500
TT Her	.036	.033	− .016	− .013	.041	.039	− .021	− .019	5290
X Tri	.045	.045	− .027	− .027	.054	.054	− .036	− .036	5290
RV Oph	.021	.022	+ .015	+ .014	.024	.025	+ .012	+ .011	5290
β Per	.036	.040	− .006	− .010	.041	.046	− .011	− .016	4500
SZ Her	.046	.049	− .016	− .019	.054	.066	− .024	− .036	5290
U Cep	.053	.063	− .010	− .020	.063	.075	− .020	− .032	5290
RZ Cas	.047	.060	+ .010	− .003	.055	.070	+ .002	− .013	5290
	.047	.064	+ .010	− .007	.056	.075	+ .001	− .018	5290
W UMi	.049	.069	− .011	− .031	.058	.083	− .020	− .045	5290
	.046	.067	− .008	− .029	.053	.079	− .015	− .041	5290
μ' Sco	.017	.040	+ .018	− .005	.011	.033	+ .024	+ .002	4500
VV Ori	.009	.022	+ .019	+ .006	.008	.023	+ .020	+ .005	4500
	.007	.018	+ .021	+ .010	.007	.018	+ .021	+ .010	4500
TT Aur	.009	.028	+ .041	+ .022	.010	.032	+ .040	+ .018	5290
U Oph	.017	.032	− .004	− .019	.019	.037	− .006	− .024	5290
TV Cas	.044	.070	+ .030	+ .004	.051	.082	+ .023	− .008	5290
GO Cyg	.032	.058	+ .024	− .002	.036	.067	+ .020	− .011	5290
u Her	.023	.054	− .005	− .036	.028	.064	− .010	− .046	4500
XX Cas	.015	.038	+ .061	+ .038	.016	.042	+ .060	+ .034	5290
RS Vul	0.032	0.058	+0.046	+0.020	0.038	0.067	+0.040	+0.011	5290

Figure 1 shows the distribution of $2A_1 - 2A_1^T$ against E_b/E_f. For stars with more than one solution the mean of these quantities is plotted. Figure 2 shows the distribution of $2A_1 - 2A_1^\lambda$ against E_b/E_f. Applying the analysis of linear correlation in both cases, we obtain the results shown in the accompanying table.

	$2A_1-2A_1^T$	$2A_1-2A_1^\lambda$
Correlation coefficient	$r=0.705\pm0.021$(p.e.)	$r=0.081\pm0.137$(p.e.)
Standard deviation	$\sigma=0.024$	$\sigma=0.025$
	mean $2A_1-2A_1^T=0.005$	mean $2A_1-2A_1^\lambda=-0.002$

There is a conspicuous correlation between the ratio of the luminous efficiencies and the difference between the observed coefficient of the reflection effect and that computed for total radiation; whereas, if the effect is computed for the wave length of observation, the correlation is negligible.

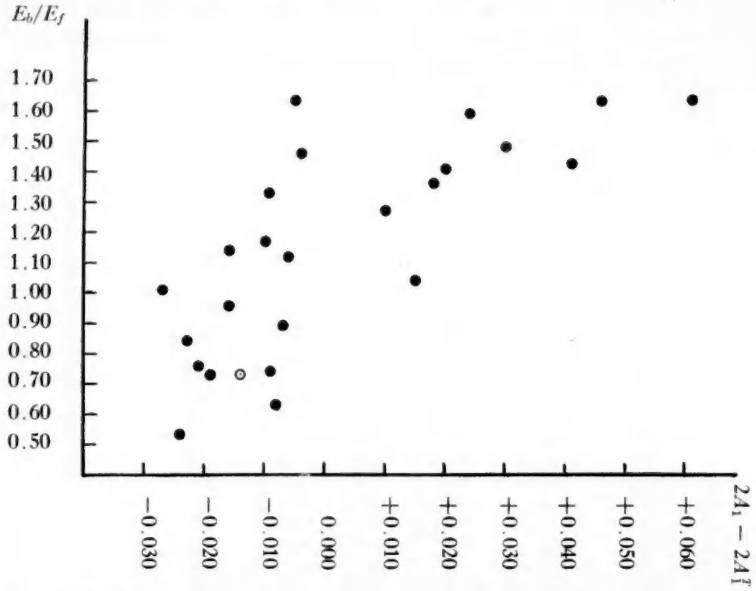

FIG. 1.—Diagram showing the distribution of $2A_1 - 2A_1^T$ against E_b/E_f

Comparison has also been made with the theoretical expression given by Kopal in his recently published monograph.[5] The procedure follows closely that given by Takeda. This takes into account the fact that the part of the comparison nearest the primary is most strongly illuminated. The expression reads as follows:

$$A_1^T = \tfrac{1}{3}\,(L_b r_f^2 - L_f r_b^2) + \tfrac{1}{4}\,(L_b r_f^3 - L_f r_b^3)\,. \qquad (2')$$

The formula for the effect is for total radiation. The corrections for luminous efficiency have been made as above:

$$A_1^\lambda = \frac{1}{3}\left(\frac{E_f}{E_b} L_b r_f^2 - \frac{E_b}{E_f} L_f r_b^2\right) + \frac{1}{4}\left(\frac{E_f}{E_b} L_b r_f^3 - \frac{E_b}{E_f} L_f r_b^3\right). \qquad (1')$$

Columns 6 and 7 in Table 1 give the reflection effects computed by formulae (2′) and (1′), respectively. The quantity r^2, as before, is taken as the square of the geometric mean of the minor equatorial and polar semi-axes; whereas r^3 is taken as abc—the product of the three semi-axes. This procedure should give a closer approximation in the case of ellipsoidal stars. Columns 8 and 9 give the $2A_1 - 2A_1^T$ and $2A_1 - 2A_1^\lambda$, respectively. Diagrams with the new data are so similar to Figures 1 and 2, respectively, that it has not seemed worth while to reproduce them here.

The correlation analysis of the data of $2A_1 - 2A_1^T$ and $2A_1 - 2A_1^\lambda$ against E_b/E_f yields the results given in the accompanying tabulation. As before, the correlation is marked for the total radiation and insensible for the known wave length.

[5] *Harvard Obs. Mono.*, No. 6, 1946.

	$2A_1-2A_1^T$	$2A_1-2A_1^\lambda$
Correlation coefficient	$r=0.690\pm0.069$	$r=-0.082\pm0.137$
Standard deviation	$\sigma=0.026$	$\sigma=0.020$
	mean $2A_1-2A_1^T=0.001$	mean $2A_1-2A_1^\lambda=-0.008$

In all cases, whether we use expressions (1), (2), or expressions (1′), (2′), for the computation of the reflection effect, there appears a considerable scatter in the residuals, be it for total radiation or for a given wave length; and this scatter is larger than the errors of observation.

It seems hardly justifiable to stress at this stage the significance of these deviations, since the formulae used are based on simplified assumptions. The complete solution of

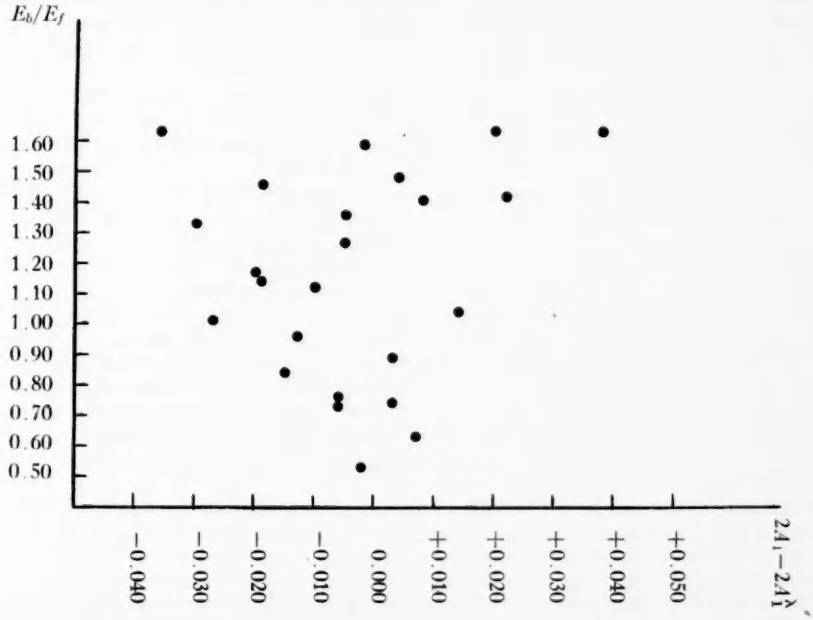

FIG. 2.—Diagram showing the distribution of $2A_1 - 2A_1^\lambda$ against E_b/E_f

the problem of reflection should include such effects as ellipticity of both components, limb darkening, and gravity darkening.

As the correlation between $2A_1 - 2A_1^T$ and E_b/E_f persists for $2A_1^T$ computed by either formula (2) or (2′) and as it is removed by the application of bolometric corrections, we can conclude that the process of "reflection" is probably one of absorption and re-emission and that the assumption that the stars considered radiate like black bodies is a fair one.

The writer takes great pleasure in expressing to Professor H. N. Russell her deep appreciation for having suggested the problem, for many helpful discussions, and for the privilege of working at the Princeton Observatory. She is also grateful to Professor L. E. Erro, of Tonanzintla Observatory, for giving her leave of absence.

REVIEWS

Theorieen der Kosmologie. By OTTO HECKMANN. ("Fortschritte der Astronomie," No. 2.) Berlin: Springer, 1942. Pp. 110+vii.

In order to appreciate the aims and achievements of this book, we have to recall the course of development of the subject during the last thirty years—surely, one of the oddest chapters in the history of science. The "De Sitter universe" of 1917 might well have served to predict the leading features of subsequent observational discoveries concerning the apparent expansion of the actual universe. It failed to do so, owing largely to the use of an unsuitable co-ordinate system. The "Einstein universe" of the same year served to demonstrate the impossibility of a static universe, of nonzero mean density, obeying the relativistic law of gravitation unless this law was modified by the rather artificial inclusion of the "cosmical term." But then the supposed necessity for a static model was taken as strong evidence for the necessity of this term. During the following ten years the nonstatic models, which form the basis of present-day relativistic cosmology, were studied mainly by Friedmann (1922) and Lemaitre (1927). They attracted little notice, however, until Eddington showed in 1930 how Lemaitre's work had implicitly demonstrated the instability of the Einstein universe. The work showed, in effect, that *no* static relativistic model is possible.

In addition, the work had already predicted the simple proportionality of speed to distance for matter in a nonstatic universe (apart from subsequent refinements depending on the precise definition of "distance"). When this law was announced by Hubble in 1929 as an empirical property of the external galaxies, a result foreshadowed by Slipher's earlier determinations (1922), it was therefore received as a great confirmation of the relativistic treatment.

There was, consequently, some natural consternation when Milne ventured in 1932 to remark upon the fact that the main characteristics of the expansion of the universe would be reproduced by the most trivial kinematics of any cloud of freely moving particles in "ordinary" space. But this elementary discussion was quickly followed by Milne's brilliant development of kinematical relativity, which, in turn, produced a model of the universe possessing much formal similarity to those of general relativity. So interest was shifted to the examination of the foundations of the two theories; also, incidentally, the reputation of the whole subject for mysteriousness was largely reinstated!

Finally, in 1934, Milne made the further crucial discovery that the problem solved by the relativistic treatment can also be solved by purely Newtonian theory. He and the present reviewer went on to establish not only a complete correspondence between Newtonian universes and those of general relativity but also the formal identity of the mathematical expression of some of their fundamental properties. Of course, for the familiar reasons depending ultimately upon the finiteness of the velocity of light, the Newtonian method is not really adequate. What is important is the insight it gives by showing that the physical situation under discussion involves only perfectly familiar physical phenomena.

The state of affairs about 1935 was therefore that, on the one hand, the immediate physical interpretation of the expansion of the universe had been found to be apparently quite simple and to account at once, to a first approximation, for the observed characteristics. On the other hand, there was no escape from the fact that a proper analysis of the problem does require all the resources of some form of relativity theory. Such analysis had led to a variety of theoretically possible models. Attention was then focused on the critical testing of these models by the most refined analysis to which the observational data could be submitted.

About that time there were published several important monographs, each giving an account of the problem from some special aspect. But a balanced appreciation of the whole situation could be had only by those who had had the opportunity closely to follow its curious history. There has been a clear need for a general survey which would present the whole subject in some sort of natural sequence calculated to make explicit the logic of its development. Dr. Heckmann's book is a very skilful survey of just this type. Unfortunately, copies will presumably not be easily available; so a review must summarize its contents more fully than would otherwise be necessary.

Part I, on "Dynamical Cosmology," develops a new presentation of the Newtonian treatment of the expanding universe referred to above. The "cosmological principle" is carefully formulated. The necessary discussion of Newtonian gravitation in an infinite distribution of matter is critically set out, and the formal possibility of modifying Newton's law by the inclusion of a cosmic term is demonstrated. The results due to Milne and to Milne and McCrea are recovered. In addition, Heckmann derives the path of a test-particle freely moving in the universe but not belonging to the substratum of galaxies—a result which is of assistance in the subsequent comparison of the various theories. He also considers briefly the thermodynamics of the universe, so as to derive a classical analogue of some results of Tolman for relativistic systems. Finally, he exposes the difficulties encountered in applying classical ideas concerning light-propagation to a Newtonian expanding universe. He shows that the assumption that the velocity of light is a function of the epoch (without further particularization) would go some way toward resolving these difficulties; though the assumption is arbitrary, it proves to be instructive for comparison with the relativistic treatment.

Part II, on "Metrical Cosmology," succeeds in giving, first, in less than twenty pages, an extraordinarily well-digested summary of the general relativity theory of the expanding universe. It does so, despite the fact that the author starts with a brief formulation of general relativity theory itself, which he finds to be necessary for his critical comparison with other theories. Then, as in Part I, he discusses the motion of a test-particle. He goes on to treat the relativity theory of light-propagation by a rather novel and powerful method which reproduces in a nicely connected fashion the results concerning Doppler effects, apparent brightness, etc., required for deriving "observable relations" in relativistic models. There follows a valuable rediscussion of the comparison of theory and observation, having, of course, the same objective as the well-known work of Hubble and Tolman and others (see Hubble, *Realm of the Nebulae* [1936], and *The Observational Approach to Cosmology* [1937]). This objective is to determine whether the observational data on the spectral shift, z, of external galaxies of apparent magnitude, m, and on the number, $N(m)$, of galaxies brighter than m can be represented sufficiently closely by any particular relativistic model and to determine its characteristics. Heckmann's first method is substantially similar to Hubble's and yields a substantially similar representation by a "closed" universe, whose small size and high mean density are quite implausible on general grounds. But he remarks that the numerical results are such as to cast doubt upon the approximations used to derive them. So he proceeds to a fresh examination of the data by using a certain function of m, z, and N which can be studied without such dubious approximations. However, his new results are essentially the same as the old ones. He then emphasizes that all such results are highly sensitive to any systematic errors in the data. By taking a hypothetical, though not impossible, example of such an error, he shows how it would lead to the replacement of the apparently too small closed space by an infinite flat space. In short, as Heckmann's summing-up makes evident, while the broad features of the observations are well reproduced by the elements common to Newtonian and relativity theories, the existing data are overstrained by the attempt to make them discriminate between the various theoretical models.

Part III, on "Kinematical Cosmology," opens with a concise survey of Milne's theory, in so far as it bears upon the cosmological problem (for kinematical relativity as a whole embraces much more than the consideration of this problem). Following the work of H. P. Robertson and of A. G. Walker, Heckmann then compares the theory with that of Part II. He concludes that the difference between the treatments of the cosmological problem is due not so much to their very different starting-points as to the part played in Milne's theory by his "dimension-hypothesis," whereby he specializes certain functions by denying the existence of universal constants possessing nonzero dimensions in length or time. Heckmann then poses certain questions, the answers to which would serve to clarify the cosmological significance of Milne's work.

There is appended to the book a valuable bibliography of nearly two hundred items for the years 1933–1940, earlier literature having been listed by Robertson (*Rev. Mod. Phys.*, Vol. 5 [1933]).

Dr. Heckmann's general arrangement of the work seems to the reviewer by far the most natural one to adopt in describing the present state of the subject. To have achieved such a well-balanced account in the space of a hundred-odd pages is a notable feat. Indeed, the book is in all essentials a model of what one of a series of "Fortschritte" should be; it is comprehensive but not too detailed; it is closely reasoned but lucid; it is critical without being partisan.

Perhaps the best virtue of the book is that it leaves one eager to see how the subject will de-

velop in the future. In this connection, the most obvious consideration is that observations by the Mount Palomar telescope are anxiously awaited. But another type of consideration also presents itself: Since the history of the subject has been so remarkable for the missing, if not of the obvious, at any rate of the simple, may we not still be overlooking yet some other vital simplification? If so, thanks in particular to certain suggestive ideas of Milne (*Ap.J.*, **91**, [1940], 129) but also, in keeping with a present trend in physical thought, we may guess what its effect should be. For, whereas existing theories yield *various* "possible" models for the universe, it would seem that there ought to be some principle according to which the actual universe is the *only* possible one.

W. H. McCrea

Royal Holloway College
London, England

Isaac Newton, 1643–1727: A Collection of Essays Dedicated to the Tercentenary of His Birth. Edited by Academician S. I. Vavilow. Academy of Sciences, U.S.S.R., 1943.

Galileo Galilei, 1564–1642: A Collection of Essays Dedicated to the Tercentenary of His Death. Edited by Academician A. M. Deborin. Academy of Sciences, U.S.S.R., 1943.

In the midst of a devastating war the Russian Academy of Sciences found it possible to publish, among many other things, these two remarkable volumes. Such devotion to the ideals of science is worthy of notice. Moreover, the contents of both volumes are of high intrinsic value. In fact, the reviewer has no hesitation in pronouncing the Newton volume one of the most significant contributions ever made in that field, indispensable for any serious study of the subject. Both volumes are in Russian, necessitating a more extended review than is customary.

The outward appearance of these two books is strikingly different. The large Newton volume (437 pp.) is printed on cheap paper and is very indifferently bound. The Galileo volume is a small book (190 pp.) printed on excellent paper and beautifully made up. Both volumes are edited very carefully with hardly any misprints. The type in both is excellent, and the Newton volume has initial blocks for each article derived from contemporary sources.

In reading these volumes one gets an impression of tremendous activity going on in modern Russia in the field of the history and philosophy of science. On page 17 of the Newton volume we learn that Euler's complete works are to be published in sixty-nine large volumes. Of these, forty-three have already been printed. The collected works of A. N. Krylov, many of which are devoted to Newton, are being continuously published, and Volume **7** (1936) isquoted on page 261. Several books on Newton, recently published in Russia, are mentioned; and from page 94 of the Galileo volume we see that even the works of Leonardo da Vinci have been translated. There is also a very large number of articles on similar subjects scattered through various Russian periodicals.

1. *Newton.*—It is obvious that it would be nearly impossible to write a comprehensive evaluation of Newton in one volume, especially if one considers his predecessors and his influence on the development of science, which is the attitude adopted by many of the contributing authors. In fact, this would amount essentially to a complete history of science and philosophy. Consequently, many topics, such as Newton's investigations in chemistry and his work at the mint have not been touched upon. It is of interest to note that these topics are treated in the American volume on Newton (*Sir Isaac Newton, 1727–1927* [History of Science Society, 1928]), so that the two volumes are in many respects complementary to each other.

There is another and greater difficulty about Newton. We refuse to treat him as a personality, and to most scientists Newton means only his *Principia* and his work in mathematics and optics. But this is not the whole of Newton. The real Newton has always been a psychological enigma, a man with a marvelous mathematical gift, yet reluctant to use it. There is much to say in favor of L. T. Moore's view (*Isaac Newton* [1934], p. 608) that the historical and theological work was of major importance to Newton. He himself considered it so, "even to the point of stating that the chief value of his scientific work lay in its support of revealed religion."

Scientists are prone to overlook the striking fact that practically all of Newton's contributions to science were made before he was forty-five years of age. So strange does it appear to us that the author of the *Principia* should bother about the interpretation of the Apocalypse that a hypothesis of his temporary insanity has actually been advanced.

Newton's psychology and attitude toward his own work is not discussed in the Russian volume, but it contains a very detailed article by S. J. Lurye, "Newton as an Historian of Antiquity," which is almost the only serious treatment of this aspect of Newton's activity to be found anywhere. The author's estimate of Newton's work is very high. He finds that Newton anticipated many methods of modern historical chronology, introducing the use of astronomical data for this purpose, comparative study of mythology, the influence of trade and commerce on the development of ancient astronomy, etc. The reason why Newton did not succeed in getting very far in his investigations was primarily the fact that the time was not yet ripe for such investigations. We must remember that even in our own day, with all the wealth of archeological data, a wide divergence of opinion on Egyptian chronology is still possible.

To the purely mathematical topics are devoted four articles: "Newton and the Theory of Similarity," by M. V. Kirpichev; "Newton's Theory of Limits," by N. N. Luzin; "Newton's Predecessors in the Philosophy of Infinitesimals," by S. J. Lurye; and "Newton's Polygon and Its Role in the Present Development of Mathematics," by N. G. Chebotarev. These articles occupy eighty-one pages, and are full of interesting information, and contain numerous references. It is quite impossible to discuss here their contents, but the first three titles are self-explanatory. The last article deals with the theory of the function

$$f(x, y) = A_n(x)\, y^n + A_{n-1}(x)\, y^{n-1} + \ldots + A_1(x)\, y + A_0(x),$$

where

$$A_k(x) = A_k x^{\rho_k} + A_{k+1} x^{\rho_{k+1}} + \ldots .$$

The development of the ideas concerning this function is traced up to the present time, even including unpublished work by the author's pupils.

There are several articles on the influence of Newton on the development of science, on which the large article of A. D. Lublinskaya, "Newton's Influence on French Science," is remarkable for the erudition shown by the author (189 references for 26 pp. of text). The problem treated in the article is the conflict of the ideas of Newton and Descartes in France. The hold that Descartes exercised on French science is evident when one recalls that the first Cassini still tried to reconcile the laws of Kepler with the vortex hypothesis. But already in 1751 the vortices appeared to D'Alembert "almost ridiculous." The author, in spite of the title, stops at about this time—just before the flowering of Newtonianism in the works of Lagrange and Laplace.

Of very great interest are the articles on the reaction that Newton's work caused in Russia. In "Newton and the Study of His Works in Russia," T. P. Kravetz notes that in the very first report of the St. Petersburg Academy of Sciences (1725) we meet with the name of Newton. However, the Academy was founded with the help of Leibniz, and the first native scientist, M. V. Lomonosov, was under the influence of Christian Wolf, who himself was a great admirer of Leibniz. The mood of the Academy was at first definitely anti-Newtonian. But as early as 1749 the Academy contributed substantially to the development of the law of gravitation by offering a prize for the best lunar theory to prove or disprove that law. This resulted in the famous essay of Clairaut, to be discussed later.

Although there were books and articles on Newton in Russia before the revolution, the more recent development of interest in Newton has been phenomenal. A. N. Krylov's work is of fundamental importance, and the author mentions several recent books on Newton, of which L. Zeitlin's *Science and Hypothesis* and S. I. Vavilow's biography of Newton should be noted.

A closely allied topic is discussed by T. I. Rainov in "Newton and Science in Russia." The article consists of the study of the influence of Newton on Lomonosov, Mendeleyev, and Krylov.

A great deal of attention is now devoted in Russia to M. V. Lomonosov, the first Russian scientist; but it is quite evident that Lomonosov's influence on the development of science in Russia and abroad was negligible. Undoubtedly, he was a many-sided genius, anticipating some later discoveries in physics and chemistry—and a good poet, too; but he was an isolated phenomenon in the sea of Russian ignorance and inertia. It is with the generation of Mendeleyev, Bredichin, and Chebyshev, which is almost within our memory, that native Russian science began to assume world-wide significance. And why, with the resources of a great empire and with the continuous encouragement of science by the government, no response in the native population was found for a hundred and fifty years after the founding of the Academy is a very interesting historical problem. Russia made contributions to world science by importing such great figures as L. Euler, the brothers Bernoulli, and many others. It may be recalled here that the founder and the first director of the Pulkovo Observatory, W. Struve, also was not a Russian by birth.

In the above article Rainov goes into a rather detailed study of Lomonosov's objections to Newton's conception of mass and the corpuscular theory of light and comes to the conclusion that most of the disagreement was due to misunderstanding. Newton was never easy to understand. D. I. Mendeleyev, known mostly as a chemist, was an admirer of Newton and wrote on many subjects besides chemistry. He adopted Newton's idea that mass is the fundamental property of matter and, following this line of thought, came to the formulation of his periodic law. But this law means that there is no progressive change of chemical properties as a function of the atomic weight but, instead, a recurrence of the same properties in a periodic fashion. Mendeleyev had to introduce the concept of the individuality of atoms, coming to the realization that mass alone is not sufficient to account for chemical properties; but the influence of Newton was too strong, and to the end of his days Mendeleyev maintained that "the understanding of the laws of harmony in chemical phenomena is possible only under the banner of the Newtonian dynamics." Therefore, Newton's influence on Mendeleyev, positive at the beginning, became negative at the end, preventing this great chemist from a deeper insight into atomic structure and even leading him to deny the reality of radioactive phenomena.

A. N. Krylov's work on Newton is discussed in the last chapter of Rainov's essay. From the Russian point of view the greatest contribution made by Krylov to the study of Newton was his translation of the *Principia* (first published in 1916), with very copious notes and explanations. It was necessary to translate not only the Latin text into Russian but also Newton's geometrical method of demonstration into the modern analytical method, in order to make it intelligible to the vast majority of readers. Krylov also published a large number of articles elucidating many points in Newton's mathematics and astronomy.[1]

A. M. Deborin's article, "Newton in the History of Culture," is not exactly what its title would suggest. Newton's law of gravitation, so dramatically demonstrated by the predicted return of Halley's Comet in 1759 and by the discovery of Neptune in 1846, has tremendously impressed every thinking individual. It is hardly possible to find a treatise on philosophy without at least a mention of Newton's name. The topic is therefore important, although hardly touched upon previously, but its treatment by the author is rather curious. After going into much detail concerning Voltaire, Saint-Simon, Fourier, and Kant and giving the reader much interesting information, the author comes to Hegel. There he stops, saying: "However, Hegel was an idealist." Did Newton's influence stop with Kant, or was there any culture after Kant worth talking about? The author ends with a general statement that "the great movement in the realm of philosophy, historical science, sociology and economics was consummated by Marx, Engels, Lenin and Stalin who worked out in the spirit of dialectic materialism all the substantial achievements of their predecessors." What the contributions were of the above-named individuals to the history of culture in connection with Newton the author does not say, apparently assuming that all this is well known.

Historical articles include also "Cambridge University and Newton," by E. C. Skrjinskaya, and "Portraits of Isaac Newton," by P. M. Dulsky. The first article deals with the history of Cambridge University before Newton and his connection with the university but makes no attempt to explain why the work of Newton was not continued at Cambridge. The other article suffers from the lack of portraits, only two of them being reproduced in the whole book.

The physics of Newton is discussed by S. I. Vavilow in "Ether, Light, and Matter in Newton's Physics" and by G. G. Slusarev in "Newton's Work in Geometrical Optics."

From the astronomical point of view the most interesting are the four articles: "Newton and the Development of the Theory of Refraction in the Earth's Atmosphere," by I. A. Khvostikov; "The Law of Universal Gravitation and Lunar Theory," by N. I. Idelson; "Newton's Tidal Theory and the Figure of the Earth," by L. N. Sretensky; and "Comets and Their Significance in the General System of Newton's *Principia*," by A. D. Dubiago. The amount of material covered in these articles is so large that it is hardly possible to indicate here more than their general idea.

The author of the article on refraction has to face the fact that there is no theory of refraction worked out by Newton. There are only two tables of refraction by Newton, never published by him, and the restoration of Newton's method used for the construction of these tables was made by Krylov in 1935. The method was equivalent to a numerical integration of the differ-

[1] In the *Russ. A. J.*, **22**, 375, 1945, two new books on related subjects are announced: *Lomonosov, Lobachevsky, and Mendeleyev*, by B. G. Kuznetsov (1945), and *Academician Alexei Nikolaievich Krylov*, by C. J. Streich (1944).

ential equations. It is rather curious that in this detailed article, full of historical references, the Pulkovo refraction tables are nowhere mentioned.

Idelson's article on lunar theory is one of the longest in the symposium (50 pp.) and one of the best. The author succeeds in making this complicated subject very clear. The role of the Russian Academy of Sciences in promoting the lunar theory by offering a prize is described in considerable detail. The prize was awarded in 1752 to Clairaut, who was able to explain the motion of the moon on the theory of gravitation. This was Clairaut's second paper on the subject. In 1743 he thought the Newtonian law required a correction. To the doubts entertained by Clairaut (and shared by D'Alembert) are devoted several interesting pages.

In the article on the tides the author goes into a thorough analysis of Newton's numerical results, which greatly exceed those derived by the modern theory. The difference is due to the fact that Newton computed the maximum height of the tides, assuming the earth to be of liquid composition throughout.

In the article on comets, Dubiago considers in detail Newton's method for the determination of parabolic orbits but hardly touches the physical theory of comets, which was of great interest to Newton.

The last article to be considered (it is the first in the symposium) is by the greatest authority on Newton in Russia (and perhaps in the world), A. N. Krylov on "Newton and His Significance in World Science." The reviewer, perhaps expecting too much after constant references to Krylov's work in other articles of the volume, can only express his disappointment. The treatment is so condensed and fragmentary that it is often reduced to a catalogue of names. For instance, exactly one line is devoted to E. W. Brown's lunar theory!

However, the article is of interest, inasmuch as the work of Russian mathematicians and astronomers hardly known abroad is emphasized, and at the end, in the appendix, is given an exposition of A. M. Liapounov's work on the equilibrium of rotating fluid masses.

We close this extended review with the hope that the Anglo-American world, so proud of the genius of Newton, will not overlook this remarkable contribution made by Russian scientists toward the understanding of Newton.

2. *Galileo.*—Here we meet with the same authors as in the volume on Newton: "Galileo in the History of Optics," by S. I. Vavilow; "Galileo as the Founder of Mechanics," by A. N. Krylov; and "Galileo in the History of Astronomy," by N. I. Idelson. There is also a translation of Galileo's letter (41 pp.) to Francesco Ingoli (1624), made by Idelson and supplied with several pages of notes.

In the first article the development of optics up to Galileo's time is carefully described. Especial emphasis is laid on the work of Leonardo da Vinci, following recent research by D. Argentieri. Several reproductions from Leonardo's notebooks are given in the article, including that of a machine for the grinding of concave mirrors. There is hardly any doubt that Leonardo understood and used a refracting telescope. The author is justly sarcastic about textbooks still passing the old yarn about the chance invention of the telescope by Lippershey or Janssen, in spite of the latter's admission that he copied his telescope from an Italian model made in 1590. To several examples quoted by the author of the use of the telescope before 1600 the reviewer may add that in Thomas Digges's *Pantometria*, published in 1571, the use of the telescope is described in detail. However, the first effective use of the telescope for astronomical observations was undoubtedly made by Galileo. There is also no doubt that Galileo made and used microscopes.

Less well known are Galileo's experiments to determine the speed of light and his views and observations of phosphorescence, described in Vavilow's article.

The short article by Krylov contrasts the views of Aristotle and of Galileo on the laws of motion of bodies.

The longest article is that by Idelson. The author is heavily indebted to Duhem, but other investigations of fundamental importance in the history of Galileo, such as those of Wohlwill, are hardly mentioned.

In general, the authors have succeeded in producing a well-balanced book without glorifying Galileo until he becomes a martyr of science and a universal genius. Besides his undoubted contributions to science, Galileo wrote much nonsense, and if he ever read Kepler he certainly did not understand him. To deny that the Catholic church persecuted Galileo is impossible, but the reasons for persecution are not so clear as they seemed to be fifty years ago. Idelson has a sufficiently balanced point of view to note that many Catholic dignitaries were on the side of

Galileo, and he mentions with especial approval Brother Campanella. Campanella was also persecuted (and, in fact, wrote most of his work in jail), but not by the church.

The fate of Michael Servetus in Calvinistic Geneva, and before him of Socrates in Athens, shows that the picture of the Catholic church versus science is a bit too naïve. New ideas are seldom tolerated under despotism, no matter what its origin.

The reviewer notes with satisfaction that this is the first popular book on Galileo that he has read in which the discredited episode of the Leaning Tower is not even mentioned. The book, although not on such a high level of scholarship as the volume on Newton, is nevertheless a valuable contribution to the history of science.

The reviewer ventures to make a few remarks here not in direct connection with the reviewed books. We live in a closely knit world, and mutual understanding between the nations is of the greatest importance. Yet it is extremely difficult to get hold of the material published in Russia. Before the war it was often impossible to get Russian books through the usual channels, while books published anywhere else in the world could be had almost by return mail. That Russian astronomy and allied disciplines are developing very rapidly is quite obvious, but we need more substantial evidence than mere hearsay to appreciate and evaluate Russian contributions to science and culture. We may not share Russian political ideas, but in science we form a truly international fellowship, in which the accidents of race, language, and political persuasion may be forgotten.

N. T. Bobrovnikoff

Perkins Observatory
May 21, 1946